Exploring the therapeutic potential and cellular mechanisms of BH3 mimetic-mediated apoptosis in cancer

Thesis submitted in accordance with the requirements of the University of Liverpool for the degree of Doctor in Philosophy

Mateus Milani

August 2019

DECLARATION

This thesis is the result of my own work. The material contained within this thesis has not been presented, nor is currently being presented, either wholly or in part for any other degree or qualification.

Mateus Milani

This research was carried out in the Department of Molecular and Clinical Cancer Medicine, University of Liverpool, UK.

Thesis contents

Acknowledgements

Firstly, I would like to thank Shankar for accepting an unknown Brazilian "hippie" into his lab and the timely despair to start his own group. During these 4+ years I have never learned so much about the practical science in my life. 874 western blots later I guess now I can say I've grasped a thing or two. Thank you for teaching me how to plan and design complicated experiments, how to work efficiently in the lab and for never stop talking during a half marathon in a foreign country. You have taught me more than you can imagine, and although is your job, I will be eternally grateful for it. Secondly, I would like to thank you, Gerry, for calmly trying to understand my accent and for guiding me with your knowledge and experience, helping me to understand how to be critical of other peers' data and most importantly, how to be critical of my own data, with a neutral eye.

Also, I thank my lab colleagues, Ahoud and Ammar, for all the support during the last year or two of my journey. Thank you, Aoula, for all the radioactivity that we shared together and for always being supportive in the lab. Thank you, Govinda, for all the deep conversations, for the companionship and for all the help during these years. Thank you, Rachel, for bringing me exotic beverages, for the non-science-y updates and for being so helpful with the science bits too. Thank you, Michael, for your patience, for teaching me all the tricks and shortcuts in the lab during the first years and for being a great and welcoming tour guide. Thank you, Georgia, for trailblazing the uncharted territories of the Varadarajan's lab with me, for being there when I needed and for at least trying to not make a mess on my bench. Once again, thank you very much lab people, you made this journey extra special!

I would like to thank my family, especially my father, my mother, Di and Dan. Thank you for always being there for me, for all the support and for the great times we had together during those years. Thank you for completely backing me up on this adventure, I couldn't do it without your encouragement.

Finally, I can't thank you more, Bia. For coming to the UK with me, plunging into the unknown enterprise of doing a PhD abroad. For being present at all times, pushing me forward, helping me to endure the tough times and to savour the nice moments. For being a partner in philosophy, in science and in life.

List of Publications

1. **MILANI, MATEUS**; BECKETT, ALISON J.; AL-ZEBEEBY, AOULA, LUO, XU; PRIOR, IAN A.; COHEN, GERALD M.; VARADARAJAN, SHANKAR. DRP-1 functions independently of mitochondrial structural perturbations to facilitate BH3 mimetic-mediated apoptosis. *Cell Death Discovery* **5**, 117 (2019).

2. YEDIDA, GOVINDA R.; **MILANI, MATEUS**; COHEN, GERALD M.; VARADARAJAN, SHANKAR. 2019. Apogossypol-mediated reorganisation of the endoplasmic reticulum antagonises mitochondrial fission and apoptosis. *Cell Death and Disease* **10**, 521 (2019).

3. **MILANI, MATEUS**; BYRNE, DOMINIC P; GREAVES, GEORGIA; BUTTERWORTH, MICHAEL; COHEN, GERALD M; EYERS, PATRICK A; VARADARAJAN, SHANKAR. DRP-1 is required for BH3 mimetic-mediated mitochondrial fragmentation and apoptosis *Cell Death Disease* **8**, 1–9 (2017).

4. GREAVES, GEORGIA; **MILANI, MATEUS**; BUTTERWORTH, MICHAEL; CARTER, RACHEL J.; BYRNE, DOMINIC P.; EYERS, PATRICK A.; LUO, XU; COHEN, GERALD M.; VARADARAJAN, SHANKAR. BH3-only proteins are dispensable for apoptosis induced by pharmacological inhibition of both MCL-1 and BCL-XL. *Cell Death Differ.* **6**, 1037–1047 (2018).

5. AL-ZEBEEBY, AOULA; VOGLER, MEIKE; **MILANI, MATEUS**; RICHARDS, CAITLIN; ALOTIBI, AHOUD; GREAVES, GEORGIA; DYER, MARTIN J.S.; COHEN, GERALD M.; VARADARAJAN, SHANKAR. Targeting intermediary metabolism enhances the efficacy of BH3 mimetic therapy in hematologic malignancies. *Haematologica* **104**, 1016–1025 (2019).

6. LUCAS, C M; **MILANI, M**; BUTTERWORTH, M; CARMELL, N; SCOTT, L J; CLARK, R E; COHEN, G M; VARADARAJAN, S. High CIP2A levels correlate with an antiapoptotic phenotype that can be overcome by targeting BCL-XL in chronic myeloid leukemia. *Leukemia* **42**, 1–9 (2016).

7. VARADARAJAN, SHANKAR; POORNIMA, PARAMASIVAN; **MILANI, MATEUS**; GOWDA, KRISHNE; AMIN, SHANTU; WANG, HONG-GANG; COHEN, GERALD M. Maritoclax and dinaciclib inhibit MCL-1 activity and induce apoptosis in both a MCL-1-dependent and -independent manner. *Oncotarget* **6**, 10–15 (2015).

Abstract

Evasion of apoptosis is one of the main hallmarks of cancer. The BCL-2 family of proteins are the main mediators of the intrinsic pathway of apoptosis and the interactions between the pro- and anti-apoptotic members of this family of proteins control the fate of a cell towards life or death. Anti-apoptotic members of the BCL-2 family, such as BCL-2, BCL-X_L and MCL-1, are frequently overexpressed in a plethora of cancers promoting abnormal cell survival. During the last ten years, several small molecule inhibitors called BH3 mimetics were developed to inhibit these anti-apoptotic proteins. The potency and specificity of the BH3 mimetics make them valuable tools for targeting the pro-survival pathways in different cancers. The first known *bona fide* BH3 mimetic, ABT-737, has now been replaced by more selective inhibitors, such as ABT-199 (BCL-2-specific inhibitor), A-1331852 (BCL-X_L-specific inhibitor), A-1210477 and S63845 (both MCL-1-specific inhibitors), all of which have been employed in the different experiments detailed in this thesis. ABT-199 has been successfully used in the treatment of haematological malignancies, such as chronic lymphocytic leukaemia. Experiments are now in progress to reproduce this success using other BH3 mimetics in a wide variety of cancers.

This study is aimed at exploring (1) whether BH3 mimetic therapy can help improve on current therapy in certain haematological malignancies, (2) whether BH3 mimetics can be used as single agents or in combination with existing therapy to target certain solid tumours, and (3) the underlying cellular and molecular mechanisms by which BH3 mimetics induce apoptosis.

In order to explore the therapeutic potential of BH3 mimetics in haematological malignancies, the cancer types chosen for this work were chronic and acute myeloid leukaemia (CML and AML). Tyrosine kinase inhibitors (TKIs) are the preferred drugs for treating CML, whereas AML is treated with anthracyclines such as daunorubicin. Using a series of genetic knockdown experiments, it was identified that CML is a BCL-X_L dependent malignancy and that targeting BCL-X_L with A-1331852 resulted in rapid and extensive apoptosis not only in the established CML cell lines but also in primary patient samples. In marked contrast, using a panel of AML cell lines, it was shown that AML cell lines and patient samples demonstrated a dual dependency on BCL-2 and MCL-1 for cell survival, which was overcome by a combination of ABT-199 and S63845.

These observations were extended to solid tumours, with a focus on head and neck squamous cell carcinoma (HNSCC) and pancreatic ductal adenocarcinoma (PDAC). Unlike the dependency on BCL-X_L for CML and BCL-2 and MCL-1 for AML, these solid tumours demonstrated a dual dependency on BCL-X_L and MCL-1 for survival. In agreement, tissue microarray (TMA) analysis revealed high expression levels of both BCL-X_L and MCL-1 in the tumour cores of these cancer patients. Furthermore, dual inhibition of these BCL-2 family proteins by a combination of A-1331852 and S63845 induced cell death and reduced clonogenic potential of several cell lines derived from these solid tumours, indicating that a combination of these inhibitors could be valuable in treating certain solid tumours.

A closer analysis of the intracellular effects caused by exposure to BH3 mimetics indicated that BH3 mimetic-mediated apoptosis was accompanied by mitochondrial ultrastructural changes. BH3 mimetics induced extensive mitochondrial fragmentation, which was dependent on the mitochondrial fission

machinery, of which DRP-1 is the major player. It was shown that BH3 mimetic-mediated induction of key steps of the intrinsic pathway of apoptosis, such as cytochrome *c* release and BAK activation, were dependent on DRP-1. This strongly suggested a linkage between the regulation of mitochondrial membrane dynamics with the mechanisms that control cell death.

Assessment of the involvement of the endoplasmic reticulum (ER) in BH3 mimetic-mediated mitochondrial membrane dynamics and cell death uncovered new roles for ER shaping proteins, such as RTN-4 and CLIMP-63. Genetic silencing of these proteins indicated that, similar to DRP-1, ER shaping proteins, play an important role both in mitochondrial fission and also in the effective induction of BH3 mimetic-mediated apoptosis.

Overall, this study highlights the potential of BH3 mimetics as therapeutic intervention for haematological malignancies, such as CML and AML, as well as for hard-to-treat solid tumours, such as HNSCC and PDAC. In addition, this study underscores the importance of assessing unanticipated effects of BH3 mimetics, such as mitochondrial fission. Finally, this study sheds light on how ER and mitochondrial membrane dynamics regulate key steps of the intrinsic pathway of apoptosis, by showing for the first time that ER shaping proteins can regulate mitochondrial fission and cell death.

Abbreviations

ABL	Abelson murine leukaemia viral oncogene homolog 1
AF	Advancing front
ALL	Acute lymphoblastic leukaemia
AML	Acute myeloblastic leukaemia
ANOVA	Analysis of variance
APAF-1	Apoptotic protease activating factor-1
BAD	BCL-2-associated death promoter
BAK	BCL-2 homologous antagonist killer
BAX	BCL-2-associated X protein
BCL-2	B-cell lymphoma 2
BCL-2A1	BCL-2-related protein A1
BCL-W	BCL-2-like protein 2
BCL-X_L	B-cell lymphoma-extra large
BCR-ABL	Breakpoint cluster region
BFL-1	BCL-2 related gene expressed in foetal liver
BH	BCL-2 homology domain
BID	BH3 interacting-domain death agonist
BIK	BCL-2-interacting killer
BIM	BCL-2-like protein 11
BMF	BCL-2-modifying factor
CCCP	Carbonyl cyanide m-chlorophenyl hydrazone
CDK	Cyclin-dependent kinase
CLIMP-63	Cytoskeleton-linking membrane protein 63
CLL	Chronic lymphoblastic leukaemia
CML	Chronic myeloblastic leukaemia
DISC	Death-inducing signalling complex
DKO	Double knock-out
DRP-1	Dynamin-1-like protein
ECL	Electrochemiluminescence
EGFR	Epidermal growth factor receptor
EM	Electron microscopy
EMEM	Eagle's minimal essential medium
ER	Endoplasmic reticulum
ERK	Extracellular signal-regulated kinase
FACS	Fluorescence-activated cell sorting
FBS	Foetal bovine serum
FITC	Fluorescein isothiocyanate
FLT3	FMS-like tyrosine kinase 3
GAPDH	Glyceraldehyde 3-phosphate dehydrogenase
HDAC	Histone deacetylase
HNSCC	Head and neck squamous cell carcinoma
HPV	Human papillomavirus
HRK	Harakiri
HSP	Heat-shock protein

IAP	Inhibitor of apoptosis
IHC	Immunohistochemistry
IMDM	Iscove's modified Dulbecco's medium
IMM	Inner mitochondrial membrane
LNP-1	Lunapark-1
MAM	Mitochondria associated membranes
MAPL	Mitochondrial-anchored protein ligase
MCL-1	Myeloid cell leukaemia 1
MEK	Mitogen-activated protein kinase
MFF	Mitochondrial fission factor
MFN1	Mitofusin 1
MFN2	Mitofusin 2
MiD49	Mitochondrial elongation factor 2
MiD51	Mitochondrial elongation factor 1
MNC	Mononuclear cells
MOMP	Mitochondrial outer membrane permeabilisation
NF-κB	Nuclear factor kappa-light-chain-enhancer of activated B cells
NOXA	Phorbol-12-myristate-13-acetate-induced protein 1
NSCLC	Non-small cell lung cancer
OC	Oral cavity
OMA1	Oma1 zinc metallopeptidase
OMM	Outer mitochondrial membrane
OPA-1	OPA1 mitochondrial dynamin like GTPase
p53	Tumour protein p53
PARP	Poly (ADP-ribose) polymerase
PDAC	Pancreatic ductal adenocarcinoma
PI	Propidium iodide
PS	Phosphatidylserine
PUMA	BCL-2 binding component 3
RAS	Rat sarcoma
ROS	Reactive oxygen species
RPMI	Roswell park memorial institute
RTN-1	Reticulon-1
RTN-4	Reticulon-4
SEM	Standard error of the mean
STAT	Signal transducer and activator of transcription
TBS-T	Tris-buffered saline-tween
TKI	Tyrosine kinase inhibitor
TMA	Tissue microarray
USP9X	Ubiquitin specific peptidase 9 x-linked
WT	Wild type
YME1L	ATP-dependent metalloprotease YME1L1
Z-VAD.FMK	N-Benzyloxycarbonyl-Val-Ala-Asp(O-Me) fluoromethyl ketone

CHAPTER 1

INTRODUCTION

Chapter contents

1.1 Apoptosis – Overview

Apoptosis is a programmed cell death pathway comprised of a coordinated set of cellular events, all of which lead to key changes in the cell and ultimately, killing the cell. The etymology of the word derives from an antient Greek term that translates to "falling off",[1] coined due to the resemblance of apoptotic cells to leaves falling off a tree. Apoptosis is crucial for the maintenance of homeostasis, occurring in aging, for cellular turnover; during development for the recycling of unnecessary vestigial parts of the body, such as the tadpole tail metamorphosis and digit formation in several animals; during clearance of cells that are infected/damaged by disease or noxious agents.[2] Morphologically, apoptotic cells undergo shrinkage and pyknosis (excessive chromatin condensation), DNA and nuclear fragmentation,[3] followed by blebbing of cell fragments into "apoptotic bodies", consisting of organelles and cytoplasm bodies tightly packed by the plasma membrane, which are then cleared by macrophage phagocytosis. This ensures that the cells are eliminated with no triggers for inflammation or cytokine mediated responses.[4]

Apoptosis is initiated *via* either an extrinsic (death receptor) pathway or intrinsic (mitochondrial) pathway (Figure 1.1). The extrinsic pathway occurs at the level of cell surface, and is executed by the recruitment of death ligands on transmembrane death receptors of the tumour necrosis factor (TNF) superfamily.[5] This results in the recruitment of adaptor proteins, like FADD, and initiator caspases, such as caspase-8 to a death inducing signalling complex (DISC), leading to the apoptotic cascade. In contrast, the intrinsic pathway occurs at the level of mitochondria and is tightly regulated by different members of the BCL-2 family of proteins (discussed in detail later). This apoptotic pathway is initiated by disruptions to the mitochondrial membrane integrity, characterised by the formation of a pore in the outer

mitochondrial membrane (OMM) in a process known as mitochondrial outer membrane permeabilisation (MOMP), typically considered as the "point of no return" on the apoptotic pathway, which is mediated by proteins such as BAX and BAK.[6,7] This results in the release of cytochrome *c*, from being initially trapped within the mitochondrial cristae into the cytosol, where it interacts with and induces the oligomerisation of APAF-1 (apoptotic protease activating factor 1), which in turn recruits pro-caspase-9.[8] APAF-1 bound to cytochrome *c* and pro-caspase-9 forms a structure called apoptosome. By interacting with the apoptosome,[9] caspase-9 undergoes dimerization and activation.[10,11] This often accompanies the cleavage of pro-caspase-9, which is thought to regulate the activity of the apoptosome.[12] Upon activation, caspase-9 initiates the so-called caspase cascade, a powerful signalling pathway that activates the executioner caspases-3 and -7.[13] These executioner caspases, namely capsase-3, caspase-7 and caspase-6 are activated by dimerization followed by cleavage of their pro-domain.[14,15] The active caspase then induces the cleavage of several different protein substrates, including PARP (poly ADP ribose polymerase), culminating in an organised mechanism of cell death.[2,13,16]

1.2 BCL-2 family of proteins

BCL-2 family of proteins coordinate the initial stages of the intrinsic pathway by regulating mitochondrial integrity. The BCL-2 family of proteins is comprised by over 25 different members, which are categorised according to their function as either anti-apoptotic (prevent apoptosis) or pro-apoptotic (promote apoptosis). The pro-apoptotic members are further subdivided according to their specific functions as activators, sensitisers and effectors. The balance between the expression levels of the pro- and anti-apoptotic members are thought to dictate mitochondrial integrity and apoptosis.[17]

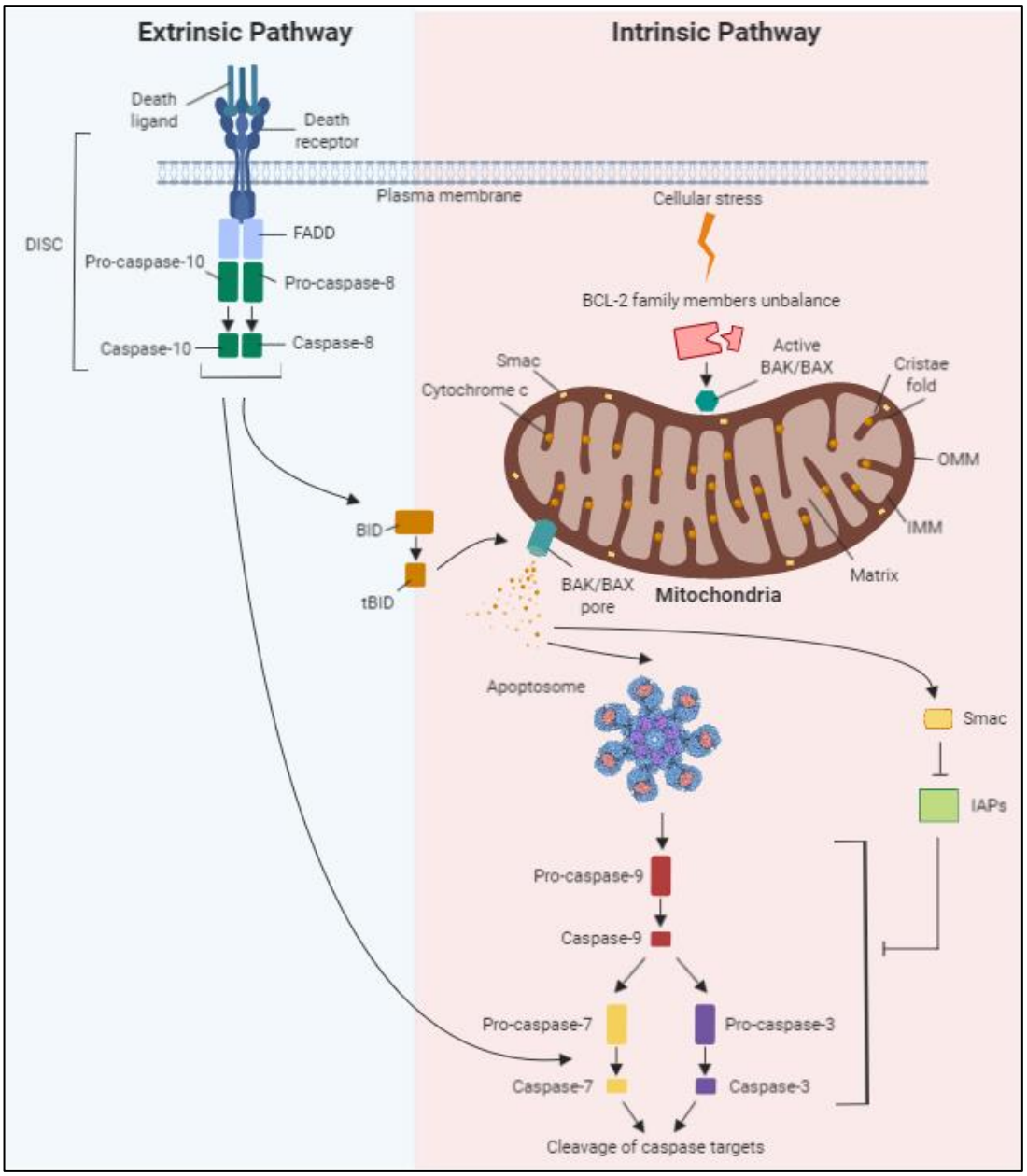

Figure 1.1 Pathways of apoptosis. The extrinsic pathway of apoptosis is initiated in by death receptors and ligands in the plasma membrane, whilst the intrinsic pathway occurs at the level of mitochondria via proteins of the BCL-2 family. Upon binding of death ligand to a death receptor, DISC is assembled to trigger the auto-catalytic activation of procaspase-8 and procaspase-10.[18] Active capase-8 cleaves procaspase-3 and BID to form the executor caspase-3, and a truncated form called tBID, respectively. tBID translocates to the mitochondria to facilitate BAX/BAK-mediated release of cytochrome *c*. In the intrinsic pathway, stress signals induce BAX/BAK activation and oligomerisation at the OMM to release cytochrome *c* and form the apoptosome. Another molecule called Smac[19] is also released from the mitochondria, to bind and inhibit the inhibitor of apoptotic proteins (IAPs) to relieve their repression of caspase activation.[20] Both apoptotic pathways culminate in the activation of the executioner caspases, ultimately promoting organised cell death.

All BCL-2 family of proteins share conserved BCL-2 homology (BH) domains, which are short amino acid sequences and classified into distinct motifs, numbered BH1-BH4. Of these, the BH3 domains share a signature sequence of LXXXGDE,[21] which is highly conserved and often exploited in cancer therapy.

1.3 The antiapoptotic members of the BCL-2 family of proteins

The main function of the anti-apoptotic members of the BCL-2 family in apoptosis lies in binding and inhibiting the activity of their pro-apoptotic counterparts, thus antagonising apoptosis. Not surprisingly, the anti-apoptotic members of the BCL-2 family are often overexpressed in different kinds of cancers, which become addicted to these proteins, as they are required for tumour cell survival. For these reasons, the anti-apoptotic members have been identified as promising targets for cancer therapy. Five members of the anti-apoptotic BCL-2 family, namely BCL-2, BCL-X_L, MCL-1, BCL-w and BCL-2A1 have been recognised so far. Of these, the first three have been heavily characterised in a wide range of malignancies. Inhibitors that selectively target these members are currently available, either for use in patients or at least in clinical trials.

1.3.1 BCL-2

BCL-2, as the name suggests, is the founder member of the BCL-2 family and was the first pro-survival protein to be discovered[22] and characterised in follicular lymphomas with a t(14;18) chromosomal translocation.[23] Overexpression of BCL-2 has been shown to play important survival roles in several solid tumours, such as brain,[24] bladder,[25] breast,[26] colorectal,[27] lung[28] and prostate[29] cancer and also in haematological malignancies such as acute myeloid leukaemia (AML),[30] chronic lymphocytic leukaemia (CLL)[31] and non-Hodgkin's lymphoma.[32] BCL-2 exists as

two isoforms: BCL-2α, which corresponds to the widely known anti-apoptotic protein and BCL-2β, that is found overexpressed in blood and bone marrow cells of chronic myeloid leukaemia (CML) patients, however with no described function until now.[33] BCL-2 is a 26 kDa protein that is mainly localised mainly within the membranes of endoplasmic reticulum (ER), and outer mitochondrial membrane (OMM), with no apparent re-localisation upon apoptotic stimuli.[17] In addition to its well-established role in apoptosis, BCL-2 has been shown to play a role in autophagy, *via* its interaction with Beclin-1.[34]

1.3.2 BCL-X_L

BCL-X_L (B-cell lymphoma extra-large) shares 44% amino acid identity to BCL-2 and has been linked to several tumours, such as CML,[35,36] head and neck,[37] colorectal[38] and prostate cancer.[39,40] The gene that codes for BCL-X_L (*BCL-X*) also codes for another isoform, BCL-X_S, by alternative splicing. While BCL-X_L is anti-apoptotic, BCL-X_S has pro-apoptotic functions.[41,42] BCL-X_L prevents BAX and BAK activation, whereas BCL-X_S disrupts BAK interaction with VDAC2 (voltage-dependent anion channel 2) facilitating BAK activation.[43] Under reducing conditions, BCL-X_L can be detected as a doublet at approximately 28 and 30 kDa which represent BCL-X_L and its phosphorylated form respectively.[44] BCL-X_L is normally localised in the cytosol and to some extent, in the OMM. During apoptosis, most cytosolic BCL-X_L gets translocated to the ER and OMM.[17] In the cytosol, BCL-X_L exerts its anti-apoptotic functions by mediating BAX retrotranslocation from mitochondria to cytosol, thus inhibiting BAX activation and subsequent anchoring in the OMM.[45] Moreover, BCL-X_L is also known to regulate autophagy by binding to Beclin-1.[34]

1.3.3 MCL-1

MCL-1 (myeloid cell leukaemia 1) was firstly discovered as a proliferation inducer in ML-1 myeloid leukaemia cells.[46] MCL-1 is one of the most overexpressed genes with oncogenic potential in several cancers.[47] highly expressed or mutated in solid tumours such breast,[48–50] lung,[51,52] ovaries,[53] head and neck,[54] thyroid,[55] pancreas[56] and prostate cancer[57] as well as in haematological malignancies, such as multiple myeloma[58] and AML.[59] Furthermore, MCL-1 is also linked to chemoresistance to cisplatin[54,60] and radiotherapy.[56,61] MCL-1 has 3 isoforms, MCL-1L (long isoform), which is the "classic" anti-apoptotic isoform and the pro-apoptotic, MCL-1S (short) and MCL-1ES (extra-short) isoforms, which have not been studied extensively so far.[33] Moreover, other isoforms of MCL-1 have been identified in the OMM, mitochondrial matrix and even nucleus.[62,63] In addition to these subcellular locations, MCL-1 has also been detected in the cytosol, ER and the inner mitochondrial membrane (IMM).[17] Under reducing conditions, MCL-1 is detected as three main bands at approximately 40, 38 and 36 kDa, which correspond to full-length MCL-1 and two isoforms, one cleaved at isoleucine-10 and localised at the OMM and the shorter one cleaved at leucine-33 localised in the IMM/matrix.[62] MCL-1 has a N-terminus motif that has not been identified in other members of the BCL-2 family. This region is enriched with proline (P), glutamic acid (E), serine (S) and threonine (T), which confers its name, PEST.[46] This motif is commonly found in short-living proteins and confers a labile feature to MCL-1.[64] The rapid turnover of MCL-1 (attributed to post-translational modifications, such as ubiquitination and proteasomal degradation)[65,66] has been exploited in cancer therapy by translationally repressing MCL-1 synthesis (for example, using a CDK inhibitor like dinaciclib).[67,68]

1.3.4 Other anti-apoptotic BCL-2 family members

Besides the above-mentioned members of the BCL-2 family, other anti-apoptotic members, such as BCL-w and BCL-2A1 also are expressed in several cancers. BCL-w overexpression has been correlated with various kinds of cancers, such as breast,[69] melanoma,[70] colorectal[71] and B cell malignancies.[72] Similarly, BCL-2A1 (BCL-2 related protein A1) also known as BFL-1 (BCL-2 related gene expressed in foetal liver) is another protein of the BCL-2 family, commonly associated with breast[73,74] and stomach cancers,[74] acute lymphoblastic leukaemia (ALL)[75] and CLL.[76,77]

1.4 BAX and BAK, the pro-apoptotic effectors of the BCL-2 family of proteins

Of the pro-apoptotic members of the BCL-2 family, the effector proteins have been extensively investigated due to their critical function in the intrinsic pathway of apoptosis. The effector proteins, BAX and BAK are known for their ability to homo or heterodimerise to form pores that permeabilise the OMM to release cytochrome *c* from the IMM.[78] In gastric and colon cancers, BAX and BAK have been found to be potentially mutated, thereby driving enhanced cell survival.[79–81]

BAX (BCL-2 associated X), was originally identified as a BCL-2 associated protein,[82] and later characterised to possess specific functions in the permeabilisation of mitochondria.[83–85] Since then, several studies have focused in elucidating the intricate molecular mechanisms behind BAX activation, oligomerisation and pore formation (reviewed in [86]). Soon after, BAK (BCL-2-homologous antagonist killer) was identified by three distinct groups and published as back-to-back articles in *Nature*, which demonstrated its similarly to BAX and its interactions with BCL-2

and BCL-X_L.[87–89] BAX also has been shown to interact with all anti-apoptotic BCL-2 family members,[90] whereas BAK binds all but BCL-w.[17,90,91]

Under normal conditions, BAX shuttles back and forth between the cytosol and mitochondria with the help of proteins such as BCL-X_L,[45] preventing BAX activation and thus, keeping control on MOMP and apoptosis. Upon activation, BAX also undergoes conformational changes, including the exposure of the 6A7 epitope in its α1 and BH3 domains,[92] which can be used as marker to assess BAX activation in cells.[93] Although to a lesser extent than BAX, BAK also shuttles between the cytosol and mitochondria, however due to lower shuttling rates BAK is normally found inserted into the OMM,[94,95] presumably *via* its α9 helix (Figure 1.2).[96] Upon interaction with pro-apoptotic members of the BCL-2 family to the BH3 domain of BAK, it becomes activated and undergoes conformational changes such as exposure of AB1 epitope which can be as marker to assess BAK activation in cells.[92]

Once activated, BAX and BAK oligomerise at the OMM, by engaging their BH3 domain with their hydrophobic surface groove and exposing lipophilic residues, which in turn can penetrate the OMM and displace phospholipids to form a puncture in the membrane, in a similar fashion to certain bacterial toxins such as melittin (Figure 1.2).[97,98]

In addition, BOK (Bcl-2-related ovarian killer), a less well understood pro-apoptotic effector of the BCL-2 family, plays unclear roles in the intrinsic pathway of apoptosis, as it has been shown to promote cell death when overexpressed[99–102] and increase ER-stress induced apoptosis when knocked-out.[99,103]

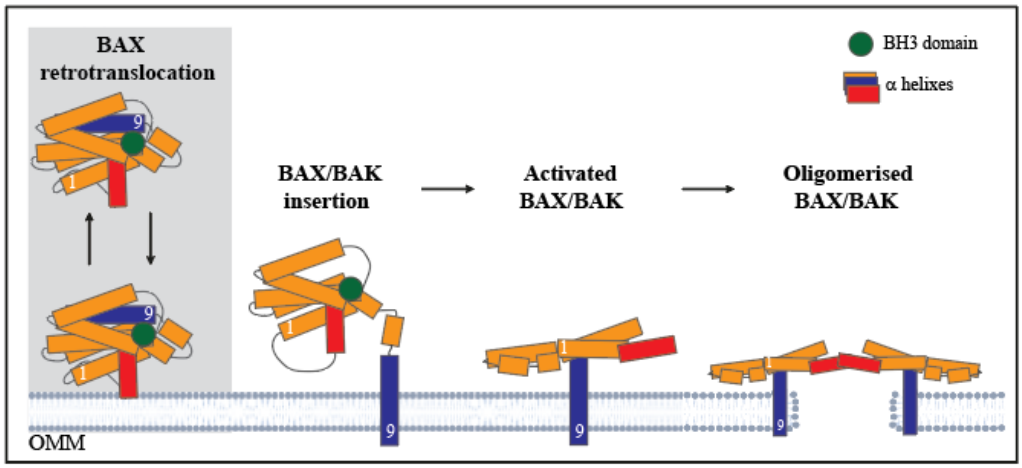

Figure 1.2. Mechanisms of BAX and BAK activation and oligomerisation. Under normal conditions, BAX, and to a lesser extent, BAK, shuttles between cytosol and mitochondria.[95] Upon apoptotic stimuli, after interactions via its BH3 domain, BAX/BAK gets inserted in the OMM by release of its α9 helix. Activated BAX/BAK changes its conformation allowing for the oligomerisation with other BAX/BAK molecules and for the opening of a pore in the OMM.

Primarily localised at the ER, BOK is constitutively bound to IP3Rs (inositol 1,4,5-triphosphate receptors), where it seems to stabilise ER-mitochondria interactions and regulate mitochondrial fusion.[104]

1.5 Protein-protein interactions within the BCL-2 family of proteins

The anti-apoptotic members, such as BCL-2 and BCL-X_L was originally thought to antagonise apoptosis by just binding and inhibiting BAX.[105] However, with the discovery of new members of the BCL-2 family, this simple model has been revisited with further improvements in our understanding of their mechanisms. Besides the effector proteins, BAX and BAK, there exists a collection of pro-apoptotic activators and sensitisers, all of which regulate the different interactions and interplay among the different members of the BCL-2 family of proteins. Unlike the other members of the BCL-2 family, the activators and sensitisers possess only the BH3 domain and hence, are collectively known as the BH3-only proteins.

Two distinct models detailing possible mechanisms by which the anti-apoptotic BCL-2 family members, pro-apoptotic effectors (BAX and BAK) and BH3-only members come together to execute the apoptotic pathway have been proposed. In the 'direct' model, the activators (BH3-only proteins) bind and directly activate effectors (BAX and BAK) to induce apoptosis, while the anti-apoptotic members sequester and inhibit the function of these activator proteins, thus antagonising apoptosis. In this model, the sensitisers (another group of the BH3-only proteins) facilitate apoptosis by disrupting the interactions between the anti-apoptotic members and the activators, thus liberating the activators to activate BAX and BAK (Figure 1.3) [106–109]

In the indirect model, the anti-apoptotic members are thought to interact with the effectors (BAX and BAK), which is disrupted by the BH3-only members to result in

apoptosis (Figure 1.3).[110–112] Later, a unified model has been proposed to integrate the pre-existing direct and indirect models to include three different "modes of action".[113] In mode 1 (derived from the direct model), anti-apoptotic members inhibit the function of the BH3-only members to prevent BAX and BAK activation. In mode 2 (derived from the indirect model), anti-apoptotic members interact and inhibit BAX and BAK. In a new mode 0, anti-apoptotic members mediate BAX translocation to mitochondria, thus affecting how BAX may interact with other BCL-2 family members to induce apoptosis (Figure 1.3).[7] The probability of these three modes to occur concomitantly is high, as the complexity of these molecules are still being uncovered.

1.6 The pro-apoptotic activators of the BCL-2 family of proteins

Three major proteins – BIM, BID and PUMA are categorised as pro-apoptotic factors of the BCL-2 family. Of these, BIM (BCL-2 interacting mediator of cell death) is a major player in apoptosis due to its ability to bind multiple members of the BCL-2 family of proteins (Figure 1.4). BIM expression is found altered in some malignancies such as lung cancers, which present low expression of BIM.[114–116] In addition, BIM deletions have been reported in mantle cell lymphoma.[117] BIM exists as three main different isoforms, extra-long (BIM_{EL}), long (BIM_L) and short (BIM_S). Under normal conditions, both BIM_{EL} and BIM_L are associated to microtubules, translocating to the OMM upon apoptotic stimuli,[17] while BIM_S is constitutively mitochondrial.[118] All these three isoforms of BIM present pro-apoptotic functions, interacting with all anti-apoptotic members of the BCL-2 family (Figure 1.4).[119]

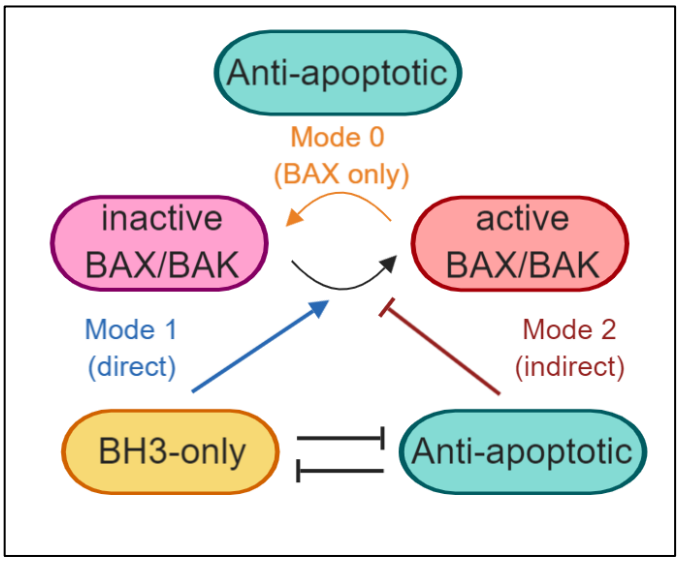

Figure 1.3. Models of interactions among the BCL-2 family members for the dictation of cell fate. Several models for the activation of BAX and BAK have been proposed. The direct model suggests that the activators of BCL-2 family activate the effectors BAX/BAK to induce apoptosis when not being repressed by the anti-apoptotic members. The indirect model proposes that the anti-apoptotic members interact with BAX/BAK, inhibiting their activation. The BH3-only proteins release this inhibition, inducing activation of the effectors. The unified model, encompasses the first two models, using modes as different ways for BAX and BAK being activated. Mode 1 derives from the direct model, mode 2 derives from the indirect model and a new mode 0, suggests that the anti-apoptotic members can prevent BAX retrotranslocation and activation in the OMM.

Unlike BIM, BID (BH3 interacting-domain death agonist), is cleaved by caspases 8 and 10 (in the extrinsic apoptotic pathway) to tBID, which facilitates BAX[120] and BAK[121] translocation to the OMM, thus serving as a mediator between the extrinsic and intrinsic pathways of apoptosis.[122–124] Normally cytosolic, BID translocates to OMM upon cleavage, binding preferentially to BCL-X_L and BCL-w, but BID also interacts with MCL-1 and BCL-2 to induce apoptosis (Figure 1.4).[17] BID expression has been found altered in different malignancies, such as gastric cancer, in which a frameshift mutation in *BID* promoted resistance to chemotherapy,[125] and in ovarian cancer, inhibition of BID expression led to resistance to TRAIL-induced apoptosis.[126]

In contrast to BIM and BID, PUMA (p53 upregulated modulator of apoptosis) is regulated by p53, which is the most mutated gene in cancer.[127] PUMA has been reported to be localised mostly in the cytosol and in the OMM to some extent,[17] interacting with all anti-apoptotic members of the BCL-2 family (Figure 1.4). PUMA expression in cancer is often dysregulated, either *via* p53 regulation or by other pathways. Furthermore, PUMA downregulation has been linked to chemoresistance in lung[128] and colorectal cancer.[129]

1.7 The pro-apoptotic sensitisers of the BCL-2 family of proteins

Five major proteins – BAD, HRK, NOXA, BIK and BMF are categorised as sensitisers in the BCL-2 family of proteins (Figure 1.4). Of these, BAD (BCL-2-associated agonist of cell death) is mainly localised in the cytosol, where it is bound to 14-3-3 proteins,[130] which in turn prevent BAD from binding to its anti-apoptotic counterparts BCL-2 and BCL-X_L.[17,131] Upon apoptotic stimuli, BAD is dephosphorylated and translocated to OMM to specifically inhibit BCL-2, BCL-X_L

and BCL-2, but not BCL-2A1 or MCL-1.[17,132] In cancer, BAD phosphorylation and overexpression was found to be associated with chemoresistance in ovarian[133] and prostate cancer.[134] Similar to PUMA, NOXA (also known as PMAIP, Phorbol-12-myristate-13-acetate-induced protein 1) is another BCL-2 family protein regulated by p53.[135] Both in normal and apoptotic conditions, NOXA is located in the OMM, where is binds exclusively with MCL-1 and BFL-1 (Figure 1.4). HRK (harakiri) interacts almost exclusively to BCL-X_L in the OMM.[17,90,136] HRK inactivation has been associated with reduced apoptosis in glioblastomas,[137] ovarian [138] and prostate cancer.[139] Localised mainly at the ER, BIK (BCL-2 interacting killer) plays important roles in breast cancer[140–142] and facilitates Ca^{2+} release from ER to mitochondria.[143,144] BMF (BCL-2 modifying factor) interacts with the cytoskeleton compartment, promoting apoptosis *via* stress in the cellular morphology and changes in the extracellular matrix.[145] Of the BCL-2 family members, BMF inhibits BCL-2 BCL-w and BCL-X_L (Figure 1.4).[17]

1.8 Targeting the BCL-2 family in cancer – BH3 mimetics

During the last 30 years, the study of cell death has become an important field of investigation in relation to cancer therapy. With the discovery of the BCL-2 family of proteins and the development of a deeper understanding of the mechanisms by which cells undergo apoptosis, researchers started to focus on identifying ways to disrupt the interactions between the anti- and pro-apoptotic BCL-2 family members to induce cell death in cancer cells. As the BH3-only proteins displace the anti-apoptotic members of the BCL-2 family from BAK/BAX to induce apoptosis, it was hypothesised that designing a compound that could occupy the BH3 domain of the anti-apoptotic BCL-2 family proteins could displace the pro-apoptotic BH3-only members or BAX/BAK to result in apoptosis. With that in mind, small molecule

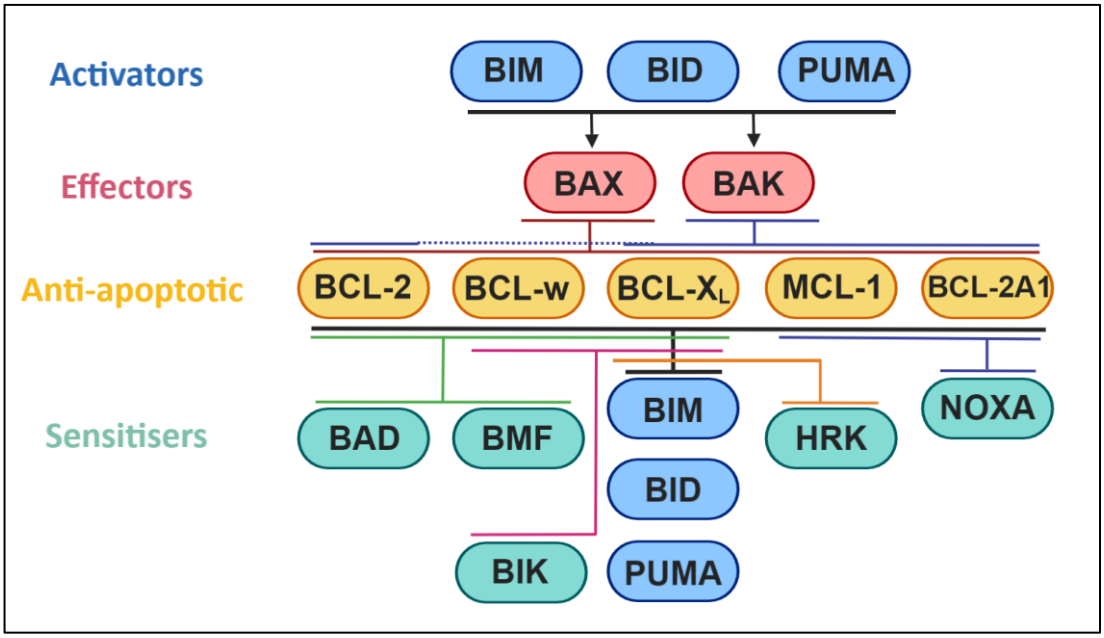

Figure 1.4 The network of interactions among the major BCL-2 protein family members. Anti-apoptotic BCL-2 family proteins (yellow) are proposed to interact with activators (blue), sensitisers (green) and effectors (red) of the BCL-2 family for the induction of apoptosis. The activators BIM, BID and PUMA are promiscuous and can interact with all major anti-apoptotic members, while the sensitisers perform specific interactions with different anti-apoptotic members. For instance, NOXA can only bind to MCL-1 and BCL-2A1, while BAK strongly interacts with all major anti-apoptotic members but BCL-w. Full lines represent a strong interaction between different proteins and dashed lines represent no interaction (used only for graphical purposes). Note that some of these interactions were observed *in vitro* and need to be further assessed *in vivo*.[17,90,91]

inhibitors called BH3 mimetics were developed. Early attempts to generate specific and potent BH3 mimetics were not highly successful, as most putative inhibitors were ineffective at low concentrations and required high micromolar concentrations to induce apoptosis. Moreover, apoptosis induced as a result appeared to occur in a BAX/BAK-independent manner, thus making the inhibitors both ineffective and toxic.[146–149] Continuous efforts to develop promising BH3 mimetics carried on, which led to the development of the first *bona fide* BH3 mimetic called ABT-737.

Developed by Abbot Laboratories (now AbbVie Inc.), ABT-737 was initially discovered by screening of a compound library to identify small molecules capable of binding to the BH3 groove of BCL-X_L.[150] From the screen, were selected two distinct molecules that exhibited binding affinities, similar to that of BH3-only peptides, to BCL-X_L.[151] By substituting regions and linking proximal fragments of these two molecules, the newly generated structure showed improved affinity with BCL-X_L, which was further enhanced by subsequent structural modifications to reduce serum binding. After a final modification, to promote better binding to BCL-2, ABT-737, with a chemical structure similar to that of the BH3-only protein BAD, was generated.[150] Similar to BAD, ABT-737 is capable of binding and inhibiting BCL-2, BCL-X_L and BCL-w, and it was shown to singlehandedly induce apoptosis in haematological malignancies and solid tumours at nanomolar concentrations in cell lines and in xenograph mice models.[150] To this date, there are approximately 700 publications in PubMed exploring the effects of ABT-737. However, despite its high potency and specificity, ABT-737 did not present good prospects to be employed as a therapeutic agent due to its poor oral bioavailability and low aqueous solubility, rendering the clinical translatability of ABT-737 challenging. For that reason a new

compound, ABT-263, which is both structurally similar to ABT-737 and also orally available and equally potent, was generated in 2008.[149]

ABT-263 (also known as Navitoclax) like ABT-737, binds and inhibits BCL-2, BCL-X_L and BCL-w promoting effective cytochrome *c* release and apoptosis in solid tumours and haematological malignancies in a BAX/BAK-dependent manner.[149] In addition, ABT-263 is also effective in reducing tumour burden in mice xenograph models at clinically relevant doses.[149] Soon after its discovery, ABT-263 was extensively investigated in approximately 400 studies, with many of these highlighting an obstacle to the employment of ABT-263 in cancer therapy. Patients administered with ABT-263 demonstrated thrombocytopenia, which was later identified to be due to enhanced platelet apoptosis, as platelets depend on BCL-X_L for survival and ABT-263 by also inhibiting BCL-X_L resulted in on-target toxicity.[152,153] This undesired toxicity threatened the potential of ABT-263 to be used in the clinic and led to the development of another BH3 mimetic by AbbVie in 2013, called ABT-199.

Also called Venetoclax, ABT-199 was developed to specifically inhibit BCL-2 to be used in CLL, as the malignancy is highly dependent on BCL-2 for survival.[154,155] The success of ABT-199 as a therapeutic compound started to rise when it was shown to induce apoptosis in several BCL-2-dependent malignancies and in non-Hodgkin's lymphoma cell lines.[154,155] Furthermore, *in vivo* studies with xenograph mice models have shown that ABT-199 can be used in combination with other agents to reduce chemoresistance and remission.[155] Since its development, ABT-199 has been investigated in approximately 600 publications and 200 clinical trials. Furthermore, it has recently been approved by the FDA for the treatment of refractory CLL[156] and is currently being trialled in other malignancies, such as

AML,[157] multiple myeloma[158,159] and non-Hodgkin's lymphoma[160] In addition to AbbVie, other pharmaceutical companies have also been developing BCL-2 inhibitors. In 2018, Servier released a new BH3 mimetic called S55746 (or BCL201), which is specific for BCL-2, orally active and induces apoptosis in a BAX/BAK-dependent manner at nanomolar concentrations in CLL and mantle cell lymphoma patients.[161] Moreover, S55746 interacts with a different binding pocket of BCL-2 than ABT-199, which could be beneficial in the case of development of resistance due to mutations in BCL-2.[161] S55746 has been, so far, used in 2 clinical trials (Clinicaltrials.gov; identifiers NCT02920697 and NCT02603445).

After the successful development of ABT-263 and ABT-199, efforts have been focused on the inhibition of other anti-apoptotic members of the BCL-2 family. In case of BCL-X_L inhibition, several compounds were released by different companies. The first of them, WEHI-539, came from the Walter and Elisa Hall Institute of Medical Research.[162] The compound presented nanomolar affinity for BCL-X_L and induced apoptosis in a BAK-dependent manner in MCL-1-defficient mouse embryonic fibroblasts.[162] As expected from a strong BCL-X_L inhibitor, WEHI-539 induced high levels of apoptosis in platelets. One year later, AbbVie released two BCL-X_L inhibitors, A-1155463[163] and A-1331852[164] which interacted with BCL-X_L at nanomolar concentrations. Of these two compounds, A-1331852 performed better, being 50-fold more potent than A-1155463, while still being orally available.[164] Up until this date, both WEHI-539 and A-1331852 have been reported in 15 publications according to PubMed. No clinical trials have been carried out so far using these compounds.

With the development of specific and potent BCL-2 and BCL-X_L inhibitors, MCL-1 emerged as the next protein to be targeted. However, the development of a

reliable inhibitor for MCL-1 has been a challenge. As previously mentioned, MCL-1 has molecular characteristics that differ from the other anti-apoptotic members of the BCL-2 family. These include a more rigid conformation of its hydrophobic binding groove and a higher affinity to its BH3-only protein binding partners.[165] In spite of these difficulties, AbbVie successfully developed the first MCL-1 inhibitor, A-1210477,[166] which specifically displaced ligands from the binding groove of MCL-1, inducing apoptosis in MCL-1-dependent cell lines. Furthermore, A-1210477 was shown to synergise with ABT-263 to promote cell death in multiple cancer cell lines.[166] However, A-1210477 was only effective *in vivo* at micromolar concentrations, curbing its potential for translation into clinical trials.[166] Since the release of A-1210477, other companies have started to release their own MCL-1 inhibitors. In 2018, Amgen Inc. released AMG-176, a compound with picomolar affinity for MCL-1, capable of promoting rapid apoptosis in several haematological cancer cell lines, patient samples and tumour xenograft mouse models.[167] In addition, AMG-176 presented synergy with other BH3 mimetics, such as Venetoclax.[167] Due to its high specificity to MCL-1 and good success in reducing tumour burden *in vivo*, AMG-176 is currently being used in 2 clinical trials to treat relapsed or refractory multiple myeloma as well as AML, non-Hodgkin lymphoma and diffuse large B-cell lymphoma in combination with venetoclax (Clinicaltrials.gov; identifiers NCT03797261 and NCT02675452). Servier also released their MCL-1 inhibitor, S63845, soon after the initial A-1210477 publication. S63845, has been shown to effectively bind to the BH3 groove of MCL-1 to induce rapid apoptosis, in a BAX/BAK-dependent manner, at nanomolar concentrations in several cell lines and in mouse models of haematological malignancies, while being well tolerated in mice at efficacious doses.[168] Until now, S63845 has been reported in approximately 20

publications, some of which have demonstrated that S63845 can be potentially used in combination with other chemotherapeutic agents in various cancers, such as breast cancer[50] and AML.[169]

Despite the successful development of specific and potent BH3 mimetics, it is not surprising that limitations of their use are starting to emerge, as the knowledge about these compounds increases. Indeed, the development of resistance to ABT-199 has been reported in haematological malignancies, which has been attributed to overexpression of MCL-1 or BCL-X_L[170,171] and to downregulation or mutations in BCL-2.[172,173] As mentioned before, a marked limitation of BCL-X_L inhibition is the development of thrombocytopenia, due to its crucial role in the survival of platelets.[152,153] The limitations of inhibiting MCL-1 arise from the great diversity of functions that MCL-1 and its isoforms appear to regulate.[62,174] Furthermore, MCL-1 is highly expressed in cardiomyocytes, which could increase toxicity. For instance, genetic knockout of MCL-1 in mice has showed pronounced cardiotoxicity, which is linked to MCL-1 involvement in mitochondrial bioenergetics.[175,176] However, the recently developed BH3 mimetics were shown to be highly potent and specific, with great potential for being used in the clinic, especially in lower concentrations. Furthermore, the use of BH3 mimetics in combination with existing therapy can potentially lower toxicity, while targeting diverse pathways for a more effective induction of apoptosis.

1.9 Aims of the study

The anti-apoptotic members of BCL-2 family of proteins are often overexpressed in cancer. During the last ten years, efforts to generate molecules to inhibit these anti-apoptotic proteins have been successful with the development of potent and specific BH3 mimetics, which have been successfully used in treating patients with CLL, as well as investigated in experimental models of myelomas, lymphomas, breast, ovarian and colorectal cancers.[177] In this study, it was intended to extend this knowledge to AML and to two hard-to-treat solid tumours, such as HNSCC and PDAC. In addition, despite the mechanistic understanding of how BH3 mimetics exert their functions at the molecular level, a deeper understanding on how BH3 mimetics can affect other facets of the apoptotic pathway, such as mitochondrial membrane dynamics remains elusive. Therefore, this study aims:

1. To investigate the potential of BH3 mimetics in enhancing the effectiveness of current treatments in CML and AML.
2. To assess the potential of BH3 mimetics in enhancing the effectiveness of current treatments in head and neck and pancreatic cancer.
3. To examine whether BH3 mimetics induce mitochondrial structural changes, either upstream/downstream/independent of the apoptotic cascade and how such structural perturbations could relate to apoptosis.
4. To investigate the involvement of endoplasmic reticulum in BH3 mimetic-mediated apoptosis and mitochondrial structural changes.

CHAPTER 2

MATERIALS AND METHODS

Chapter contents

2.1 Cell culture

All cells were obtained from American Type Culture Collection (ATCC, Manassas, VA, USA) or from *Deutsche Sammlung von Mikroorganismen und Zellkulturen* (DSMZ, Braunschweig, Germany), unless otherwise specified in Table 2.1. Cells were grown in appropriate cell culture media obtained from Life Technologies Inc (Paisley, UK) and supplemented with 10% foetal bovine serum (FBS) (Table 2.1). Cells were grown at 37°C, 5% CO_2 until they reached ~80% confluence. Sub-culturing adherent cell lines was carried out by aspirating the spent media, washing with warmed PBS (ThermoFisher Scientific, MA, USA) and then incubating with 0.05% trypsin-EDTA (Gibco, ThermoFisher Scientific) at 37°C for 5 min. Trypsinised cells were collected and then distributed into multiple plates. Suspension cell lines had media changed every 48 - 72 h.

Primary CML and AML patient samples were obtained from Liverpool Biobank and approved by the Liverpool Central Ethics Committee. All patients gave informed consent. Patient mononuclear cells from chronic phase CML were separated by density-dependent centrifugation (Lymphoprep Axis-Shield, Oslo, Norway), then washed in RPMI 1640 and resuspended in 10% dimethyl sulfoxide (DMSO), 10% FBS in RPMI at 4°C and cryopreserved in liquid nitrogen. Cells were cultured with StemSpan SFEMII media (Stemcell Technologies, Cambridge, UK). Primary AML patient samples were thawed by adding 4 ml of IMDM complete media (Gibco, ThermoFisher Scientific) supplemented with 10% FBS, 1% penicillin/streptomycin and 1% L-glutamine Sigma-Aldrich/Merck (Darmstadt, Germany) dropwise over 3 minutes. Further 8 ml of IMDM media was added over 3 more minutes. Cells were centrifuged at 2000 rpm for 5 minutes and pellet resuspended in IMDM media for culture.

2.2 Cell lines

Table 2.1 – Cell lines, growing media and additional information. "NSCLC" stands for non-small cell lung carcinoma, "AML" stands for acute myeloid leukaemia, "CML" stands for chronic myeloid leukaemia, "MCL" stands for mantle cell lymphoma, "MM" stands for multiple myeloma, "BC" stands for breast cancer, "CEC" stands for cervical carcinoma, "PC" stands for pancreatic carcinoma, "PDAC" stands for pancreatic adenocarcinoma, "SCC" stands for squamous cell carcinoma, "COC" stands for colon carcinoma. "RPMI" stands for Roswell Park Memorial Institute (RPMI) 1640, "HCM" stands for Hybri-Care medium (ATCC 46-X), "EMEM" stands for Eagle's minimum essential medium, "DMEM" stands for Dulbecco's modified Eagle Medium, "MC5A" stands for McCoy's 5A Modified. "NEAA" stands for non-essential amino acids, "BME" stands for 2-mercaptoethanol. All culture media were supplemented with 10% FBS (Gibco, ThermoFisher Scientific).

Cell line	Tumour origin	Culture media	Source
H1299	NSCLC	RPMI	ATCC
H23	NSCLC	RPMI	ATCC
MV-4-11	AML	RPMI	ATCC
OCI-AML3	AML	RPMI	ATCC
HL-60	AML	RPMI	ATCC
U937	AML	RPMI	ATCC
THP-1	AML	RPMI	ATCC
MOLM-13	AML	RPMI	ATCC
K562	CML	RPMI	Prof. R. Clark (University of Liverpool)
KCL22	CML	RPMI	
MAVER-1	MCL	RPMI	Dr. J. Slupsky (University of Liverpool)

H929	MM	RPMI + 0.02% BME	ATCC
AU565-A	BC	RPMI	Prof. C. Palmieri (University of Liverpool)
HCC1937D	BC	RPMI	
BT-474	BC	HCM+1.5 g/L $NaHCO_3$	
HCC70	BC	RPMI	Prof. P. Meier (Institute of Cancer Research)
MCF7	BC	EMEM + 1% NEAA	ECCAC
HeLa	CEC	DMEM	ATCC
MIA PaCa-2	PC	DMEM	Prof. B. Greenhalf (University of Liverpool)
BxPC-3	PDAC	DMEM	
PANC-1	PC	DMEM	Dr. A. Mielgo (University of Liverpool)
UM-SCC-1	oral cavity SCC	DMEM + 1% NEAA	Prof. T. Carey (University of Michigan, USA)
UM-SCC-11B	laryngeal SCC	DMEM + 1% NEAA	
UM-SCC-17A	laryngeal SCC	DMEM + 1% NEAA	
UM-SCC-17AS	laryngeal SCC	DMEM + 1% NEAA	
UM-SCC-74A	tongue SCC	DMEM + 1% NEAA	
UM-SCC-81B	tonsillar SCC	DMEM + 1% NEAA	
HCT116 WT and DKO	COC	MC5A	Dr. X. Luo (University of Nebraska, USA)
SW48	COC	MC5A	Prof. I. Prior (University of Liverpool)

2.3 Reagents and compounds

Reagents, chemicals and buffers, were obtained from Sigma-Aldrich/Merck (Darmstadt, Germany) unless otherwise specified. Compounds used are indicated in Table 2.3.

Table 2.3 – Compounds, targets and sources. Selleck stands for Selleck Chemicals Co (Houston, TX, USA), Abbvie stands for Abbvie (Chicago, IL, USA), AB stands for Active Biochem (New Jersey, USA), Stratech stands for Stratech Scientific Ltd. (Suffolk, UK), Sigma stands for Sigma-Aldrich/Merck (Darmstadt, Germany).

Inhibitor	Target	Source
ABT-199	BCL-2	Selleck
ABT-737	BCL-2, BCL-X_L, BCL-w	Selleck
A-1331852	BCL-X_L	Abbvie
A-1210477	MCL-1	Abbvie
S63845	MCL-1	Selleck
MG-132	Proteasome	AB
Z-VAD-FMK	Caspases	Selleck
Dinaciclib	Cyclin-dependent kinases	Stratech
CCCP	Mitochondria	Sigma
Cisplatin	DNA (alkylating agent)	Selleck
Gemcitabine	DNA (anti-metabolite)	Selleck
Imatinib	Tyrosine-kinase	Selleck
Nilotinib	Tyrosine-kinase	Selleck
Dasatinib	Tyrosine-kinase	Selleck

2.4 Antibodies

Table 2.4 – Antibodies specifications. Clone numbers (brackets, when available), epitopes, applications, sources and catalogue numbers of antibodies used. "AA" stands for Amino acids, "IB" stands for immunoblotting, "ICC" stands for immunocytochemistry, "IF" stands for immunofluorescence, "IHC" stands for immunohistochemistry, "IP" stands for immunoprecipitation, "SC" stands for Santa Cruz Biotechnology (CA, USA), "CST" stands for Cell Signalling Technologies (MA, USA), Abcam (Cambridge, UK), "BD" stands for BD BioSciences (CA, USA), "MP" stands for Millipore/Merck (Darmstadt, Germany), "Enzo" stands for Enzo Biochem. Inc (NY, USA), "Calbio" stands for Calbiochem Research Biochemicals (now Merck), "Upstate" stands for Upstate USA Inc (NY, USA).

Antibody	Epitope	Application	Source	Cat. #
BCL-2 family				
BCL-2	N/A	IB	CST	4223
BCL-2 (124)	AA 41-54	IHC	CST	15071
BCL-X_L	Around Asp61	IB and IHC	CST	2762
BCL-X_L (E-18]	AA 1-100	IP	Abcam	ab32370
MCL-1 (S-19)	AA 89-139	IB	SC	sc-819
MCL-1 (Y-37)	AA 100-200	IP	Abcam	ab32087
MCL-1 (D5VL5)	Around L210	IHC	CST	39224
BCL-w (31H4)	Around Ala39	IB	CST	2724
BIK (N-19)	N-terminal	IB	SC	sc-1710
BFL-1	Custom-made	IB	Gift from J. Borst	N/A
PUMA	C-terminal	IB	CST	4976
BIM (C34C35)	Around Pro25	IB	CST	2933
BAD	Around Ser112	IB	CST	9292
BMF	Around Gly81	IB	CST	5889
HRK	AA 30-50	IB	SC	sc-6971

NOXA (114C307)	FL protein	IB	Calbio.	OP180
BID	Cleavage site	IB	CST	2002
BAK (AB-1)	Active Site	IF (FACS)	Calbio.	AM-03
BAK	Internal	IB	SC	sc-832
BAX (C3)	AA 55-178	IB	BD	610983
Apoptosis				
Cytochrome *c*	Around AA 62	ICC and IB	BD	556432
Caspase-3	N/A	IB	CST	9662
Cleaved caspase-9	Around Asp315	IB	CST	9505
Caspase-7	FL protein	IB	CST	9494
Cleaved PARP (D64E10)	Around Asp214	IB	CST	5625
Mitochondrial fusion and fission				
DRP-1 (8/DLP-1)	AA 601-722	IB and ICC	BD	611113
DRP-1 S616	Around Ser616	IB	CST	3455
DRP-1 S367	Around Ser637	IB	CST	4867
MFN1 (D6E2S)	C-terminal	IB	CST	13196
MFN2 (D2D10)	Around Val573	IB	CST	9482
OPA-1 (18/OPA1)	AA 708-830	IB	BD	612607
Endoplasmic reticulum shaping proteins				
RTN-1	AA 159-208	IB	Abcam	ab83049
RTN-4	AA 1-50	IB	Abcam	ab47085
LNP-1	AA 304-426	IB	Sigma	HPA014205
CLIMP-63 (G1/296)	N/A	IB	Enzo	ALX-804-604
Miscellaneous				
Tubulin (6-11B-1)	Around Lys40	IB	Abcam	ab24610
GAPDH (FL-335)	AA 1-335	IB	SC	sc-25778
HSP70 (JG1)	AA 661-679	ICC	Abcam	ab2799

2.5 RNA interference

siRNAs (small interfering RNA oligoduplexes) obtained from Qiagen (Cambridge, UK) or Ambion (Austin, TX, USA) were transfected in cells at a final concentration of 10 nM, using OptiMEM Reduced Serum Media (Life Technologies) and Interferin transfection reagent (Polyplus, Illkirch, France).

Table 2.5 – siRNAs targets, catalogue numbers, source and target regions. siRNA catalogue number with source between brackets and the sequence targeted. (Q) stands for Qiagen and (A) stands for Ambion obtained siRNAs.

Protein targeted	Cat. # (source)	Sequence Targeted
BCL-X_L	SI03025141 (Q)	TTGGCTTTGGATCTTAGAAGA
MCL-1 (#1)	SI02781205 (Q)	CCCGCCGAATTCATTAATTTA
MCL-1 (#2)	S102781205 (Q)	CCCGCCGAATTCATTAATTTA
BAX	1299001 (A)	CCCACCAGCUCUGAGCAGAUCAUGA
BAK	4390824 (A)	GGUUUUCCGCAGCUACGUUTT
BIM	4427038 (A)	CAUGAGUUGUGACAAAUCATT
BID	S102654568 (Q)	TAGGGACTATCTATCTTAATA
PUMA	4390828 (A)	GGAUAGGUUGCAGUCCAUCTT
NOXA	SI00129430 (Q)	TGGGCTATATACAGTCCTCAA
HRK	4427037 (A)	GAGCGAUCGUAGAAACACATT
BMF	16104 (A)	GCUAAGUGACUUUUAGAGUTT
BIK	4390824 (A)	GGACUUCGAUUCUUUGGAATT
BAD	SI00299348 (Q)	ACGAGTTTGTGGACTCCTTTA
BCL-w	4390824 (A)	CAGACUUUGUAGGUUAUAATT
BFL-1	AM16104 (A)	GAGTTCATAATGAATAACACA
DRP-1	S104274235 (Q)	CACGGTGGGCGCCGACATCAT
DRP-1	SI02661365 (Q)	CAGGAGCCAGCTAGATATTAA
OPA-1	SI03019429 (Q)	CCGGACCTTAGTGAATATAAA
RTN-1	SI04178545 (Q)	CACGGACTGCCTGCAGTTCTA
RTN-4	4392420 (A)	CCAUCAGCUUUAGGAUAUATT
RTN-4	s32767 (A)	GGCCACCCGGGGAGTACCCA
LNP-1	SI00460355 (Q)	CACGATGTTCTTGATGATAAT
CLIMP-63	SI00347242 (Q)	CCAAGTGGAGGCGGACTTGAA
CLIMP-63	4427037 (A)	CTCTTCAAATCAGGCAACTTCCA
Non-targeting control	1027310 (Q)	AACTGGGGGAGGATTGTGGCC

2.6 Overexpression studies

For transient transfections of DRP-1 K38A plasmid (gift from Dr. E. Bampton, University of Leicester), cells were seeded at a determined density to reach 80% of confluency in 3-4 days. On the day after seeding, cells were transfected using TransIT-LT-1 transfection reagent (Mirus Bio LLC, Madison, WI, USA) in a 3:1 ratio (DNA:LT-1) with 10% of final media volume of OptiMEM serum free media. Transfection rates were observed in an EVOS FLoid Cell Imaging Station (ThermoFisher Scientific, MA, USA) under the green channel.

2.7 Immunoblotting (SDS-PAGE)

Immunoblotting was performed using acrylamide gels made in-house with Protogel acrylamide (30%) (National Diagnostics, Atlanta GA, USA), lower gel buffer (1.5 M Tris-HCL, 0.4% SDS, pH 8.8), upper gel buffer (Tris-HCL 0.5 M, 0.4% SDS, pH 6.8), 10% ammonium persulphate and TEMED. Cells were collected, centrifuged and pellets were lysed in radioimmunoprecipitation assay (RIPA) buffer (10 mM Tris-Cl (pH 8.0), 1 mM EDTA, 0.5 mM EGTA, 1% Triton X-100, 0.1% sodium deoxycholate, 0.1% SDS, 140 mM NaCl) with 20 µM MG-132 and one protease inhibitor tablet (Roche, Basel, Switzerland). For lysis, cells were incubated on ice for 15 min in RIPA lysis buffer and sonicated with a Bandelin SONOPULS ultrasonic homogeniser (Bandelin, Berlin, Germany). Colorimetric Bradford assay (BioRad Protein Assay Dye Reagent, BioRad, CA, USA) was used to determine protein concentration. Samples optical density at 600 nm (OD600) were measured with a spectrophotometer (Eppendorf, Hamburg, Germany) and standardised with a solution of bovine serum albumin (BSA) which concentration was pre-determined to obtain samples protein concentrations.

Protein lysates with concentrations ranging from 10-50 µg were added to 4x NuPAGE LDS sample buffer (Life Technologies) and boiled for 5 min at 70°C (ThermoFisher Scientific). Samples were loaded in acrylamide gels alongside 5 µl of protein ladder SeeBlue™ Plus2 Pre-stained Protein Standard (ThermoFisher Scientific) and subjected to SDS-PAGE in electrode buffer (25 mM Tris-HCL, 192 mM glycine, 10% SDS) at 130 V for 100 min and then transferred to Amersham ProTran nitrocellulose membranes (VWR, Radnor, PA, USA) in transfer buffer (25 mM Tris-HCL, 192 mM glycine, 20% methanol) at 100 V for 90 min. Membranes were blocked in non-fat 5% milk in TBS-T (Tris-buffered saline with 0.1% Tween, 20 mM Tris-HCL, 150 mM NaCl, 0.1% Tween-20) for 30 min, incubated overnight at 4°C with the indicated primary antibodies, with a 1:1000 dilution in TBS-T. Next, membranes were rinsed with TBS-T and incubated with anti-mouse or anti-rabbit IgG HRP-linked secondary antibodies (Cell Signalling Technology) for 1 h, then washed three times in TBS-T before revealing of protein bands with ECL reagents (GE Healthcare, IL, USA) either by X-ray film (GE Healthcare) or via ChemiDoc Imaging system (BioRad).

2.8 Immunoprecipitation

Protein G Dynabeads (ThermoFisher Scientific) (30 µl/sample) were washed three times with PBS-T (0.05% Tween-20 in PBS) and resuspended with 5 µg of antibody against BCL-X_L or MCL-1 (see Table 2.4). Beads with antibodies were incubated under rotation for 4 h at 4°C, followed by two washes with triethanolamine (0.2 M). Beads were crosslinked to antibodies using dimethylpimelidate (5.4 mg/ml) at room temperature for 30 min. Crosslinking reaction was neutralised with Tris-HCL pH 7.5 (50 mM) at room temperature for 15 min. Beads-antibody conjugates

were washed three times with PBS-T and resuspended in 500 µg of cell lysate for a total volume of 100 µl per sample.

Cells were collected, centrifuged and lysed in 1% CHAPS lysis buffer (150 mM KCl, 50 mM HEPES (pH 7.4), 1% CHAPS) added with 20 µM MG-132 and a protease inhibitor tablet (Roche, Basel, Switzerland) for 1 h on ice and centrifugated at 14,000 RPM for 10 min at 4°C. 500 µg of protein from the supernatant was incubated overnight with beads-antibody conjugate, under rotation at 4°C. Beads were collected, washed three times with PBS-T and protein was eluted from beads using 2x NuPAGE LDS sample buffer (Life Technologies) at 55°C for 10 min under constant shaking. Samples were loaded into gels for immunoblotting analysis of protein levels. A lane with bead control (beads with no antibody) was added to assess for antibody specificity.

2.9 Clonogenicity assay

Cells were seeded at a 500, 1000 or 2000 cells per well of a 12 well plate and monitored daily for the formation of colonies. On the first day after seeding, cells were exposed to different compounds used throughout the studies. Upon reaching ~50 cells per colony (at around day 7) cells were washed with PBS, fixed with fixing solution (1:7 v/v ratio acetic acid to methanol) for 5 min at room temperature and stained with staining solution (20 ml methanol, 80 ml H_2O, 0.5 g crystal violet) for 2 h at room temperature. Next, cells were de-stained under running water and left for drying for 1 day. Colonies were counted using a GelCount instrument (Oxford Optronix, Oxford, UK). Surviving fraction was determined by the following equation:

$$Surviving\ fraction = \frac{\#colonies\ formed}{\#cell\ seeded}\ x100$$

2.10 Tissue micro array analysis

Tissue micro array (TMA) slides were obtained from Liverpool Biobank, (University of Liverpool). TMA analysis was performed using QuPath software.[178] Electronic scans of TMAs were uploaded to the software and the basic wizard protocol was used to assess for the intensity of staining of BCL-2, BCL-X_L and MCL-1 in the tissues and H-scores were obtained from the final analysis. H-score values were then used in conjunction with patient data to generate Kaplan-Meier estimators.

2.11 Flow cytometry - apoptosis

Suspension cells were collected directly in tubes, washed and pelleted, while adherent cells were trypsinised and washed in PBS before being pelleted. Cell pellets were resuspended in 500 µl of 1x Annexin Binding Buffer (10 mM HEPES, 140 mM NaCl, 2.5 mM $CaCl_2$, pH 7.4) with Annexin-V-FITC (1:20,000 dilution, made in-house) and incubated at room temperature for 7 min. 5 µl of propidium iodide (PI) (Sigma-Aldrich/Merck, Darmstadt, Germany) was added to cell suspension just before analysis. For assessment of the extent of Annexin-V/PI labelling, cells were passed through an Attune NxT flow cytometer (ThermoFisher) using the red and blue lasers for PI and Annexin V staining respectively. 10,000 events per sample were recorded and a minimum of 3 replicates were assessed for each experiment.

2.12 Flow cytometry – BAK activation

BAK activation by FACS was performed by collecting cells and fixing them with 2% paraformaldehyde (PFA) at room temperature for 10 min. Fixed cells were washed with PBS and re-suspended in FACS buffer (0.1% saponin, 0.5% BSA in PBS) for 10 min. Primary antibody anti-BAK AB-1 (0.1 mg/ml) was added to the

cells at a volume FACS buffer and cells were incubated for 1 h at 4°C. Cells were pelleted by centrifugation and goat-anti-mouse IgG-AlexaFluor-488 conjugated secondary antibody was then added to cells in FACS buffer and incubated for 1 h at 4°C. The extent of BAK activation was detected by flow cytometry using a blue (BL1) laser (530/30 nm emission filter) as recommended for AlexaFluor-488 secondary antibodies.

2.13 Immunocytochemistry

Cells were seeded on sterile coverslips in a 24 well plate to reach 80% confluency by the day of treatment and fixation. On the determined day, media was removed from wells and coverslips were washed with PBS twice. Cells were fixed with 4% (w/v) paraformaldehyde for 10 min at room temperature and permeabilised in 0.5% (v/v) Triton X-100 in PBS for 10 min at room temperature. Coverslips were removed from wells and incubated in a humidified chamber with primary antibody diluted in 3% BSA in PBS for 1 h. Next, coverslips were incubated with species-specific AlexaFluor (Life Technologies) secondary antibody diluted 1:1000 in 3% B BSA in PBS. Next, coverslips were washed in dH_2O three times, dried with lint-free paper towels and mounted in glass slides with Polymount (Polysciences, PA, USA) mounting solution. Finally, cells were imaged in a 3i Marianas spinning disk confocal microscope, fitted with a Plan-Apochromat × 63/1.4 NA Oil Objective, M27 and a Hamamatsu ORCA-Flash4.0 v2 sCMOS Camera (Intelligent Imaging Innovations, GmbH, Gottingen, Germany). For quantitation of mitochondrial fragmentation using HSP70 antibody, only cells with fine punctate mitochondrial staining were considered as having fragmented mitochondria.

2.14 Immunohistochemistry

Explants, surgically resected from patients, were acclimatized overnight to the culture conditions before exposure to BH3 mimetics for 48 h. Explants were fixed in 4 % paraformaldehyde at 4 °C for 24 h and processed using a HistoCore PEARL Tissue Processor (Leica). Following paraffin embedding, tissues were cut into 5 μm sections. Sections from TMAs were processed and stained using the Bond RXm autostainer (Leica). TMA sections were deparaffinised, subjected to heat induced epitope retrieval and incubated with the relevant primary antibodies and a non-species-specific linker and HRP, which was detected using DAB+ chromogen. Sections were counterstained with hematoxylin, dehydrated, cleared and mounted using EcoMount (Biocare Medical). Images were acquired at 20x magnification using a Nikon Eclipse E800 microscope and MetaMorph 6.3r7 software or by scanning at 40x magnification using an Aperio slide scanner (Leica). Antibody staining intensity was analyzed using QuPath software.[178] The cytoplasmic DAB optical density was measured for each tumor cell within a tissue sample, and a histo-score (H-score; a quantitative measurement of the intensity of staining for a particular antibody) generated for that sample. The H-score was averaged between two or three tissue samples available per patient and thresholds applied to designate each patient's overall H-score as low, moderate or high for the appropriate antibody. Explant staining was quantified by counting the HNSCC nuclei in each image and determining the percentage of positively stained cells.

2.15 Transmission Electron Microscopy

Cells were fixed in 2.5% (w/v) glutaraldehyde and 2 mM calcium chloride in 0.1 M cacodylate buffer (pH 7.4), followed by heavy metal staining, consisting of

two consecutive osmium tetroxide steps (2% (w/v) OsO4 in ddh2O), followed by 1% (w/v) aqueous uranyl acetate. All fixation and staining steps were performed in a Pelco Biowave®Pro (Ted Pella Inc., Redding, California, USA) at 100w 20Hg, for 3 min and 1 min, respectively. Dehydration steps were conducted in a graded ethanol series before filtration and embedding in medium premix resin (TAAB, Reading, UK). 70- 74 nm serial sections were cut using a UC6 ultra micro- tome (Leica Microsystems, Wetzlar, Germany) and collected on Formvar (0.25% (w/v) in chloroform (TAAB, Reading, UK) coated Gilder 200 mesh copper grids (GG017/C; TAAB, Reading, UK). Images were acquired using a 120 kV Tecnai G2 Spirit BioTWIN (FEI, Hillsboro, Oregon, USA) with a MegaView III camera and analySIS software (Olympus, Germany).

2.16 Serial block face scanning electron microscopy (3view microscopy)

Cells were fixed in 2.5% (w/v) glutaraldehyde with 2 mM calcium chloride in 0.1 M cacodylate buffer (pH 7.4). Heavy metal staining consisted of reduced osmium (2% (w/v) OsO4, 1.5% (w/v) potassium ferrocyanide in ddh2O), 1% (w/v) thiocarbohydrazide (RT), 2% OsO4 (w/v in ddh20), then 1% (w/v) aqueous uranyl acetate overnight at 4°C. The next day cells were stained with Walton's lead aspartate (0.02 M lead nitrate, 0.03 M aspartic acid, pH 5.5) at RT. Fixation and staining steps were performed in a Pelco Biowave®Pro (Ted Pella Inc.Redding California, USA) at 100 w 20 Hg, for 3 mins and 1min respectively. Dehydration was performed in a graded series of ethanol before filtration and embedding in hard premix resin (TAAB, Reading, UK). Images were obtained from Gatan 3View serial block-face system (Gatan, Pleaseanton, CA) installed on a FEI Quanta 250 FEG scanning electron microscope (FEI Company, Hillsboro, OR). Each z-section had a thickness of 75 nm and the images had a resolution of ~20 nm. Images were double

binned for faster render and were processed, analysed and quantified using Thermo Scientific Amira Software 6. For quantification of ER-mitochondria contact points, we considered the number of times that an ER membrane overlapped with a mitochondrial membrane in the same 3D reconstruction for the chosen mitochondrion.

2.17 Synergy studies

Synergistic analysis was carried out using a multiple-ray experimental design with a fixed order of magnitude increase between the assessed compounds. Cell death output from FACS analysis was fed to the Combenefit[179] software to generate a *Bliss Independence* score heatmap. Bliss Independence scores range from -100 to 100, representing at -100, antagonistic effects, at 0, additive effects and at 100, synergistic effects for the combination of the two compounds tested.

2.18 Statistics

Two-way ANOVA was performed for studies using two numerical variables. For studies involving a single numerical variable, one-way ANOVA was performed. Multiple comparison tests were conducted using Fisher's LSD test. For continuous variables, Mann-Whitney *U*-test was used to compare independent samples. For estimation of survival function from lifetime data, Kaplan-Meier estimator was used. Asterisks depicted correspond to the following p values: * for $p \leq 0.05$, ** for $p \leq 0.005$ and *** for $p \leq 0.001$.

CHAPTER 3

Evaluating the potential of BH3 mimetic therapy in haematological malignancies

Chapter contents

3.1 Introduction

Chronic myeloid leukaemia (CML) is a disorder that arises from the myeloid lineage of haematopoietic stem cells. The disease is characterised by abnormal growth and accumulation of granulocytes and their precursors in the bone marrow. In a typical case, the disease begins at the chronic phase, which comprises around 85% of diagnosed patients. In the absence of successful treatment, the disease can evolve to the accelerated phase, characterised by a gradual increase (10-20%) of immature blast cells in peripheral blood. This signals for rapid disease progression and imminent transition to blast crisis (with blast cell count in peripheral blood >20%).[180] Blast crisis is the last phase of CML, progressing rapidly and ultimately leading to bone marrow failure by massive undifferentiated cell infiltration.

The main genetic feature of CML is a reciprocal chromosomal translocation between chromosomes 9 and 22, which results in the formation of the Philadelphia chromosome coding for BCR-ABL, a chimeric tyrosine kinase signalling protein. This aberrant protein is constitutively active and signals downstream targets resulting in uncontrolled cell proliferation.[181] The mRNA transcript of BCR-ABL is found in more than 90% of CML cases, and therefore targeting the kinase activity of this protein is a major approach for therapy.[181] The first tyrosine kinase inhibitor (TKI) – Imatinib – discovered by Novartis in 1992, acts by preventing ATP from binding its site in the ABL pocket, blocking the catalytic function of the enzyme (Figure 3.1). Although treatment with imatinib achieved low relapse and high response rates, with overall survival rates of ~80% after 8 years, some patients developed resistance to imatinib, through accumulation of mutations in the BCR-ABL protein or through independent mechanisms, such as drug efflux or activation of alternative signalling pathways.[182] To circumvent imatinib resistance, second generation TKIs – nilotinib

and dasatinib - were developed and shown to directly inhibit specific mutant forms of BCR-ABL.[183] However, in spite of being effective against the great majority of mutations associated with imatinib resistance, the second generation TKIs do not target the T315I mutant of BCR-ABL (often referred to as the gatekeeper mutation).[184] In 2010, a new compound named ponatinib addressed this issue by effectively binding to the pocket of the BCR-ABL T315I mutant and also to other known mutants. Ponatinib has recently been approved for phase II clinical trials.[185]

Acute myeloid leukaemia (AML), like CML, also derives from the myeloid lineage of haematopoietic stem cells compartment. The malignancy is the most common acute leukaemia in adults, accounting for ~80% of cases.[186] In AML, the undifferentiated myeloid cells accumulate in the bone marrow, peripheral blood and other organs, leading to anaemia, thrombocytopenia and bone marrow failure.[187] The stratification of different risk groups in AML is based primarily on the expression levels of fusion proteins, such as RUNX1-RUNX1T1 and PML-PARA, which occur as a consequence of the chromosomal translocations, t(8;21) and t(15;17) respectively.[187,188] In addition to chromosomal abnormalities, FLT3 (FMS-like tyrosine kinase 3) receptor gene mutations are the most common somatic mutations in AML, leading to a constitutive activation of this protein and consequently cytokine-independent proliferation of myeloblasts. The presence of a mutated FLT3 receptor has been linked to poor prognosis.[189] The current main line of treatment for AML consists of a combination of cytarabine and anthracyclines.[187] In the last decade, TKIs, such as sorafenib and midostaurin, have been used to treat AML.[190–192]

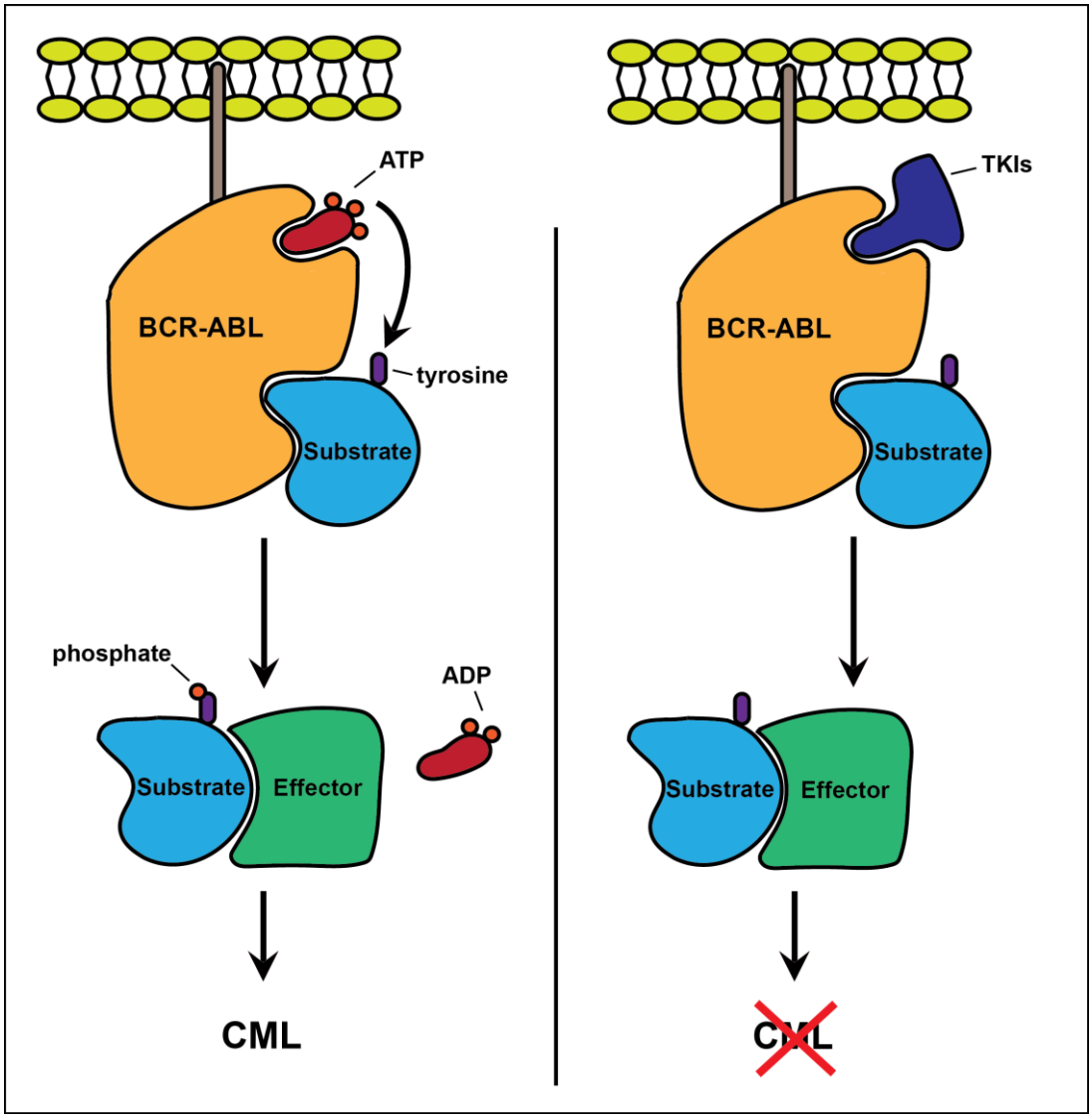

Figure 3.1. Scheme representing the mechanism of action of TKIs. In CML, the BCR-ABL tyrosine kinase is constitutively active by binding to ATP, leading to a signalling cascade that promotes cell division and inhibition of apoptosis. The TKIs bind to the ATP binding site of BCR-ABL, thus preventing downstream signalling.

The members of the BCL-2 family of proteins are key regulators of the intrinsic pathway of apoptosis. These proteins are highly expressed in CML. Furthermore, it has been shown that cells that express BCR-ABL have high levels of the anti-apoptotic members, BCL-X_L and MCL-1, as well as the pro-apoptotic BIM.[193] Resistance to TKIs in CML has been attributed to the increased expression/activity of BCL-2, BCL-X_L and MCL-1.[36] Moreover, BCR-ABL modulates the expression levels and/or the phosphorylation status of several BCL-2 family members, thus exerting important regulatory effects on apoptosis.[194–196] In addition, high expression levels of BCL-2 have been connected to a bad prognostic in AML,[30] posing ABT-199 as a good candidate for therapy.[197] These findings suggest that BH3 mimetic therapy could be beneficial in the treatment of CML and AML.

In this chapter, using a panel of BH3 mimetics, the potential of targeting distinct members of the BCL-2 family of proteins to enhance the effectiveness of current treatments in CML and AML is investigated.

3.2 Results

3.2.1 CML cell lines undergo TKI-mediated apoptosis in a concentration-dependent manner

Since TKI-mediated cell death has been observed in CML cell lines[36] and TKIs are commonly used in therapy,[198] the extent of apoptosis in CML cell lines following exposure to first (imatinib) and second (nilotinib and dasatinib) generation TKIs was compared. Apoptosis was assessed by measuring the extent of phosphatidylserine (PS) externalisation following caspase activation in these cells. Since the protein Annexin-V specifically recognises the externalised PS molecules, the cells were stained with Annexin V, conjugated to FITC and the extent of FITC fluorescence (indicative of PS externalisation) was measured by flow cytometry. For the following experiments, two CML cell lines, K562 and KCL22, which were originally derived from blast crisis patients, were chosen.[199,200] The cells were exposed for 48 h to a concentration range of imatinib (10 nM - 10 µM), nilotinib (1 nM - 3 µM), dasatinib (0.1 nM - 10 nM) and assessed for PS externalisation (Figure 3.2). In both cell lines, dasatinib was most effective in inducing apoptosis, followed by nilotinib and imatinib, possibly due to its higher affinity for the ATP binding site of the BCR-ABL protein.[201] In addition, KCL22 cells were slightly more sensitive to all the TKIs used. This experiment was used to identify appropriate concentrations of the different TKIs for further studies. Imatinib (1 µM), nilotinib (50 nM) and dasatinib (3 nM) induced comparable levels of apoptosis (Figure 3.2) and hence these concentrations were chosen for the following experiments.

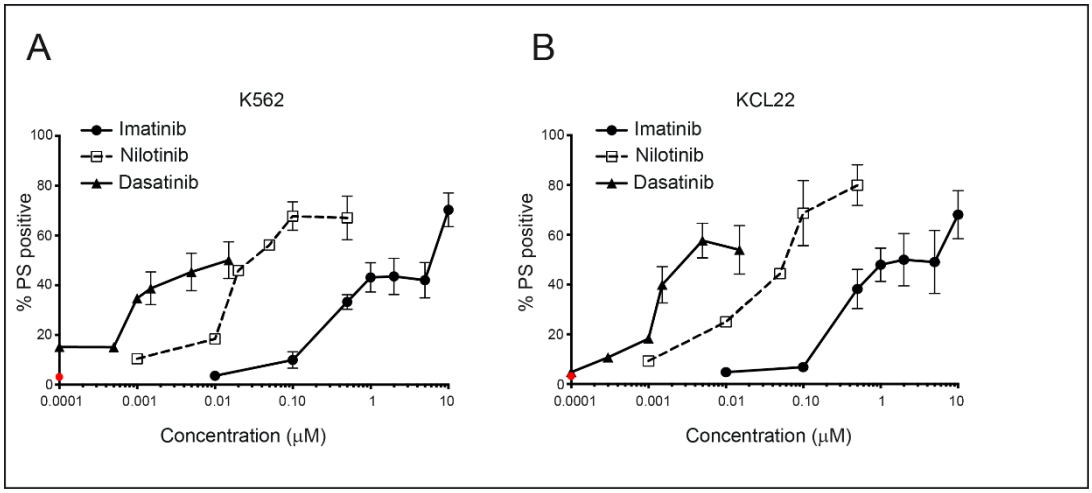

Figure 3.2. CML cell lines undergo TKI-mediated apoptosis in a concentration-dependent manner. (A) K562 and **(B)** KCL22 cells were exposed for 48 h to a concentration range of TKIs, imatinib (bold lines with filled circle), nilotinib (dotted lines with hollow square) and dasatinib (bold lines with filled triangle) and assessed for the extent of PS positivity by flow cytometry. In the graph, the extent of apoptosis in untreated cells is represented by a red circle. Error bars represent standard error of mean (S.E.M.) from at least three independent biological replicates.

3.2.2 TKIs induce apoptosis in a BAX/BAK-dependent manner

The induction of the intrinsic pathway of apoptosis is initiated by the release of the pro-apoptotic BCL-2 family members from their anti-apoptotic counterparts, which in turn activates BAK and/or BAX in the OMM to facilitate cytochrome *c* release and apoptosis. Since TKIs induced apoptosis in a concentration-dependent manner, studies were performed to assess if TKI-mediated apoptosis was BAK and BAX-dependent. For this, K562 and KCL22 cells, were transfected with siRNAs against both BAK and BAX for 48 h and the extent of TKI-mediated apoptosis assessed. In both cell lines, BAK and BAX knockdown did not enhance basal cell death, with less than 10% of the cells exhibiting basal apoptosis (Figure 3.3 A). Downregulation of BAX and BAK resulted in a significant decrease of TKI-mediated apoptosis (Figure 3.3 B - E). These results indicate that TKIs induce the intrinsic pathway of apoptosis in a BAX and/or BAK-dependent manner.

3.2.3 TKIs induce the intrinsic pathway of apoptosis in a BIM, BID and PUMA-dependent manner

Next, to assess the involvement of the pro-apoptotic activators, BIM, BID and PUMA in TKI-mediated apoptosis, K562 and KCL22 cells were transfected for 48 h with siRNAs against BIM, BID and PUMA and TKI-mediated apoptosis assessed. In both cell lines, downregulation of BIM, BID or PUMA significantly reduced the extent of TKI-mediated apoptosis. This was more evident following exposure to nilotinib and dasatinib than imatinib (Figure 3.4 B - E). These results indicate a dependence of TKIs on the activators BIM, BID and PUMA to induce apoptosis.

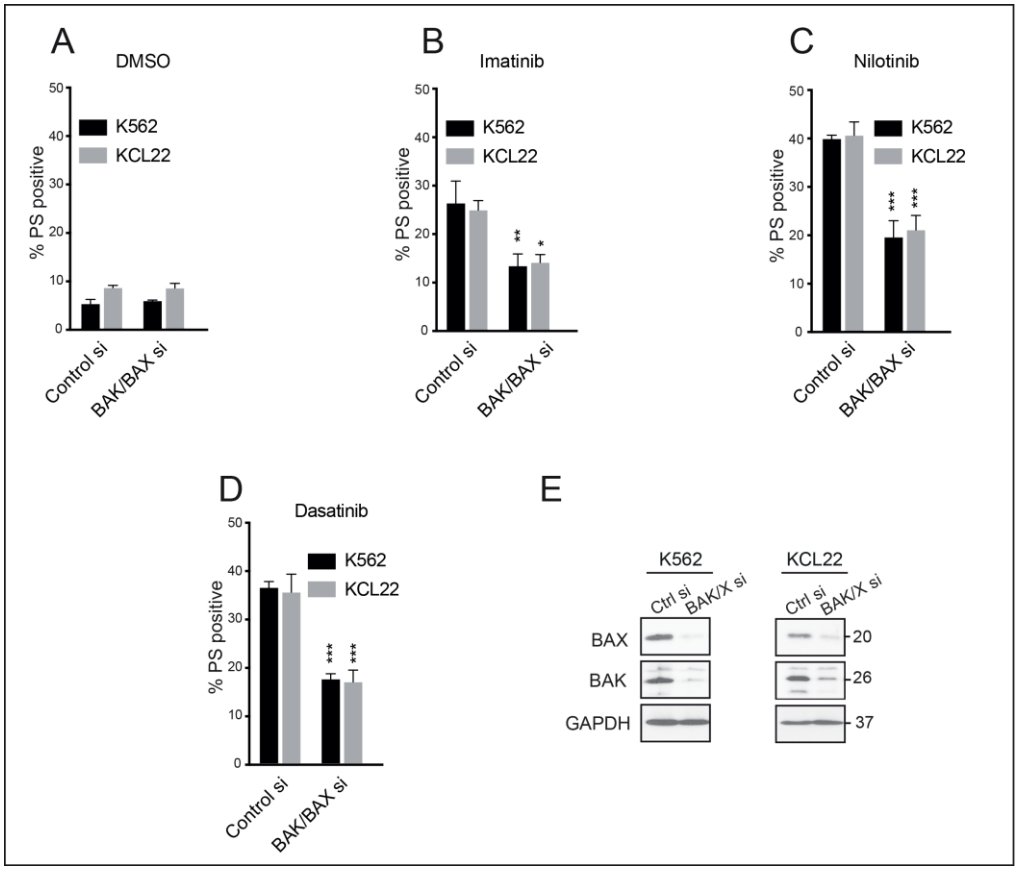

Figure 3.3. **TKIs induce BAX and BAK dependent-intrinsic pathway of apoptosis.** K562 and KCL22 cells were transfected with siRNAs against BAK and BAX for 48 h and further exposed for 48 h to **(A)** DMSO, **(B)** imatinib (1 μM), **(C)** nilotinib (50 nM) or **(D)** dasatinib (3 nM) and assessed for PS positivity by flow cytometry **(E)** Western blots confirming the knockdown efficiency of siRNA targeting mRNAs of the indicated proteins. GAPDH was used as loading control. Error bars represent standard error of mean (S.E.M.) from at least three independent biological replicates. Western blots were performed 72 h after siRNA transfection. Statistical analysis was conducted using one-way ANOVA and multiple comparison tests were conducted using Fisher's LSD test (***$p \leq 0.001$; ** $p \leq 0.01$; * $p \leq 0.05$).

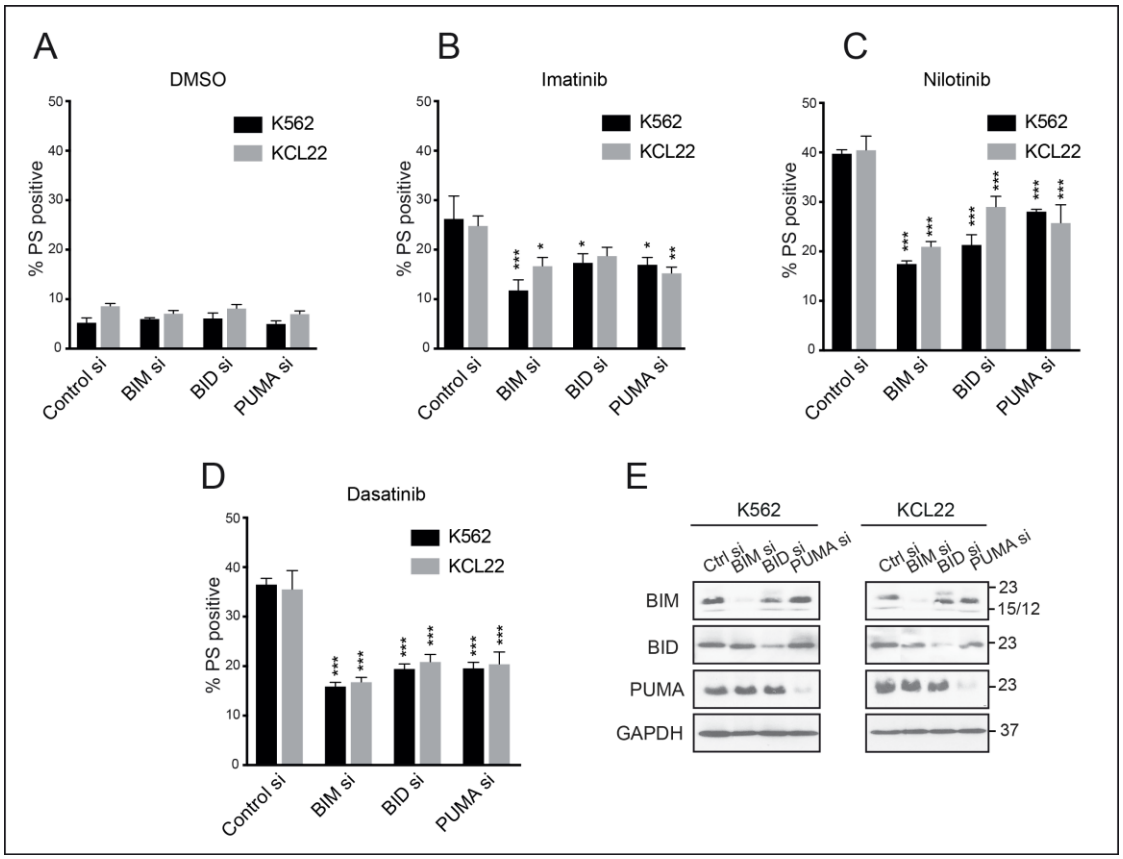

Figure 3.4. **TKIs induce apoptosis in a BIM, BID and PUMA-dependent manner.** K562 and KCL22 cells were transfected with siRNAs against BIM, BID or PUMA for 48 h and exposed for a further 48 h to **(A)** DMSO, **(B)** imatinib (1 μM), **(C)** nilotinib (50 nM) or **(D)** dasatinib (3 nM) and assessed for PS positivity by flow cytometry **(E)** Western blots confirming the knockdown efficiency of siRNA. GAPDH was used as loading control. Error bars represent standard error of mean (S.E.M.) from at least three independent biological replicates. Western blots were performed 72 h after siRNA transfection. Statistical analysis was conducted using one-way ANOVA and multiple comparison tests were conducted using Fisher's LSD test (***$p \leq 0.001$; ** $p \leq 0.01$; * $p \leq 0.05$).

3.2.4 TKIs induce apoptosis in HRK- and BAD-dependent manner

The sensitisers BH3-only members, NOXA, HRK, BMF, BIK and BAD, do not interact with BAX and BAK but can bind specifically to anti-apoptotic BCL-2 family members to release BH3-only activators and induce apoptosis. Therefore, K562 and KCL22 cells were transfected with siRNAs against NOXA, HRK, BMF, BIK and BAD for 48 h, and assessed for TKI-mediated apoptosis. Downregulation of HRK and BAD, but not NOXA, BMF or BIK inhibited TKI-mediated apoptosis in both K562 and KCL22 cells (Figure 3.5 B - E). Although HRK levels were not clearly detected by western blot, HRK mRNA levels were detected by qPCR (data shown in the published version and in Appendix).

3.2.5 BCL-X_L is an essential requirement for CML cell lines survival

The sensitisers, BAD (binds BCL-2, BCL-X_L and MCL-1) and HRK (specifically binds BCL-X_L) share BCL-X_L as their common binding partner (Figure 1.3).[202] Data demonstrating that TKI-mediated apoptosis occurred in a BAD- and HRK-dependent manner highlight a possible role for BCL-X_L in TKI-mediated cell death in CML. Therefore, K562 and KCL22 cells were transfected with siRNAs against BCL-2, BCL-X_L, BCL-W, BFL-1 and MCL-1 for 48 h and assessed for changes in TKI-mediated apoptosis. Downregulation of BCL-X_L but not the other members resulted in high levels of apoptosis in both K562 and KCL22 cells (Figure 3.6 A and B). Furthermore, silencing of BCL-X_L also increased TKI-mediated cell death (Figure 3.6 A and C).

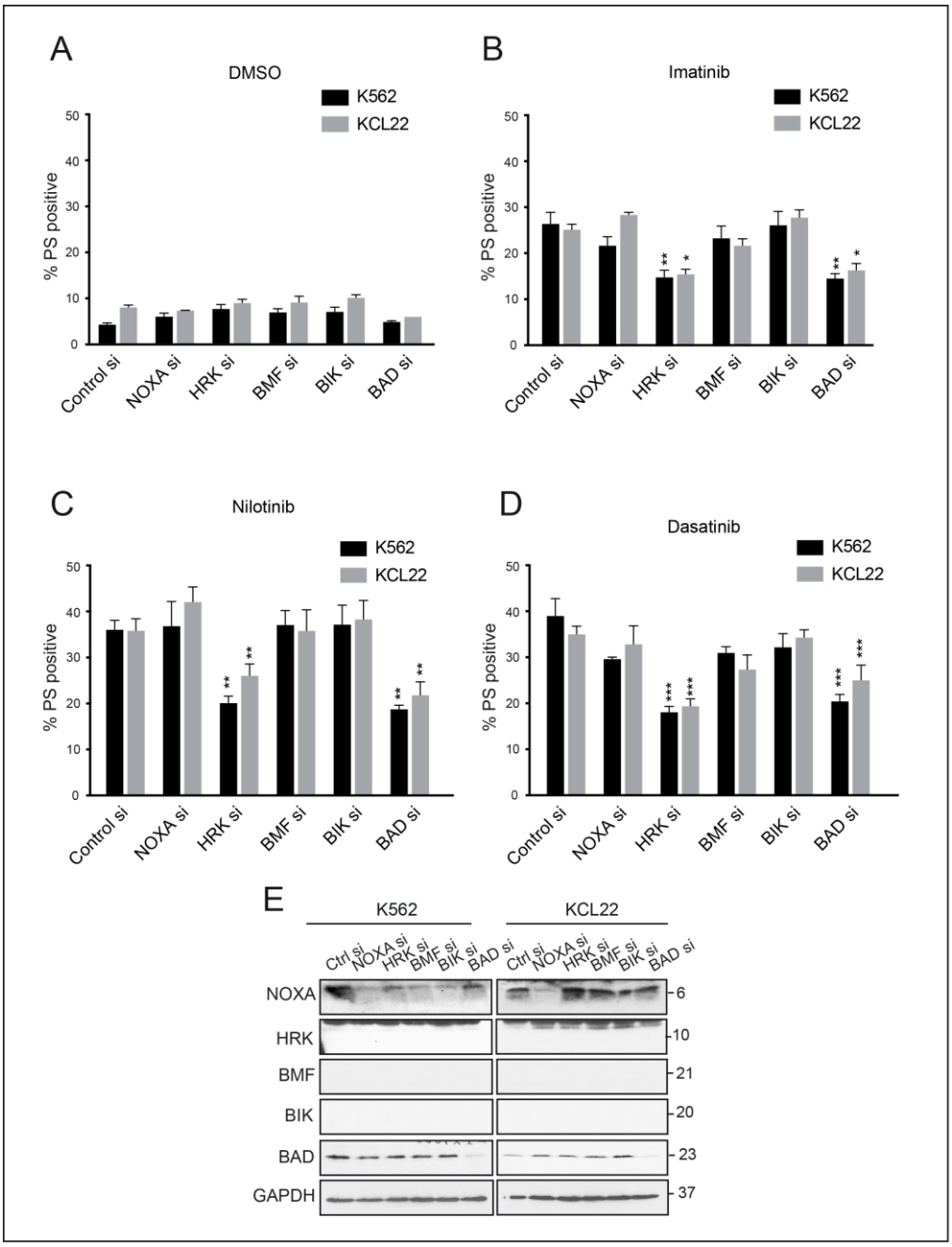

Figure 3.5. **TKIs induce apoptosis in an HRK and BAD-dependent manner.** K562 and KCL22 cells were transfected with siRNAs against NOXA, HRK, BMF, BIK or BAD for 48 h and further exposed for 48 h to **(A)** DMSO, **(B)** imatinib (1 µM), **(C)** nilotinib (50 nM) or **(D)** dasatinib (3 nM) and assessed for PS positivity by flow cytometry **(E)** Western blots confirming the knockdown efficiency of siRNAs. Levels of BMF and BIK were undetectable in the experiments. GAPDH was used as loading control. Error bars represent standard error of mean (S.E.M.) from at least three independent biological replicates. Western blots were performed 72 h after siRNA transfection. Statistical analysis was conducted using one-way ANOVA and multiple comparison tests were conducted using Fisher's LSD test (***$p \leq 0.001$; ** $p \leq 0.01$; * $p \leq 0.05$).

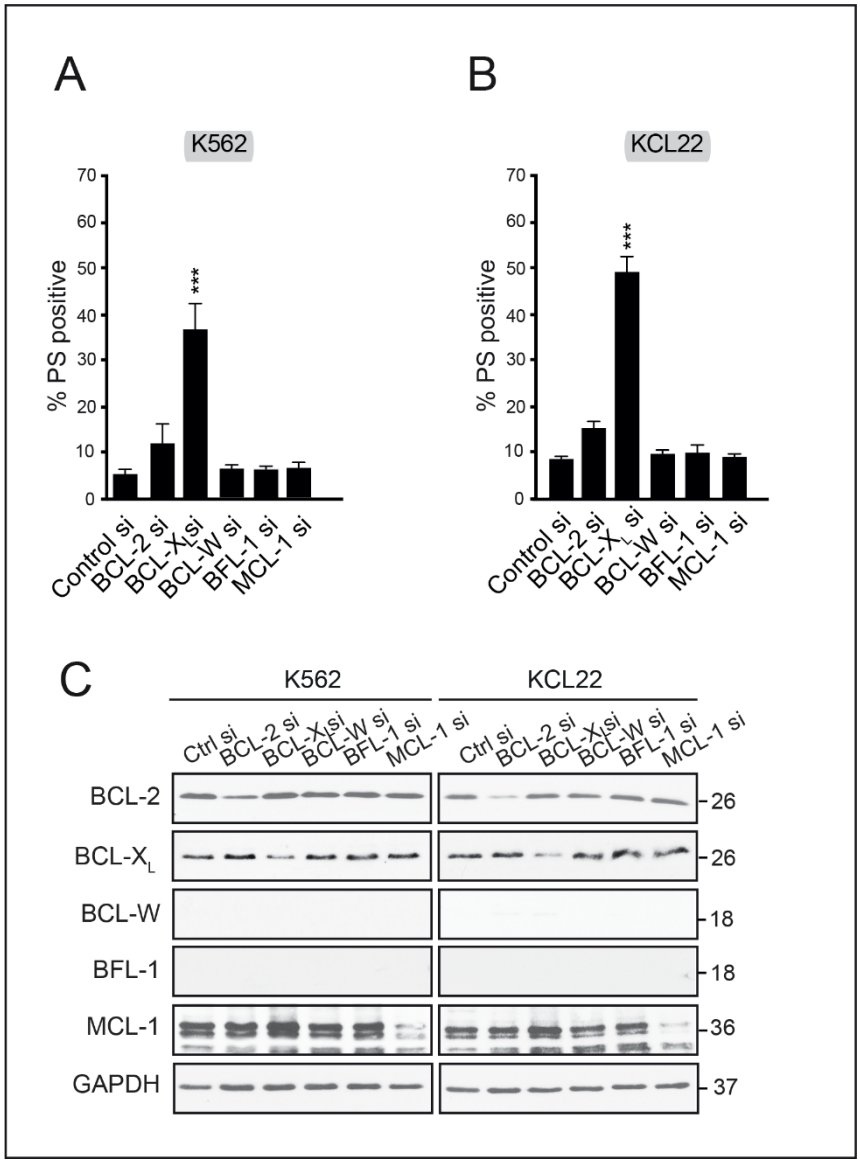

Figure 3.6. **BCL-X_L is critical for the survival of CML cell lines. (A)** K562 and **(B)** KCL22 cells were transfected with siRNAs against BCL-2, BCL-X_L, BCL-W, BFL-1 or MCL-1 for 48 h and further exposed for 48 h to either DMSO, imatinib (1 µM), nilotinib (50 nM) or dasatinib (3 nM) and assessed for PS positivity by flow cytometry **(C)** Western blots confirming the knockdown efficiency of siRNAs. GAPDH was used as loading control. Error bars represent standard error of mean (S.E.M.) from at least three independent biological replicates. Western blots were performed 72 h after siRNA transfection. Statistical analysis was conducted using one-way ANOVA and multiple comparison tests were conducted using Fisher's LSD test (***$p \leq 0.001$; ** $p \leq 0.01$; * $p \leq 0.05$).

3.2.6 The BCL-X_L inhibitor, A-1331852, induces apoptosis in CML cell lines

As CML cells appeared to depend on BCL-X_L for survival (Figure 3.6), K562 and KCL22 cells were exposed to increasing concentrations of ABT-737 (a BAD mimetic that inhibits BCL-2, BCL-X_L and BCL-w), ABT-199 (a BCL-2 inhibitor), A-1331852 (a BCL-X_L inhibitor) and A-1210477 (a MCL-1 inhibitor) and assessed for PS positivity. In accordance with previous results (Figures 3.5 and 3.6), inhibition of BCL-X_L by A-1331852 was by far the most effective in promoting apoptosis in both cell lines compared to the other inhibitors (Figure 3.7).

3.2.7 TKI-induced apoptosis is enhanced by chemical or genetic inhibition of BCL-X_L

After establishing that the CML cell lines require BCL-X_L for apoptosis, experiments were performed to verify how pharmacological or genetic inhibition of BCL-X_L would affect TKI-induced apoptosis. Downregulation of BCL-X_L resulted in 50-60% apoptosis, which was greatly increased when exposed to the different TKIs (Figure 3.8 A and B). To assess whether A-1331852 enhanced TKI-mediated apoptosis, K562 cells were exposed to a sub-lethal concentration of A-1331852 (1 nM), which did not induce any apoptosis. The three different TKIs alone induced ~50% of apoptosis, which was significantly increased when cells were exposed to a sub-lethal concentration (1 nM) of A-1331852 (Figure 3.8 C). These results further confirmed that A-1331852 induced extensive apoptosis in CML cell lines and also synergised with TKIs to result in enhanced apoptosis.

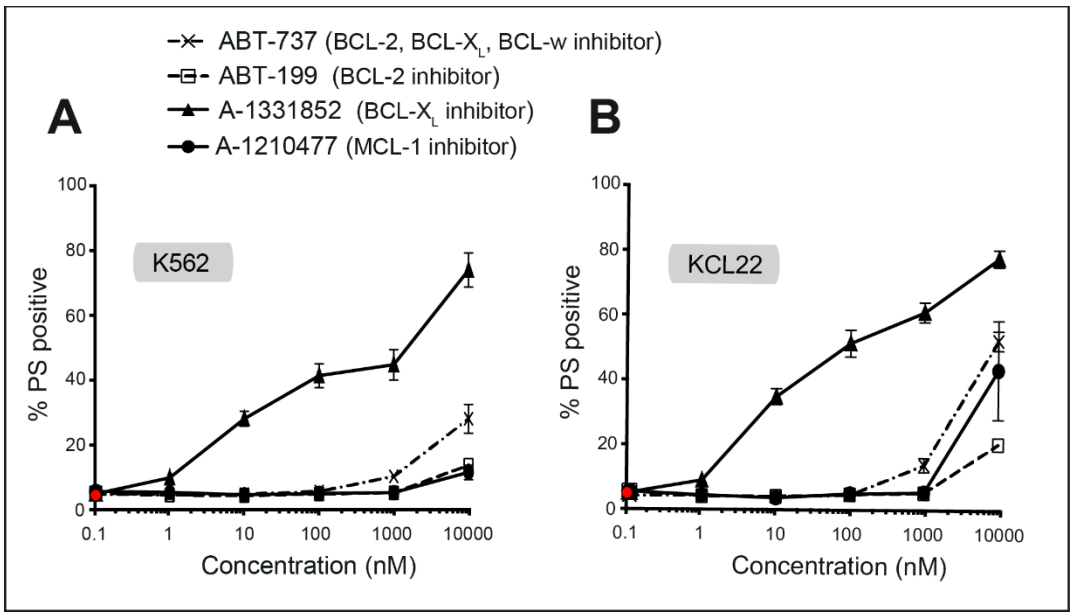

Figure 3.7. A **BCL-X_L inhibitor induces apoptosis in CML cell lines. (A)** K562 and **(B)** KCL22 cells were exposed for 4 h to a concentration range of BH3 mimetics: ABT-737 (dotted lines with cross), ABT-199 (dotted lines with hollow square), A-1331852 (bold lines with filled triangle) and A-1210477 (bold lines with filled circle) and assessed for PS positivity by flow cytometry. In the graph, the extent of apoptosis in untreated cells are represented by a red circle. Error bars represent standard error of mean (S.E.M.) from at least three independent biological replicates.

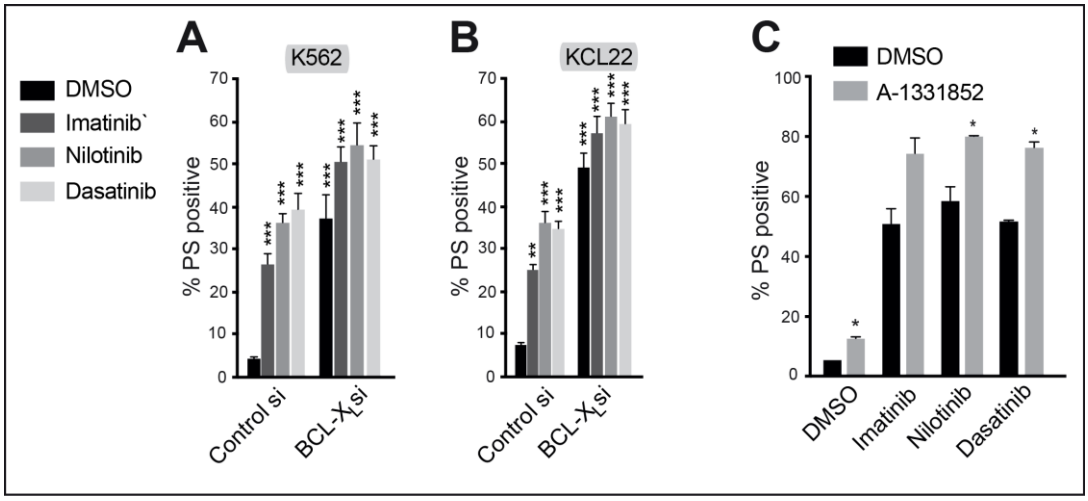

Figure 3.8. Inhibition of BCL-X_L enhances TKIs-induced apoptosis in CML cell lines. **(A)** K562 and **(B)** KCL22 cells, transfected with siRNA against BCL-X_L for 48 h, were further exposed to DMSO, imatinib (1 µM), nilotinib (50 nM) or dasatinib (3 nM) for 48 h and assessed for PS positivity by flow cytometry. **(C)** K562 cells, exposed to DMSO, imatinib (1 µM), nilotinib (50 nM) or dasatinib (3 nM) for 48 h, were further exposed to A-1331852 (1 nM) for 1 h and assessed for PS positivity by flow cytometry. Error bars represent standard error of mean (S.E.M.) from at least three independent biological replicates. Statistical analysis was conducted using one-way ANOVA and multiple comparison tests were conducted using Fisher's LSD test (***$p \leq 0.001$; ** $p \leq 0.01$; * $p \leq 0.05$).

3.2.8 Inhibition of BCL-X_L induces rapid apoptosis in primary CML cells with no effect in normal mononuclear cells (MNC)

To extend the observations in cell lines to primary patient samples, $CD34^+$ (haematopoietic stem cell marker) progenitor CML cells and MNCs from healthy volunteers were exposed to increasing concentrations of A-1331852 and the extent of PS positivity assessed. At low concentrations (1 nM), A-1331852 resulted in enhanced apoptosis in $CD34^+$ progenitor cells within 1 h of exposure, with higher concentrations (10 nM) further increasing the extent of apoptosis (Figure 3.9 A). In contrast, survival of MNCs from healthy volunteers was not affected by A-1331852 (Figure 3.9 B). Thus A-1331852 could selectively kill CML cells while sparing normal cells.

3.2.9 AML cell lines depend on MCL-1 and BCL-2 but not BCL-X_L for survival

Several studies have shown that AML cells can be targeted by inhibiting BCL-2 and/or MCL-1.[170,203–205] However, some reports indicate that AML cells depend primarily on BCL-2 for survival.[197,206] To study this further, 6 AML cell lines, namely MV-4-11, MOLM-13, THP-1, AML-3, U937 and HL-60, were exposed to increasing concentrations of the different BH3 mimetics, namely ABT-199, A-1331852 and S63845 to inhibit BCL-2, BCL-X_L and MCL-1, respectively. S63845 was used instead of A-1210477 in these experiments, as it was recently reported as the most potent and specific MCL-1 inhibitor.[168] Of the six cell lines used, MV-4-11 and MOLM-13 exhibited marked sensitivity to either ABT-199 (IC_{50} ~ 100 nM) or S63845 (IC_{50} ~ 10 nM). THP-1 and AML-3 cells were highly sensitive to only S63845 (IC_{50} ~ 50 nM and 500 nM respectively), but not to ABT-199. U937

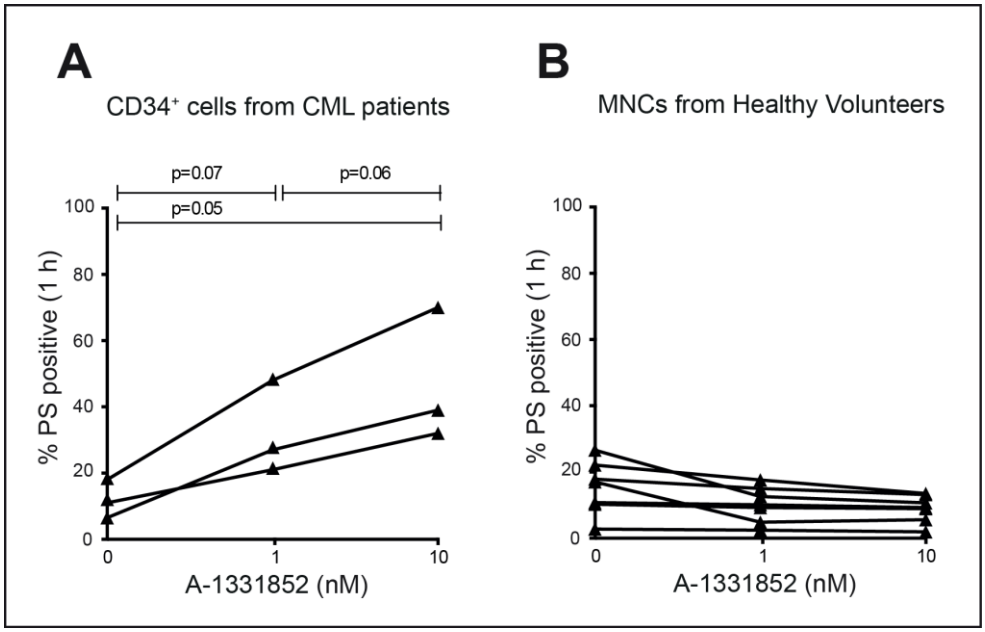

Figure 3.9. **Inhibition of BCL-X_L induces rapid apoptosis in primary CML cells but not in normal MNC**. **(A)** Primary $CD34^+$ cells from CML patients (n=3) and **(B)** MNCs from healthy volunteers (n=8) were exposed to 0, 1 or 10 nM of A-1331852 for 1 h and assessed for PS positivity by flow cytometry. In the graphs, each line represents the same pool of cells. P values correspond to Mann-Whitney *U*-test, where significant.

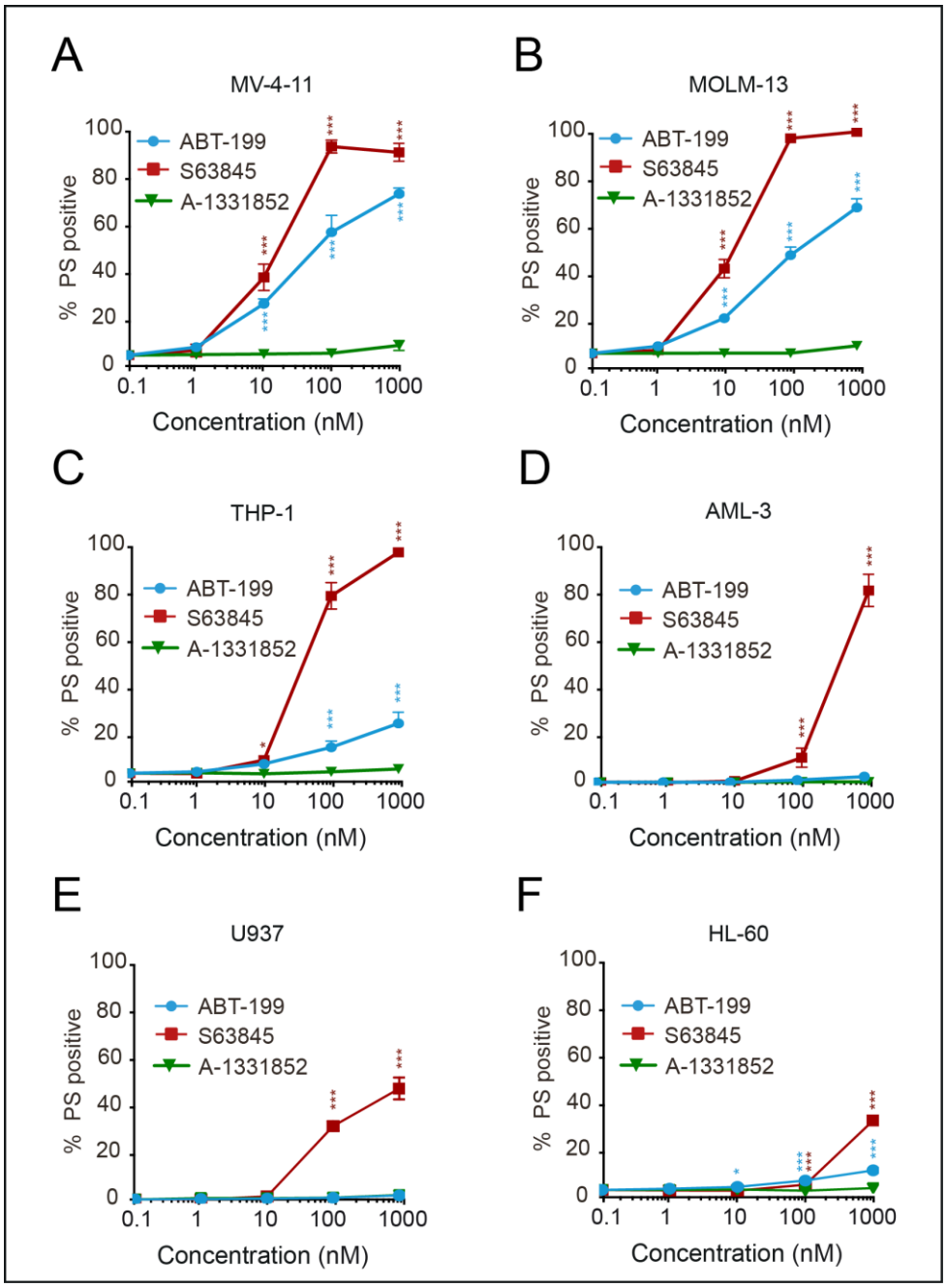

Figure 3.10. **Inhibitors of BCL-2 and/or MCL-1 induces apoptosis in AML cell lines.** **(A)** MV-4-11, **(B)** MOLM-13, **(C)** THP-1, **(D)** AML-3 (OCI), **(E)** U937 and **(F)** HL-60 cell lines were exposed to a concentration range of ABT-199 (BCL-2 inhibitor), S63845 (MCL-1 inhibitor) or A-1331852 (BCL-X_L) inhibitor for 24 h and assessed for PS positivity by flow cytometry. Results are shown as Mean ± SEM (standard error of the mean) from at least three independent experiments. Statistical analysis was conducted using two-way ANOVA and multiple comparison tests were conducted using Fisher's LSD test (***$p \leq 0.001$; ** $p \leq 0.01$; * $p \leq 0.05$).

cells showed mild resistance to S63845 (IC_{50} ~ 1 µM) and great resistance to ABT-199. HL-60 cells were the most resistant cells from the panel. None of the cells showed sensitivity to BCL-X_L inhibition by A-1331852 (Figure 3.10).

3.2.10 Inhibition of both MCL-1 and BCL-2 exhibits synergy in the induction of apoptosis in AML cell lines

Single inhibition of MCL-1 or BCL-2, but not BCL-X_L, induced varying levels of apoptosis in most of the AML cell lines used, indicating that these cells might depend on either MCL-1 or in some cases, BCL-2 for survival. Based on a multiple-ray experimental design to achieve an ideal concentration ratio between S63845 and ABT-199, the cells were exposed to varying concentrations of a combination of the two inhibitors and assessed for PS positivity. Cell death percentages were fed to the Combenefit software[179] to generate a *Bliss Independence* score heatmap. The *Bliss Independence* model is based on the assumption that the effects of the drugs used are due to a probabilistic chance, and a zero interaction is comparable to a probabilistic independence. This synergy model works analogously to the concept of epistasis in molecular biology, which is the phenomenon where the effect of a particular gene is dependent on the presence of at least one other gene.[207,208] Using this approach, the effect of the two BH3 mimetics were compared to answer whether the presence of one of them affects the extent of apoptosis mediated by the other and *vice-versa*. Although all cell lines showed differing levels of synergy between S63845 and ABT-199, MV-4-11 and MOLM-13 exhibited better synergy at lower concentrations, which was not apparent in the most resistant U937 and HL-60 cells (Figure 3.11). It is important to note that MV-4-11 and MOLM-13 showed high levels of cell death even at low concentrations of ABT-199 and S63845

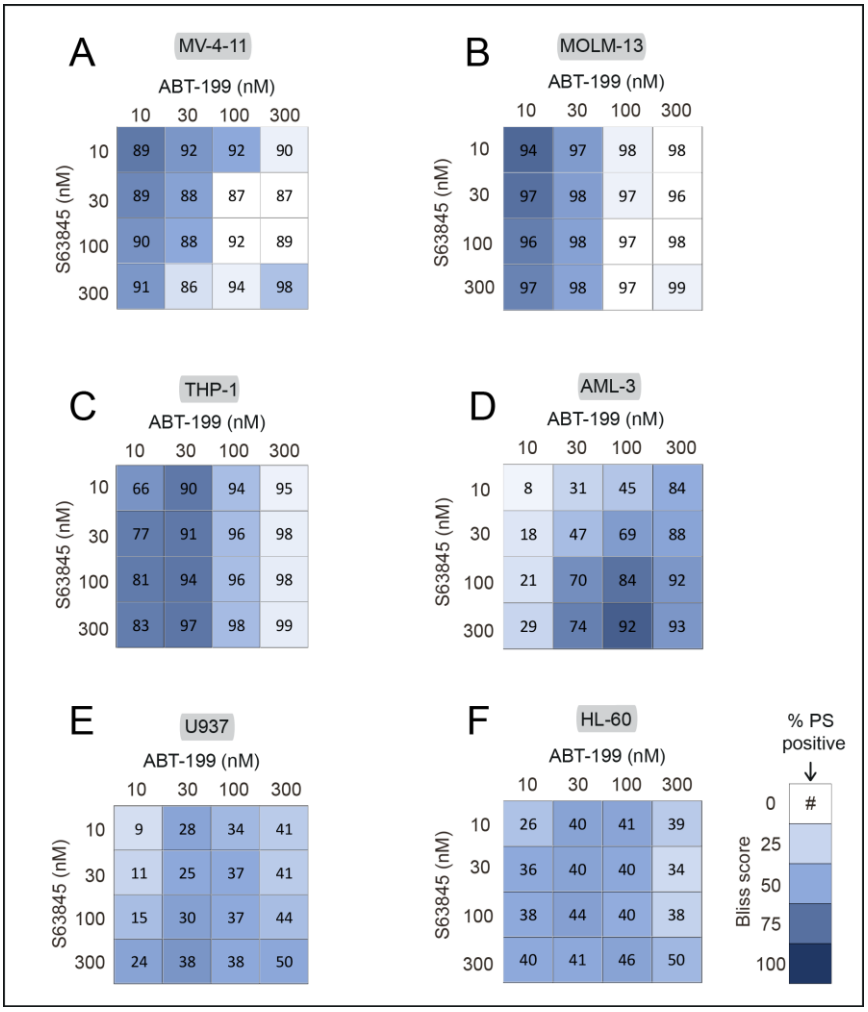

Figure 3.11. **Inhibitors BCL-2 and MCL-1 synergise with each other to induce apoptosis in AML cell lines. (A)** MV-4-11, **(B)** MOLM-13, **(C)** THP-1, **(D)** AML-3 (OCI), **(E)** U937 and **(F)** HL-60 cell lines were exposed to a combination of varying concentrations of ABT-199 and S63945 for 24 h and assessed for PS positivity by flow cytometry. The Bliss score ranging from 0 (white) to 100 (dark blue) depicts the strength of the synergistic effect and the extent of PS positivity for the different combinations is shown inside each quadrant. Shown values correspond to the average of at least 3 independent experiments.

alone, which affected the calculation of synergy, since the effect of one compound by itself can explain the amount of cell death observed.

3.2.11 Dual inhibition of MCL-1 and BCL-2 in primary AML cells induces apoptosis in an additive manner

Next, primary AML cells isolated from patients, were exposed to increasing concentrations of S63845 and/or ABT-199 for 4 h, and the extent of PS positivity subjected to Bliss score analysis (Figure 3.12). ABT-199 in combination with S63845 induced apoptosis in primary AML cells in an additive manner for all the samples tested, with some cells being similarly to sensitive to both ABT-199 and S63845 (#3621 and #3624), while the rest being more sensitive to S63845 than to ABT-199. Taken together, these results indicate that a combination therapy, involving both ABT-199 and S63845, could be a better therapeutic strategy in AML.

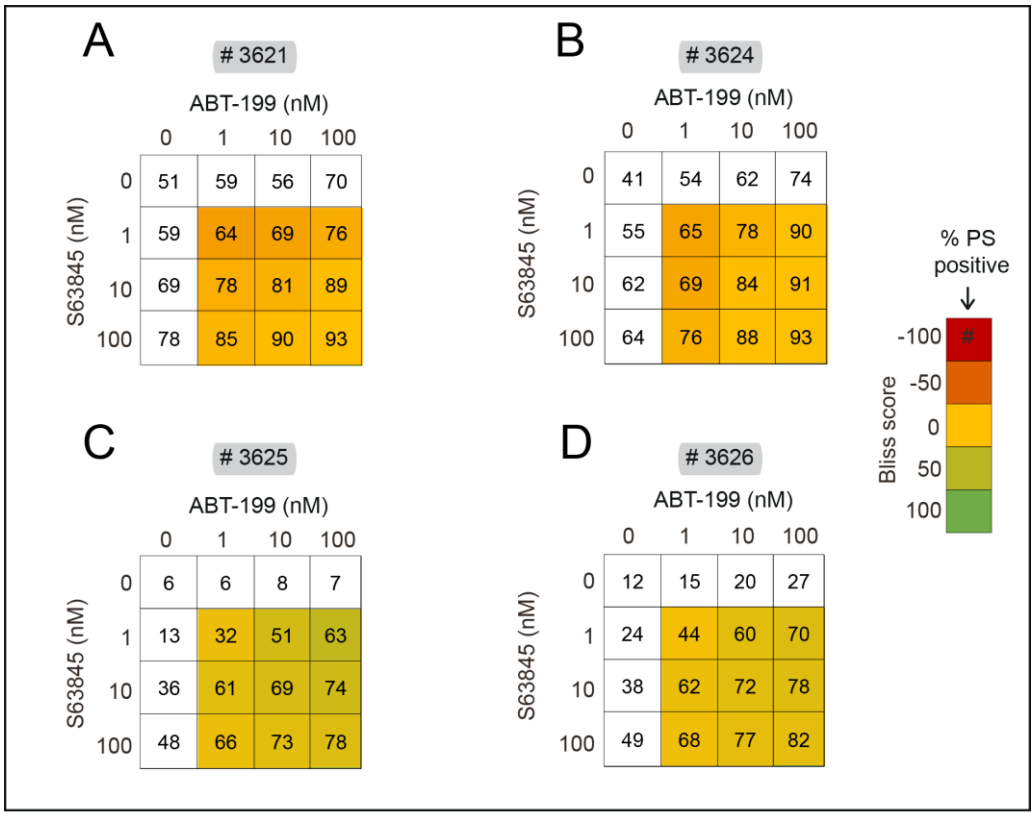

Figure 3.12. **Exposure to ABT-199 and S63845 in primary AML cells induces apoptosis in an additive manner.** Primary AML cells isolated from patients **(A-D)** were exposed to a combination of varying concentrations of ABT-199 and S63945 for 4 h and assessed for PS positivity. The Bliss score ranging from -100 (red) to 100 (green) depicts antagonistic (red), additive (yellow) or synergistic (green) effects by the inhibitors. The extent of PS positivity for the different combinations is shown inside each quadrant. The Bliss score was calculated only for combination exposures to inhibitors, single drug exposures have a white background.

3.3 Discussion

The constitutively active kinase activity of BCR-ABL1 contributes to disease progression in CML and hence has been exploited in the design and successful use of TKIs. Several TKIs display great potency in inhibiting BCR-ABL1 kinase activity and reducing the frequency of CML disease progression to blast crisis. Although imatinib has greatly improved patient outcome, approximately one third of patients still fail treatment.[209] In this study, using RNA interference in CML cell lines, specific members of the BCL-2 family, such as BAX/BAK, BIM, BID, PUMA, BAD and HRK, have been identified to be critical in the induction of apoptosis following exposure to TKIs (Figures 3.3-3.5). Intriguingly, these findings also appeared to extend to CML patients, as increased expression of specific pro-apoptotic BH3-only members *PUMA*, *HRK* and possibly *BIM* correlated with progression free survival in CML patients.[35] This was the first study to link several pro-apoptotic BCL-2 family members to progression free survival in imatinib–treated CML patients.

Targeting the BCL-2 family of proteins with selective antagonists may offer novel therapeutic approaches in this malignancy. BCL-X_L has been associated with the development and maintenance of TKI resistance as well as disease progression in CML.[36,194,210–212] In agreement, A-1331852 displayed remarkable potency, both as a single agent and in combination with TKIs, to facilitate apoptosis both in cell lines and in the progenitor $CD34^+$ primary cells. Notably, the insensitivity of these quiescent $CD34^+$ progenitor cells has limited the potential of imatinib to cure CML and is a major factor in the recurrence of the disease on discontinuation of therapy. Previous studies have shown a BCL-X_L dependence of stem cell survival for human embryonic stem cells as well as non-small cell lung cancer cells.[213,214] The sensitivity of $CD34^+$ progenitor cells to BCL-X_L inhibition offers much promise towards the

introduction of BH3 mimetic therapy in CML. The results presented in this study indicate that targeting of BCL-X_L in CML in combination with TKIs could be a very beneficial adjunct to current therapy, taking into consideration the effects of BCL-X_L inhibition for platelet survival.[215]

Chromosomal abnormalities and mutations in the FLT3 receptor gene are responsible for the onset of the great majority of AML types.[187,216] Besides the common cytarabine and anthracycline therapy, TKIs have been developed to inhibit the FLT3 receptor.[187] The potential of BH3 mimetic therapy in AML has been explored in conjunction with standard chemotherapy, such as sorafenib,[217] HDAC inhibitors[218] and MEK inhibitors.[219] Recent reports suggest that AML is a BCL-2 dependent cancer,[197,206] although recently developed MCL-1 inhibitors have entered clinical trials to treat AML.[220] In addition, ABT-199 has been used in combination with MEK inhibitors and TKIs, unveiling new ways to target AML.[197,219,221,222] The data presented in this chapter indicate that dual inhibition of BCL-2 and MCL-1 is remarkably synergistic to induce cell death in AML cell lines and additive in primary cells derived from AML patients, which could be due to the sample number limitation and patient to patient variability. Taken together, these results show that using BH3 mimetics to tackle AML could be a very appealing strategy. Moreover, it is important to emphasise that a prior knowledge on BCL-2 family member dependency would be required for a more specific and personalised therapy in the future, to account for individual patient variability.

CHAPTER 4

Evaluating the potential of BH3 mimetic therapy in solid tumours

Chapter contents

4.1 Introduction

BH3 mimetics have been successfully used in several haematological malignancies. While the use of ABT-199 in CLL has been extensively studied,[164,223,224] leading to the approval of ABT-199 for treatment against chemorefractory CLL,[225] findings from the previous chapter revealed the potential of BH3 mimetic therapy in CML and AML. To extend these observations to solid tumours, two different tumour types were chosen.

The first tumour type was from Head and neck squamous cell carcinoma (HNSCC), a highly prevalent cancer worldwide, with ~600,000 new cases every year.[226] Although the most important risk factors are alcohol consumption and tobacco use, human papillomavirus (HPV) infection has been linked to a subset of high-risk HNSCC, as HPV type-16 E6 oncogene inactivates p53. In addition, *TP53* is also mutated in 60-80% of HNSCC cases which are linked to poor prognosis.[227] The main line of chemotherapy for head and neck cancer is cisplatin, often combined with surgery and/or radiotherapy.[228] However, HNSCC treatment is hampered by development of resistance to cisplatin as well as enhanced toxicity.[229] Therefore, assessment of new promising candidates for HNSCC therapy is essential. On that note, the first successful targeted therapy for HNSCC was the use of antibodies targeting EGFR,[230] as EGFR expression has been associated with poor prognosis.[231] Studies pertaining to the BCL-2 family of proteins in HNSCC are focused on chemoresistance, which has been attributed to high expression of anti-apoptotic members of the BCL-2 family, especially BCL-X_L in HNSCC.[232] In support of this, BH3 peptides and ABT-737 have been previously used in HNSCC to enhance the extent of apoptosis following cisplatin and etoposide,[233,234] highlighting that the use of BH3 mimetics could be beneficial for the treatment of HNSCC.

The second choice of tumour type was from pancreatic ductal adenocarcinoma (PDAC), one of the most deadly tumours, responsible for ~20-25% of all cancer deaths worldwide.[235] It presents a very poor prognosis as < 20% of patients achieve cure and the 5-year survival rate is < 5%.[236] Although several environmental factors have been likely linked to PDAC, a causative role only exists for tobacco use.[237] In addition, *KRAS2* mutations and inactivation of *CDKN2A* are present in ~90% of all fully established pancreatic tumours.[238] Gemcitabine, a nucleoside analogue of deoxycytidine, is widely used as the first line treatment for pancreatic cancer, however response rates to gemcitabine treatment is as low as 25% and many patients develop resistance.[239] Gemcitabine resistance has been attributed to several factors, such as upregulation of the ribonucleotide reductase RRM1,[240] enhanced activity of the DNA repair endonuclease ERCC1,[241] or *via* miRNA regulatory pathways.[239] In addition, resistance to gemcitabine has been linked to overexpression of BCL-X_L and MCL-1.[242,243] Of interest, some reports have shown that targeting BCL-2, BCL-X_L or MCL-1 with BH3 mimetics can potentially increase gemcitabine sensitivity in PDAC, and induce caspase-dependent cell death, highlighting the potential of using BH3 mimetics in PDAC therapy.[244–247]

In this chapter, using cell lines and patient material derived from cancers of the head and neck and pancreas, the potential of BH3 mimetic therapy in these malignancies is investigated.

4.2 Results

4.2.1 Several solid tumour cell lines depend on both MCL-1 and BCL-X_L for survival

Haematological malignancies generally depend on a single anti-apoptotic member of BCL-2 family for survival.[35,155,248] However, several reports indicate that the majority of solid tumours depend on both BCL-X_L and MCL-1 for survival,[249] thus requiring inhibition of the two anti-apoptotic proteins to undergo apoptosis.[250,251] To confirm that, cell lines derived from different solid tumours, namely breast, pancreas, lung and colon, were exposed to S63845 and/or A-1331852 and PS positivity assessed. All cell lines exhibited marked PS externalisation when exposed to a combination of S63845 and A-1331852 but not when exposed to either of those BH3 mimetics individually (Figure 4.1), indicating these cell lines depend on both BCL-X_L and MCL-1 for survival. The 4 h exposure to BH3 mimetics in these experiments was chosen based on hourly observations under a light microscope for detached and apoptotic cells.

4.2.2 Several HNSCC cell lines express high levels of BCL-X_L and MCL-1

In order to check the expression levels of BCL-2, BCL-X_L and MCL-1 in HNSCC, several head and neck cancer cell lines derived from distinct anatomical sites, namely oral cavity (UM-SCC-1), larynx (UM-SCC-11B, UM-SCC-17A and UM-SCC-17AS) and oropharynx (UM-SCC-74A and UM-SCC-81B), were immunoblotted for the major BCL-2 anti-apoptotic proteins. The chosen cells showed varying levels of BCL-2, but high expression levels of both MCL-1 and BCL-X_L (Figure 4.2), indicating that inhibiting these proteins could potentially induce apoptosis in these cells.

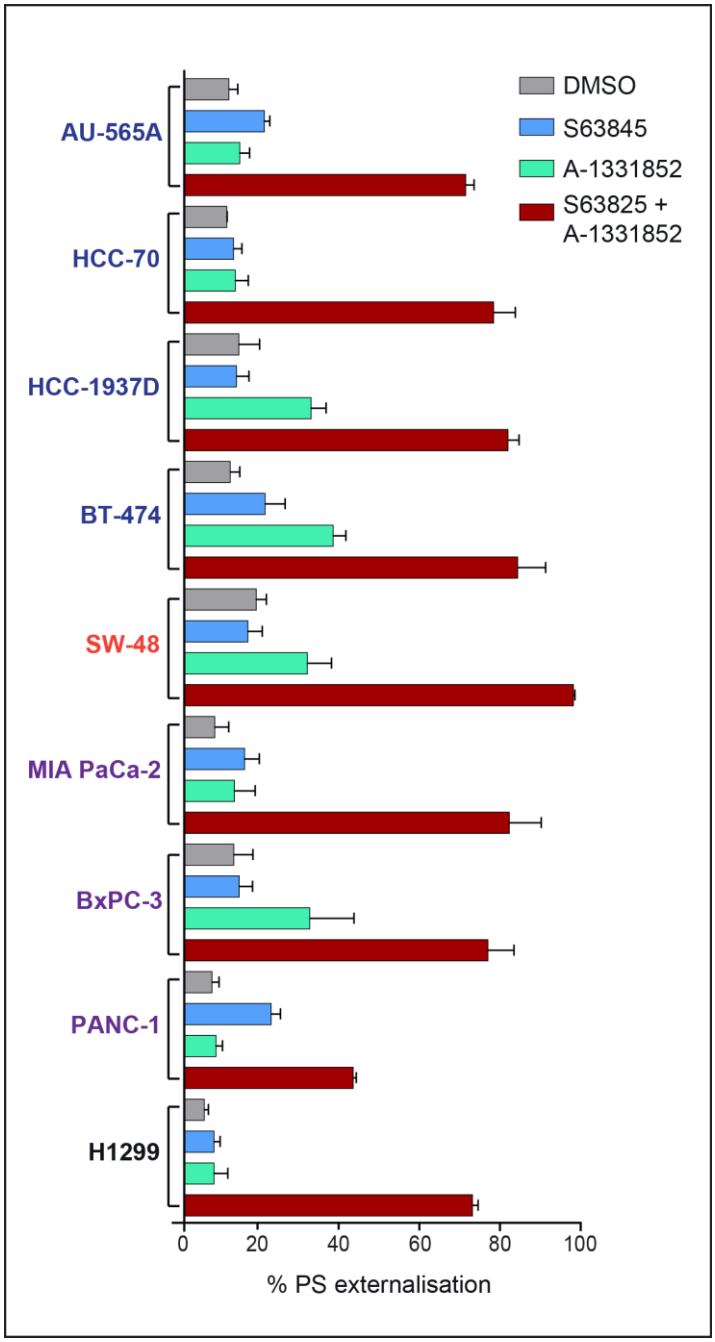

Figure 4.1. MCL-1 and BCL-X_L inhibition induces apoptosis in several solid tumours cell lines. Breast cancer cell lines, AU-565A, HCC-70, HCC-1937D and BT-474; a colon cancer cell line, SW-48; a pancreatic cancer cell lines, MIA PaCa-2, BxPC-3 and PANC-1 and a non-small cell lung cancer cell line, H1299 were exposed to S63845 (100 nM), A-1331852 (100 nM) or a combination of both for 4 h and assessed for the extent of PS externalisation by FACS. Error bars represent the S.E.M. for at least three independent biological replicates.

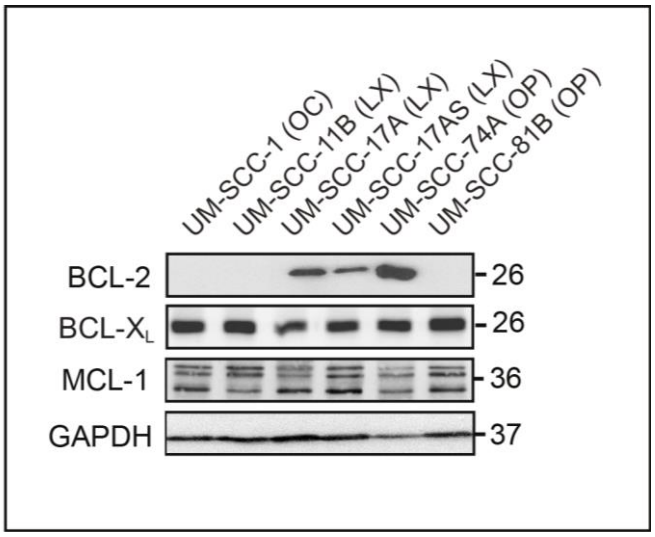

Figure 4.2. BCL-2 anti-apoptotic family members protein expression levels in several HNSCC cell lines. Immunoblot of several HNSCC cell lines derived from different head and neck tissues showing expression levels of BCL-1, BCL-X_L and MCL-1. GAPDH was used as loading control. OC (oral cavity); LX (larynx); OP (oropharynx).

4.2.3 BCL-2 is poorly expressed in the oral cavity tissue of HNSCC patients

As some of the HNSCC cell lines expressed varying levels of BCL-2, studies were carried out to confirm whether this result translated to patient samples. Oral cavity (OC) TMA (tissue microarray) cores from normal, tumour core and advancing front of HNSCC patients were immunostained with BCL-2 antibody and the staining intensity (H-score) quantified to assess BCL-2 expression levels. Normal cores from healthy patients, tumour cores from HNSCC patients as well as tumour tissues from the advancing front of the tumour core from HNSCC patients exhibited similar H-scores, averaging below 100, which is considered a low value.[178] Statistical analysis showed that there were no significant differences between BCL-2 expression levels of normal, tumour core and tumour advancing front TMAs. A representative image of each category illustrates BCL-2 expression levels of the tissues analysed (Figure 4.3).

4.2.4 BCL-X_L is highly expressed in HNSCC oral cavity tissue

Similarly, the expression levels of BCL-X_L in normal and HNSCC patients were assessed in the relevant TMAs. In contrast to the expression profile of BCL-2, BCL-X_L expression levels were overall high. Normal patient cores showed considerably lower levels of BCL-X_L expression when compared to tumour cores and tumour advancing front (Figure 4.4), in agreement with previous data showing high levels of BCL-X_L expression in HNSCC cell lines (Figure 4.2). This indicated that BCL-X_L may be a good marker for HNSCC prognosis and that it could be potentially targeted in a therapeutic context.

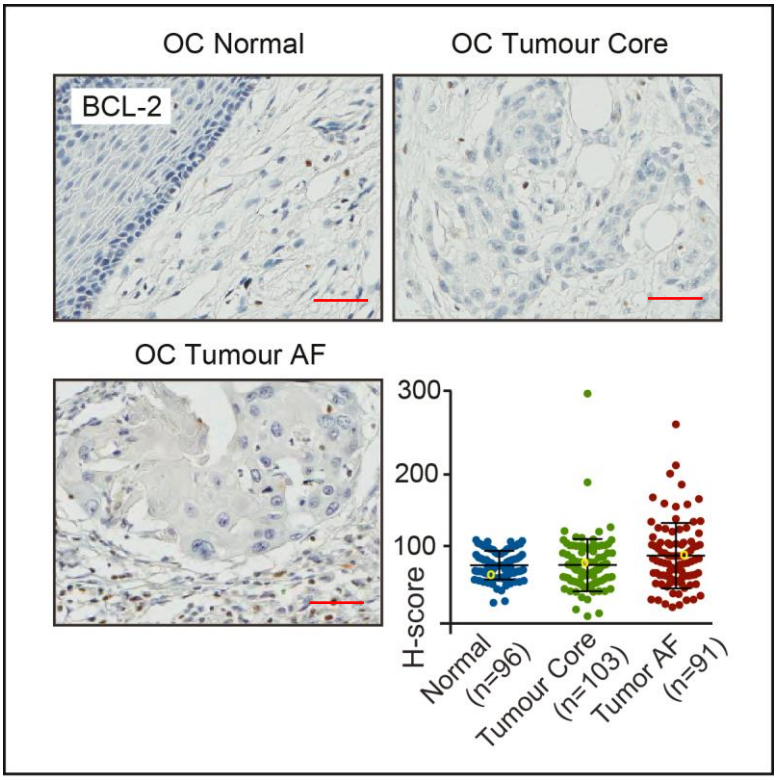

Figure 4.3. BCL-2 is poorly expressed in HNSCC oral cavity. TMAs of oral cavity (OC) obtained from normal patients, tumour core and tumour advancing front (AF) stained with anti-BCL-2 antibody and counter-stained for haematoxylin. Scale bar: 50 µm. TMA cores were assessed for the intensity of BCL-2 antibody staining using QuPath software (H-score). Yellow hollow circles represent the core section chosen as a representative image. Statistical analysis was conducted using one-way ANOVA and multiple comparison tests were conducted using Fisher's LSD test (***P≤0.001). Work done in collaboration with Dr. Rachel Carter.

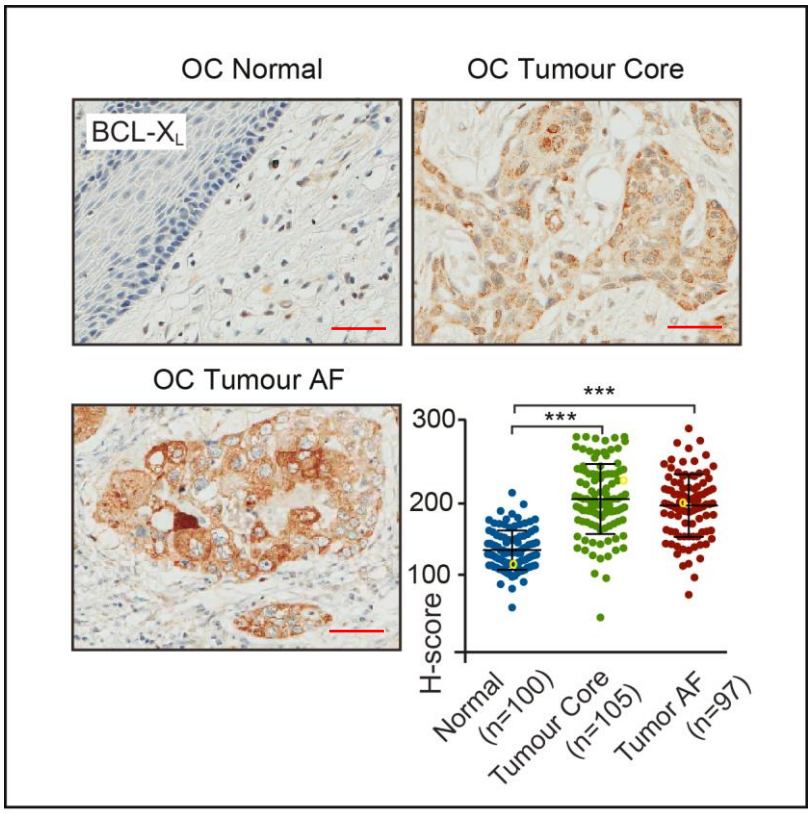

Figure 4.4. BCL-X_L is highly expressed in HNSCC oral cavity. TMAs of oral cavity (OC) obtained from normal patients, tumour core and tumour advancing front (AF) stained with anti-BCL-X_L antibody and counter-stained for haematoxylin. Scale bar: 50 µm. TMA cores were assessed for the intensity of BCL-X_L antibody staining using QuPath software (H-score). Yellow hollow circles represent the core section chosen as a representative image. Statistical analysis was conducted using one-way ANOVA and multiple comparison tests were conducted using Fisher's LSD test (***P≤0.001). Work done in collaboration with Dr. Rachel Carter.

4.2.5 MCL-1 is highly expressed in HNSCC oral cavity tissue

Similar to BCL-X_L, MCL-1 expression levels were higher in the tumour core and advancing front than normal tissues. In addition, oral cavity tumour cores exhibited higher levels of MCL-1 expression than advancing front cores, which could indicate that the role of MCL-1 in this cancer might be involved in precursor tumour cells (tumour core) but not so much in the derived cells (advancing front) (Figure 4.5). These data confirm that HNSCC tumours express high levels of MCL-1 and therefore MCL-1 could be a good target for potential BH3 mimetic therapy.

4.2.6 BH3 mimetics do not accentuate the effects of cisplatin in reducing the clonogenic potential of HNSCC cell lines

Since cisplatin is the first-line chemotherapy for HNSCC, the specified cell lines were exposed to cisplatin in combination with the different BH3 mimetics and assessed for changes in their clonogenic potential. This was performed by quantifying the percentage of colonies that survived the specific treatments (surviving fraction). Cisplatin exposure alone greatly reduced clonogenicity of UM-SCC-11B, -17A and -74A, however this was not exacerbated when combined with BH3 mimetics. UM-SCC-1 cells exhibited mild reduction of clonogenicity by cisplatin and A-1331852 was the only BH3 mimetic capable of further reducing the clonogenic potential of this cell line. UM-SCC-17AS and 81B were the most resistant cells, showing a small reduction of clonogenic potential by cisplatin alone, which was not exacerbated when combined with any of the BH3 mimetics (Figure 4.6). These results indicate that co-administration of BH3 mimetics with cisplatin may not offer any therapeutic benefit over cisplatin monotherapy in HNSCC.

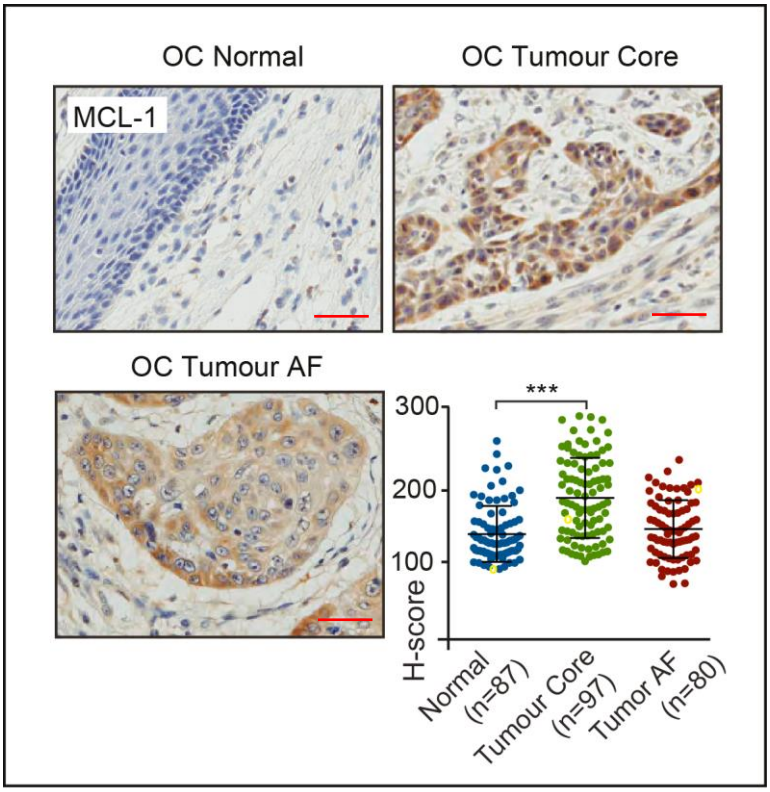

Figure 4.5. MCL-1 is highly expressed in HNSCC oral cavity. TMAs of oral cavity (OC) obtained from normal patients, tumour core and tumour advancing front (AF) stained with anti-MCL-1 antibody and counter-stained for haematoxylin. Scale bar: 50 µm. TMA cores were assessed for the intensity of MCL-1 antibody staining using QuPath software (H-score). Yellow hollow circles represent the core section chosen as a representative image. Statistical analysis was conducted using one-way ANOVA and multiple comparison tests were conducted using Fisher's LSD test (***P≤0.001). Work done in collaboration with Dr. Rachel Carter.

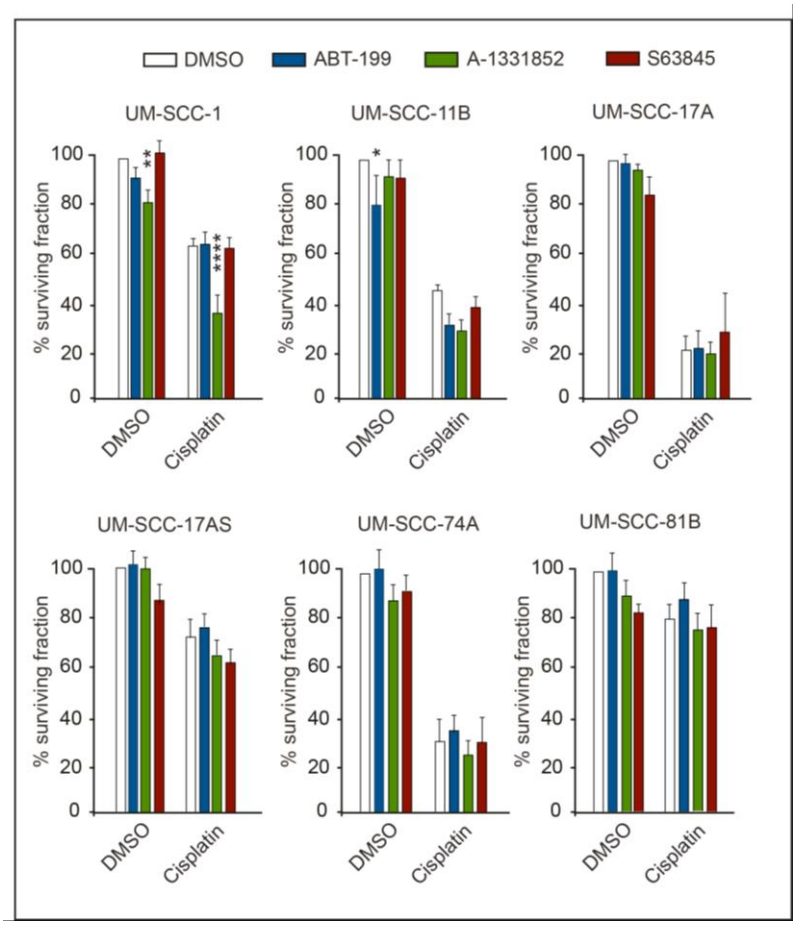

Figure 4.6. Single inhibition of BCL-2, BCL-X_L or MCL-1 does not affect native or cisplatin-induced clonogenic survival of several head and neck cancer cell lines. Several head and neck cancer cell lines were exposed to ABT-199 (100 nM), A-1331852 (100 nM) or S63845 (100 nM) alone or in combination with cisplatin (1 μM) for 7 days and assessed for clonogenic survival. Error bars represent the S.E.M. for at least three independent biological replicates. Statistical analysis was conducted using one-way ANOVA and multiple comparison tests were conducted using Fisher's LSD test (***P≤0.001).

4.2.7 Inhibition of both BCL-X_L and MCL-1 induce apoptosis in HNSCC cell lines

Since exposure to individual BH3 mimetics did not reduce clonogenic potential of HNSCC cells, these studies were extended to assess whether exposing the HNSCC cell lines to a combination of BH3 mimetics could induce apoptosis. As expected, BH3 mimetics, when used as single agents, were not capable of promoting apoptosis in these cells, confirming that these cells must depend on more than one anti-apoptotic member of the BCL-2 family (Figure 4.7 A). Similarly, inhibiting both BCL-2 and BCL-X_L (by ABT-199 and A-1331852, respectively) or both BCL-2 and MCL-1 (by ABT-199 and S63845, respectively) did not induce apoptosis in any of the cell lines (Figure 4.7 B and C). However, a dual inhibition of BCL-X_L and MCL-1 (by A-1331852 and S63845, respectively) greatly induced apoptosis in all HNSCC cell lines (Figure 4.7 D). These results are in accordance to the initial findings on several solid tumour cell lines, showing dependence on both BCL-X_L and MCL-1 for survival and indicate that HNSCC cells also depend on these two proteins.

4.2.8 The clonogenic survival of HNSCC cell lines is greatly impaired by inhibition of both BCL-X_L and MCL-1

As inhibition of both BCL-X_L and MCL-1 induced apoptosis, experiments were performed to investigate whether a combination of A-1331852 and S63845 would also decrease clonogenic potential of these cells. Indeed, targeting both BCL-X_L and MCL-1 with A-1331852 and S63845, respectively greatly reduced the clonogenic potential of all HNSCC cell lines used in this study (Figure 4.8), further confirming the dual dependency on BCL-X_L and MCL-1 of HNSCC cells and unveiling a potential new therapy for HNSCC.

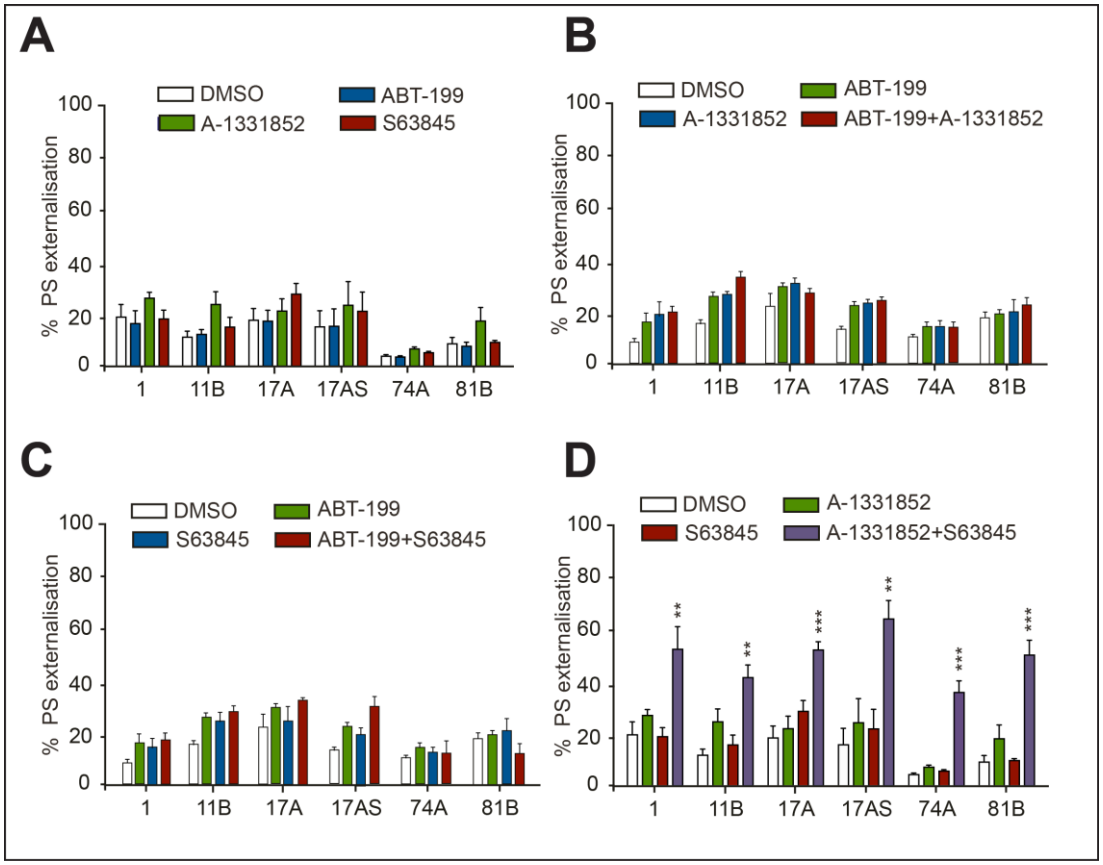

Figure 4.7. HNSCC cell lines depend on both BCL-X_L and MCL-1 for survival. HNSCC cell lines were exposed to ABT-199 (100 nM), A-1331852 (100 nM), S63845 (100 nM) alone or in combination for 24 h and assessed for the extent of PS externalisation by FACS. **(A)** Single BH3 mimetics exposure. **(B)** Inhibition of BCL-2 and BCL-X_L **(C)** Inhibition of BCL-2 and MCL-1**. (D)** Inhibition of BCL-X_L and MCL-1. Error bars represent the S.E.M. for at least three independent biological replicates. Statistical analysis was conducted using one-way ANOVA and multiple comparison tests were conducted using Fisher's LSD test (***P≤0.001).

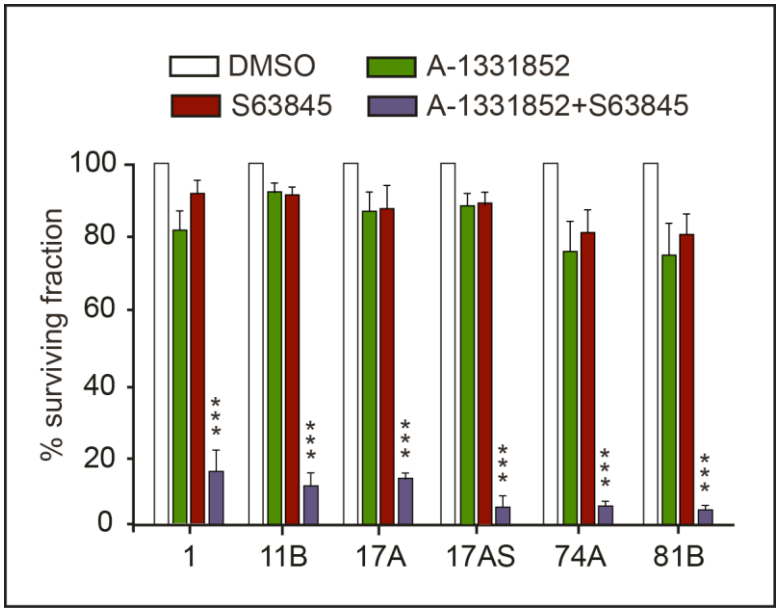

Figure 4.8. Inhibition of both BCL-X_L and MCL-1 greatly impairs clonogenic survival of several HNSCC cell lines. Indicated HNSCC cell lines were exposed to A-1331852 (100 nM), S63845 (100 nM) or a combination of both for 7 days and assessed for clonogenic survival. Error bars represent the S.E.M. for at least three independent biological replicates. Statistical analysis was conducted using one-way ANOVA and multiple comparison tests were conducted using Fisher's LSD test (***P≤0.001).

4.2.9 Inhibition of both BCL-X_L and MCL-1 induce apoptosis in primary tumours derived from head and neck cancer patients

To corroborate the previous observations that targeting both BCL-X_L and MCL-1 induced apoptosis in HNSCC cell lines, and thus could form a new potential therapy in HNSCC, similar treatments of the specific BH3 mimetics were carried out on the ex-vivo explant cultures of the tumour tissues, freshly resected from patients. The tumour tissues, post-surgery, were collected, treated with BH3 mimetics, fixed, processed, sectioned and stained for apoptosis markers (cleavage of PARP) by Dr. Rachel Carter in our research group. I assisted Dr. Carter in quantifying the cleaved PARP-positive tumour nuclei, and the results from these studies were plotted. As expected, A-1331852 and S63845, when used in combination but not as singe agents, resulted in pronounced apoptosis in patient tissues (Figure 4.9), further confirming the rationale for using this combination therapy in HNSCC.

4.2.10 Several PDAC cell lines express similar levels of the anti-apoptotic BCL-2 family of proteins

Following a similar strategy used to investigate the potential of BH3 mimetic therapy in head and neck cancer, efforts were made to extend these observations to pancreatic cancer. Firstly, the expression levels of BCL-2, BCL-X_L and MCL-1 were assessed in 3 pancreatic cell lines, MIA PaCa-2, PANC-1 and BxPC-3. All 3 cells showed similar expression levels of the proteins (Figure 4.10). Although these cells express considerable amounts of BCL-2, as already demonstrated in Figure 4.1, these cells depend on both BCL-X_L and MCL-1 for survival.

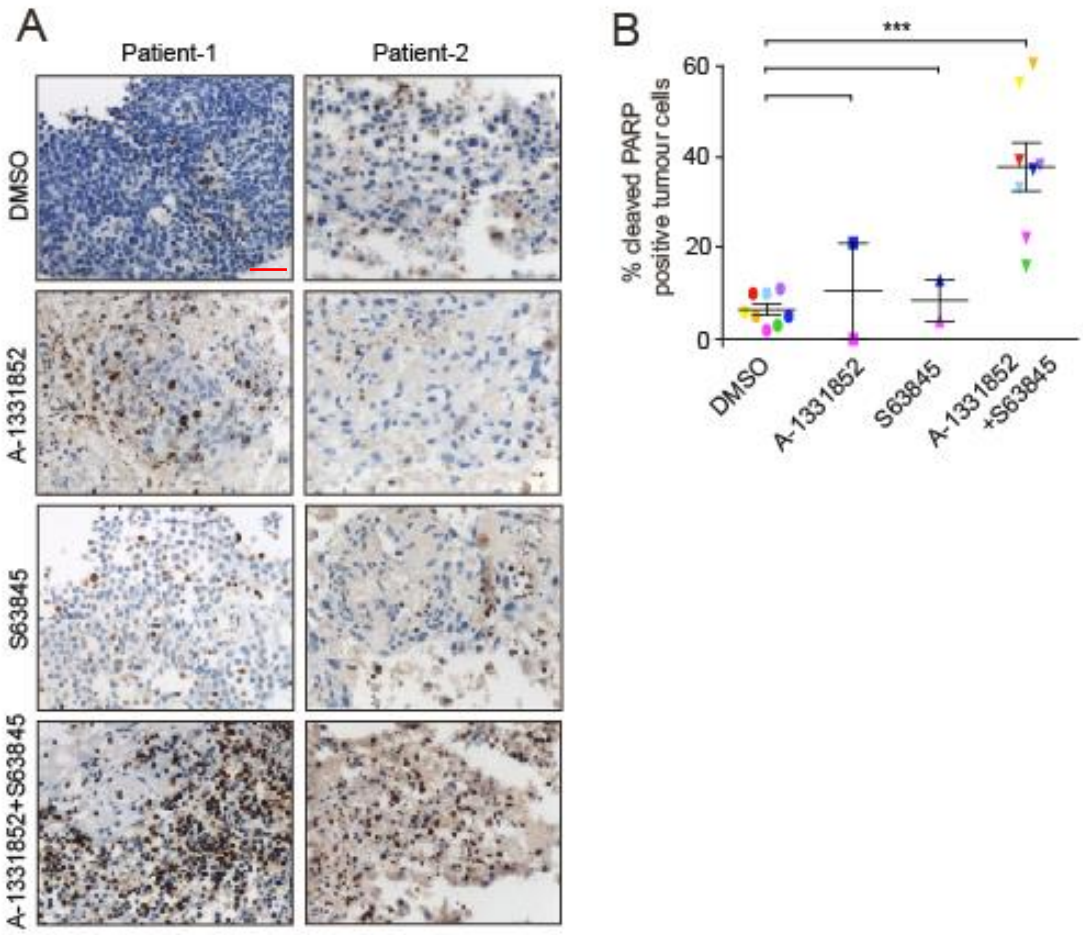

Figure 4.9. Inhibition of both BCL-X_L and MCL-1 induces apoptosis in HNSCC patient tissues. (A) Freshly resected patient tissues of HNSCC were obtained from Aintree University Hospital, cut to 1 mm^3 pieces and exposed to A-1331852 (1 µM), S63845 (1 µM) or a combination of both for 48 h and processed for immunohistochemistry with cleaved PARP antibody (brown staining) and counterstained with haematoxylin (blue staining). Scale bar: 50 µm. **(B)** The percentage of cells positively stained for cleaved PARP was quantified for different patient-derived tissues (colour coded for each patient). Statistical analysis was conducted using one-way ANOVA and multiple comparison tests were conducted using Fisher's LSD test (***P≤0.001). Work done in collaboration with Dr. Rachel Carter.

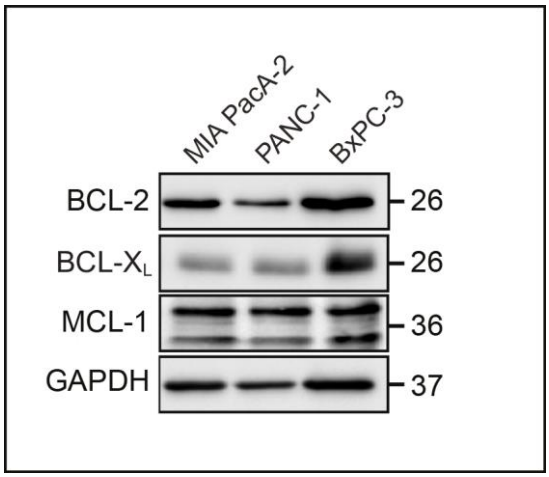

Figure 4.10. Protein expression levels of the anti-apoptotic BCL-2 family members in several PDAC cell lines. Immunoblot of several pancreatic cancer cell lines showing expression levels of BCL-1, BCL-X_L and MCL-1. GAPDH was used as loading control.

4.2.11 BCL-2, BCL-X_L and MCL-1 are highly expressed in pancreatic cancer

Similar to the TMA analysis that was carried out using HNSCC patient samples, pancreatic cancer TMAs obtained from Liverpool biobank were immunostained with BCL-2, BCL-X_L and MCL-1 antibodies and H-score was determined using QuPath analysis. Expression levels of BCL-2 were variable among the TMA cores, with slightly more cores expressing low levels of the protein (Figure 4.11). In contrast, BCL-X_L was highly expressed in the great majority of the cores, with a few cores showing moderate staining and no core exhibiting low staining (Figure 4.12). MCL-1 expression levels were also variable, with most of the cores expressing moderate amounts of the protein (Figure 4.13).

4.2.12 Expression levels of BCL-2, BCL-X_L and MCL-1 in pancreatic cancer TMAs do not correlate with overall patient survival

Next, the expression levels of BCL-2, BCL-X_L and MCL-1 were correlated with overall survival in the corresponding pancreatic cancer patients. Using data obtained from TMA analysis and patient data obtained from Liverpool biobank, Kaplan-Meier estimators were generated to verify whether expression levels of BCL-2, BCL-X_L and MCL-1 would be good estimators of overall patient survival. Statistical analysis by logrank test indicated that expression levels of BCL-2, BCL-X_L and MCL-1 are not good estimators for overall patient survival (Figure 4.14). These results suggested that expression levels of these anti-apoptotic BCL-2 family of proteins may not necessarily contribute to disease progression in pancreatic cancer. Nevertheless, targeting these proteins have been shown to be effective in inducing apoptosis, and hence a reasonable strategy to be taken forward.

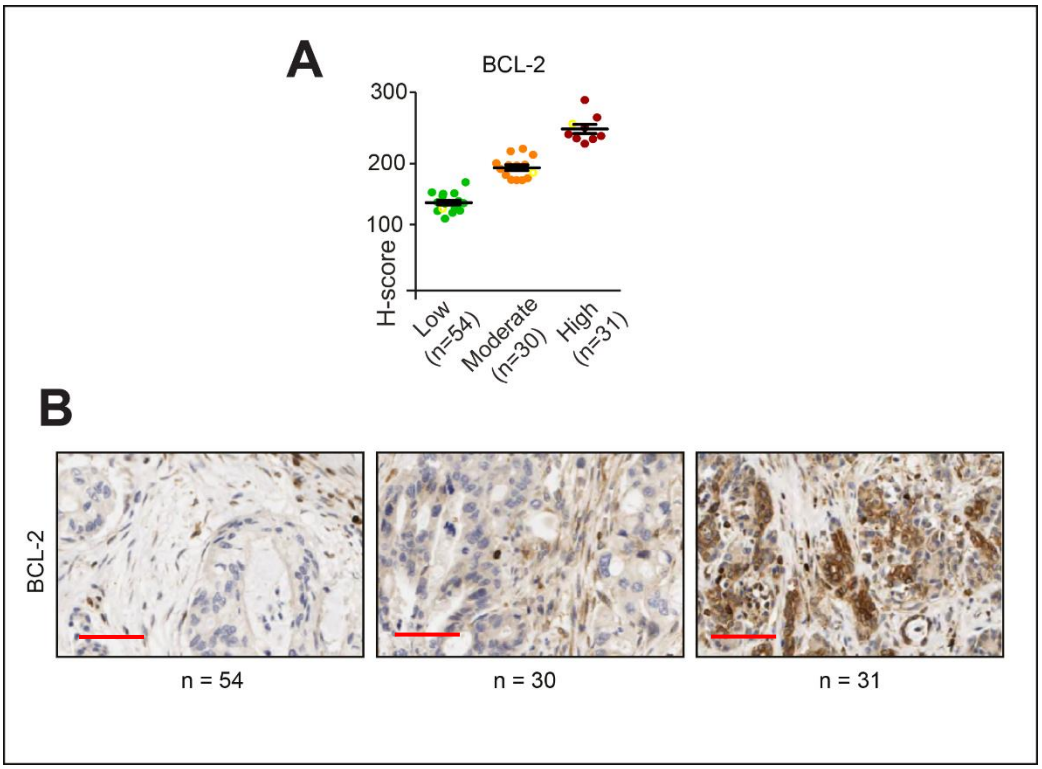

Figure 4.11. BCL-2 expression is evenly distributed among the tumour cores of PDAC patients. TMAs from PDAC patients were stained with anti-BCL-2 antibody, counter-stained for haematoxylin and H-score on QuPath software. **(A)** TMA cores were assessed for the intensity of antibodies staining using QuPath software (H-score). Yellow hollow circles represent the core section chosen as a representative image **(B)** Representative images of TMA cores for BCL-2 staining levels and respective n numbers for each *stratum*. Scale bar: 50 μm.

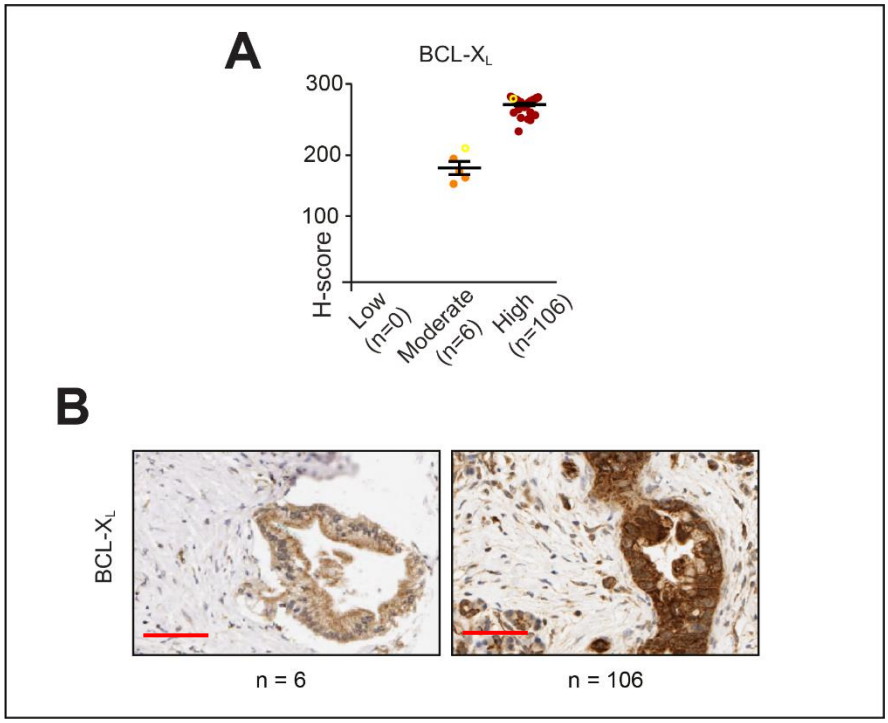

Figure 4.12. BCL-X_L expression is generally high in the tumour cores of PDAC patients. TMAs from PDAC patients were stained with anti-BCL-X_L antibody, counter-stained for haematoxylin and H-score on QuPath software. **(A)** TMA cores were assessed for the intensity of antibodies staining using QuPath software (H-score). Yellow hollow circles represent the core section chosen as a representative image **(B)** Representative images of TMA cores for BCL-X_L staining levels and respective n numbers for each *stratum*. Cores with low levels of BCL-X_L could not be detected. Scale bar: 50 µm.

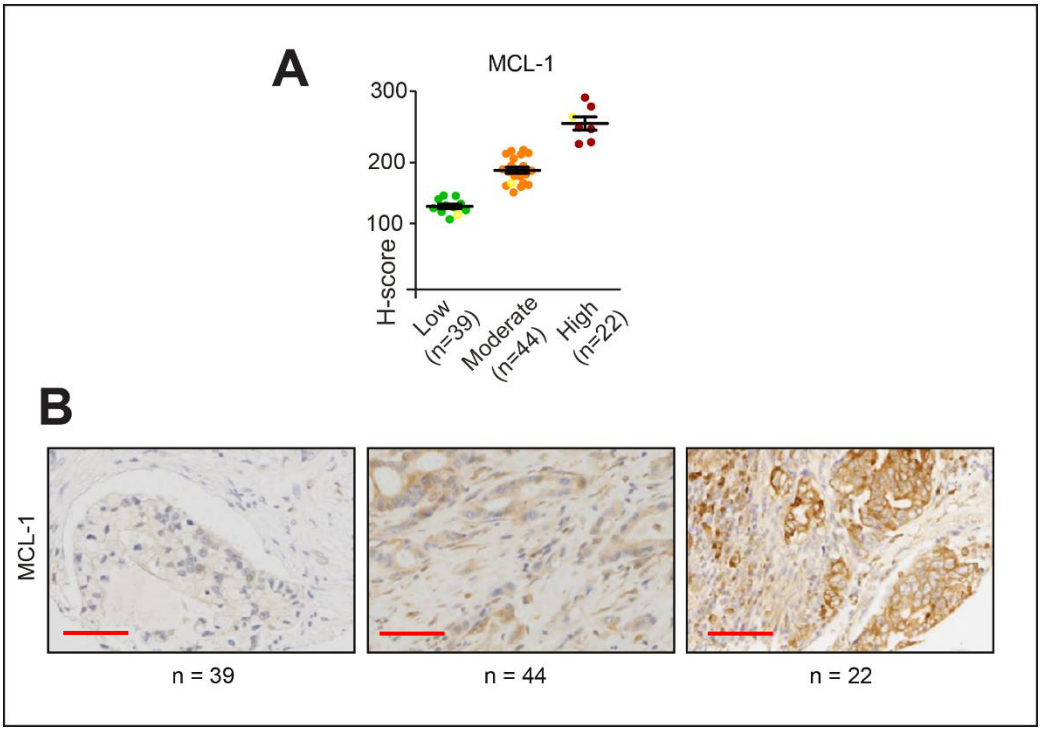

Figure 4.13. MCL-1 expression is evenly distributed among the tumour cores of PDAC patients. TMAs from PDAC patients were stained with anti-MCL-1 antibody, counter-stained for haematoxylin and H-score on QuPath software. **(A)** TMA cores were assessed for the intensity of antibodies staining using QuPath software (H-score). Yellow hollow circles represent the core section chosen as a representative image **(B)** Representative images of TMA cores for MCL-1 staining levels and respective n numbers for each *stratum*. Scale bar: 50 μm.

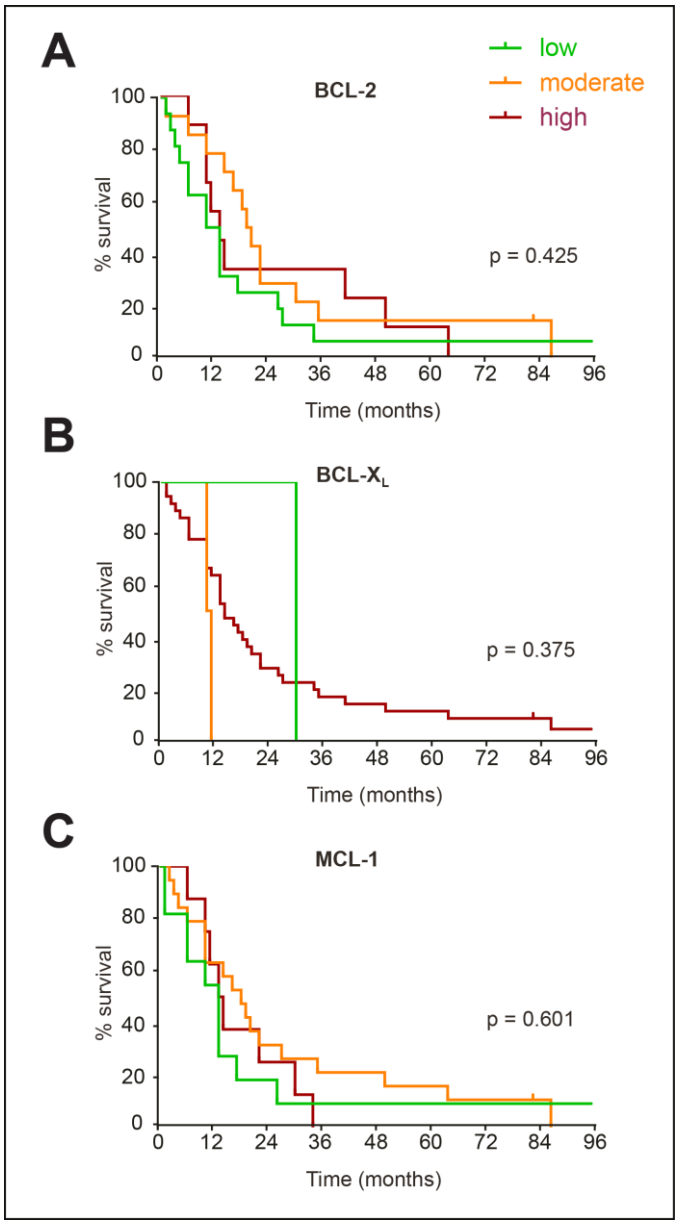

Figure 4.14. Kaplan-Meier plots reveal no correlation between the overall survival of patients and expression levels of anti-apoptotic BCL-2 family members. Low, moderate and high expression levels of **(A)** BCL-2 **(B)** BCL-X_L and **(C)** MCL-1 obtained from H-scores of TMA cores of pancreatic cancer patients (showed in Figures 4.11, 4.12 and 4.13), were analysed against patient survival time after diagnostic. Stratification for low, moderate and high expression levels were obtained from QuPath recommendations for 3 bins based on H-score. Statistical analysis was conducted by using logrank test, $p \leq 0.05$.

4.2.13 BH3 mimetics may enhance gemcitabine-mediated apoptosis in PDAC

In order to assess whether targeting BCL-X_L or MCL-1 would synergise with a standard treatment such as gemcitabine in inducting apoptosis in pancreatic cancer, MIA PaCa-2, PANC-1 and BxPC-3 cells were exposed to increasing concentrations of gemcitabine alone or in combination with A-1331852 or S63845 and assessed for changes in the extent of apoptosis. While A-1331852 but not S63845 in combination with gemcitabine enhanced apoptosis in BxPC-3 cells, no such effects were observed in MIA Paca-2 and PANC-1 cells (Figure 4.15).

4.2.14 Inhibition of BCL-X_L in combination with gemcitabine decreases the clonogenic potential of PDAC cell lines

Next, the treatments mentioned above were carried out in the same cell lines to measure their clonogenic potential. Exposure to A-1331852 diminished the ability of the cells to form distinct colonies, especially when gemcitabine was simultaneously administered (Figure 4.16). This effect was more pronounced in BxPC-3 cells compared to the other two cell lines, indicating that inhibiting BCL-X_L in combination with gemcitabine treatment could be beneficial to some pancreatic cancer patients. However, this study could not be extended to tumour samples from patients due to the unavailability of PDAC patient tumour tissues during this study.

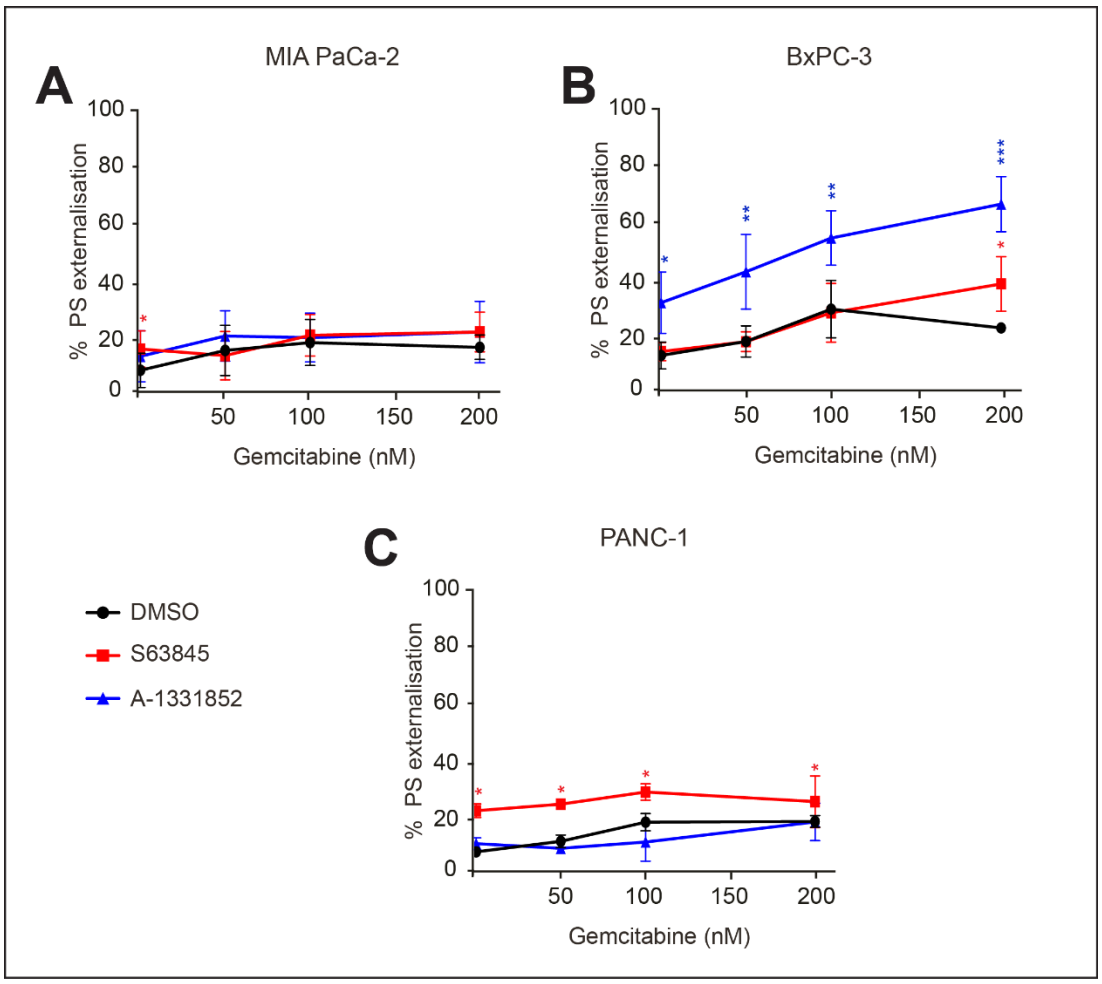

Figure 4.15. Gemcitabine-mediated apoptosis is enhanced by inhibition of BCL-X_L or MCL-1. The PDAC cell lines **(A)** MIA PaCa-2, **(B)** BxPC-3 and **(C)** PANC-1 were exposed to different concentrations of gemcitabine alone (black line) or in combination with S63845 (100 nM; red line) or A-1331852 (100 nM; blue line) for 24 h and assessed for the extent of PS externalisation by FACS. Statistical analysis was conducted using two-way ANOVA (***P≤0.001).

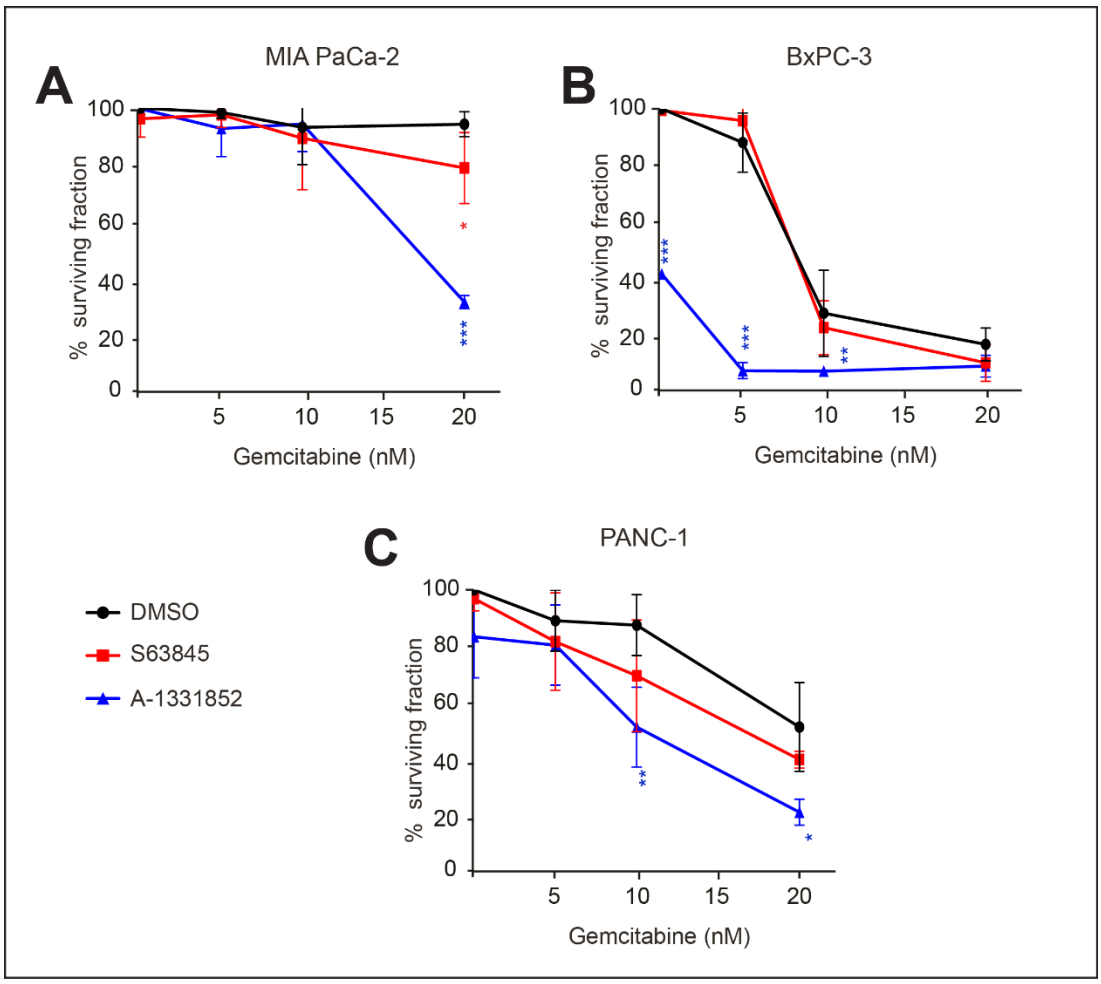

Figure 4.16. Gemcitabine-mediated decrease in clonogenic potential is further decreased by inhibition of BCL-X_L or MCL-1. The PDAC cell lines **(A)** MIA PaCa-2, **(B)** BxPC-3 and **(C)** PANC-1 were exposed to different concentrations of gemcitabine alone (black line) or in combination with S63845 (10 nM; red line) or A-1331852 (10 nM; blue line) for 7 days and assessed for clonogenic survival. Statistical analysis was conducted using two-way ANOVA (***P≤0.001).

4.3 Discussion

HNSCC and PDAC comprise together approximately 20,000 new cases per year in the UK.[252] Main line of chemotherapy for both of these cancers are agents that target DNA (antimetabolites and alkylating agents) that have been used for more than 25 years. The problems associated with such therapy (resistance/toxicity) emphasise the need for newer, more specific and more potent treatments.[229,239,253,254] Screening several cell lines from HNSCC and PDAC to assess dependencies on the different anti-apoptotic BCL-2 family members revealed that BCL-X_L and MCL-1 are promising therapeutic targets (Figure 4.1). Furthermore, protein expression analysis of head and neck cell lines showed high expression levels of BCL-X_L and MCL-1 (Figure 4.2), which was confirmed by patient TMA analysis (Figures 4.3 - 4.5), thus raising the potential of BH3 mimetic therapy in HNSCC.

BH3 mimetics such as ABT-737 and gossypol have been studied as potential therapy for head and neck cancer, especially when used in combination with cisplatin.[234,255] However, the data presented here suggests that targeting BCL-X_L, MCL-1 or BCL-2 with more specific BH3 mimetics does not improve cisplatin-mediated decrease in clonogenicity of HNSCC cell lines (Figure 4.6). Nevertheless, inhibition of both BCL-X_L and MCL-1 drastically reduced clonogenic potential and induced apoptosis in all HNSCC cell lines tested (Figure 4.7 and 4.8), indicating that co-administration of these inhibitors could be valuable to head and neck cancer patients. Moreover, this strategy could potentially benefit patients by reducing cisplatin-related toxicity side effects such as myelosuppression, nephrotoxicity, vomiting and others.[228]

Similarly, expression profile of pancreatic cancer cell lines and TMAs revealed that MCL-1 and BCL-X_L were highly expressed in PDAC (Figures 4.12 and 4.13). In pancreatic cancer, the use of BH3 mimetics has been studied more extensively in comparison to head and neck cancer. BH3 mimetics such as sabutoclax and apogossypol have been shown to enhance the sensitivity if pancreatic cancer cells to gemcitabine.[256,257] However, these BH3 mimetics are much less specific than the recently developed inhibitors, such as A-1210477 and S63845.[168,251,258] Moreover, a recent study showed that ABT-199 alone enhanced sensitivity to gemcitabine by reducing BCL-2 protein expression, indicating BCL-2 could also be an important target in pancreatic cancer.[245] This is not in line with the results presented in this chapter, as expression levels of BCL-2 were generally low in the PDAC patient TMAs (Figure 4.11). Nevertheless, genetic inhibition of BCL-X_L and MCL-1 has been shown to induce apoptosis in pancreatic cancer cells,[250] in agreement to the data shown here (Figures 4.12 and 4.13), suggesting that these two proteins could be potentially targeted to improve therapy.

Taken together, the results presented in this chapter show that using BH3 mimetics in solid tumours and more specifically in head and neck and pancreatic cancer, could be beneficial and that BCL-X_L and MCL-1 play an important role in regulating the survival of these cancer cells, thus making them potential targets for chemotherapy.

CHAPTER 5

Characterisation of the mitochondrial structural changes during BH3 mimetic-mediated apoptosis

Chapter contents

5.1 Introduction

Having emerged as an endosymbiont from ancient bacteria,[259] the subcellular organelle, the mitochondrion, possesses its own DNA, proteins and division processes.[260] Recent studies have redefined the intricacies around mitochondrial structure and function, and confirmed that the mitochondrial network acts in tight conjunction with the host cell, sharing proteins and processes that are fundamental for cellular homeostasis. This complex mitochondrial dynamic network that spreads throughout the cell is organised and maintained by a balance of mitochondrial fission and fusion events, named mitochondrial membrane dynamics.[260]

Mitochondrial membrane dynamics are orchestrated by GTPases proteins of the dynamin superfamily. Fission events are catalysed mainly by DRP-1, which is recruited transiently from the cytosol to its receptors, MFF, MiD49, MiD51 and Fis1, at the mitochondrial fission sites.[261] DRP-1 contains a highly conserved N-terminal GTPase domain that homodimerizes in the presence of GTP.[262] This self-assembly mechanism continues to recruit additional DRP-1 molecules in a ring like structure transversally around the mitochondria. In the following steps, this newly assembled DRP-1 ring undergoes further conformational changes, tightening the target membrane and inducing fission of the mitochondrial membrane.[261] Notably, DRP-1 overexpression does not directly induce mitochondrial fission, as DRP-1 activity is dependent of different post-translational modifications, such as phosphorylation, which is controlled by proteins regulating different pathways within the cell. Of those, kinases such as cyclin-dependent kinases phosphorylate DRP-1 at Ser616, inducing activity of the GTPase.[263] On the other hand, DRP-1 activity can be inhibited by phosphorylation at Ser637 by protein kinase A,[264] which in turn can be counteracted by calcineurin.[265]

Fusion events are catalysed by mitofusins 1 and 2 (MFN1 and MFN2), responsible for outer mitochondrial membrane fusion and OPA-1, responsible for inner mitochondrial membrane fusion (Figure 5.1).[261] After mRNA splicing OPA-1 exists as 2 long (L-OPA-1) and 3 short (S-OPA-1) variants[266] which control the closure and maintenance of the structure of the mitochondrial cristae, crucial for trapping cytochrome *c* in the electron transport chain and for proper functioning of mitochondrial oxidative phosphorylation.[267] Upon mitochondrial stress, membrane-bound L-OPA-1 can be proteolysed by the metalloproteases YME1L (ATP-dependent metalloprotease YME1L1) and OMA1 (Oma1 zinc metallopeptidase), which cleave L-OPA-1 to produce S-OPA-1.[268,269] Notably a balance between the long and short isoforms of OPA-1 is a pre-requisite for a healthy mitochondria, while a shift towards the short isoforms promotes mitochondrial dysfunction.[266] Moreover, it has been shown that inhibition of ATP-synthase reduces OPA-1 processing by OMA1, altering mitochondrial remodelling dynamics induced by DRP-1 and hindering mitochondrial fission in an attempt to prevent cell death.[270,271] In addition, DRP-1 function can be regulated by mitochondrial redox status. Enhanced mitochondrial respiration induces production of ROS which stimulates DRP-1 phosphorylation at Ser616, promoting mitochondrial fission.[272] Moreover, mitochondrial membrane dynamics also play an important role during cell death, as mitochondria constitute the initiation sites of the intrinsic apoptotic pathway. It has been known that cytochrome *c* release requires inner mitochondrial membrane remodelling and OPA-1 proteolysis for a successful release to the intermembrane space and to further reach the cytosol via BAK and BAX pores (Figure 5.2).[273,274]

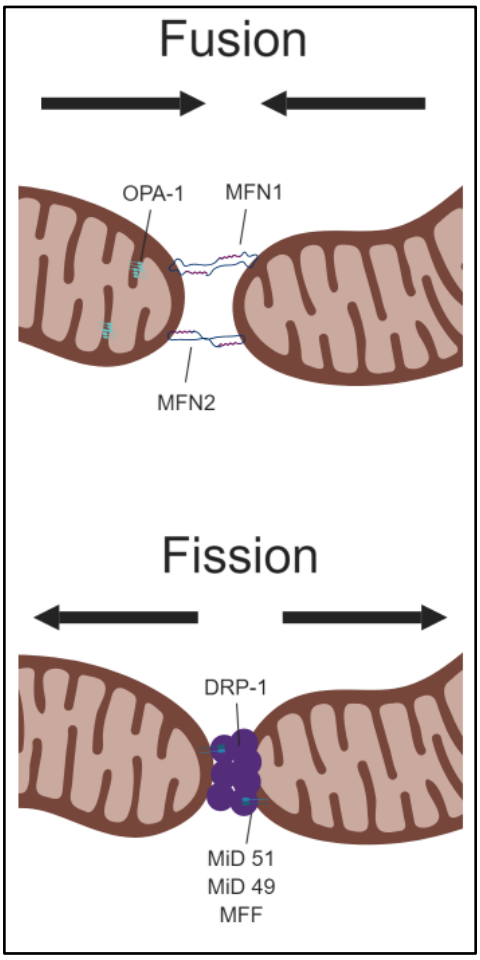

Figure 5.1. The main processes of mitochondrial membrane dynamics. Mitochondrial fusion is mediated by MFN1 and MFN2 in the OMM and by OPA-1 in the IMM, whereas mitochondrial fission is mediated by binding of DRP-1 to its receptors in the OMM, which in turn forms a constriction ring to tighten mitochondrial surface, ultimately parting a mitochondrion.

These studies have focussed on unravelling the mechanisms of mitochondrial membrane dynamics and multi-organelle interplay by monitoring the molecular changes of mitochondrial membranes, fission/fusion proteins and ionic exchange with other organelles.[275–278] However, most of these studies lack detailed information on how these events relate to apoptosis. In addition, the assessment of mitochondrial membrane dynamics and cell death, in the context of BH3 mimetics has been minimal. Previously, it has been shown that ABT-737 induces OMM breaks in primary B-cell malignancies cell lines independently of caspase activity, which could be due to changes in the mitochondrial ionic influx.[279] Furthermore, putative MCL-1 inhibitors such as sabutoclax, BI112D1 and maritoclax have been shown to induce mitochondrial fragmentation independently of MCL-1, DRP-1, BAX or BAK by a mechanism not yet elucidated.[68,280]

There is clearly a lack of clear understanding on the mitochondrial ultrastructural changes that occur during BH3 mimetic-mediated apoptosis. This chapter is aimed at understanding whether BH3 mimetics induce mitochondrial structural changes, either upstream/downstream/independent of the apoptotic cascade. The study further extends to answer whether such mitochondrial changes, if upstream or independent from apoptosis, are a prerequisite for the efficient execution of apoptosis.

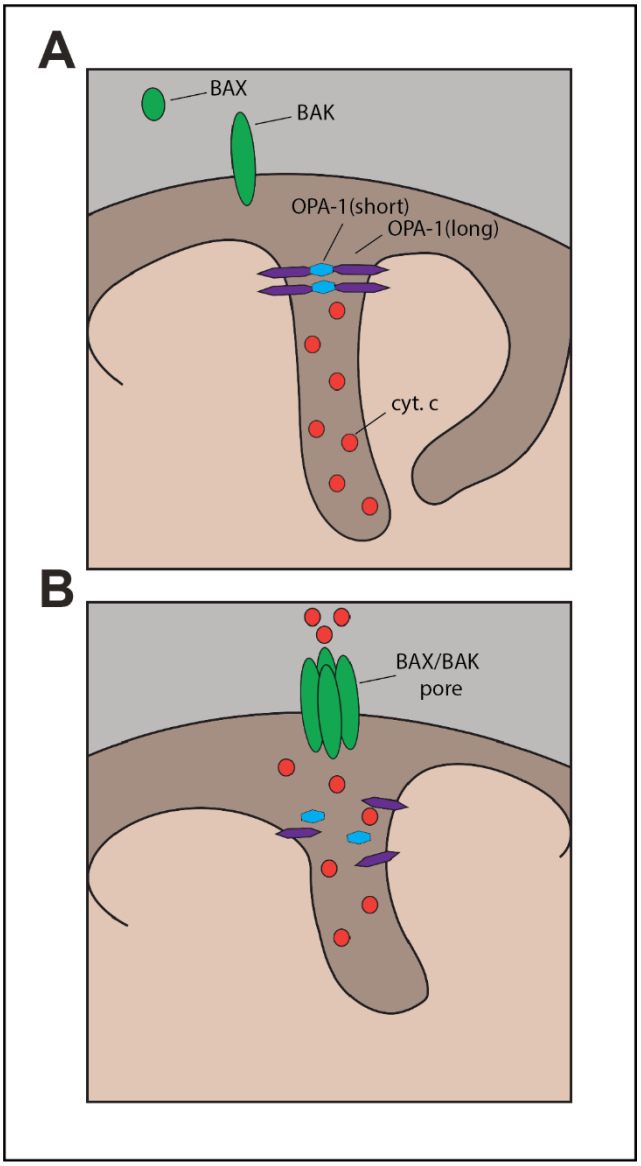

Figure 5.2. Control of cristae structure by OPA-1. (A) Under normal conditions, BAX and BAK are inactive and OPA-1 is engaged in trapping cytochrome *c* within mitochondrial cristae. **(B)** Under apoptotic conditions, OPA-1 is proteolysed, which facilitates the release of cytochrome *c* to the cytosol via BAX/BAK pores in the OMM.

5.2 Results

5.2.1 BH3 mimetics induce rapid mitochondrial structural perturbations

BH3 mimetics were designed to specifically induce apoptosis *via* the intrinsic pathway,[281] therefore experiments were performed to verify how these small molecules affect mitochondrial structure and function in different cell lines. For this, three haematological cancer cell lines that depend on distinct BCL-2 family members for survival were chosen. The cell lines were - H929 (derived from multiple myeloma and depend on MCL-1 for survival), K562 (derived from CML and depend on BCL-X_L) and MAVER-1 (derived from mantle cell lymphoma and depend on BCL-2).[248] Those three cell lines were exposed to the corresponding BH3 mimetics and subjected to electron microscopy to observe mitochondrial structural changes. In the control cells exposed to DMSO, mitochondria appeared intact with a defined double membrane and organised cristae. Upon exposure to specific BH3 mimetics, these cells showed marked OMM breaks, as well as cristae remodelling, as evidenced by the excessive swelling of the mitochondrial matrix (Figure 5.3, yellow arrowheads).

Since these structural changes were observed following exposure to a single BH3 mimetic in a single-dependent cell line, studies were carried out to assess whether mitochondrial changes would be evident in dual-dependent cell lines derived from solid tumours. The cell lines - H1299 (derived from NSCLC) and HCT-116 (derived from colon cancer), both dependent on BCL-X_L and MCL-1 for survival, as detailed in the previous chapter – were exposed to a combination of A-1210477 and A-1331852 and assessed them for mitochondrial ultrastructural changes. In both cell lines, similar structural perturbations to mitochondria were observed (Figure 5.4), similar to those seen in haematological cell lines, indicating that BH3 mimetics

induce profound mitochondrial structural changes in multiple cell lines. It is important to note that all these experiments were performed in the presence of Z-VAD.FMK, a broad-spectrum caspase inhibitor, to ensure that the observed mitochondrial changes were not due to caspase activation or downstream the apoptotic cascade.

5.2.2 BH3 mimetic-mediated mitochondrial changes are BAX- and BAK-dependent

To further characterise the involvement of BAK and BAX in BH3 mimetic-mediated mitochondrial ultrastructural changes, HCT-116 – both WT (wildtype) and BAX/BAK DKO (double knockout) were exposed to a combination of A-1210477 and A-1331852 and assessed for mitochondrial ultrastructural changes by electron microscopy. WT HCT-116 cells exposed to BH3 mimetics showed extensive mitochondrial deformation, outer membrane breaks and matrix swelling, whereas mitochondria of DKO HCT-116 cells exposed to BH3 mimetics were not affected, showing a similar phenotype to untreated cells (Figure 5.4). These results indicate that BAX and BAK are important for BH3 mimetic-mediated mitochondrial ultrastructural changes and could potentially couple these changes to the intrinsic pathway of apoptosis.

5.2.3 BH3 mimetic-mediated mitochondrial fission occurs before apoptosis

Previous results clearly demonstrate that BH3 mimetics induce drastic perturbations to mitochondrial structure at the level of electron microscopy. However, since the technique is both time consuming and expensive, other avenues were explored to study BH3 mimetic-mediated mitochondrial changes. Immunocytochemistry using an antibody raised against a mitochondrial marker such

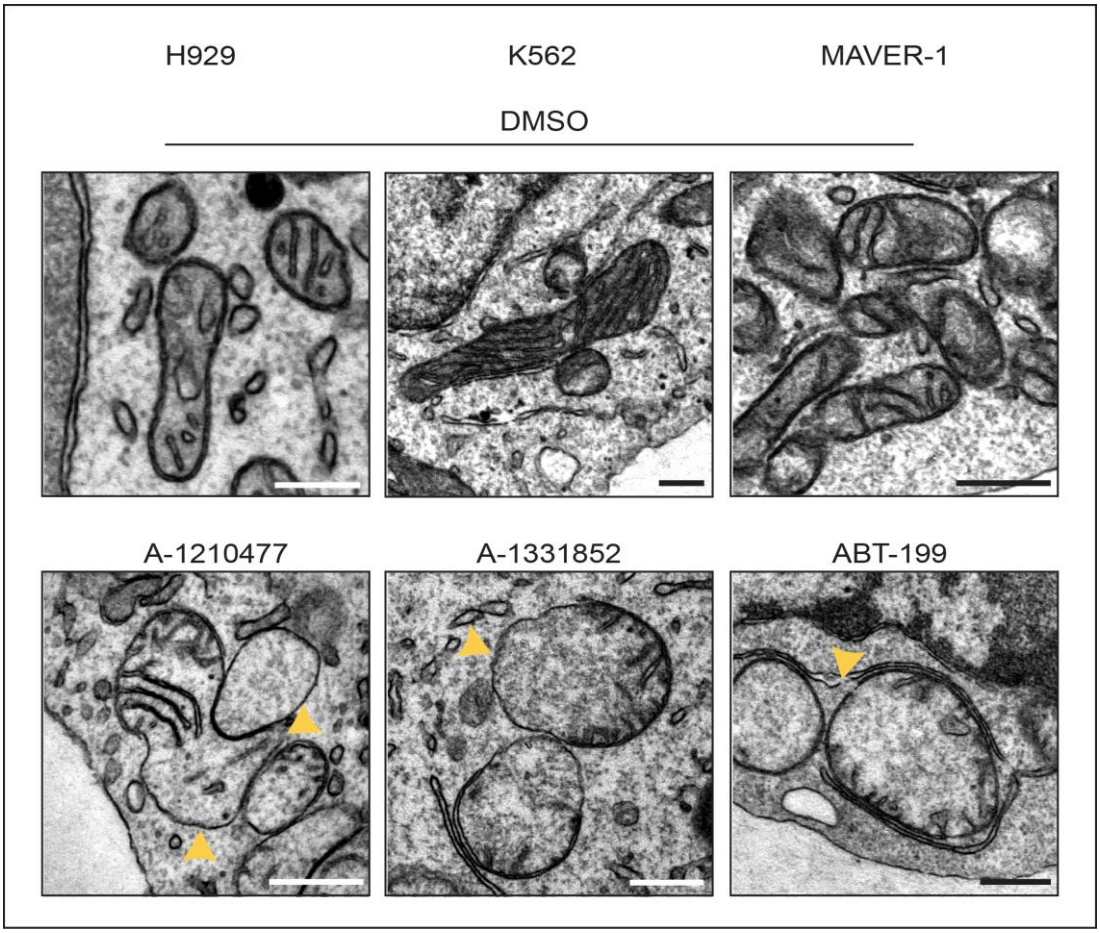

Figure 5.3. BH3 mimetics induce marked mitochondrial ultrastructural changes. H929, K562 and MAVER-1 cells were exposed to A-1210477 (10 µM), A-1331852 (100 nM) or ABT-199 (100 nM) respectively for 4 h and assessed by EM for mitochondrial structural changes. Yellow arrowheads: outer mitochondrial membrane breaks and matrix swelling. Scale bars: 500 nm.

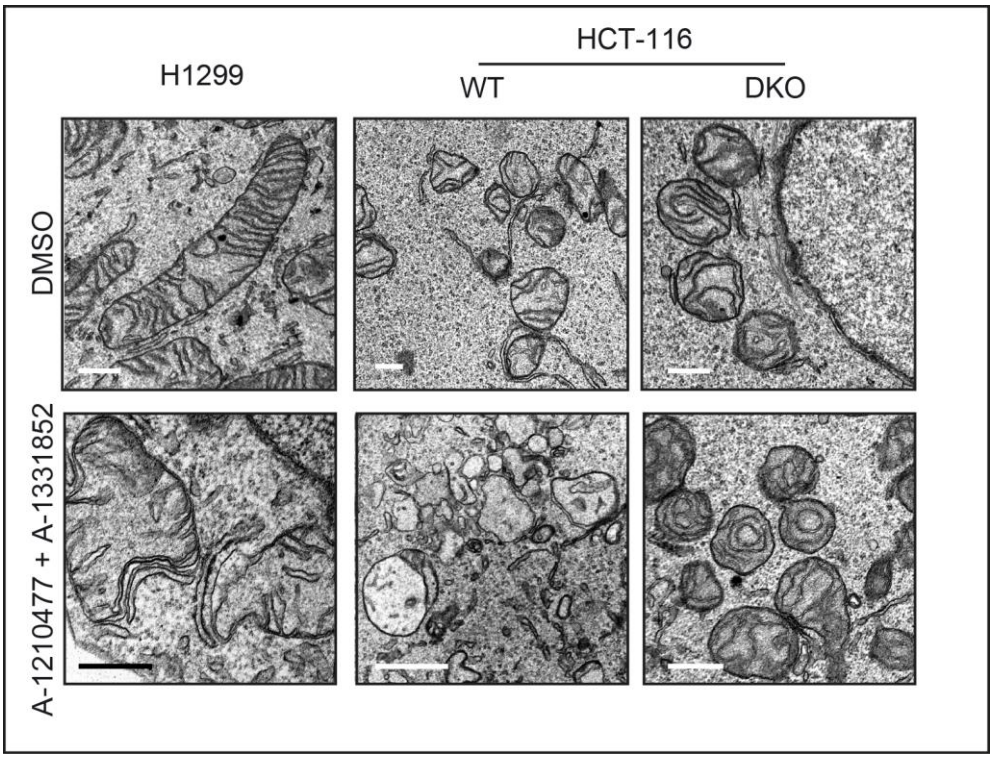

Figure 5.4. BAX and BAK are required for BH3 mimetic-mediated apoptosis-related mitochondrial ultrastructural changes. H1299 and WT or DKO (BAX and BAK deficient) HCT-116 cells were exposed to a combination of A-1210477 (10 μM) and A-1331852 (100 nM) for 4 h and processed for EM for mitochondrial structural changes. Scale bars: 500 nm.

as HSP70 was used to characterise mitochondrial structural changes using confocal microscopy. To assess whether BH3 mimetics mediate mitochondrial structural changes upstream of or independent of apoptosis, the dual (BCL-X_L and MCL-1-) dependent H1299 cells were transfected with siRNAs against BCL-X_L (to render them MCL-1-dependent) or MCL-1 (to render them BCL-X_L-dependent), exposed to either A-1210477 or A-1331852 and subjected to immunocytochemistry and confocal microscopy. Immunolabeling with HSP70 antibody revealed a filamentous mitochondrial network in the control as well as in the BCL-X_L or MCL-1-downregulated cells. However, exposure to A-1210477 induced mitochondrial fragmentation in the cells independently of MCL-1 or BCL-X_L (Figure 5.5). This is line with the extensive mitochondrial fragmentation previously observed with several putative inhibitors of MCL-1.[68,280] Exposure to A-1331852 also resulted in mitochondrial fragmentation but this occurred only when H1299 cells were rendered BCL-X_L-dependent by the removal of MCL-1 (Figure 5.5). Moreover, the fragmented mitochondria in this instance appeared more swollen unlike the more punctate-distribution of mitochondria, observed following A-1210477. These results suggested that A-1210477-mediated mitochondrial fragmentation could be distinct from the mitochondrial fragmentation observed during apoptosis, following the neutralisation of both MCL-1 and BCL-X_L in the H1299 cells.

5.2.4 A-1210477 induces extensive mitochondrial fission in several cell lines, most likely in an MCL-1-dependent but BH3 only-independent manner.

Since A-1210477 induced mitochondrial changes in H1299 cells, studies were performed to verify whether this effect was specific to H1299 cells, or if it can

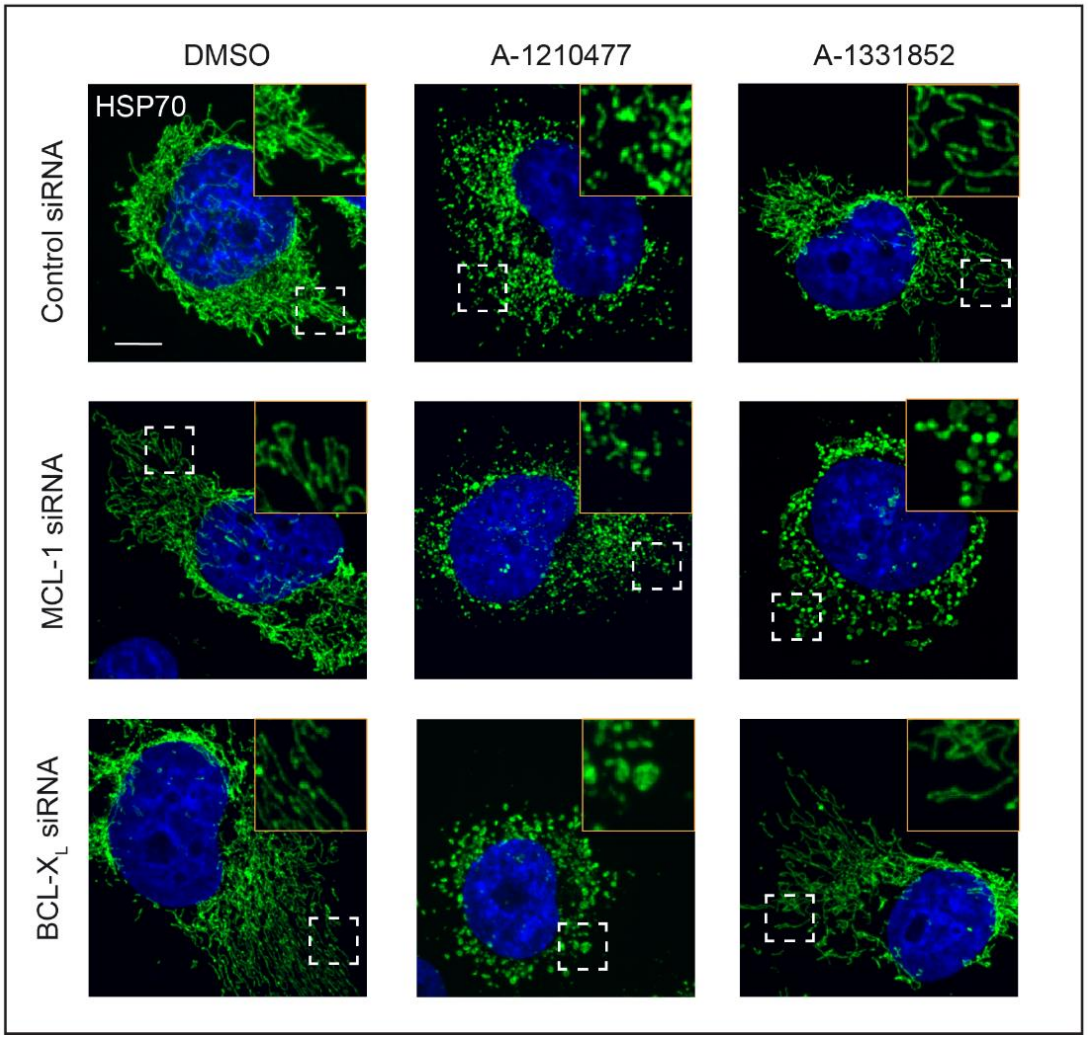

Figure 5.5. Mitochondrial fragmentation mediated by different BH3 mimetics appear to exhibit distinct structural characteristics. H1299 cells were transfected with control, MCL-1 or BCL-X_L siRNA and exposed to DMSO, A-1210477 (10 μM) or A-1331852 (100 nM) for 4 h in the presence of Z-VAD-FMK (30 μM) and assessed for mitochondrial integrity by immunofluorescence with HSP70 antibody. Areas inside dashed line boxes have been zoomed. Scale bar: 10 μm. Images representative of a cell population.

be replicated in several cancer cell lines. Exposure of H23 (a NSCLC cell line), HeLa (a cervical adenocarcinoma cell line) and MCF7 (a breast cancer cell line) to A-1210477 also showed extensive mitochondrial fission compared to the control cells (Figure 5.6). In order to resolve if the mitochondrial fragmentation mediated by A-1210477 was solely due to inhibition of MCL-1 or other nonspecific effect(s), three different strategies were employed to downregulate MCL-1, following which mitochondrial structural changes were assessed. The first strategy involved downregulation of MCL-1 using a genetic knockdown (RNA interference), while the second strategy utilised the short half-life of MCL-1,[64] involving transcriptional repression of MCL-1 using the CDK inhibitor, Dinaciclib.[68] The final strategy was to perform similar studies with the more potent and specific inhibitor of MCL-1, S63845, which has been established to inhibit MCL-1 and induce apoptosis at low nanomolar concentrations.[168,249]

Downregulation of MCL-1 using two different MCL-1-targeting siRNAs or transcriptional repression by Dinaciclib failed to mimic A-1210477 in inducing mitochondrial fragmentation, despite effectively depleting MCL-1 protein levels (Figure 5.7). This suggested that mitochondrial fragmentation observed following exposure of cells to A-1210477 could be due to potential off-target effects of A-1210477, or an on-target activity on MCL-1 affecting protein-protein interactions as part of a large scaffold in which MCL-1 could play a vital role. The latter possibility is speculated to be more likely as multiple putative inhibitors of MCL-1 have previously been reported to induce such mitochondrial fragmentation.[68,280] To gain more clarity on this issue, the third strategy of inhibiting MCL-1 using S63845 was executed. In marked contrast to the observations made with A-1210477, S63845 at a

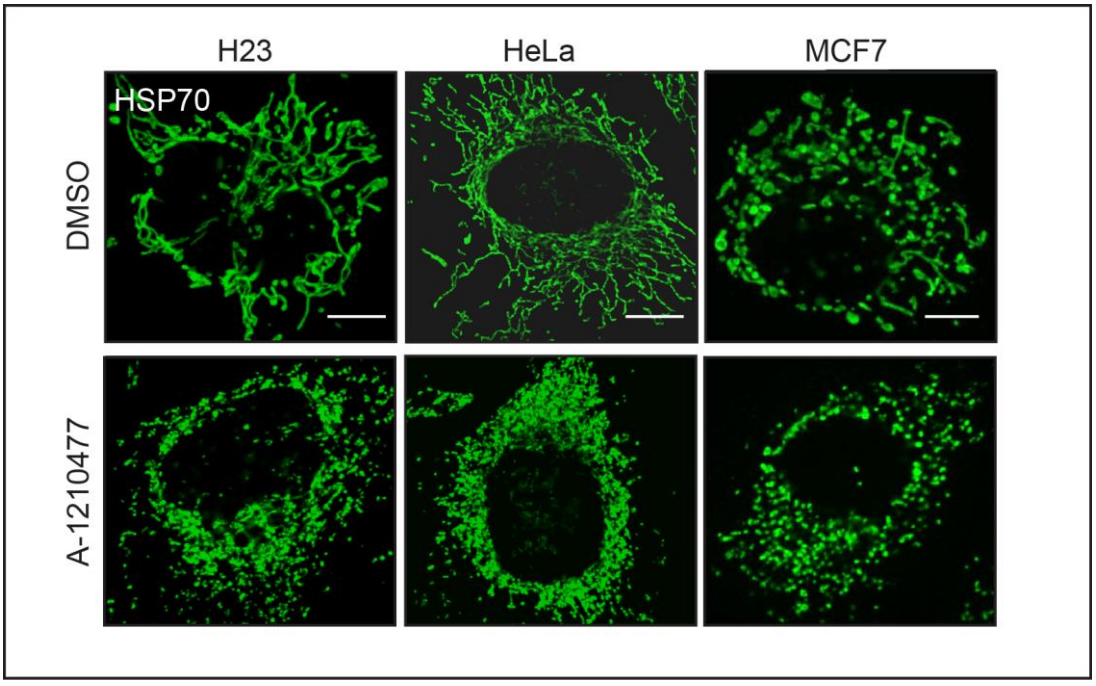

Figure 5.6. A-1210477 induces mitochondrial fragmentation in several cell lines. H23, HeLa and MCF7 cells were exposed to A-1210477 (10 µM) for 4 h and assessed for mitochondrial integrity by immunofluorescence. Scale bar: 10 µm.

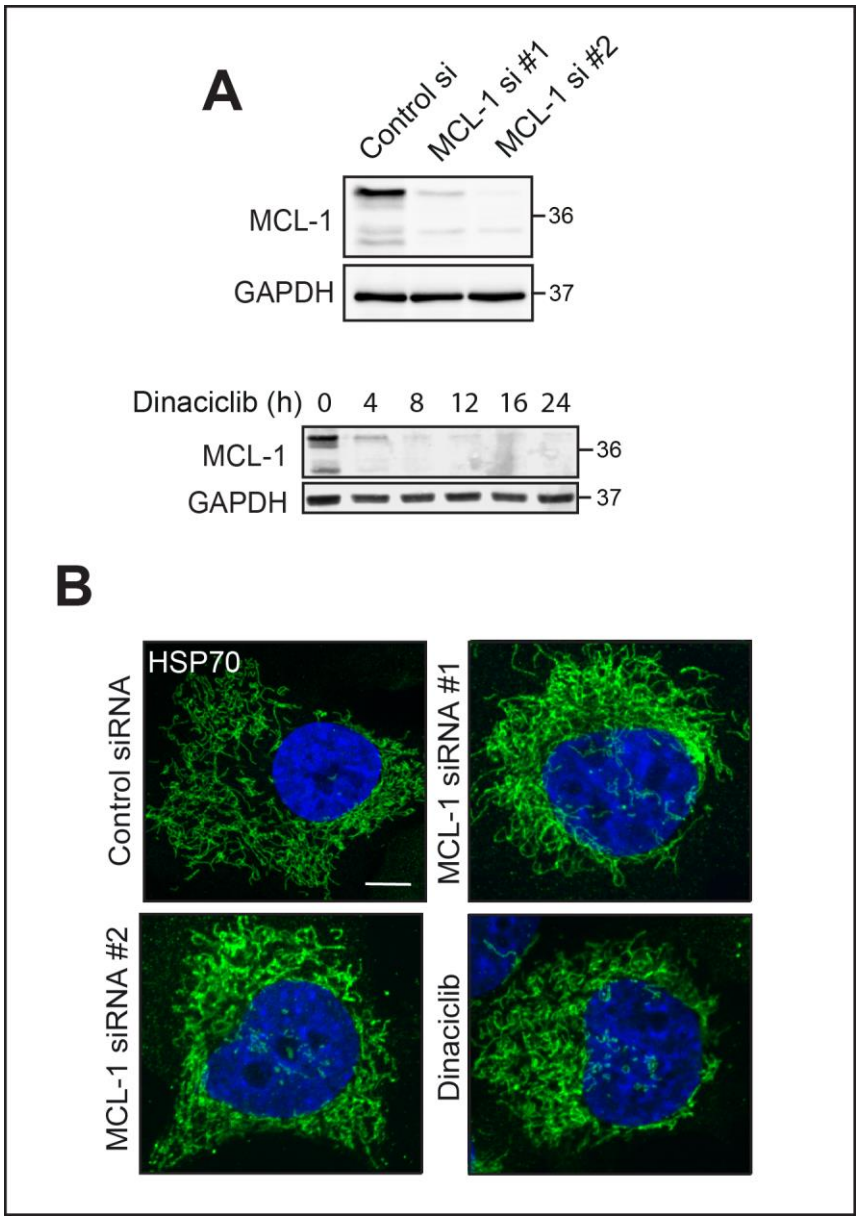

Figure 5.7. Mitochondrial ultrastructural network is not altered by genetic or translational inhibition of MCL-1. (A) Immunoblotting showing silencing efficiency for the MCL-1 siRNAs and MCL-1 downregulation by Dinaciclib. **(B)** H1299 cells were transfected with control siRNA and two different MCL-1-targeting siRNAs for 72 h or exposed to Dinaciclib (30 nM) for 4 h and assessed for mitochondrial integrity by immunofluorescence. Scale bar: 10 µm.

concentration (1 μM), sufficient to induce apoptosis in a MCL-1-dependent manner,[168] failed to demonstrate extensive mitochondrial fragmentation (Figure. 5.8). In addition, A-1210477 when used in conjunction with A-1331852 resulted in mitochondrial structural changes that resembled the swollen mitochondria observed during apoptosis, as previously observed (compare Figures 5.8 and 5.5). Taken together, these results suggested that mitochondrial fission mediated by A-1210477 and induction of apoptosis induction are distinct effects.

5.2.5 Expression levels of mitochondrial fusion/fission proteins are not affected by A-1210477

Next to assess whether A-1210477-mediated mitochondrial fragmentation was due to changes in the levels of key mitochondrial fission and fusion proteins, H1299 cells were exposed to A-1210477 for 4 h, and the expression levels of the mitochondrial fusion proteins OPA-1, MFN1, MFN2 and fission protein, DRP-1 were assessed. Since no major changes were detected in the total levels of these proteins (Figure 5.9), efforts were carried out to assess the phosphorylation states of these proteins, in particular DRP-1, as DRP-1 has been shown to be phosphorylated at Ser 616 to induce mitochondrial fission[282] and at Ser 637 to inhibit mitochondrial fission.[282–284] Surprisingly, despite the extensive induction of mitochondrial fragmentation in these cells, A-1210477 did not result in any consistent changes to the phosphorylation status of DRP-1 (Figure 5.9), thus negating a role for DRP-1 phosphorylation in A-1210477-induced mitochondrial fission. It must be noted that these studies were not performed using higher concentrations of S63845, as the inhibitor was not commercially available when these experiments were carried out.

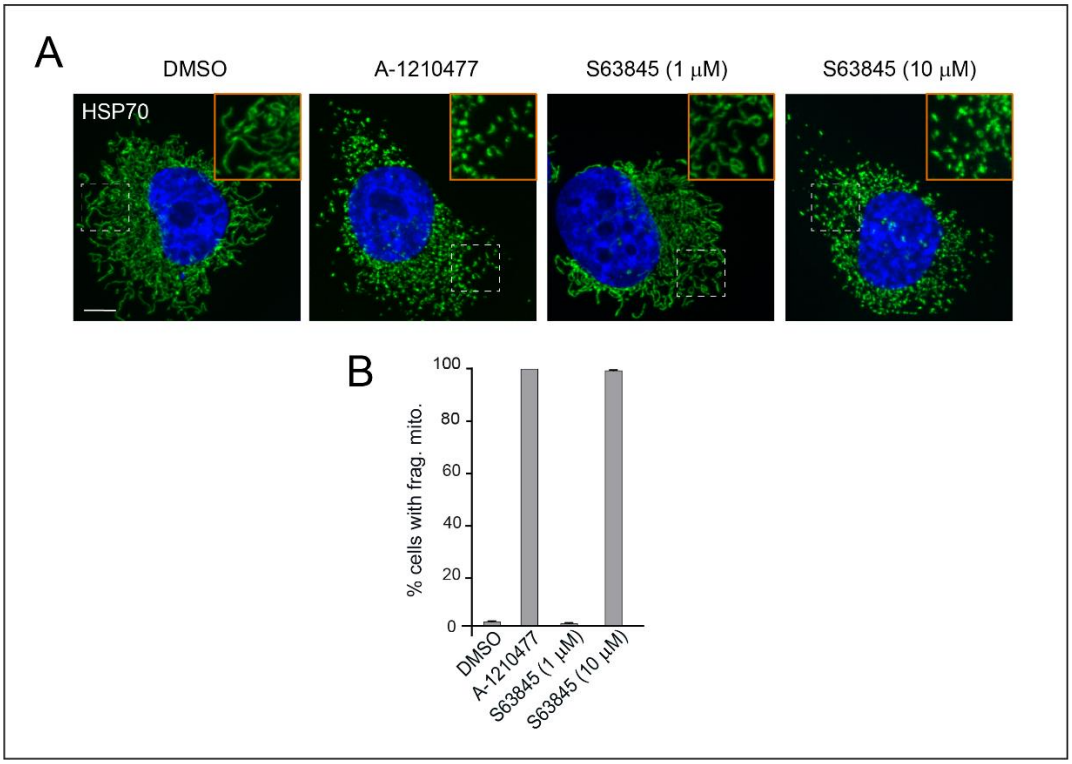

Figure 5.8. S63845 induces mitochondrial fragmentation only at high concentrations. **(A)** H1299 cells were exposed to A-1210477 (10 μM) or S63845 (1 μM, 10 μM) for 4 h and assessed for mitochondrial integrity by immunofluorescence with HSP70 antibody. Areas inside dashed line boxes have been zoomed. Scale bar: 10 μm. **(B)** Quantification for the extent of mitochondrial fragmentation showed in A. At least 100 cells were counted for 3 independent experiments.

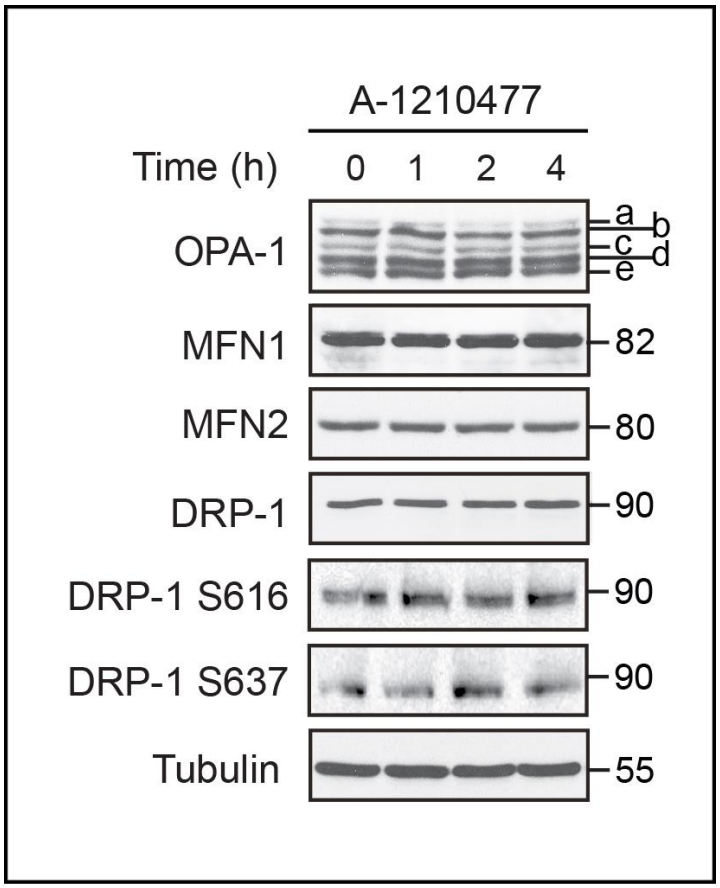

Figure 5.9. A-1210477 does not appear to alter expression levels of mitochondrial fission-fusion proteins. H1299 cells were exposed to A-1210477 (10 μM) for 0, 1, 2 or 4 h and assessed for mitochondrial fission and fusion protein levels by immunoblotting. Letters (a-b-c-d-e) represent the different OPA-1 isoforms.

5.2.6 DRP-1 foci localise at A-1210477-mediated mitochondrial fission sites

DRP-1 is the master regulator of mitochondrial fission and is recruited from the cytosol to the mitochondrial membrane to execute fission.[285] A-1210477, despite not changing DRP-1 protein levels or phosphorylation status, could still be dictating DRP-1 translocation to mitochondrial membrane resulting in excessive fragmentation. To assess that, H1299 cells were exposed to A-1210477 and processed for immunocytochemistry staining with antibodies against DRP-1 and HSP70. In control cells, DRP-1 appeared as punctate structures distributed between cytosol and mitochondrial membranes (Figure 5.10). Following A-1210477, DRP-1 did not undergo remarkable redistribution. DRP-1 punctae were clustered around the fragmented mitochondria, suggesting that DRP-1 could be involved in A-1210477-mediated mitochondrial fragmentation. However, as DRP-1 activity depends on different post-translational modifications, further analysis such as assessment for the phosphorylation status of DRP-1 will be valuable for an accurate evaluation of the role of DRP-1 in A-1210477-mediated mitochondrial fragmentation.

5.2.7 Mitochondrial fragmentation mediated by MCL-1 inhibitors occurs in a DRP-1-dependent manner

To assess whether DRP-1 is required for A-1210477-mediated mitochondrial fragmentation, H1299 cells were transfected with control or two different DRP-1 targeting siRNAs which were used on the following experiments (data shown for only one of them). On the following day, cells were exposed to A-1210477 or S63845 and immunostained for HSP60 to assess for mitochondrial ultrastructure. Indeed, mitochondrial fragmentation mediated by both these inhibitors was significantly prevented in cells lacking DRP-1, indicating that DRP-1 is necessary for A-1210477 and S63845 to induce mitochondrial fragmentation (Figure 5.11).

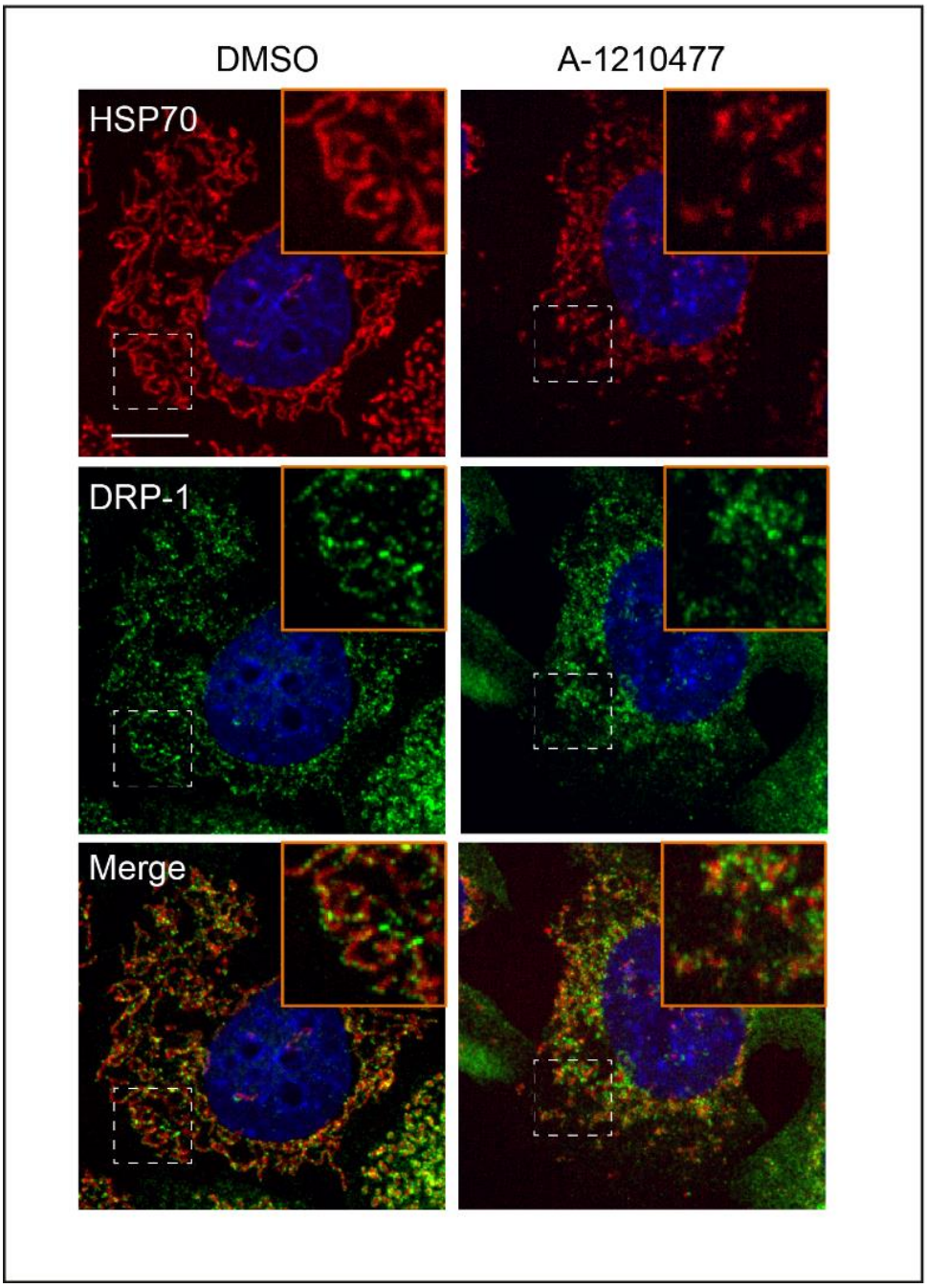

Figure 5.10. DRP-1 localises at A-1210477-induced mitochondrial fission sites. H1299 cells were exposed to A-1210477 (10 μM) for 4 h and assessed for mitochondrial ultrastructure and DRP-1 localisation by immunofluorescence. Areas inside dashed line boxes have been zoomed. Scale bar: 10 μm.

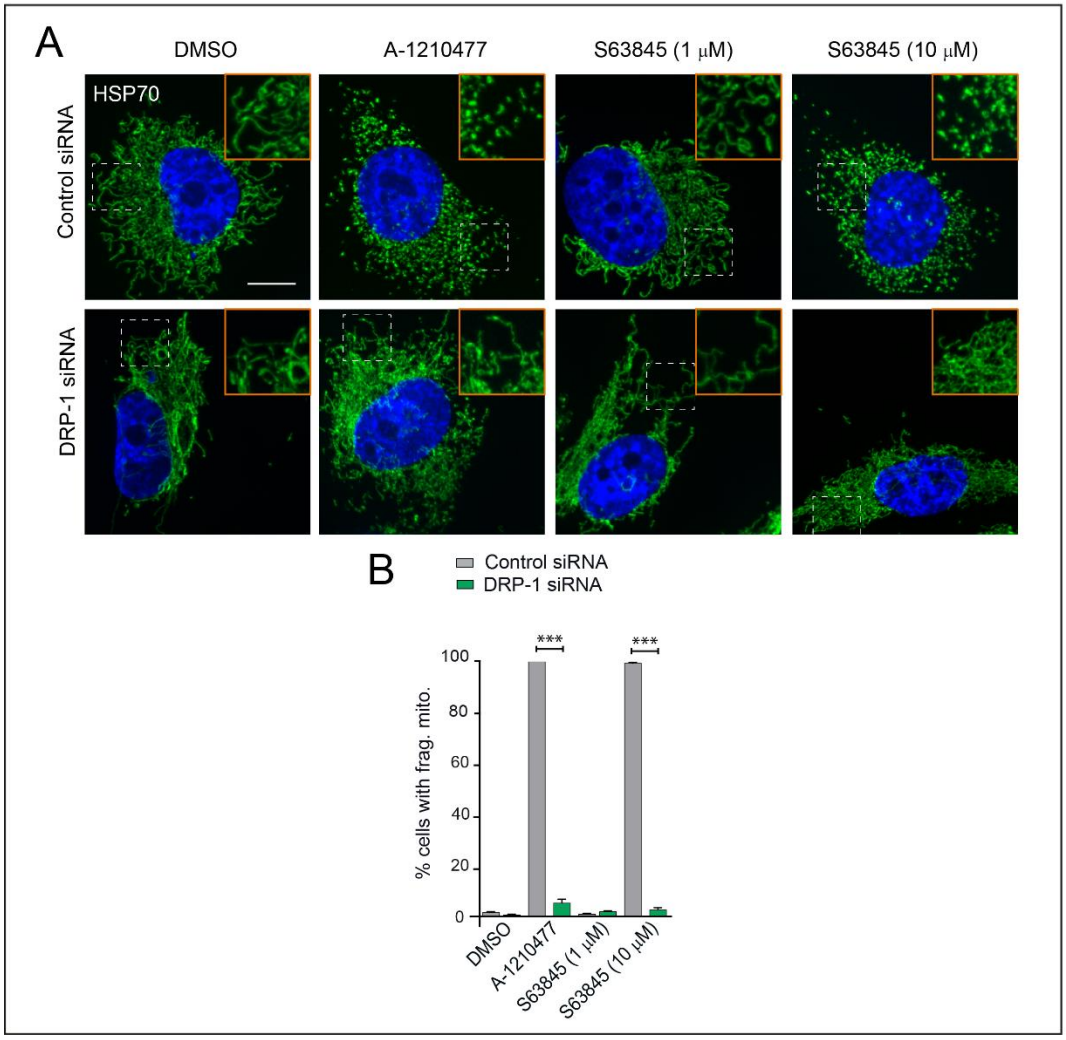

Figure 5.11. DRP-1 is required for BH3 mimetic-induced mitochondrial fragmentation. **(A)** H1299 cells were reverse transfected with control or DRP-1 siRNA for 72 h, exposed to A-1210477 (10 μM) or S63845 (1 μM, 10 μM) for 4 h and assessed for mitochondrial integrity by immunofluorescence with HSP70 antibody. Areas inside dashed line boxes have been zoomed. Scale bar: 10 μm. **(B)** Quantification for the extent of mitochondrial fragmentation showed in A. At least 100 cells were counted for 3 independent experiments. Statistical analysis was conducted using one-way ANOVA (***P≤0.001).

5.2.8 DRP-1 is not required for mitochondrial structural changes that occur during apoptosis

Although A-1210477-mediated fragmentation appeared structurally different from mitochondrial fission following BH3 mimetics, the requirement of DRP-1 for the former could potentially delineate these ultrastructural changes. To elucidate that, H1299 cells were transfected with DRP-1 siRNA in combination with suitable apoptotic stimuli (as previously shown in Figure 5.5, which forms the negative control for this experiment) and subjected to immunocytochemistry and confocal microscopy. The apoptotic stimuli used here was a combination of siRNA against either MCL-1 or BCL-X_L (to render the cells depend on one or the other member for survival) and BH3 mimetics, targeting BCL-X_L or MCL-1 (to neutralise both proteins and induce apoptosis). The results indicated that downregulation of DRP-1, despite preventing A-1210477-mediated mitochondrial fragmentation (as previously shown in Figure 5.11), does not alter mitochondrial fragmentation induced by apoptotic stimuli (Figure 5.12). Collectively, this data revealed that DRP-1 is not required for these early mitochondrial fission events observed during apoptosis.

5.2.9 BH3 mimetic-induced apoptosis is DRP-1-dependent

Although DRP-1 does not seem to be required for early mitochondrial fission events observed during apoptosis, it is extensively characterised as a fission GTPase, with implications in apoptosis (Figure 5.13 A). In support, a recent study has shown that DRP-1 could play a role in apoptosis by preventing staurosporine-induced cytochrome *c* release.[275] To investigate the role of DRP-1 in BH3 mimetic-mediated apoptosis, H1299 cells were transfected with control or two different DRP-1 siRNA, exposed to a combination of A-1210277 and A-1331852 and assessed for cell death.

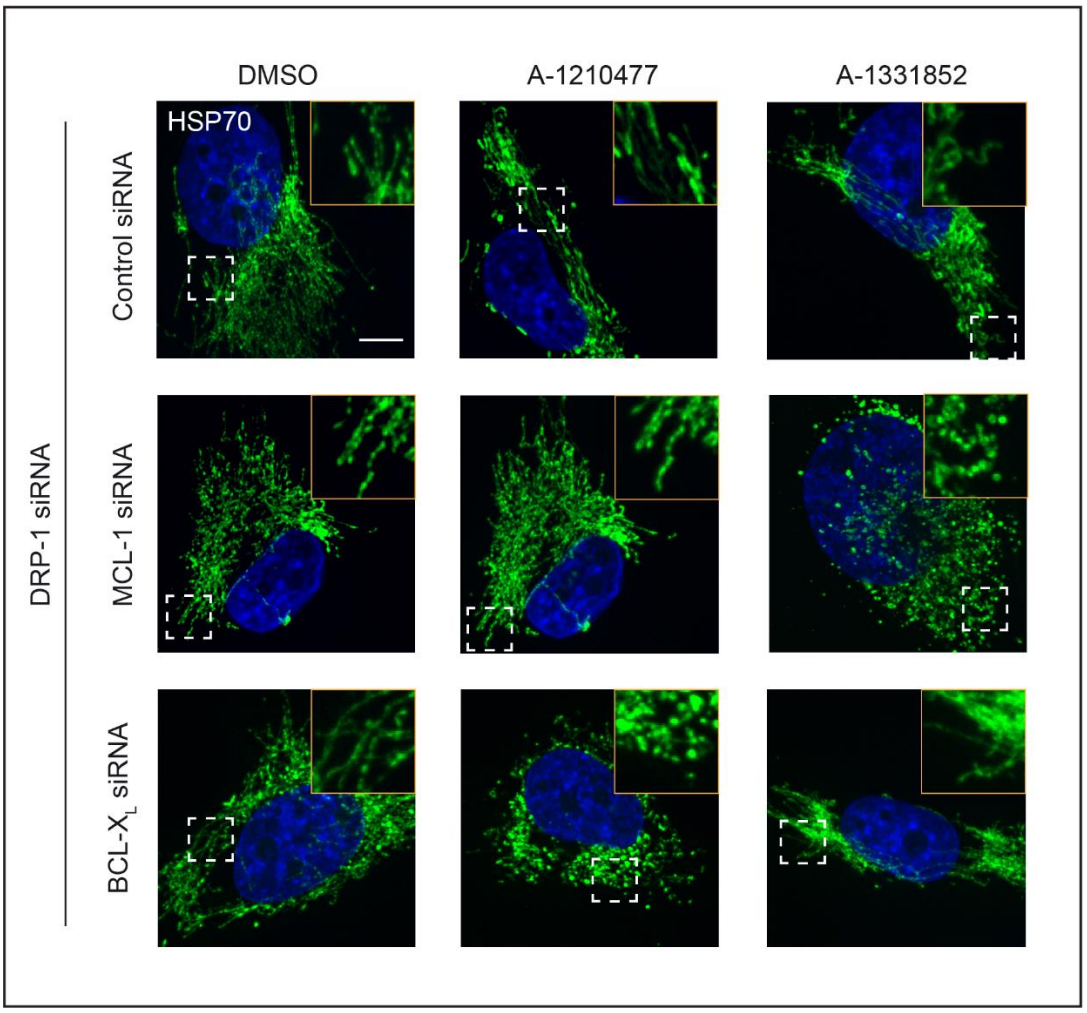

Figure 5.12. Pre-apoptotic mitochondrial fragmentation is independent of DRP-1. H1299 cells were transfected with control, MCL-1 or BCL-X_L siRNA in combination with DRP-1 siRNA and exposed to DMSO, A-1210477 (10 µM) or A-1331852 (100 nM) for 4 h in the presence of Z-VAD-FMK (30 µM) and assessed for mitochondrial integrity by immunofluorescence with HSP70 antibody. Scale bar: 10 µm. Images representative of a cell population.

DRP-1 silencing prevented A-1210477 and A-1331852-mediated PS externalisation (Figure 5.13 B) and caspase-3 processing, evident by a marked decrease of the cleaved band at ~20 kDa (Figure 5.13 C). The protective effects of DRP-1 depletion against cell death were more striking when cells were observed under bright-field microscopy, following exposure to BH3 mimetics (Figure 5.13 D). Taken together these results indicate that DRP-1 plays an important anti-apoptotic role in BH3 mimetic-mediated apoptosis.

5.2.10 BH3 mimetics-induced MOMP and cytochrome *c* release is DRP-1-dependent

To further investigate the precise step at which DRP-1 could be exerting its anti-apoptotic role, early apoptotic events were monitored. MOMP was the next logical step to analyse, as it precedes PS externalisation and caspase processing in the intrinsic pathway. MOMP was assessed by cytochrome *c* release from mitochondria to the cytosol (Figure 5.14 A). H1299 cells were transfected with DRP-1 siRNA or with a DRP-1 K38A plasmid (the K38A mutation at the GTPase domain of DRP-1 renders a kinase dead protein, non-functional and dominant-negative protein)[286] and exposed to a combination of A-1210477 and A-1331852. Cytochrome *c* release was then assessed by immunocytochemistry and immunoblotting. The combination of BH3 mimetics induced cytochrome *c* release from the mitochondria to the cytosol, which was greatly reduced by DRP-1 silencing or by K38A mutant overexpression (Figure 5.14 B-D). Interestingly, mitochondria in cells that lack DRP-1 appeared swollen following BH3 mimetics (Figure 5.14 B), possibly indicating that in the absence of DRP-1, mitochondria that has received the apoptotic insult (characterised by mitochondrial swelling) ceases to undergo fission that is required for apoptosis.

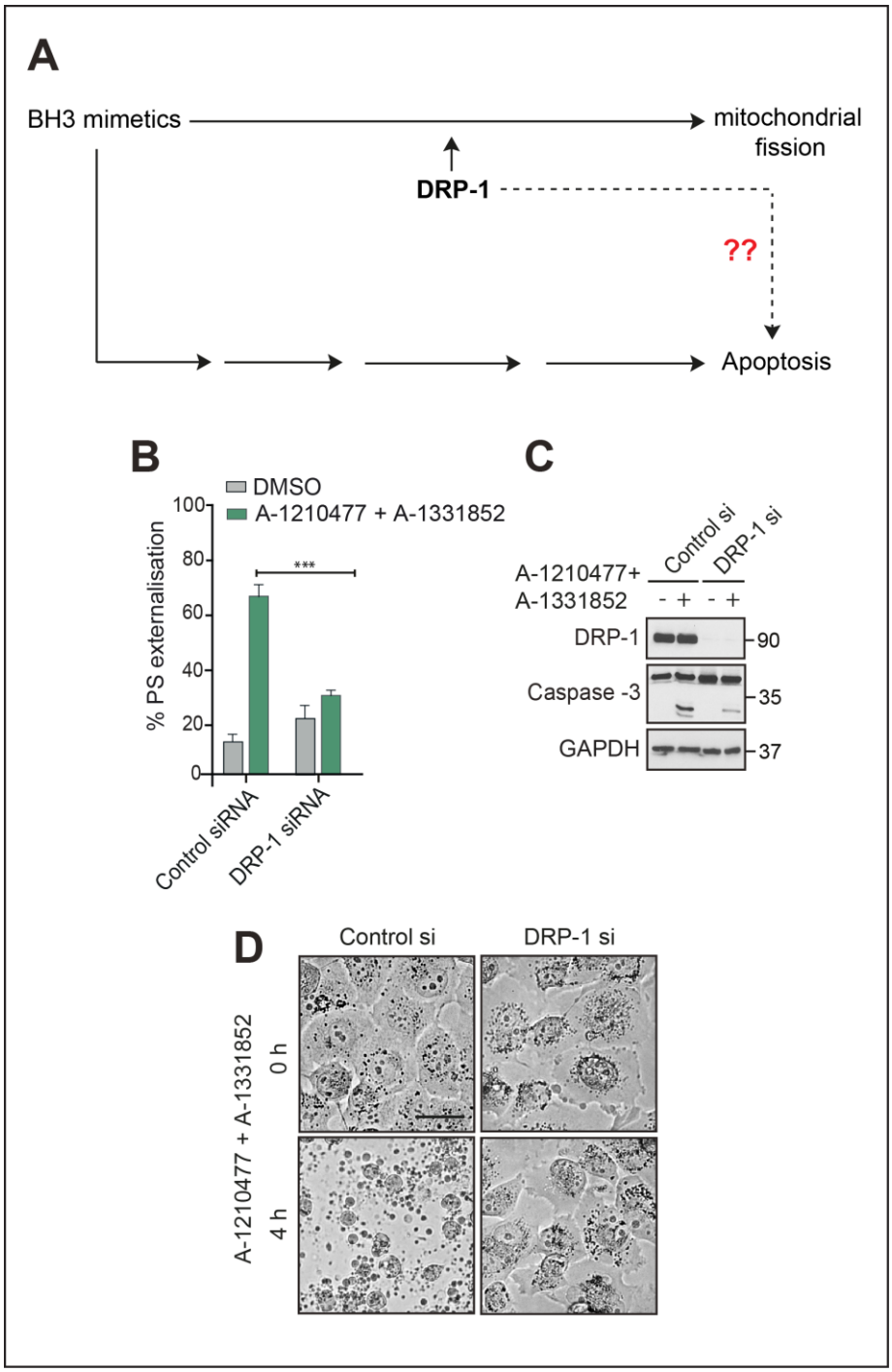

Figure 5.13. DRP-1 is required for BH3 mimetic-induced apoptosis. (A) Flowchart representing the findings of this study hitherto. **(B)** H1299 cells were transfected with control siRNA and DRP-1 siRNA, exposed to a combination of A-1210477 (10 µM) and A-1331852 (100 nM) for 4 h and assessed for the extent of PS externalisation by flow cytometry. Statistical analysis was conducted using one-way ANOVA (***P≤0.001). **(C)** Caspase-3 processing and DRP-1 silencing efficiency by immunoblotting and **(D)** overall cell death by bright field microscopy; scale bar: 30 µm.

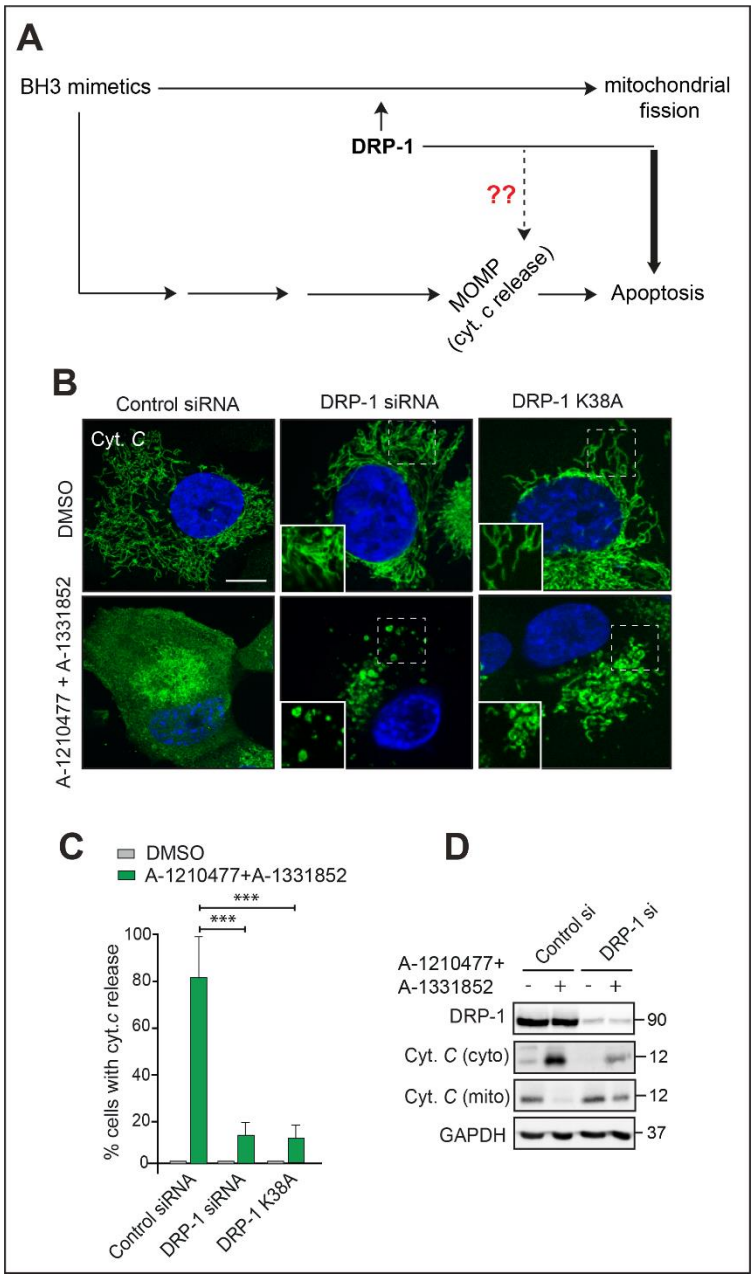

Figure 5.14. DRP-1 is required for BH3 mimetic-induced cytochrome *c* release. (A) Flowchart representing the findings of this study hitherto. **(B)** H1299 cells were transfected with control siRNA, DRP-1 siRNA or DRP-1 K38A plasmid and assessed for the extent of cytochrome *c* release by immunofluorescence upon exposure to a combination of A-1210477 (10 μM) and A-1331852 (100 nM) for 4 h. Areas inside the dashed line boxes have been zoomed. Scale bar: 10 μm. **(C)** Quantification of the extent of cytochrome *c* release showed in A. At least 100 cells were counted for 3 independent experiments. Statistical analysis was conducted using one-way ANOVA (***P≤0.001). **(D)** Immunoblot showing silencing efficiency of DRP-1 siRNA used in A and the extent of cytochrome *c* release from mitochondria to cytosol upon exposure to a combination of A-1210477 (10 μM) and A-1331852 (100 nM) for 4 h. GAPDH was used as loading control.

5.2.11 BH3 mimetic-induced BAK activation is DRP-1-dependent

Since BH3 mimetic-mediated mitochondrial swelling occurred in a BAX/BAK-dependent manner (Figure 5.4), it is possible that BAK and BAK are already activated by BH3 mimetics to facilitate mitochondrial fission, which then requires DRP-1 to induce fission and MOMP (Figure 5.15 A). Since H1299 cells (ATCC, 5803-CRL H1299) neither express BAX nor p53,[287] these experiments were altered to only assess BAK activation in the presence and absence of DRP-1. For this, H1299 cells were transfected with control or DRP-1 siRNA, exposed to a combination of A-1210477 and A-1331852 and assessed for BAK activation by FACS with anti-BAK AB1 antibody, specific for the active conformation of BAK.[288] Interestingly, DRP-1 silencing greatly reduced BH3 mimetic-mediated BAK activation in H1299 cells (Figure 5.15 B), thus placing DRP-1 upstream of BAK activation during BH3 mimetic-mediated apoptosis.

5.2.12 BH3 mimetic-mediated release of BH3-only proteins is not altered by DRP-1 downregulation

BAX and BAK are effector proteins that can be activated either upon direct release from their anti-apoptotic counterparts or by the release of BH3-only proteins, which in turn can activate BAX and BAK.[86] Immunoprecipitation of BCL-X_L and MCL-1 in H1299 cells, following BH3 mimetics revealed that BIM, BAD and BAK bound to BCL-X_L and NOXA that is bound to MCL-1 were released in cells, irrespective of the presence or absence of DRP-1 (Figure 5.16), thus suggesting that DRP-1 does not play a role in the protein-protein interactions between the anti- and pro-apoptotic BCL-2 family members.

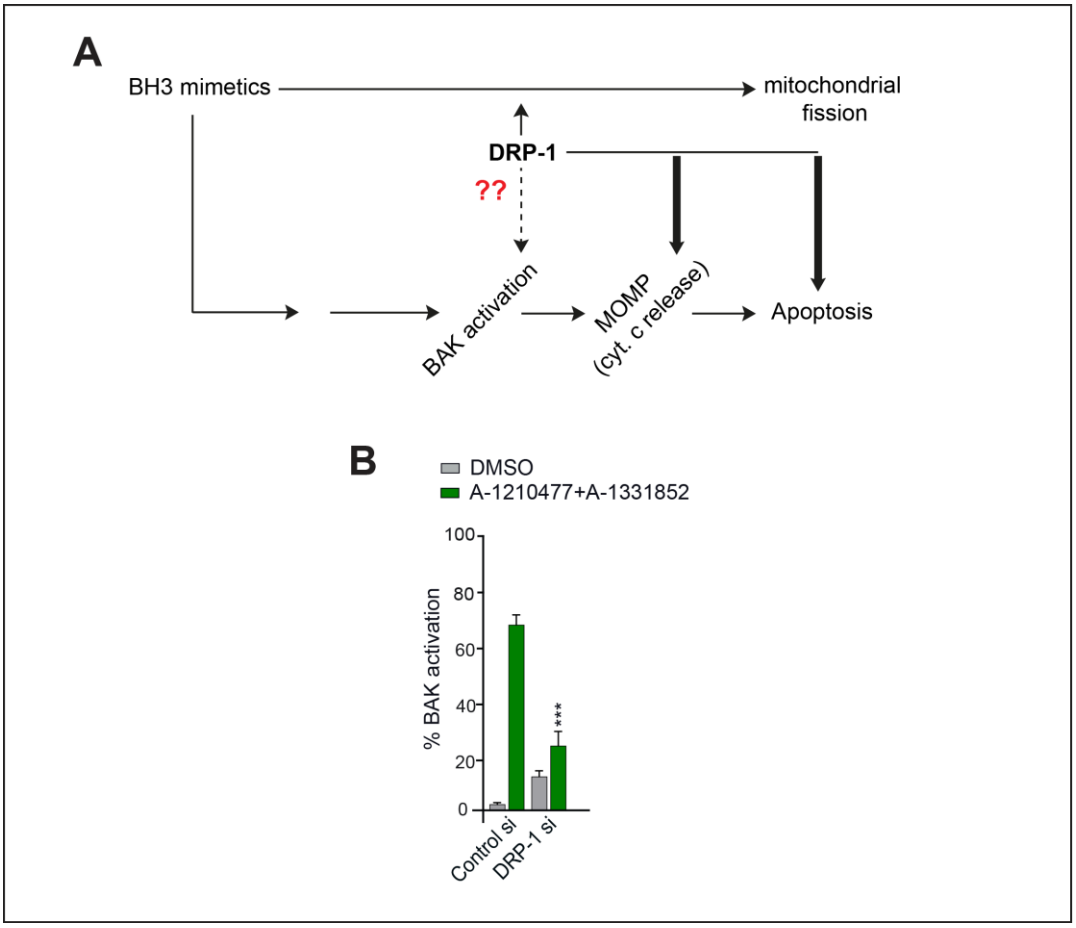

Figure 5.15. DRP-1 is required for BH3 mimetic-induced BAK activation. (A) Flowchart representing the findings of this study hitherto. **(B)** H1299 cells were transfected with control or DRP-1 siRNA and assessed for the extent of BAK activation by flow cytometry upon exposure to a combination of A-1210477 (10 μM) and A-1331852 (100 nM) for 4 h. Statistical analysis was conducted using one-way ANOVA (***P≤0.001).

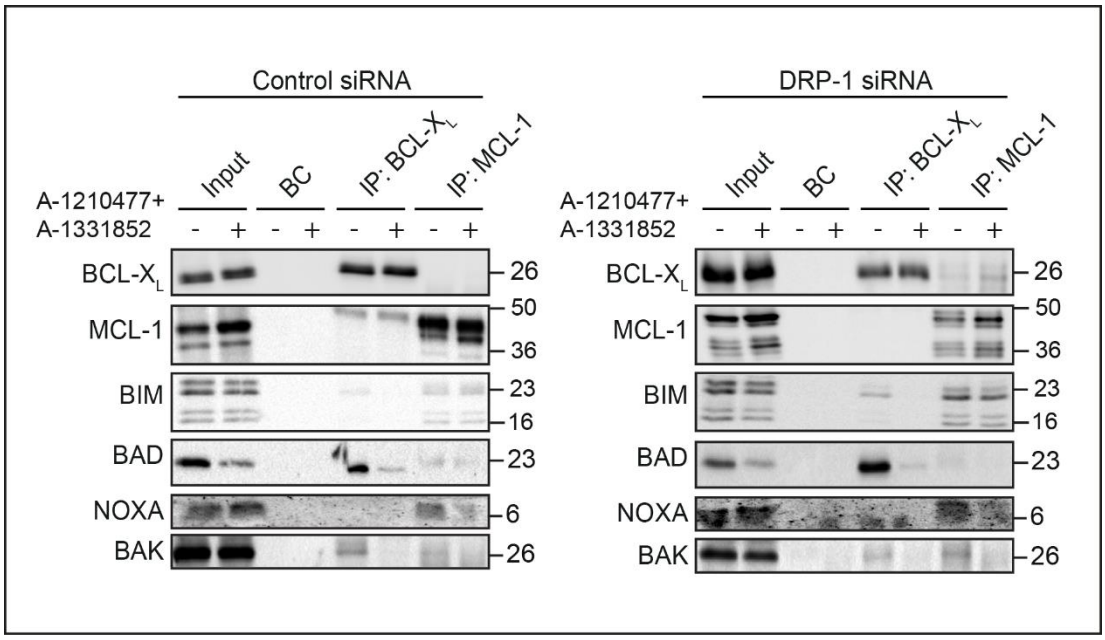

Figure 5.16. DRP-1 is not required for BH3 mimetic-release of BH3-only proteins. H1299 cells were reverse transfected with control or DRP-1 siRNA for 72 h before exposed to DMSO or a combination of A-1210477 (10 μM) and A-1331852 (100 nM) for 4 h and processed for immunoprecipitation with MCL-1 or BCL-X_L antibodies. IP indicates immunoprecipitation. BC indicates beads control, with no antibody bound.

5.2.13 DRP-1 is not required for BH3 mimetic-induced mitochondrial cristae remodelling

Previous results indicate that BAK released from the anti-apoptotic members is somehow not activated in the absence of DRP-1 (even when all other BH3-only proteins are released from both BCL-X_L and MCL-1) (Figures 5.15 B and 5.16). Since BAK is normally localised in the mitochondrial membrane, structural changes in the mitochondrial membrane following BH3 mimetics could regulate BAK activation, and it is possible that DRP-1 plays a role in this mechanism. At the level of mitochondria, BH3 mimetics result in cristae remodelling, which is largely dictated by OPA-1 processing and can occur upstream of BAK activation (Figure 5.17 A).[273,289] H1299 cells transfected with control or DRP-1 siRNA and exposed to a combination of A-1210477 and A-1331852 demonstrated clear OMM breaks, induced by BH3 mimetics exposure (yellow arrowhead, Figure 5.17 B), as expected of cells undergoing apoptosis. DRP-1 silencing induced mitochondrial elongation,[290] and following BH3 mimetics, aberrant shaped mitochondria, with extensive matrix swelling but intact double membranes, could be observed (Figure 5.17 B). Furthermore, silencing of DRP-1 neither repressed BH3 mimetic mediated cristae remodelling nor prevented OPA1 proteolysis (Figure 5.17 B and C). In the control and DRP-1 downregulated cells, exposure to BH3 mimetics induced a clear alteration in the levels of OPA-1 isoforms, with the long isoforms **a** and **b** of OPA1 being proteolyzed, compatible with an induction of cristae remodelling (Figure 5.17 C). These results indicate that the anti-apoptotic role of DRP-1 in the intrinsic pathway of apoptosis lies downstream of cristae remodelling, OPA-1 processing and release of the pro-apoptotic members from their anti-apoptotic counterparts.

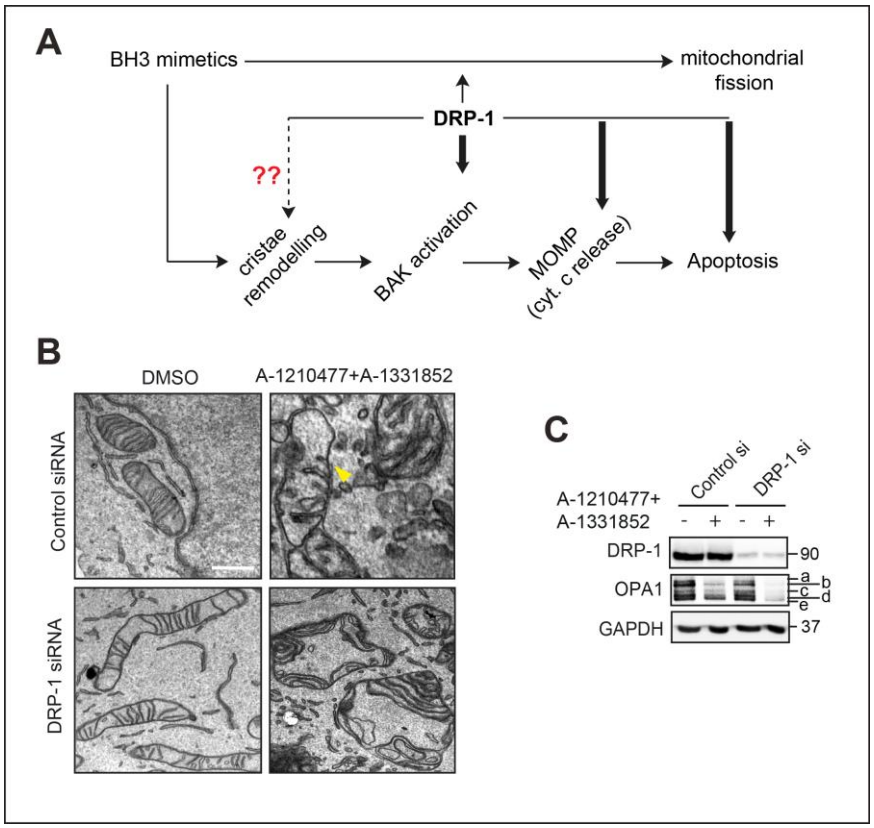

Figure 5.17. BH3 mimetics induce DRP-1 independent cristae remodelling. (A) Flowchart representing the findings of this study hitherto. **(B)** Electron micrographs of H1299 cells transfected with control or DRP-1 siRNA and exposed to a combination of A-1210477 (10 µM) and A-1331852 (100 nM) for 4 h. Scale bar: 10 nm. Yellow arrowhead points to a mitochondria outer membrane break. **(C)** Immunoblot showing silencing efficiency of DRP-1 siRNA and proteolysis of OPA-1 isoforms upon exposure to a combination of A-1210477 (10 µM) and A-1331852 (100 nM) for 4 h. GAPDH was used as a loading control.

5.2.14 DRP-1 acts downstream of OPA-1 in activating BAK to drive BH3 mimetic-induced apoptosis

As DRP-1 silencing did not prevent BH3 mimetic-mediated OPA-1 processing and cristae remodelling (Figure 5.18 A), it suggested that the role of DRP-1 in apoptosis lies downstream of OPA-1. Since OPA1 regulates the release of cytochrome *c* within the mitochondria from cristae to the inner membrane space, H1299 cells were transfected with siRNA against OPA-1 to induce in this redistribution, which was followed by exposure to A-1210477 and A-1331852 to induce BAK activation and cause MOMP. As expected, OPA-1 silencing followed by exposure to BH3 mimetics induced slightly higher levels of cytochrome *c* release and PS externalisation (most likely due to the redistribution of cytochrome *c*) compared to cells transfected with control siRNA (Figure 5.18 B - D). Interestingly, silencing of DRP-1 in these cells still prevented BH3 mimetic-induced cytochrome *c* release and PS externalisation (Figure 5.18 B - D), further confirming the requirement of active BAK to result in MOMP and PS externalisation. Thus, the results indicate that DRP-1 somehow activates BAK to facilitate BH3 mimetic-mediated MOMP and apoptosis.

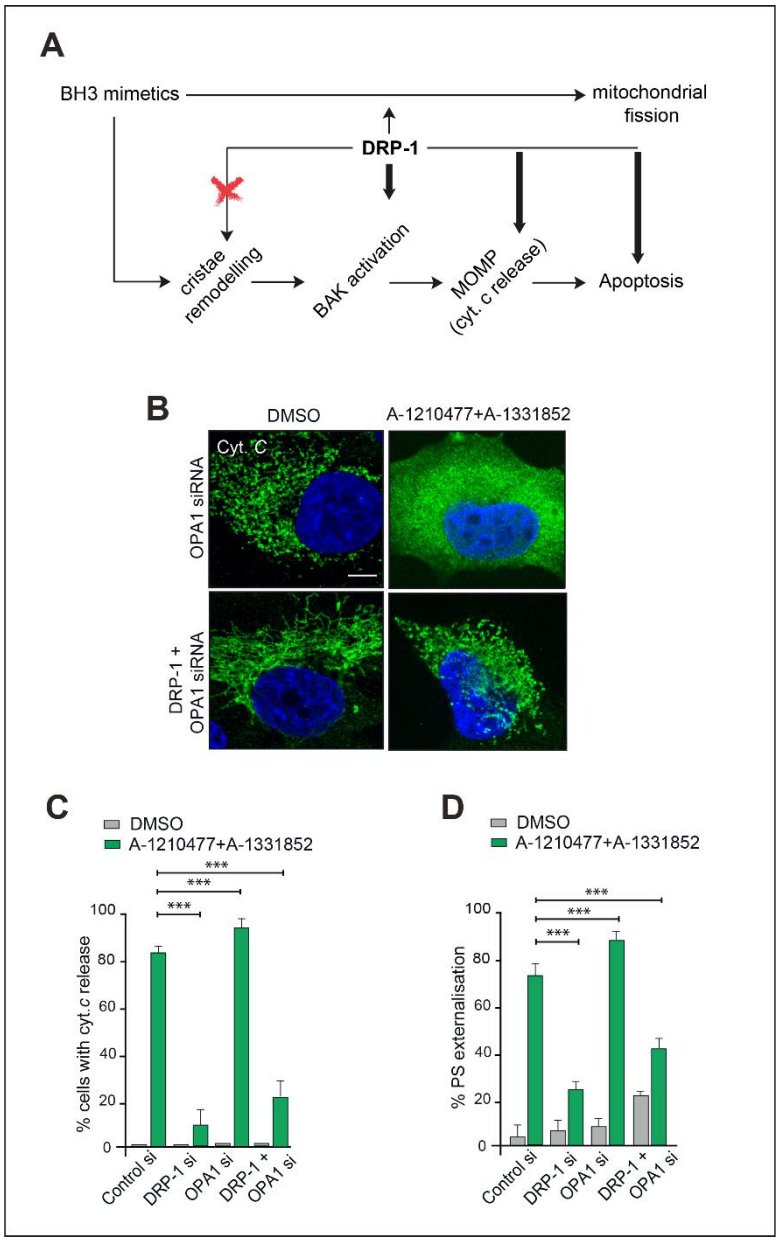

Figure 5.18. DRP-1 acts downstream of OPA-1 to regulate BH3 mimetic-induced apoptosis. (A) Flowchart representing the findings of this study hitherto **(B)** H1299 cells were transfected with OPA-1 siRNA or OPA-1 and DRP-1 siRNA and the extent of cytochrome *c* release assessed by immunofluorescence following exposure to a combination of A-1210477 (10 µM) and A-1331852 (100 nM) for 4 h. Scale bar: 10 µm. **(C)** Quantification of the extent of cytochrome *c* release showed in B. At least 100 cells were counted for 3 independent experiments. Statistical analysis was conducted using one-way ANOVA (***P≤0.001). **(D)** H1299 cells were transfected with control siRNA, DRP-1 siRNA, OPA-1 siRNA or OPA-1 and DRP-1 siRNA and assessed for PS externalisation following exposure to a combination of A-1210477 (10 µM) and A-1331852 (100 nM) for 4 h. Statistical analysis was conducted using one-way ANOVA (***P≤0.001).

5.3 Discussion

BH3 mimetics were developed based on the mechanism of interactions between the pro- and anti-apoptotic members of the BCL-2 family of proteins, which, when shifted towards cell death, culminates in the release of cytochrome *c* and activation of the caspase cascade.[22] Mitochondrial structural changes, particularly fission, have been observed during apoptosis.[284] Furthermore, MCL-1 inhibitors, such as A-1210477 and S63845 induced extensive mitochondrial fragmentation in a DRP-1-dependent manner (Figure 5.11). However, removal of MCL-1 either by genetic silencing or transcriptional inhibition did not affect the mitochondrial ultrastructural network (Figure 5.7) suggesting that the presence of MCL-1 may be critical for the induction of the structural changes, or that the fragmentation caused by these MCL-1 inhibitors derive from an off-target effect, as only high concentrations of S63845 (10 µM) but not low concentrations capable of inducing apoptosis (100 nM) promoted mitochondrial fragmentation (Figures 5.5 and 5.8). A recent report delving into the functions of different MCL-1 isoforms has shown that a truncated form of MCL-1, located in the mitochondrial matrix, regulates mitochondrial metabolism and dynamics by supporting oxidative phosphorylation and maintenance of mitochondrial membrane potential.[62,291] Moreover, deletion of MCL-1 in cardiomyocytes have been shown to induce abnormal mitochondrial structure and defective respiration.[175] Based on that, it is likely that A-1210477 could bind to these two isoforms to induce both apoptosis (by displacing the BH3-only members from the long isoform at mitochondrial outer membrane) and mitochondrial fragmentation (by displacing an unknown protein from the truncated isoform at the matrix).[62]

Several studies have shown that DRP-1 not only acts as the master regulator of mitochondrial fission, but also plays a role in the induction of apoptosis.[275,276,292]

More recently, it has been shown that the RING-finger-containing protein, MAPL, when overexpressed, induced mitochondrial fragmentation. In addition, MAPL was also identified to promote SUMOylation of DRP-1,[293] which is required for staurosporine-mediated apoptosis.[276] In this study, the data indicate that silencing of DRP-1 prevented BH3 mimetic-mediated cytochrome *c* release. Furthermore, the involvement of DRP-1 in cell death was further confirmed by overexpression of a kinase-dead dominant-negative protein with a K38A mutation in the G1 motif of the GTPase domain of DRP-1,[294] rendering DRP-1 non-functional (Figure 5.14).

Interestingly, H1299 cells transfected with DRP-1 siRNA and exposed to BH3 mimetics, despite having cytochrome *c* trapped in the mitochondria (due to the lack of DRP-1), showed unexpected spherical mitochondrial aggregates highly stained for cytochrome *c* (Figure 5.14). When analysed by EM, these aggregates seemed like bundles of altered mitochondrial cristae, localised at the periphery of the mitochondria and connected by a central swollen mitochondrial matrix (Figure 5.17). This indicates that the apoptotic effects of BH3 mimetics on mitochondria occur independently of DRP-1 up to the point of cristae remodelling and OPA-1 proteolysis (Figures 5.17 and 5.18), freeing cytochrome *c* from the OPA-1-bound cristae to the intermembrane space. At this point, DRP-1 is recruited to the fission sites and constricts the mitochondrial membrane, leading to the release of cytochrome *c* to the cytosol.

The requirement of DRP-1 for BH3 mimetics to activate BAK is another interesting finding, as BH3 mimetics appeared to displace BAK and all BH3-only members from their anti-apoptotic counterparts irrespective of DRP-1. This indicates that the released BAK still requires DRP-1 to undergo activation and mitochondrial insertion to facilitate MOMP. In agreement, previous reports have linked DRP-1 and

BAX/BAK at the level of mitochondria to regulate MOMP, where BAX/BAK stabilises DRP-1 association with mitochondria *via* SUMOylation of DRP-1.[295] However, a few years later, the same group showed that MAPL, the protein responsible for SUMOylation of DRP-1, acts downstream of BAK/BAX activation,[276] arguing that MAPL-mediated DRP-1 stabilisation could be a tipping point towards apoptosis for sub-lethal levels of BAX/BAK activation. Furthermore, it has also been shown that the dominant-negative DRP-1 K38A cannot prevent BAX clustering in the OMM, preventing cell death.[292]

Although determination of MOMP was performed *via* quantitative or qualitative assessment of cytochrome *c* release, the most modern models for MOMP consider the initial event as the formation of BAX/BAK pores on OMM.[296] This results in the release of other molecules, such as Smac and Omi.[297] Even though Smac release was not assessed throughout this study, there is evidence that it can occur independently of DRP-1,[298] indicating the complexity underlying MOMP. Nevertheless, the results presented here place DRP-1 immediately upstream of BAK activation to facilitate MOMP (cytochrome *c* release) and the downstream apoptotic cascade, reinforcing the role of DRP-1 not only in mitochondrial fission, but also in cell death.

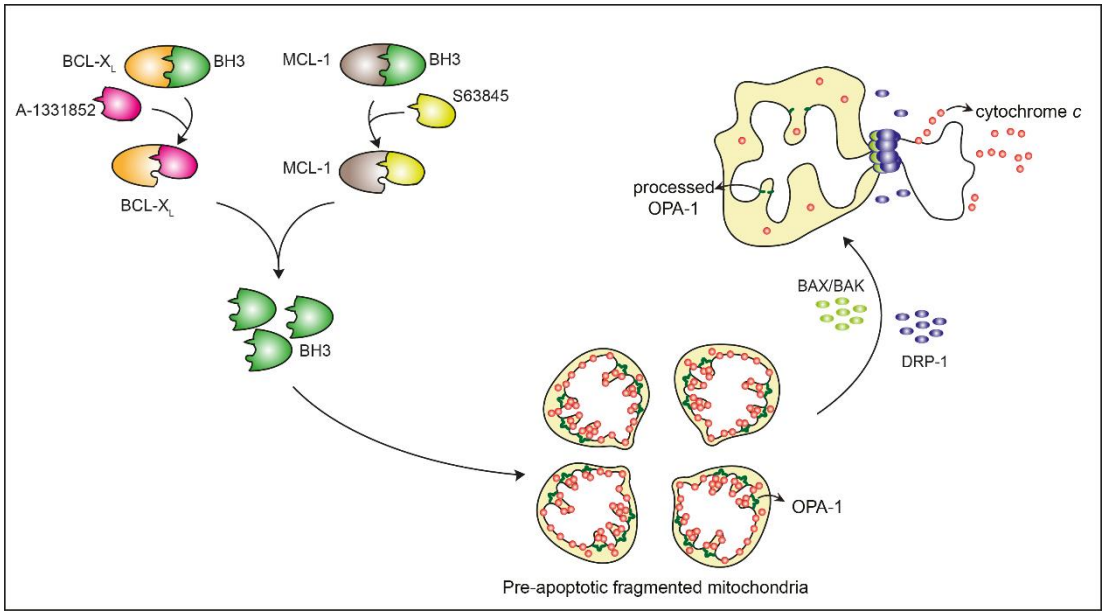

Figure 5.19. Scheme representing the mechanism of action of BH3 mimetics in pre-apoptotic mitochondrial fragmentation and cell death. A-1331852 and S63845 displace BH3-only proteins from BCL-X_L and MCL-1 respectively, inducing mitochondrial fragmentation that precedes apoptosis in a DRP-1-independent manner. The pre-apoptotic stage is followed by apoptosis *per se*, which depends on DRP-1 and requires BAK activation and oligomerisation.

CHAPTER 6

Membrane dynamics of the endoplasmic reticulum and mitochondria during BH3 mimetic-mediated apoptosis

Chapter contents

6.1 Introduction

In eukaryotic cells, the endoplasmic reticulum (ER) is formed of a highly interconnected network of tubules and sheets, which are present as one continuous membrane.[299,300] The membranes of ER tubules and sheets are maintained by curvature stabilisation, achieved by proteins called the ER shaping proteins, mainly from the reticulon family.[301,302] ER shaping proteins, such as RTN-4 are localised in the ER tubules and sheets and possess a multi-transmembrane reticulon homology domain (RHD), which is inserted across the ER membrane in a stitch or hairpin-like manner, inducing a mechanical bend in the ER membrane.[303] Besides reticulons, other proteins, such as CLIMP-63, are responsible for the maintenance of ER structure. CLIMP-63 resides in the ER sheets and creates a distance between two apposed ER membranes, creating a cisterna *via* a coiled coil domain (Figure 6.1).[304] These ER shaping proteins are vital for the normal functioning of ER and for enabling ER to interact with other organelles, such as mitochondria at the ER-mitochondria contact sites.[301] The mitochondria-associated membranes (MAMs) are the connections between the ER and mitochondria. MAMs are considered to be contiguous with the ER, but physically connected to mitochondria.[305] MAMs play important functions in maintaining cellular homeostasis by transferring diverse molecules and ions, such as Ca^{2+}, phosphatidylserine and sterols.[305,306] In addition, MAMs have also been implicated in other cellular processes, such as autophagy and mitochondrial membrane dynamics.[307–310]

Recent studies show that the onset of mitochondrial fission occurs at specific sites where ER contacts the mitochondria.[308,311] ER tubules wrap around mitochondria, for an initial constriction that initiates the recruitment of DRP-1 to its receptors, which is followed by DRP-1 oligomerisation and the assembly of the

constriction ring.[308,311] This model further integrates the ER, components of the cytoskeleton and mitochondria. An initial tether occurs between ER and mitochondria *via* INF2 in the ER membrane and Spire1C in the mitochondrial membrane through ER-derived actin and myosin IIA filaments.[312] This interaction tightens the tether and acts as a motor for the initial ER wrapping around mitochondria, which in turn recruits DRP-1 and the fission machinery.[277] In addition to those events, some studies point to the role of dynamin 2 (Dyn2) in the final scission step of mitochondrial fission.[275,313]

Recent studies have implicated a role of ER membranes in mitochondrial fission and the induction of apoptosis.[276] While the involvement of ER in mitochondrial fission is well characterised, cell death studies have been carried out with broad-spectrum, non-specific cell death inducers, such as staurosporine and etoposide.[275] When studying such critical pathways, it is crucial to employ specific and potent cell death inducing compounds, such as BH3 mimetics. To date, relatively little information is available regarding the effects of BH3 mimetics on ER-mitochondria crosstalk mechanisms. As BH3 mimetics are already being used in clinical trials for different cancers,[281,314] it is important to understand how BH3 mimetics could affect mitochondrial fission/fusion dynamics, in the context of an involvement of ER membranes. In this chapter, using RNA interference to downregulate specific ER shaping proteins, such as RTN-4 and CLIMP-63, studies have been performed to assess the involvement of ER shape in mitochondrial fission, ER-mitochondrial contacts and BH3 mimetic-mediated apoptosis.

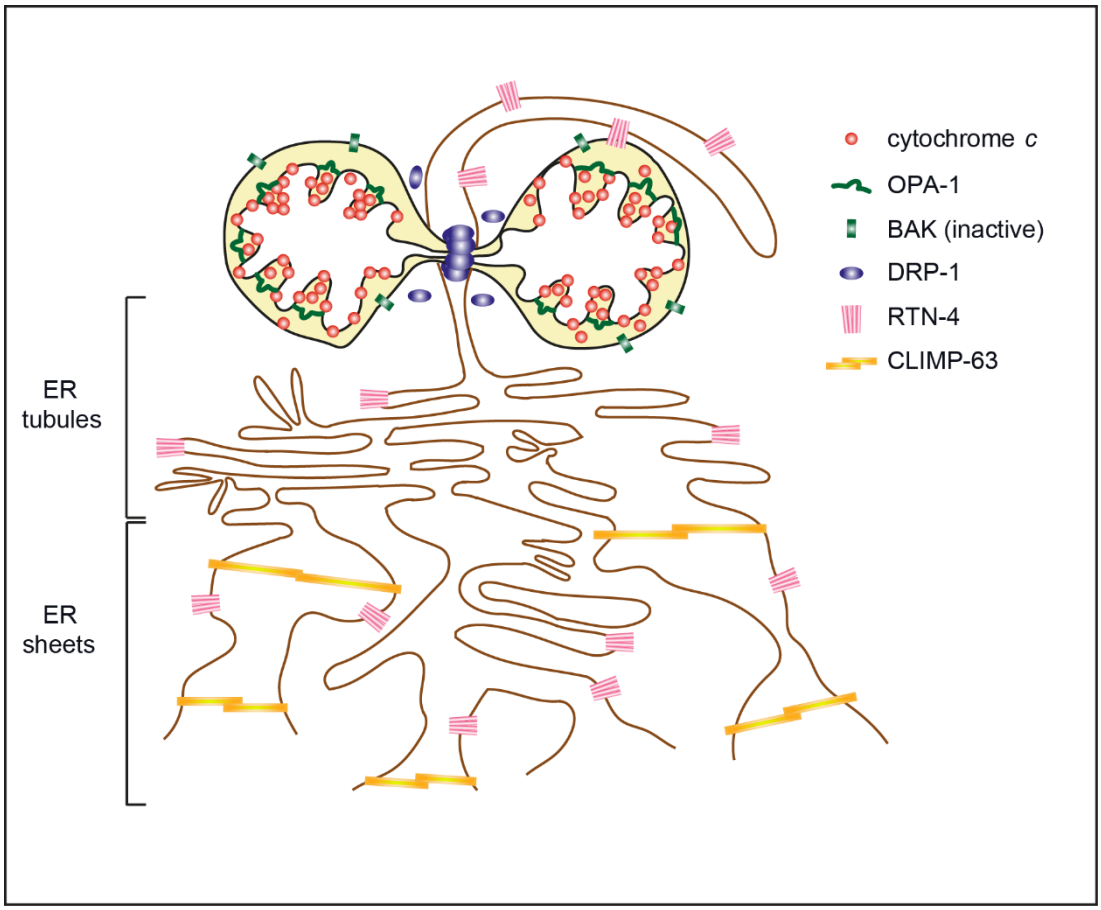

Figure 6.1. Schematic representation of mitochondria and ER, highlighting the organelle localisation of ER shaping proteins used throughout this study. ER wraps around mitochondria to facilitate DRP-1-mediated mitochondrial fission. Mitochondrial proteins cytochrome *c*, OPA-1 and BAK are shown to illustrate the possible involvement of the ER in apoptosis. ER shaping proteins RTN-4 and CLIMP-63 are shown to illustrate their ER localisation on ER tubules and/or sheets.

6.2Results

6.2.1 Silencing of ER shaping proteins alters mitochondrial ultrastructure

Over the last few years, several reports have highlighted the importance of ER membranes in regulating mitochondrial membrane dynamics.[276,315,316] ER interacts with mitochondria *via* different complexes, which could facilitate and orchestrate DRP-1-mediated mitochondrial fission.[277,312,317,318] To assess that, experiments were performed to elucidate how silencing some key ER shaping proteins, such as Reticulon-1 (RTN-1), Reticulon-4 (RTN-4), Lunapark-1 (LNP1) and CLIMP-63 could affect mitochondrial ultrastructure. While RTN-1/4 are transmembrane proteins involved in creating an ER curvature,[301,319] whereas CLIMP-63 maintains the shape of ER sheets (Figure 6.1).[301,320] LNP-1 is a three-way junction protein that resides in the ER membranes and regulates ER membrane interconnectivity.[321,322] To carry out this study, H1299 cells were transfected with siRNAs against the indicated ER shaping proteins and processed for EM. RNAi against DRP-1 was used as a positive control for demonstrating changes in mitochondrial ultrastructure. Visual analysis of EMs of these cells indicated increased mitochondrial elongation induced by silencing of DRP-1, as well as the different ER shaping proteins. Although the extent of elongation was not quantified, the same observation was made in multiple experiments in several, suggesting that DRP-1 and ER shaping proteins are playing a role in mitochondrial membrane dynamics (Figure 6.2).

6.2.2 3view EM imaging reveals a detailed analysis of the mitochondrial network

Although EM is extremely useful to visualise mitochondrial ultrastructure, a single two-dimensional micrograph does not convey the complexity of the highly

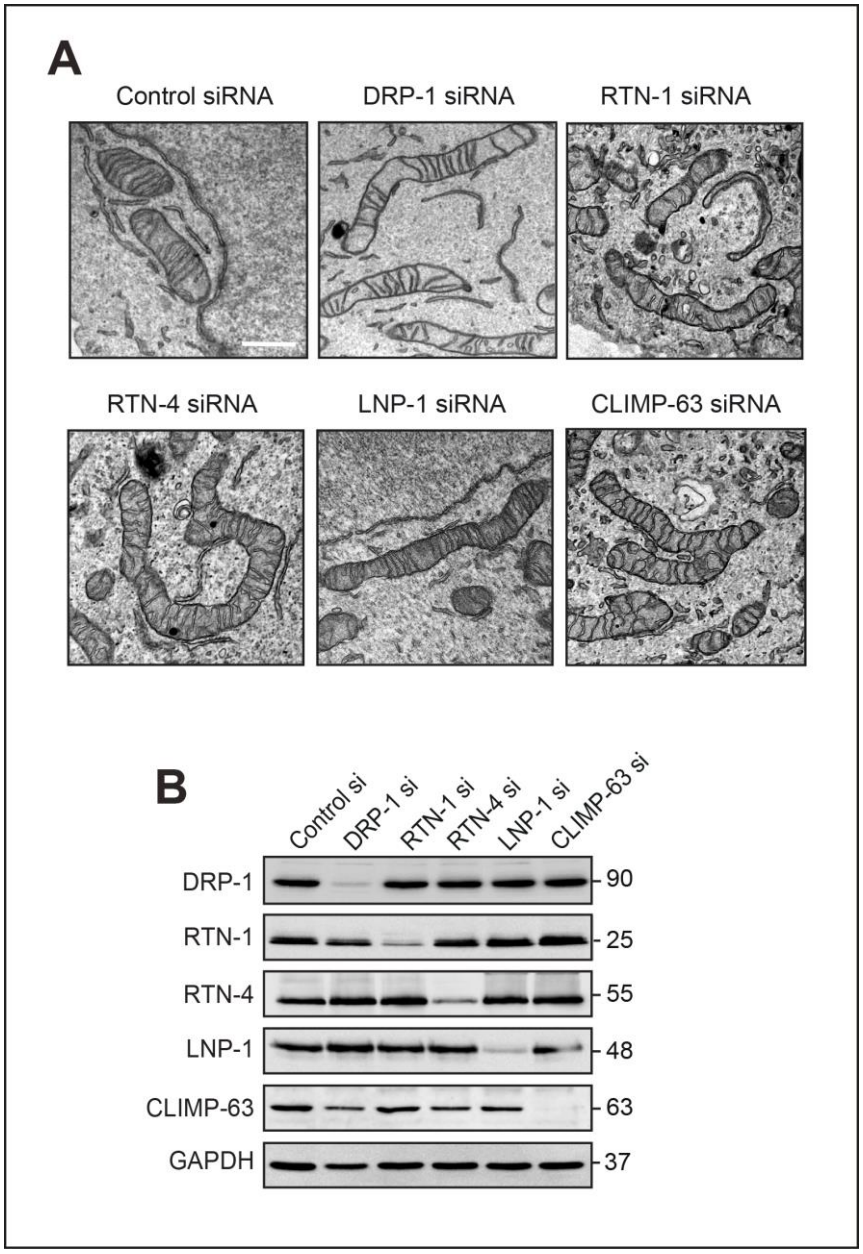

Figure 6.2. Silencing of ER shaping proteins induces mitochondrial elongation. Electron micrographs of H1299 cells transfected with control, DRP-1, RTN-4 or CLIMP-63 siRNA for 72 h. Scale bar: 500 nm. **(B)** Immunoblot showing silencing efficiency of DRP-1, RTN-4 and CLIMP-63 siRNAs in H1299 cells. GAPDH was used as a loading control.

filamentous mitochondria. Therefore, 3view EM analysis was used to render the whole mitochondrial structure from <150 serial sections (electron micrographs) of a single cell. This analysis demonstrated that mitochondria in the assessed cell were highly interconnected as the rendering revealed that the chosen mitochondrion spanned through several sections of the cell in a highly interconnected network (Figure 6.3). Furthermore, the particular cell that was analysed was rendered and quantified to comprise 145 mitochondria with a total volume of 220 μm^3 (Figure 6.3). Of the 145 mitochondria, only 2 had volumes greater than 50 μm^3 (70 and 65 μm^3), whereas the rest were discontinuous with volumes lower than 1 μm^3 (Figure 6.3).

6.2.3 Silencing of DRP-1 facilitates mitochondrial hyperfilamentation

In order to assess the effect of DRP-1 and possibly ER shaping proteins on mitochondrial structural changes, further studies involving 3view EM imaging were carried out using siRNAs against DRP-1 (positive control), as well as RTN-4 and CLIMP-63. Downregulation of DRP-1 drastically reduced the total number of mitochondria (145 in the control siRNA-transfected cell *versus* 67 for DRP-1 siRNA-transfected cell). Of the 67 mitochondria rendered in the DRP-1 siRNA-transfected cell, only 1 of the mitochondria demonstrated hyperfilamentation, defined by a single continuous mitochondrion, and mitochondrial swelling, with a total volume of 203 μm^3 (Figure 6.4, right panel, red dot) The rest of the mitochondria in this cell were discontinuous with volumes lower than 1 μm^3 (Figure 6.4).

Up to the final moments of writing this thesis, experiments are still being carried out for the assessment of mitochondrial volume and number in H1299 cells transfected with RTN-4 and CLIMP-63 siRNA.

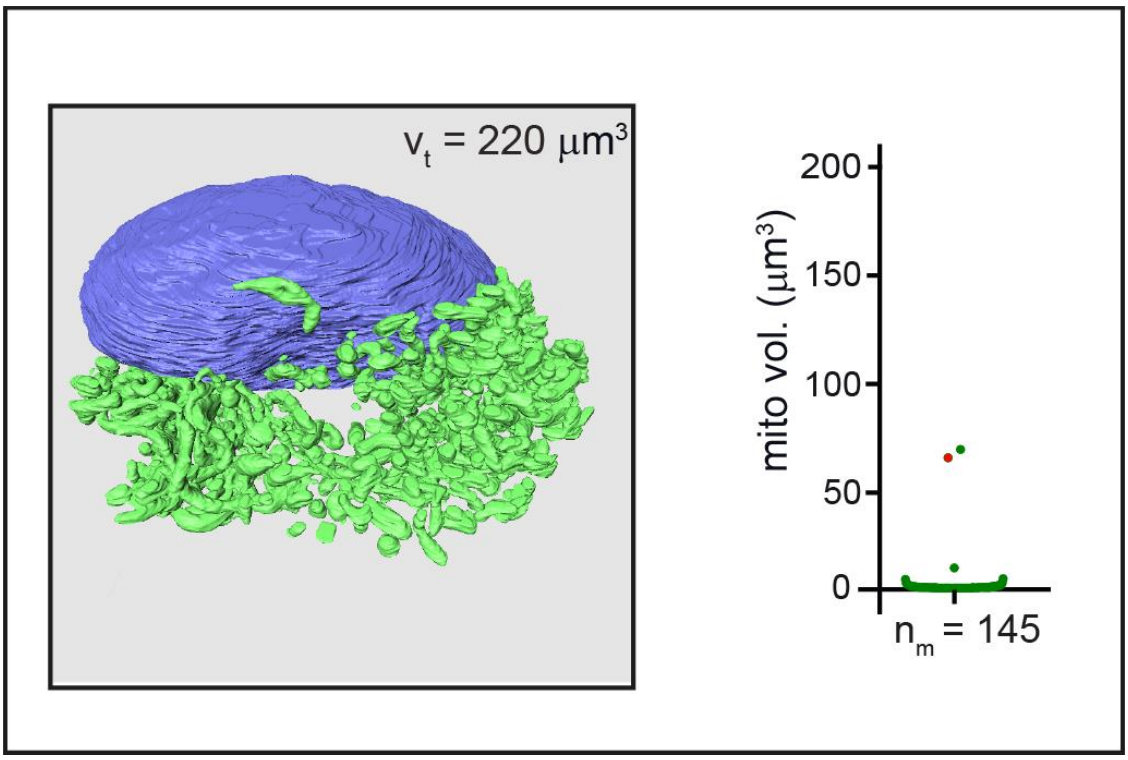

Figure 6.3. The complexity of the mitochondrial network. H1299 cells were processed for 3view electron tomography. Mitochondria (green) and nuclei (blue) were rendered and quantified for volume and number of mitochondrial fragments. Red dot corresponds to the mitochondrion used for rendering of ER in the next experiments. v_t, total volume of all mitochondria. n_m, number of mitochondria.

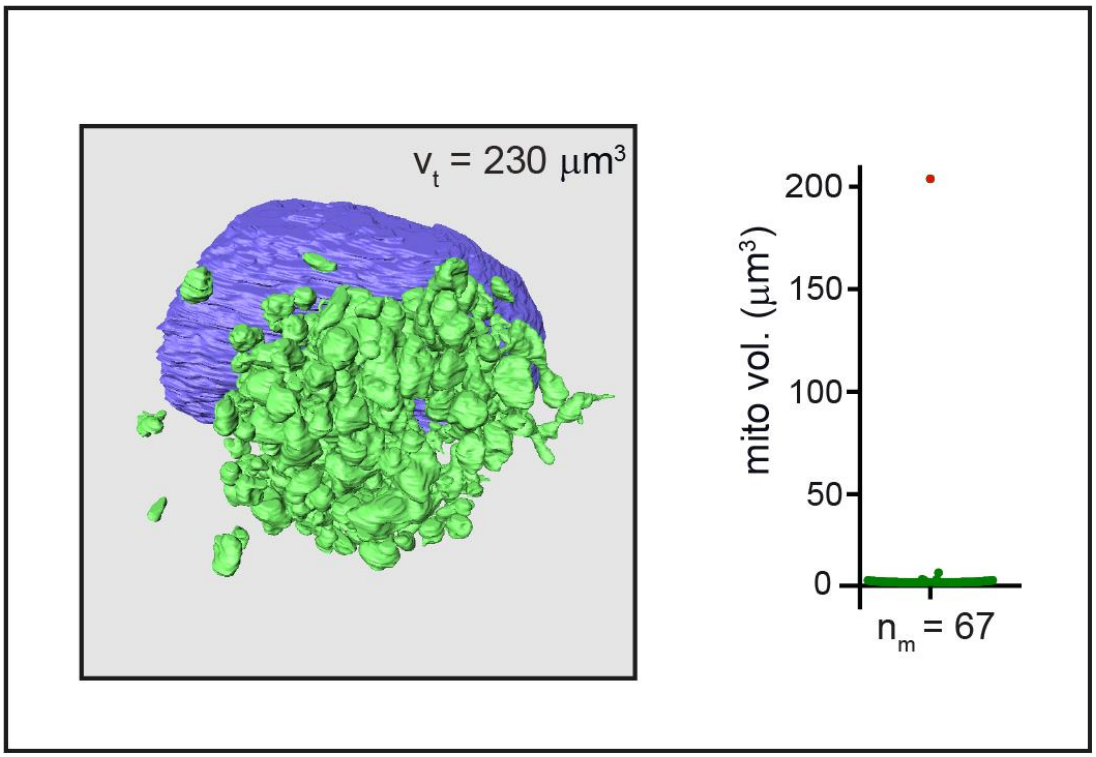

Figure 6.4. Mitochondrial network is altered by DRP-1. H1299 cells were reverse transfected with DRP-1 siRNA for 72 h and processed for 3view electron tomography. Mitochondria (green) and nuclei (blue) were rendered and quantified for volume and number of mitochondrial fragments. Red dot corresponds to the mitochondrion used for rendering of ER in the next experiments v_t, total volume of all mitochondria. n_m, number of mitochondria.

6.2.4 A-1210477 induces mitochondrial fission only in the presence of ER shaping proteins

The results shown in figure 6.2 indicated that ER shaping proteins seemed to play a role in mitochondrial membrane dynamics, possibly involving mitochondrial fission. As silencing of DRP-1 prevented A-1210477-mediated mitochondrial fragmentation (Figure 5.8), experiments were carried out to assess whether silencing the different ER shaping proteins would demonstrate similar effects. In these and the following experiments two different siRNAs targeting DRP-1, RTN-4 and CLIMP-63 were used to control for potential off-target effects. Indeed, silencing of the ER shaping proteins prevented A-1210477-mediated mitochondrial fragmentation (Figure 6.5), indicating that ER shaping proteins are important for mitochondrial fission, possibly by regulating the recruitment of DRP-1 to the mitochondria.

6.2.5 DRP-1 localisation at mitochondrial fission sites does not depend on ER shaping proteins

To examine whether the localisation of DRP-1 to mitochondrial fission sites is dictated by ER shaping proteins, H1299 cells lacking ER shaping proteins were exposed to A-1210477 and immunolabeled for both HSP70 and DRP-1. As expected, HSP70 staining showed a filamentous network of mitochondria in untreated cells, which underwent extensive fragmentation in the presence of A-1210477. DRP-1 staining in the untreated cells showed a punctate pattern and distributed evenly between the cytosol and mitochondrial membranes. Following A-1210477, one or more DRP-1 punctae were observed surrounding the fragmented mitochondrial filaments, suggesting that DRP-1 could have been recruited to the fission sites.

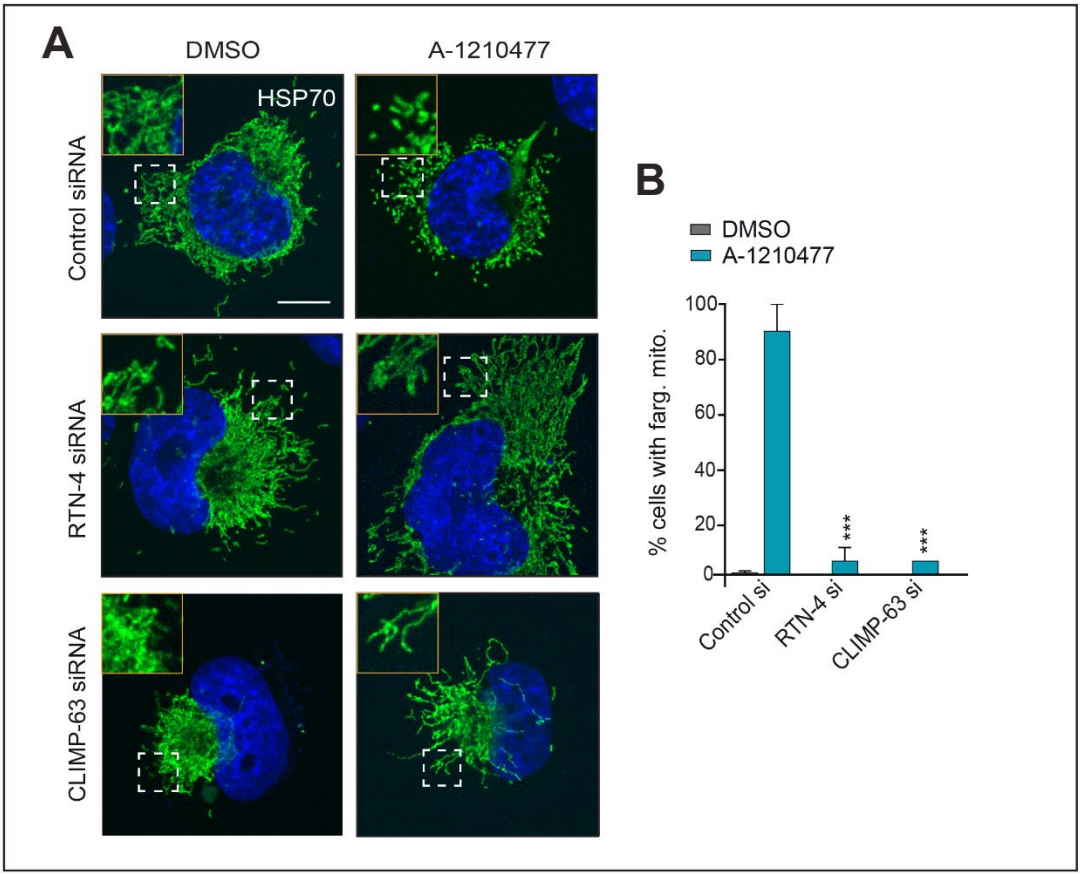

Figure 6.5. ER shaping proteins are required for A-1210477-mediated mitochondrial fragmentation. (A) H1299 cells were transfected with control siRNA, DRP-1 siRNA, RTN-4 siRNA or CLIMP-63 siRNA for 72h and assessed for mitochondrial shape by immunofluorescence with anti-HSP60 antibody upon exposure to A-1210477 (10 µM) for 4 h. Areas inside the dashed line boxes have been zoomed. Scale bar: 10 µm. **(B)** Quantification of the extent of mitochondrial fragmentation shown in A. At least 100 cells were counted for 3 independent experiments. Statistical analysis was conducted using one-way ANOVA (***P≤0.001).

Interestingly, none of the ER shaping proteins seemed to be required for A-1210477-mediated localisation of DRP-1 to the mitochondria, as a similar distribution pattern of DRP-1 was observed even in cells lacking RTN-4 and CLIMP-63 (Figure 6.6). These results could suggest that localisation of DRP-1 to mitochondria at fission sites could be dictated by mechanisms independent of these ER shaping proteins. However, as previously mentioned, assessment of DRP-1 activity/post-translational modifications and/or translocation to mitochondria would be beneficial to clarify the role of ER shaping proteins in the fission process. In this regard, time-lapse or live-cell imaging under these conditions could offer further insight.

6.2.6 CCCP induces mitochondrial fission independently of ER shaping proteins

Next, to assess whether ER shaping proteins regulated mitochondrial fission induced by other stimuli or the effect was exclusive to BH3 mimetics, H1299 cells transfected with RTN-4, and CLIMP-63 siRNA were exposed to carbonyl cyanide m-chlorophenyl hydrazine (CCCP), a proton uncoupler that rapidly depolarises mitochondria and induces mitochondrial fragmentation. While DRP-1 downregulation could overcome CCCP-mediated mitochondrial fragmentation, silencing of ER shaping proteins could not produce the same effect (Figure 6.7), possibly due to the ability of CCCP, but not A-1210477 to depolarise mitochondria in these cells.[251] This result indicates that, even in the absence of RTN-4 and CLIMP-63, CCCP could be recruiting DRP-1 to induce mitochondrial fragmentation.

6.2.7 Loss of mitochondrial fusion mediated by OPA-1 silencing does not require ER shaping proteins

Previous data suggested that DRP-1 played a critical role downstream of mitochondrial cristae remodelling and OPA-1 proteolysis in regulating apoptosis (Figure 5.17). To assess whether ER shaping proteins regulate mitochondrial fission

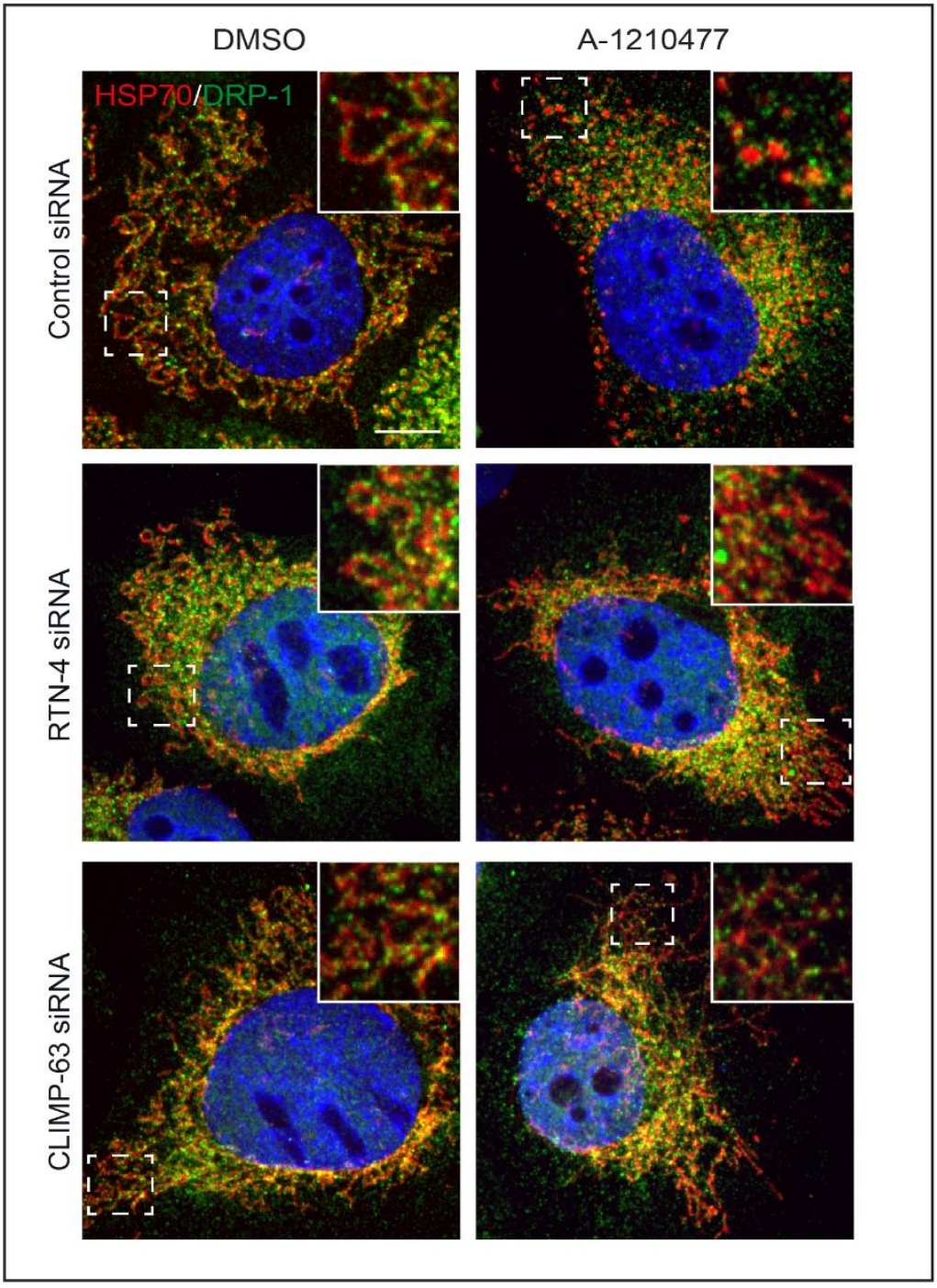

Figure 6.6. ER shaping proteins are not required for DRP-1 localisation at mitochondria fission sites. H1299 cells were transfected with control siRNA, RTN-4 siRNA or CLIMP-63 siRNA for 72 h and assessed for mitochondrial shape and for DRP-1 localisation by immunofluorescence with anti-HSP70 (red) and an anti-DRP-1 (green) antibody respectively, following exposure to A-1210477 (10 µM) for 4 h. Areas inside the dashed line boxes have been zoomed. Scale bar: 10 µm.

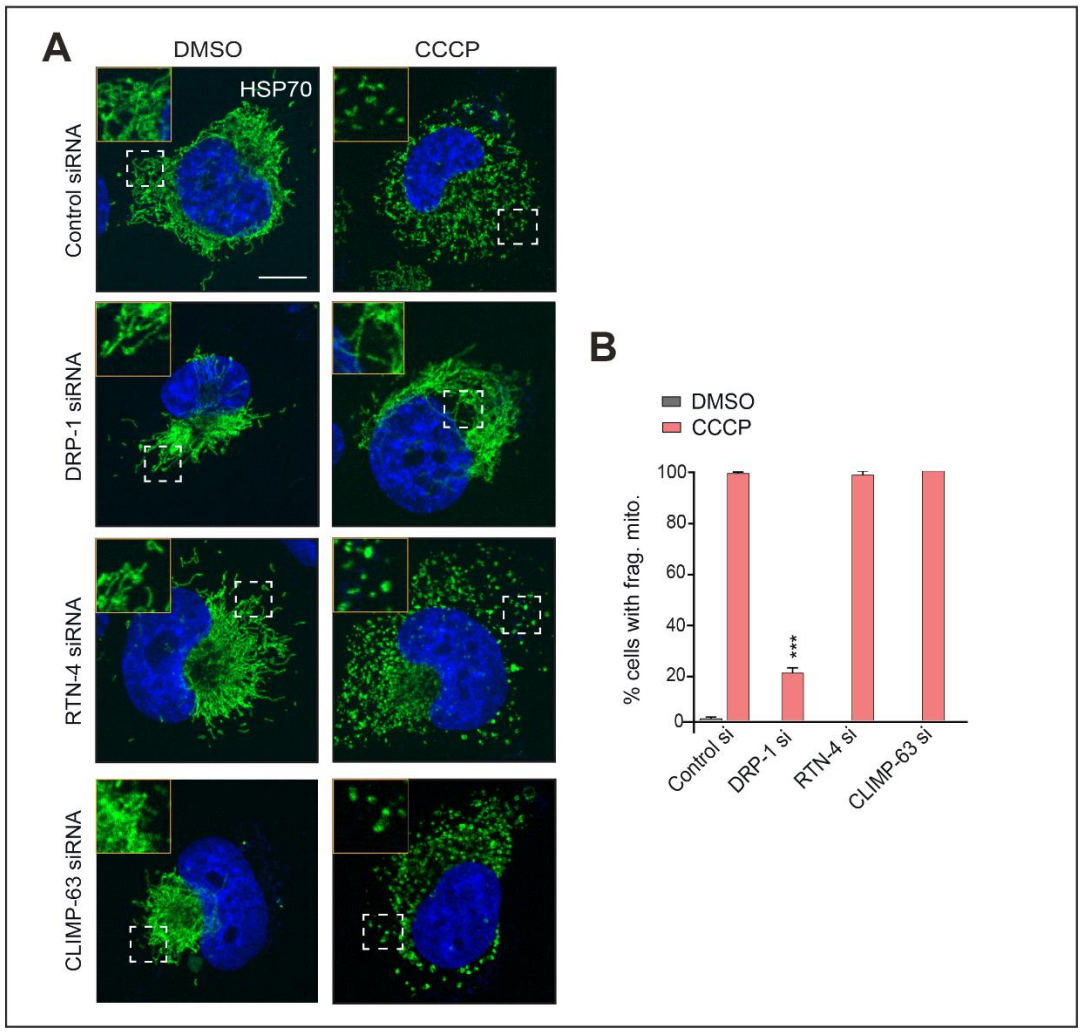

Figure 6.7. ER shaping proteins are not required for CCCP-mediated mitochondrial fragmentation. (A) H1299 cells were transfected with control siRNA, DRP-1 siRNA, RTN-4 siRNA or CLIMP-63 siRNA for 72 h and assessed for mitochondrial shape by immunofluorescence with an anti-HSP70 antibody following exposure to CCCP (20 µM) for 2 h. Areas inside the dashed line boxes have been zoomed. Scale bar: 10 µm. **(B)** Quantification of the extent of mitochondrial fragmentation shown in A. At least 100 cells were counted for 3 independent experiments. Statistical analysis was conducted using one-way ANOVA (***P≤0.001).

downstream of OPA-1 proteolysis, H1299 cells were transfected with RTN-4 and CLIMP-63 siRNA (DRP-1 siRNA was used as a positive control) in the presence and absence of OPA-1 siRNA and the extent of mitochondrial fragmentation was assessed.

Similar to the results obtained for CCCP-induced mitochondrial fragmentation, fragmentation induced by OPA-1 depletion depends on DRP-1 (Figure 6.8). This could be due to the tight connection between OPA-1, maintenance of cristae structure and mitochondrial polarisation. Furthermore, OPA-1 has been shown to stabilise different complexes of the respiratory chain, maintaining mitochondrial polarisation.[323] In marked contrast silencing of ER shaping proteins did not prevent mitochondrial fragmentation induced by OPA-1 silencing (Figure 6.8).

Taken together with previous results (Figures 6.5 and 6.7), these findings indicate that altering mitochondrial cristae either by silencing of OPA-1 or by direct mitochondrial depolarisation, resulted in extensive DRP-1-mediated mitochondrial fission, which occurred independently of the ER membranes.

6.2.8 Silencing of DRP-1 reduces the number of contact points between the ER and mitochondria

Previous results revealed that silencing of DRP-1 and ER shaping proteins reduced the total number of individual mitochondria in H1299 cells, resulting in a single, hyperfused mitochondrion (Figure 6.4). These data, combined with the model dictating that ER wraps around mitochondria to initiate mitochondrial fission, led to the hypothesis that the number of ER-mitochondria contact points could be significantly decreased following downregulation of the different ER shaping proteins. To assess this hypothesis, 3view analysis was performed in all ER

membranes around a chosen mitochondrion from a single cell (obtained from figure 6.3) was labelled and rendered to generate a composite image (Figure 6.9; left panel). The rendered image revealed that ER membranes extensively wrap the mitochondria, thus potentially making numerous contacts with the mitochondria (Figure 6.9; left panel). To quantify, the precise number of contacts that the ER makes with mitochondria, the number of ER-mitochondria contact points were calculated by counting how many times an ER membrane was in contact with a mitochondrial membrane. In the control cell, there were about 604 contact points (depicted as n_c=number of contact sites) (Figure 6.9; right panel). Due to variations in the volume between the selected mitochondrion in each condition, the number of contact points were normalised to the volume of the chosen mitochondrion. Since the volume of the chosen mitochondrion in the control cells was 65 μm^3 (Figure 6.3, right panel, red dot), the contact points for this mitochondrion was normalised by dividing n_c over mitochondrial volume to generate the number of ER-mitochondria contacts as 9.29 in the chosen mitochondrion (Figure 6.9; right panel). Interestingly, silencing of DRP-1 drastically reduced the number of ER-mitochondria contact points (Figure 6.10, right panel), from a ratio of 9.29 for control siRNA to 1.32 for DRP-1 siRNA. These results indicate that DRP-1 recruitment could facilitate the interactions between ER and mitochondria. It will be interesting to see if silencing of RTN-4 and CLIMP-63 would have similar effects in exhibiting decrease of ER-mitochondria contacts.

6.2.9 BH3 mimetic-induced PS externalisation and caspase processing require ER shaping proteins

Recent studies claim that ER plays a major role in the recruitment of DRP-1.[277] As previous results showed that DRP-1 is required for BH3 mimetic-mediated

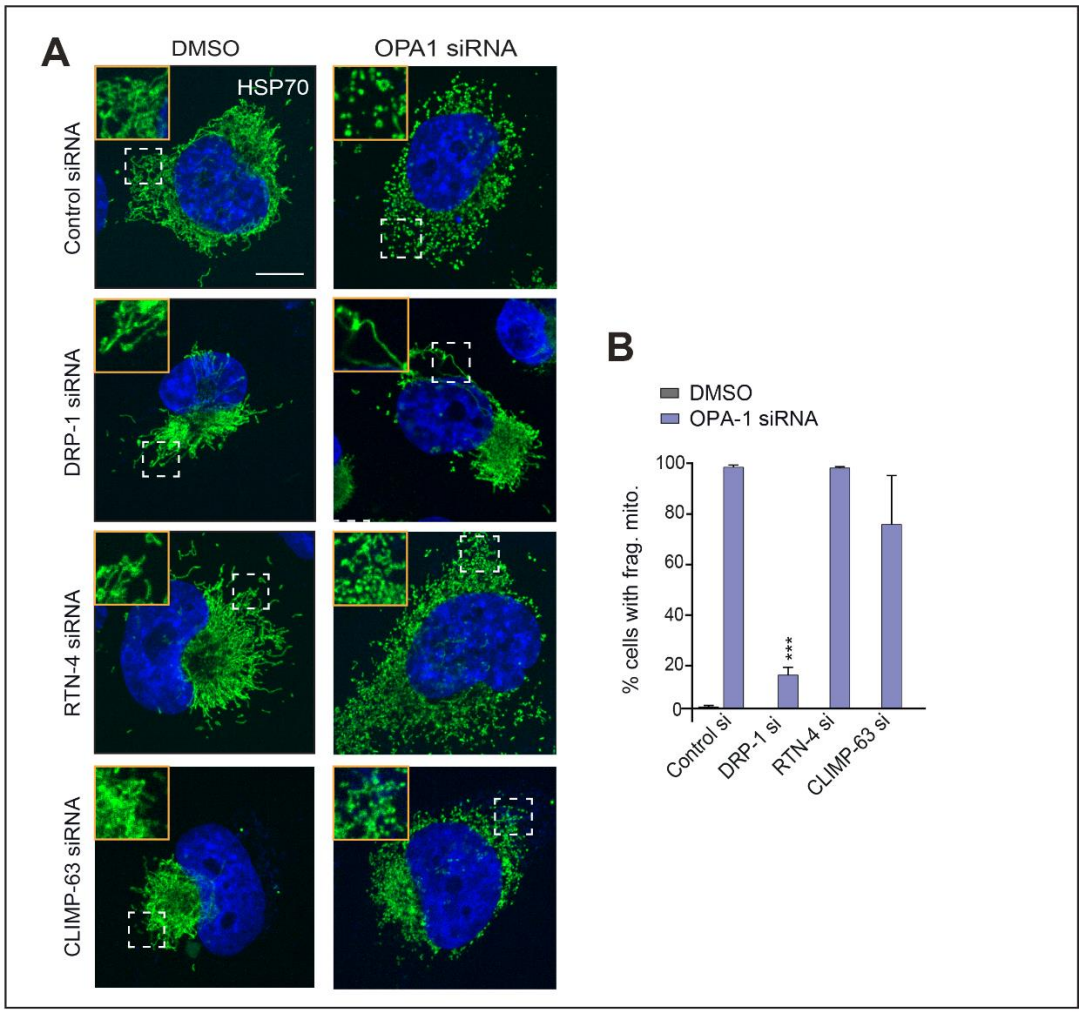

Figure 6.8. ER shaping proteins are not required for OPA-1 silencing-mediated mitochondrial fragmentation. (A) H1299 cells were transfected with control siRNA, DRP-1 siRNA, RTN-4 siRNA or CLIMP-63 siRNA alone or in combination with OPA-1 siRNA for 72 h and assessed for mitochondrial shape by immunofluorescence with anti-HSP70. Areas inside the dashed line boxes have been zoomed. Scale bar: 10 µm. **(B)** Quantification of the extent of mitochondrial fragmentation shown in A. At least 100 cells were counted for 3 independent experiments. Statistical analysis was conducted using one-way ANOVA (***P≤0.001).

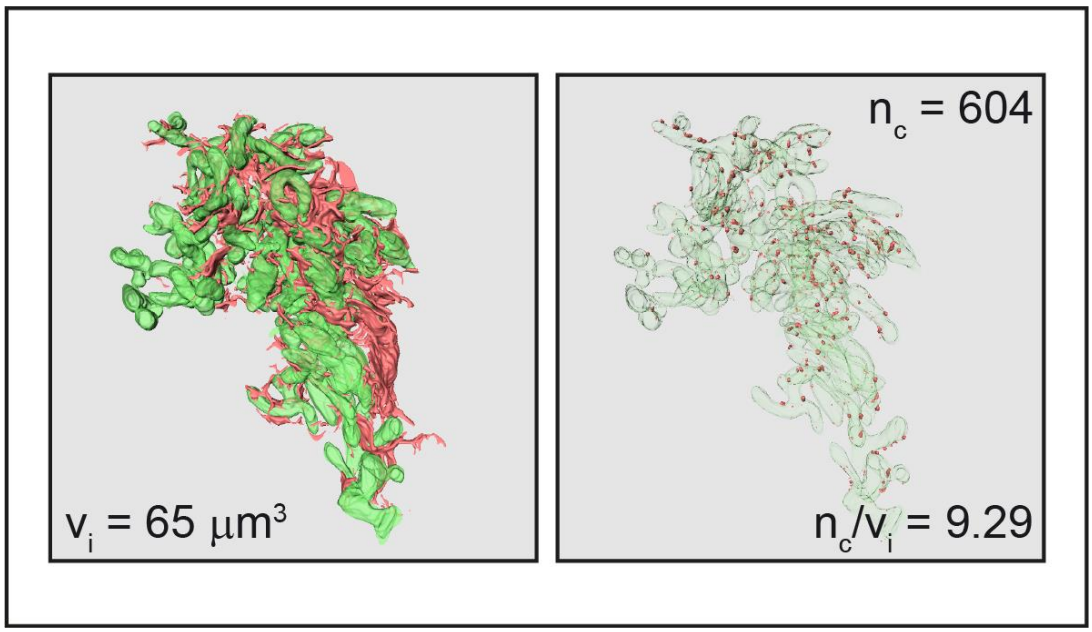

Figure 6.9. ER-mitochondrial contact sites are abundant in H1299 cells. H1299 cells were processed for 3view electron tomography. An isolated mitochondrion, obtained from figure 6.3 (green), was rendered and its volume calculated. Similarly, ER (red, left panel) at the mitochondrion surrounding were rendered and contact points were quantified (right panel, red spheroids). v_i, volume of selected mitochondrion. n_c, number of contact points.

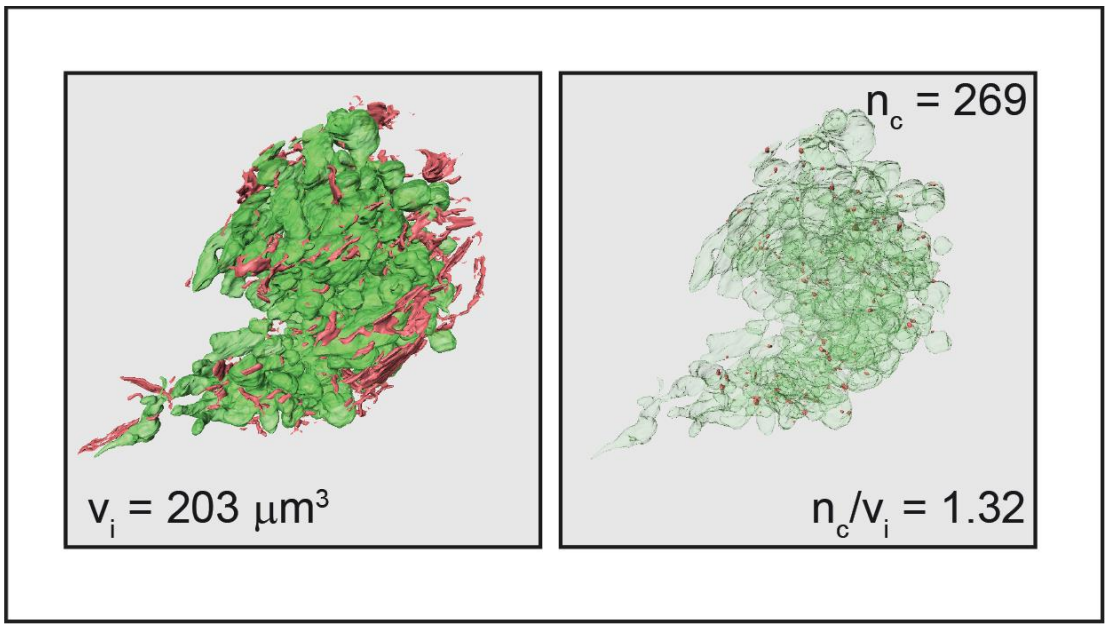

Figure 6.10. ER-mitochondrial contact sites are drastically reduced by DRP-1 silencing. H1299 cells were reverse transfected with DRP-1 siRNA for 72 h and processed for 3view electron tomography. An isolated mitochondrion obtained from figure 6.4 (green) was rendered and its volume calculated. Similarly, ER (red, left panel) at the mitochondrion surrounding were rendered and contact points were quantified (right panel, red spheroids). v_i, volume of selected mitochondrion. n_c, number of contact points.

BAK activation, cytochrome *c* release and PS externalisation (Figures 5.13 and 5.14) and ER shaping proteins seem to be important for A-1210477-mediated mitochondrial fragmentation (Figure 6.5), a strategy, similar to the one used to identify the role of DRP-1 in apoptosis, was adopted to understand how the ER shaping proteins can regulate the distinct steps of the intrinsic pathway of apoptosis (Figure 6.11 A). H1299 cells were transfected with two different DRP-1, RTN-4 or CLIMP-63 siRNAs, exposed to a combination of A-1210477 and A-1331852 and apoptosis assessed by PS externalisation and immunoblotting. Although statistically significant, the protective effect of RTN-4 and CLIMP-63 silencing was not as effective as DRP-1 siRNA in antagonising BH3 mimetic-mediated apoptosis as evidenced by PS externalisation (Figure 6.11 B). However, the appearance of the cleaved forms of caspase-9, -3 and -7 in cells exposed to BH3 mimetics was markedly inhibited by silencing of DRP-1, RTN-4 and CLIMP-63 (Figure 6.11 C). These data indicate that DRP-1, RTN-4 and CLIMP-63 are required for an effective induction of BH3 mimetic-mediated apoptosis.

6.2.10 BH3 mimetic-induced cytochrome *c* release requires ER shaping proteins

Next, the effects of silencing the ER shaping proteins on BH3 mimetic-mediated MOMP, measured by cytochrome *c* release were analysed (Figure 6.12 A). H1299 cells were transfected with two different DRP-1, RTN-4 and CLIMP-63 siRNAs, exposed to a combination of both A-1210477 and A-1331852 and assessed for the extent of cytochrome *c* release using immunocytochemistry. Similar to the results observed by PS externalisation and apoptosis silencing of CLIMP-63 effectively prevented BH3 mimetic-mediated cytochrome *c* release (Figure 6.12). Although statically significant, RTN-4 silencing was not as effective in antagonising

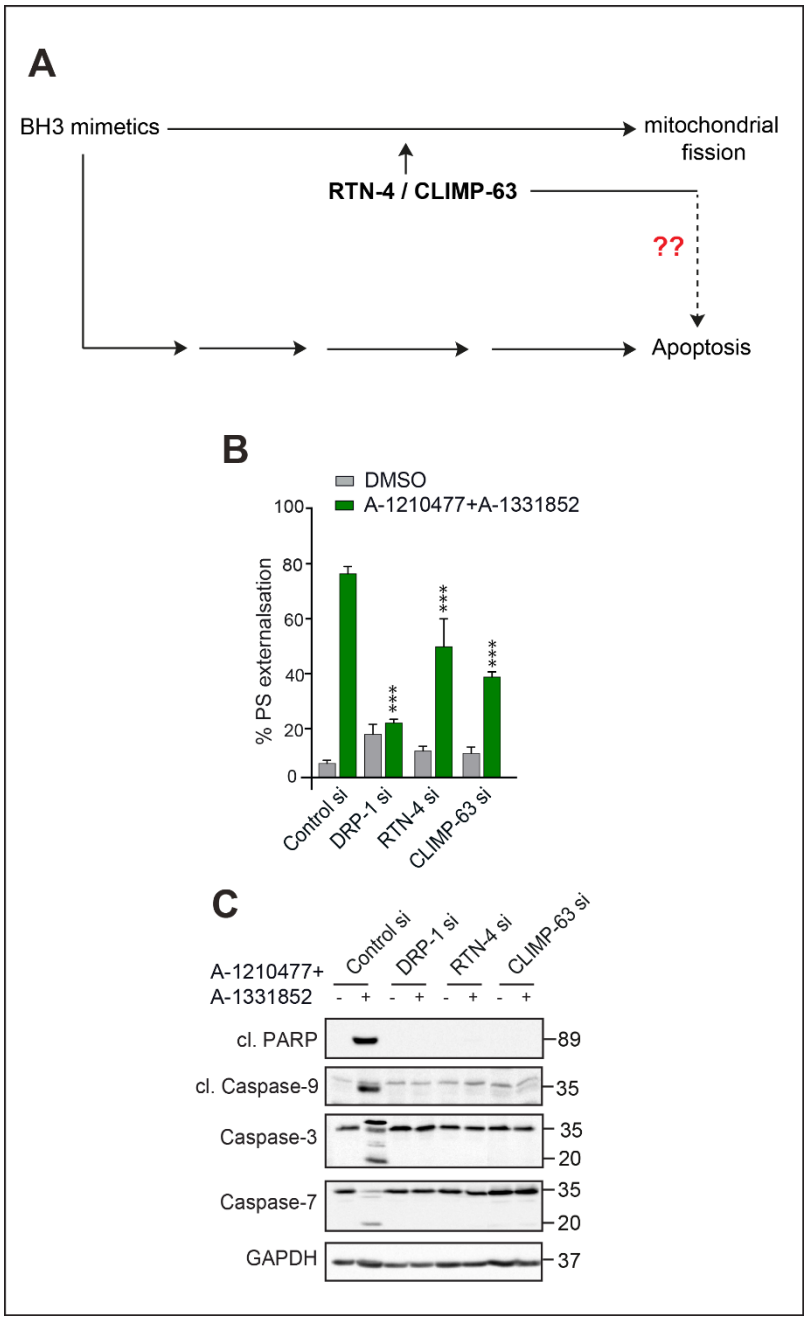

Figure 6.11. ER shaping proteins are required for BH3 mimetic-mediated apoptosis. **(A)** Flowchart representing the findings of this study hitherto **(B)** H1299 cells were transfected with control siRNA, RTN-4 siRNA or CLIMP-63 siRNA for 72 h and assessed for the extent of phosphatidylserine externalisation by FACS upon exposure to a combination of A-1210477 (10 µM) and A-1331852 (100 nM) for 4 h. Statistical analysis was conducted using one-way ANOVA (***P≤0.001). **(C)** Immunoblots of H1299 cells transfected with the same siRNAs and exposed to the same conditions as in (A) showing distinct apoptotic markers, such as PARP, Caspase-9, Caspase-3 and Caspase-7 processing. GAPDH was used as a loading control. cl: cleaved.

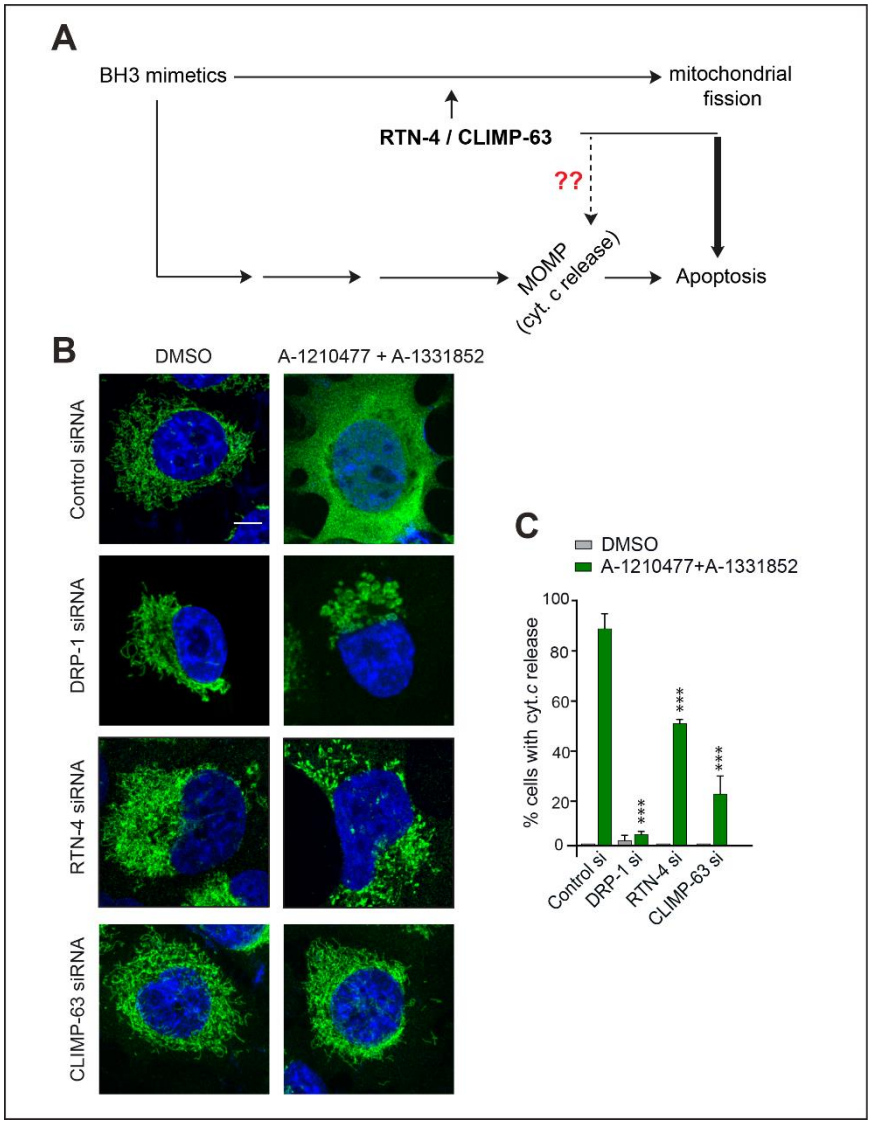

Figure 6.12. ER shaping proteins are required for BH3 mimetic-mediated cytochrome *c* release. (A) Flowchart representing the findings of this study hitherto **(B)** H1299 cells were transfected with control siRNA, RTN-4 siRNA or CLIMP-63 siRNA for 72 h and assessed for the extent of cytochrome *c* release by immunofluorescence following exposure to a combination of A-1210477 (10 µM) and A-1331852 (100 nM) for 4 h. Scale bar: 10 µm. **(C)** Quantification of the extent of cytochrome *c* release shown in A. At least 100 cells were counted for 3 independent experiments. Statistical analysis was conducted using one-way ANOVA (***P≤0.001).

BH3 mimetic-mediated release of cytochrome c (Figure 6.12 B and C). Nevertheless, these data indicate that ER shaping proteins also play a role in the regulation of MOMP.

6.2.11 BH3 mimetic-induced BAK activation requires DRP-1 and CLIMP-63, but not RTN-4

Previous results showed that DRP-1, RTN-4 and CLIMP-63 were required for BH3 mimetic-mediated cytochrome *c* release and MOMP (Figure 6.12). During the intrinsic pathway of apoptosis, cytochrome *c* is released from mitochondria to the cytosol via BAX/BAK-mediated pores in the outer mitochondrial membrane. As activation of BAK is a necessary step for the formation of the pore, the block in cytochrome *c* release induced by silencing of DRP-1, RTN-4 and CLIMP-63 could be related to BAK activation (Figure 6.13 A). It must be noted that H1299 cells do not express BAX. To assess BAK activation, H1299 cells were transfected with control, DRP-1, RTN-4 or CLIMP-63 siRNA and exposed to a combination of both A-1210477 and A-1331852 and stained with anti-activated BAK specific antibody. While silencing of DRP-1 and CLIMP-63 prevented BH3 mimetic-mediated BAK activation, in agreement with measurements of PS externalisation and cytochrome *c* release, silencing of RTN-4 did not have any protective role in BH3 mimetic-mediated BAK activation In fact, silencing of RTN-4 slightly increased the extent of BAK activation following exposure to BH3 mimetics in these cells (Figure 6.13 B). These findings uncoupled the effect of RTN-4 and CLIMP-63 in regulating the distinct steps of the intrinsic apoptotic pathway.

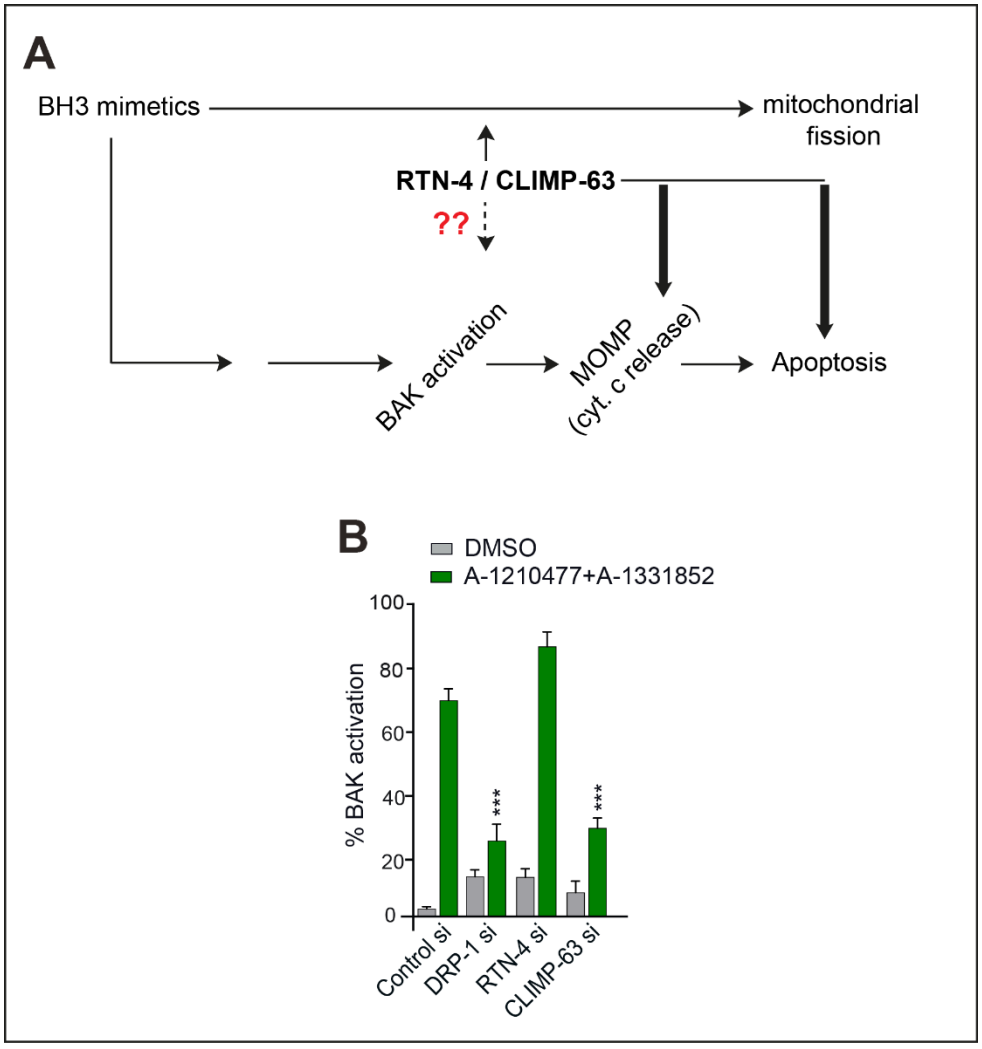

Figure 6.13. DRP-1 and CLIMP-63 are required for BH3 mimetic-mediated BAK activation. (A) Flowchart representing the findings of this study hitherto. **(B)** H1299 cells were transfected with control siRNA, DRP-1 siRNA, RTN-4 siRNA or CLIMP-63 siRNA for 72 h and assessed for BAK activation by FACS upon exposure to a combination of A-1210477 (10 μM) and A-1331852 (100 nM) for 4 h. Statistical analysis was conducted using one-way ANOVA (***P ≤ 0.001).

6.2.12 ER shaping proteins are not required for BH3 mimetic-induced mitochondrial cristae remodelling

Although only DRP-1 and CLIMP-63, but not RTN-4 silencing prevented BH3 mimetic-mediated BAK activation, it was important to ascertain whether ER shaping proteins were required for BH3 mimetic-induced cristae remodelling. To assess this, H1299 cells were transfected with control, DRP-1, RTN-4 or CLIMP-63 siRNA, exposed to a combination of A-1210477 and A-1331852 and subjected to EM analysis. Silencing of the ER shaping proteins did not prevent BH3 mimetic-mediated mitochondrial cristae remodelling as it did not inhibit the loss of mitochondrial cristae, the appearance of outer mitochondrial membrane breaks and the major mitochondrial ultrastructural changes (Figure 6.14). Taken together, these results indicate that the ER shaping proteins play a role downstream of cristae remodelling in the intrinsic pathway of apoptosis.

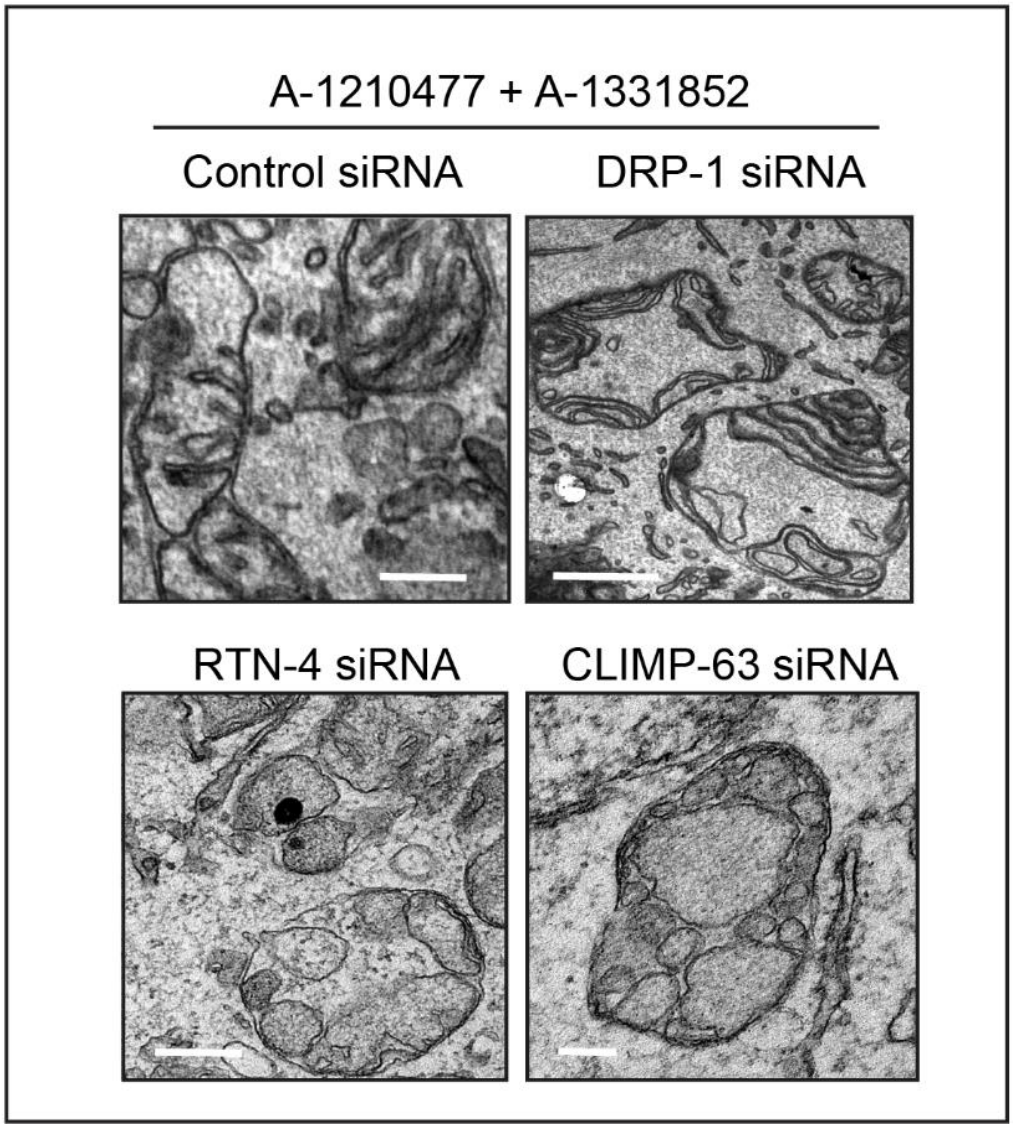

Figure 6.14. BH3 mimetics induce cristae remodelling independent of ER shaping proteins. Electron micrographs of H1299 cells transfected with control, DRP-1, RTN-4 or CLIMP-63 siRNA and exposed to a combination of A-1210477 (10 μM) and A-1331852 (100 nM) for 4 h. Scale bar: 10 nm.

6.3 Discussion

The recent model linking mitochondrial fission and apoptosis highlights the interactions between ER and mitochondria as initiators of these processes.[277] According to the model, ER wraps around mitochondria to initiate the assembly of DRP-1 constriction ring.[277] Since ER shaping proteins play an important role in the maintenance of ER structure and function,[301,302] the roles of these proteins in mitochondrial fission and apoptosis were investigated in this chapter.

The data presented here support the ER-mitochondrial fission model by indicating that silencing of RTN-4 and CLIMP-63 not only induced mitochondrial elongation (Figure 6.2), but also prevented BH3 mimetic-mediated mitochondrial fragmentation (Figure 6.5). Moreover, silencing of RTN-4 and CLIMP-63 did not seem to affect DRP-1 localisation to fission sites, although DRP-1 activity was not assessed (Figure 6.6). Further investigation using live-cell microscopy and quantitative analysis could provide further information. In this context, determination of the number of contact sites between ER and mitochondria in cells lacking RTN-4 and CLIMP-63 would be extremely valuable. In addition, it is important to underline that, despite providing highly informative data, 3view microscopy is a technique based on single cell analysis. Analysing a larger dataset or using other techniques such as standard transmission electron microscopy could be beneficial to reduce sampling bias.

Even though DRP-1 and ER shaping proteins regulate mitochondrial fission-fusion dynamics, mitochondrial fragmentation induced by CCCP or OPA-1 silencing is only dependent on DRP-1, with no role evidence for ER shaping proteins in these processes (Figures 6.7 and 6.8). OPA-1 is a major factor in mediating mitochondrial fusion and maintaining cristae stability.[266,289,324] The results presented in this chapter

also indicate that ER shaping proteins are required for BH3 mimetic-mediated OMM break but IMM cristae remodelling lies downstream of ER shaping proteins in the apoptotic pathway (Figure 6.14). Furthermore, silencing of RTN-4 and CLIMP-63 prevented BH3 mimetic-mediated cytochrome *c* release and apoptosis (Figure 6.11 and 6.12). Although there are several reports underlining the functions of RTN-4 and CLIMP-63 in the maintenance of ER shape, structure and function,[319,325–327] there are few studies linking these ER shaping proteins to cell death, to date. For instance, silencing of RTN-1, another member of the reticulon family, has been shown to reduce apoptosis during cerebral ischemia by retrotranslocating BCL-X_L from mitochondria to ER.[328] Similar interaction of a related protein RTN-XS with BCL-2 and BCL-X_L in the ER has been reported to reduce the anti-apoptotic activity of these proteins.[329] However, these studies did not focus specifically on the effects of these ER shaping proteins in apoptosis, and did not employ a *bona fide* apoptotic inducer like BH3 mimetics.

Based on the findings presented in this chapter, an integrative model of ER-mitochondrial membrane dynamics and BH3 mimetic-mediated apoptosis is shown for the first time. Therefore, we propose a model in which BH3 mimetics facilitate the recruitment of ER membranes (involving specific ER shaping proteins such as RTN-4 and CLIMP-63) and DRP-1 to mitochondrial fission sites, inducing enhanced mitochondrial fission and/or MOMP, followed by BAK activation, cytochrome *c* release and subsequent apoptosis (Figure 6.15). Further studies are required to understand the role of ER shaping proteins in cristae remodelling and possible interactions with proteins at the OMM to better characterise the effect described here. All in all, this is the first study to describe the roles of ER shaping proteins in mitochondrial membrane dynamics and cell death.

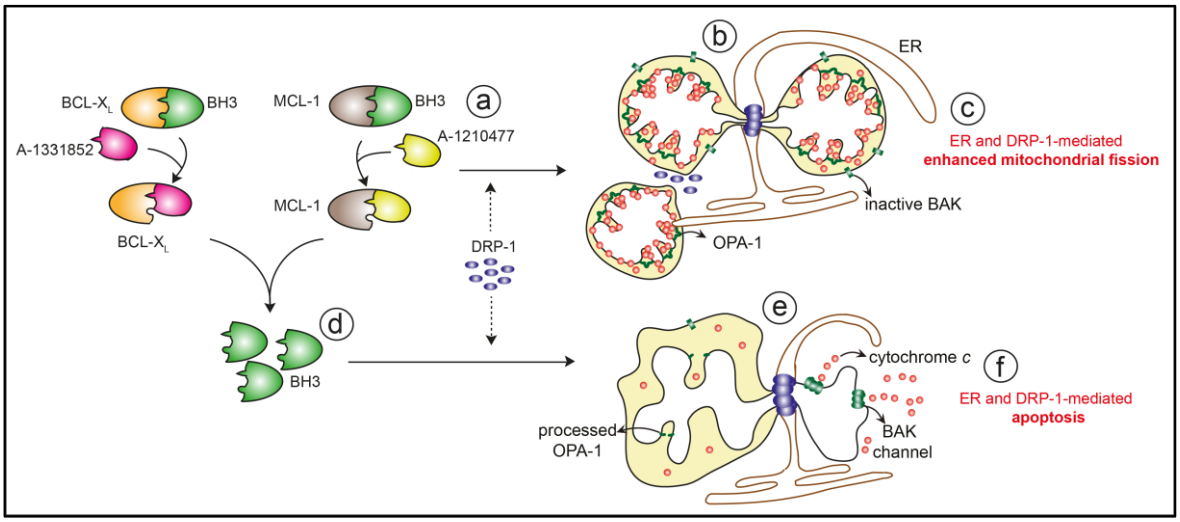

Figure 6.15. ER shaping proteins and DRP-1 are required for BH3 mimetic-mediated mitochondrial fission and apoptosis. (a) Upon exposure to A-1214077, DRP-1 is recruited and oligomerises at (b) ER-marked mitochondrial fission sites, in a process dependent on ER shaping proteins that culminates in (c) enhanced mitochondrial fission. (d) Upon exposure to both A-1210477 and A-1331852, BH3 only members are released from MCL-1 and BCL-X_L, facilitating (e) DRP-1 oligomerisation at ER-marked mitochondrial sites, culminating in (f) BAK activation, cristae remodelling, cytochrome *c* release and apoptosis dependent on DRP-1 and ER shaping proteins.

CHAPTER 7

DISCUSSION

Chapter contents

7.1 Inhibition of BCL-X_L in CML as an adjunct/alternative to TKI therapy

As development of resistance to TKIs poses a major problem for CML therapy, new efforts to target other cellular pathways to induce apoptosis in cancer cells have been widely considered[330–332] (and clinical trials NCT00006364, NCT00049192, NCT00381550). In chapter 3, BCL-X_L has been identified as a novel therapeutic target for CML. Genetic and pharmacological inhibition of BCL-X_L not only induced rapid apoptosis in CML cell lines, but also promoted cell death in patient-derived CML cells while sparing healthy MNCs. Although some studies have shown that using ABT-737 in combination with TKIs could induce apoptosis in $CD34^+$ progenitor cells, it has been speculated that Imatinib could reduce MCL-1 expression, which in combination with ABT-737 is sufficient to inhibit all major anti-apoptotic BCL-2 family members.[193] More recent papers imply a closer link to BCL-X_L inhibition and the induction of apoptosis in CML.[36,333,194] Using animal models, it has been shown that BCL-X_L is not necessary for the development of CML but it plays a major role in disease progression.[36]

The ability of A-1331852 to induce apoptosis in a BCR-ABL driven malignancy like CML could be attributed to STAT5, which is a critical substrate of BCR-ABL.[194] Upon phosphorylation of STAT5 by BCR-ABL, BCL-X_L transcription is enhanced leading to an increased anti-apoptotic phenotype.[194] In addition, overexpression of a dominant negative STAT5 ablated the increased transcription of BCL-X_L even in BCR-ABL positive cells.[194] Furthermore, decreased STAT5 activity was also linked to enhanced expression of BIM[116] and BAD,[334] further escalating the imbalance of the pro- and anti-apoptotic members of the BCL-2 family. Of interest, in a therapeutic context, a combination of ABT-263 and PP242 (a mTOR inhibitor) has been shown to induce selectively toxicity in CML $CD34^+$ progenitor cells but not

normal progenitors cells, which has been attributed to BAD activation.[36] With the recent introduction of more selective BH3 mimetics such as A-1331852, it is arguably more beneficial to directly inhibit BCL-X_L using BH3 mimetics than to alter BCR-ABL/STAT5/mTOR signalling pathways, all of which will invariably have multiple downstream effects.

Although this strategy offers much promise, it is important to consider the challenges imposed by the inhibition of BCL-X_L. BCL-X_L inhibition/depletion has been strongly linked to a decrease in platelet population, as these cells depend mainly on BCL-X_L for survival.[152] Although this is a limiting factor in cancer therapy and has paved a way for the development of ABT-199 for the treatment of CLL, thrombocytopenia following BCL-X_L inhibition could be managed clinically with platelet transfusion. Therefore, the possibility to inhibit BCL-X_L in CML still remains, especially when used in conjunction with current TKI therapies, which may facilitate lower dosage and a better clinical outcome. Another issue that can emerge from the use of BH3 mimetics in CML is the development of resistance. Recently we have shown that K562 cells can rapidly acquire resistance to A-1331852, which in turn, can be overcome by targeting other pathways of intermediary metabolism.[248] Currently several BCL-X_L inhibitors have been developed by pharmaceutical companies with great therapeutic potential for different cancers,[162,163] however these inhibitors are yet to be tested in clinical trials. Given the results of this study, clinical trials with BCL-X_L inhibitors will be beneficial for CML patients.

7.2 Inhibition of both BCL-2 and MCL-1 in AML

Despite the increasing body of knowledge towards understanding the mechanisms underlying clinical and molecular aspects of AML, an effective treatment for the disease remains elusive.[187,216,335] So far FLT3 has been the primary target in AML, since FLT3 alterations that are found in 25% of AML cases which are most aggressive than normal. Interestingly, MCL-1 was found overexpressed in FLT3 mutated AML cells resistant to TKIs, and silencing of MCL-1 in these cells rescued sensitivity to TKIs.[336] Similarly, BCL-2 has been found overexpressed in primary AML cell lines, and targeting BCL-2 with ABT-737 has been shown to synergise with FLT3 inhibitors.[337] Furthermore, BCL-2 and MCL-1 seem to play redundant roles in AML as BCL-2-bound BIM is sequestered by MCL-1 upon BCL-2 inhibition, thus causing resistance to apoptosis. [338] This could be overcome by dual inhibition of BCL-2 and MCL-1. Recent efforts have initially uncovered the potential of inhibiting both BCL-2 and MCL-1 in AML. An initial study using venetoclax and A-1210477 has shown that AML cell lines and primary patient samples underwent apoptosis upon exposure to both compounds.[338] However, the concentrations used in this study were around the micromolar range, which are not translatable to the clinical setting. This issue has been resolved by the introduction of more potent MCL-1 inhibitor such as S63845 and which induce high levels of apoptosis in AML cell lines and mouse xenograft models.[169]

In agreement, the results in chapter 3 show that dual inhibition of BCL-2 and MCL-1 by BH3 mimetics synergistically induce apoptosis in AML cell lines and promote cell death in AML patient cells in an additive manner. While this thesis was in preparation, a paper published in *Leukemia* also confirmed that a combination of BCL-2 and MCL-1 inhibition is effective in inducing apoptosis in AML.[339] The

potential of tackling MCL-1 and BCL-2 in AML offers much promise and this drug combination has entered 3 clinical trials for the treatment of AML.[169] In support of that, S63845 and AMG176 (another MCL-1 inhibitor) have entered phase I studies (individual drugs) in combination with venetoclax to treat AML (Clinical trials: NCT03672695 and NCT03797261, respectively).

7.3 The potential of using BH3 mimetics to improve therapy in solid tumours

In the last 50 years, the understanding of the biology of HNSCC has been greatly improved. Cisplatin and/or radiotherapy remain the gold standard therapy for HNSCC, however these therapeutic strategies are often plagued with resistance or undesirable side effects.[239] In HNSCC, resistance to cisplatin has been attributed to mutation or loss of p53, the most commonly altered gene in the malignancy.[340,341] Numerous strategies, including the inhibition of STAT3 and Chk1/2 to promote cell death in p53 mutated HNSCC cell lines, have been advocated to restore sensitivity to cisplatin.[341] As previously mentioned, STAT3 has been reported to upregulate MCL-1 in AML, and this could be the possible mechanism by which inhibition of STAT3 is effective in HNSCC.[342,336] Interestingly, a short nuclear isoform of MCL-1 responds to DNA damage promoting phosphorylation of Chk1, therefore inhibition of Chk1 could also be linked to nuclear MCL-1 downregulation and enhanced sensitivity to cisplatin.[174,343]

Several studies have explored the role of the BCL-2 family of proteins in HNSCC. IHC analyses of BCL-2 levels have presented indecisive results when correlated with clinical outcome. In agreement with the data presented in chapter 4, most of these studies showed that BCL-2 expression in HNSCC was low,[232,344–350] however, others have proposed BCL-2 as an early prognostic marker of HNSCC as BCL-2 protein levels were considered high in 25 to 55% of the cases analysed.[351–353]

Although BCL-2 inhibition with ABT-199 is highly effective and is currently being employed in more than 100 clinical trials, this study indicates that targeting BCL-2 in HNSCC patients would not be as effective as targeting MCL-1 and BCL-X_L, despite that only a few studies have investigated BCL-X_L and MCL-1 in HNSCC.[37,54,344,348,350] Our results showed that BCL-X_L expression is higher than MCL-1, especially when considering the advancing front of the oral cavity tumours. That could be the reason as to why a recent work has shown that ABT-737, when combined with etoposide or cisplatin, induced apoptosis and reduced clonogenic potential of HNSCC, albeit in considerably high concentrations (5 µM) and over 48 h of exposure.[234] Furthermore, the precise mechanisms dictating low MCL-1 levels in the advancing front could be due to a functional redundancy with BCL-X_L, which has been shown to promote epithelial-mesenchymal transition and tumour metastasis.[37] Nevertheless, since BCL-X_L and MCL-1 have similar roles in apoptosis and tumour survival in HNSCC, targeting these two proteins could be beneficial for HNSCC therapy.

Determination of the therapeutic index for the combination of S63845 and A-1331852 for HNSCC patients could be highly valuable, as cisplatin therapy only marginally improves overall survival with high toxicity. In addition, many HNSCC patients in advanced stages of the disease are not suitable for a cisplatin-based regimen. Although, when used as single agents, the BH3 mimetics did not synergize with cisplatin to reduce the clonogenic potential of HNSCC cell lines, dual inhibition of MCL-1 and BCL-X_L has proven to be highly effective, indicating that the combination could potentially permit lower dosage of cisplatin for patients. Furthermore, due to the high expression of these proteins in HNSCC patient tissue,

MCL-1 and BCL-X_L could also be used as potential biomarkers for this kind of cancer, rendering MCL-1 and BCL-X_L as valuable assets for HNSCC therapy.

In PDAC, K-RAS mutations are the most frequent genetic alteration observed, reaching almost 100% of all cases,[354] which is linked to the expression of anti-apoptotic BCL-2 family members *via* the NF-κB pathway. Furthermore, overexpression of a dominant-negative RAS allele abolishes NF-κB in PDAC cell lines,[355] which has been shown to upregulate expression levels of several BCL-2 family members.[356] p53 also plays an important role in PDAC,[239] as it is found mutated in 50 to 70% of PDAC cases, which upregulates expression levels of MCL-1 and BCL-X_L [354,357] Gemcitabine is the first line therapy for PDAC and, as resistance to gemcitabine-mediated cytotoxicity has been attributed to mutations in p53, BH3 mimetics could be a valuable tool to overcome gemcitabine resistance in PDAC patients.

Initial studies with BH3 mimetics in PDAC were conducted with non-specific compounds such as sabutoclax, which showed inhibition of cell proliferation and induction of apoptosis in several PDAC cell lines.[257] Similarly, ABT-737 was shown to enhance gemcitabine-mediated reduction of cell viability in the PDAC cell lines PANC-1 and BxPC-3 and in vivo models of PDAC.[247,358] Accordingly, the data presented in chapter 4 indicates that PDAC patients could benefit from BCL-X_L inhibition to possibly overcome gemcitabine resistance, as A-1331852 and gemcitabine together reduced clonogenic potential and induced apoptosis in several PDAC cell lines.

7.4 BH3 mimetics and mitochondrial membrane dynamics

BH3 mimetics were designed to mimic specific BH3-only members of the BCL-2 family, binding to the BH3 groove of anti-apoptotic members and promoting apoptosis. Following the displacement of the BH3 only members, BAX and BAK are activated, translocated and inserted in the OMM, creating a platform for the release of cytochrome *c* to the cytosol. Concomitantly, mitochondrial cristae undergo remodelling to facilitate cytochrome *c* release, contributing to an effective induction of the intrinsic pathway of apoptosis. Since BH3 mimetics act at the level of mitochondria, it is possible that they may induce mitochondrial ultrastructural changes. Indeed, as shown in chapter 5, A-1210477 and S63845 induced extensive mitochondrial fragmentation in several cell lines. Interestingly, such mitochondrial fragmentation does not result in cell death as most cell lines depend on both MCL-1 and BCL-X_L for survival. Inhibition of MCL-1 alone does not result in cell death unless BCL-X_L is also inhibited. Therefore, the role of MCL-1 inhibitor in regulating mitochondrial ultrastructure remains to be characterised. Previous reports link MCL-1 inhibition to mitochondrial membrane dynamics, by claiming that MCL-1 regulates the maintenance of normal IMM structure, mitochondrial fission and the assembly of ATP synthase oligomers.[62] In chapter 5, I showed that MCL-1 inhibitors can induce profound mitochondrial structural changes, ranging from pre-apoptotic cristae remodelling and OMM breaks to mitochondrial fragmentation, all of which occurring independently of apoptosis, which possibly occurs *via* off-target effects.

Mitochondrial membrane dynamics is mediated by a group of fission and fusion proteins, which seem to play an important role in apoptosis. Of these, DRP-1 is widely known for its role as the master regulator of mitochondrial fission. Since the early 2000, research involving DRP-1 has been increasing drastically with

numerous studies unravelling the role of DRP-1 in mitochondrial division under physiological conditions and in drug-mediated mitochondrial fission.[294,359] In chapter 5, I have identified and characterised novel roles of DRP-1 in BH3-mimetic mediated apoptosis, cytochrome *c* release and BAK activation. As previously mentioned, we have assessed MOMP *via* cytochrome *c* release, which does not comprise the full aspect of this process, as other molecules, such as Smac, are also released to the cytosol upon MOMP.[20] Nevertheless, DRP-1 depletion prevented in great extent BH3 mimetic-mediated cytochrome *c* release in H1299 cells. Indeed, similar results, using other apoptotic agents, such as staurosporine and etoposide have been reported by other groups.[275,290] This, of course it is not without its controversy as another report has argued for no role for DRP-1 in BH3 mimetic-mediated apoptosis in melanoma cells.[360] Furthermore, studies using, mdivi-1, initially considered as a DRP-1 inhibitor, showed that DRP-1 is required for tBID-mediated apoptosis and that physical topological changes induced by DRP-1 at the mitochondrial membrane facilitated BAX/BAK assembly and cytochrome *c* release.[361–363] However, mdivi-1 effects on DRP-1 are currently attributed to be indirect, as mdivi-1 has been shown to be a complex I inhibitor.[364] Furthermore, interactions of BAX and BAK with mitofusins and their coordination with DRP-1 activity have been proposed as possible mechanisms for apoptosis induction.[365] The data shown here point in the same direction, since silencing of DRP-1 decreases BH3 mimetic-mediated BAK activation. It is quite likely that the physical changes at the OMM caused by DRP-1 oligomerisation facilitates the activation and insertion of BAK at the OMM. Recently, post-translational modifications of DRP-1 such as SUMOylation by the SUMO E3 ligase MAPL have been elucidated, presenting novel insights into understanding of the role of DRP-1 in apoptosis.[276,293] This SUMOylation process is

thought to stabilise DRP-1 at the OMM to facilitate BAX/BAK assembly. Given the fast shuttling of DRP-1 oligomers for the formation of DRP-1 constriction ring in mitochondrial fission, this could be a possible explanation on how DRP-1 stabilisation could facilitate apoptosis. Moreover, other proteins contribute to the role of DRP-1 in mitochondrial fission, and possibly apoptosis.

In addition, there are other proteins involved in the intricate process of mitochondrial fission. Dynamin 2, another member of the dynamin family,[366] has been shown to play a similar role to DRP-1, but its assembly at the fission sites occurs after the initial constriction of DRP-1, acting as a final sever for mitochondrial fission.[307,367] Furthermore, silencing of dynamin 2 has been shown to prevent staurosporine-mediated mitochondrial fragmentation and, to some extent, cell death.[275] On the same note, some reports have shown that naturally formed mitochondrial DNA aggregates, also known as mitochondrial nucleoids, signal the assembly of the constriction machinery, which occurs in the vicinity of the nucleoids.[368] In addition, knockdown of DRP-1 has been shown to increase nucleoid clustering, which in turn restricts the individual nucleoids from signalling for mitochondrial constriction.[369] This further strengthens the ties for the role of DRP-1 in MOMP and apoptosis, as it has been shown that mitochondrial DNA gets released from mitochondria following MOMP in a BAX/BAK-dependent manner.[370] Another protein of interest in this process is the cytoskeleton component septin 2, which has been shown to interact with DRP-1 and regulate mitochondrial fission.[371] Interestingly, other components of the cytoskeleton have been shown to play a role in mitochondrial fission, such as actin and myosin IIA filaments, bringing together the role of ER in mitochondrial membrane dynamics.[372,373]

7.5 The role of ER membranes in the induction of apoptosis

The crosstalk between ER and mitochondria has been extensively studied in the past decades. Besides the already known functions in calcium signalling, protein trafficking and lipid exchange, recent studies have added mitochondrial membrane dynamics and apoptosis to the list of functions that have been attributed to the crosstalk mechanisms between ER and mitochondria.[374] In the context of apoptosis, widely-studied ER proteins, such as IP3R have been show to regulate ER-derived mitochondrial calcium overload and the induction of apoptosis.[375–377] In chapter 6, I showed that ER shaping proteins such as RTN-4 and CLIMP-63 are required for BH3 mimetic-mediated mitochondrial fission and apoptosis. Although the underlying mechanism of this anti-apoptotic function is yet to be characterised, there could be an important role for ER shaping proteins in ER-mitochondria calcium exchange. Studies have shown that RTN-4 couples two important calcium channels, the ER-resident STIM1 and the plasma membrane-resident Orai1, which act together to replenish ER and intracellular calcium stores.[378] Thus, silencing of RTN-4 could potentially cause a lack of intracellular calcium influx, which could impair ER-mitochondria calcium transfer and the initial signalling for apoptosis. In fact, inhibition of store-operated calcium entry has been associated with cell death resistance in prostate cancer[379] and also with a poorer prognosis in breast cancer.[380] Although the role of RTN-4 has been extensively studied in neurodegenerative diseases,[381] in cancer, more studies are required to better understand how this ER shaping protein could regulate cell death.

CLIMP-63 is essential for the interaction of ER with microtubules, hence named cytoskeleton-linking membrane protein (CLIMP-63),[382] as well as being recruited during early stages of the assembly of ER-translocon complexes.[383]

Although the role of CLIMP-63 in apoptosis has not been well characterised, enhanced expression of CLIMP-63 has been observed following chemotherapy. For instance, inhibition of CDK in leukaemia has been shown to upregulate CLIMP-63, which in turn arrests cell growth.[384] CLIMP-63 has also been linked to enhanced sensitivity to gentamicin in HEK293 cells,[385] which enhanced the binding of CLIMP-63 to 14-3-3 proteins.[385] It is possible that this interaction between CLIMP-63 and 14-3-3 could prevent BAD from being retained in the cytosol by 14-3-3.[386] Which in turn could enable the mitochondrial translocation of BAD to execute apoptosis. This could well be the reason for why silencing of CLIMP-63 prevents BH3 mimetic-mediated cell death.

In addition to RTN-4 and CLIMP-63 there are other proteins, such as INF2 and Spire1C that are involved in mitochondrial fission.[277,312,317,372] However the specific role of these proteins in apoptosis has not been studied to this date.

7.6 The role of ER membranes in other cellular functions

The mitochondria associated membranes (MAMs), especially at the ER, also play such an important role in cellular homeostasis that these connective areas are often considered as an extra intracellular environment.[307,374] Interestingly, some reports have shown a connection between MAMs and members of the BCL-2 family on the regulation of calcium signalling. For instance, BCL-X_L has been shown to interact with IP3R channels for the induction of calcium-dependent mitochondrial bioenergetics during ER stress,[387] or to block VDAC activity for the inhibition of ER-derived mitochondrial calcium influx.[388] In addition, BCL-2 has also been shown to interact with IP3R receptors to block pro-apoptotic calcium signalling to mitochondria.[389,390] Another important component of the MAMs is MFN2, which has been shown to play a crucial molecule in maintaining an appropriate distance

between ER and mitochondria. Of interest, it has been reported that knockdown of MFN2 reduces the number of ER-mitochondria contact points while not affecting calcium exchange.[391] The data presented in chapter 6 suggest that DRP-1 also plays an important role in maintaining ER-mitochondria contacts, as silencing of the GTPase drastically reduced the number of contact points. Although MFN2 and DRP-1 appear to play opposite roles in mitochondrial membrane dynamics, these data indicate that alterations in the fusion/fission balance can deeply affect ER-mitochondria interactions.

Despite the initial description of ER and mitochondria contacts in the early 50s, the importance of these intracellular microenvironment was only further explored in the 90s, in a paper describing lipid exchange between these two organelles.[305] It was demonstrated that lipid-synthesising enzymes were localised at the mitochondria-ER contacts, which were later shown to transfer phosphatidylserine from the ER.[392] Interestingly, lipid transfer has been proposed to play a role in cell death[393] by mediating the insertion of BAX/BAK and anchoring other BCL-2 family members in the OMM, a mechanism that could potentially be affected by silencing of ER shaping proteins. Additionally, a recent report has shown that DRP-1 interacts with cardiolipin for an effective induction of mitochondrial fission.[394] which was further backed by an *in vitro* study showing that cardiolipin is required for proper BAX insertion at the OMM and that process is countered by BCL-X_L.[395] Furthermore, one of the only contexts that ER shaping proteins have been associated to mitochondria is lipid exchange, by a study with yeast shows that phospholipid transfer from ER to mitochondria is significantly slower in cells lacking certain ER shaping proteins.[396]

7.7 Implications and future studies

This study reinforces the therapeutic potential and applicability of BH3 mimetics in various cancers, not only as a stand-alone therapy, but also when used in combination with other existing therapies. The data presented here highlights the necessity for the assessment of potential off-target or unforeseen effects caused by BH3 mimetics, such as the induction of mitochondrial structural changes. The results presented in this thesis show that CML cells mainly depend on BCL-X_L for survival, whereas AML cells depend on BCL-2 and MCL-1 and solid tumours on both MCL-1 and BCL-X_L. This needs to be taken into consideration when prescribing BH3 mimetics in the clinic as there are side effects, such as thrombocytopenia associated with BCL-X_L inhibition[152,153] and cardiotoxicity with MCL-1 inhibition.[175] Furthermore, as BCL-X_L and MCL-1 play redundant roles in regulating cell survival in most solid tumours, concomitant inhibition of these proteins require the achievement of a good therapeutic window to minimise side effects. Therefore, careful toxicity assessments using these BH3 mimetics alone and in combination are required, as well as studies to understand potential mechanisms of chemoresistance and drug safety.

It has been shown in this study that DRP-1 plays a crucial role in BH3 mimetic-mediated mitochondrial fragmentation and apoptosis, confirming the role of this protein as a master regulator of mitochondrial fission. Although previous studies have demonstrated that DRP-1 could play a role in apoptosis,[275,290] here it is first described that DRP-1 was also required for BH3 mimetic-mediated cell death. These findings further open numerous questions regarding the nature of the requirement of DRP-1 for apoptosis. For instance, does DRP-1 plays a similar role in alternative cell death pathways, such as ferroptosis, necrosis and pyroptosis? Of interest, a report

indicates that DRP-1 could also play a crucial role in necroptosis.[397] In addition further assessment of potential interactions between BCL-2 family members and DRP-1 at the OMM would be valuable, as well as identifying the roles of DRP-1 in apoptosis. Moreover, more studies are required to identify what mechanisms are involved in the recruitment of DRP-1 to mitochondria at the fission sites and how ER interplay with DRP-1 could be dictating its activity in mitochondrial membrane dynamics and cell death.

Also, here it has been shown that RTN-4 and CLIMP-63 play an important role for the effective induction BH3 mimetic-mediated apoptosis. The results presented in this study open a new avenue for the study of ER-mitochondria interactions, as they link ER structural maintenance to mitochondria-induced cell death. In the future, focusing on potential interacting partners for RTN-4 and CLIMP-63 by techniques such as mass spectrometry could provide a good basis towards understanding how these ER shaping proteins could be altering the apoptotic pathway and/or related pathways. On that note, it will be important to characterise the roles of these proteins in ER-mitochondrial contacts, which can affect several other pathways, such as calcium exchange, cell cycle and lipid transfer, as exemplified by the association of CLIMP-63 with the cytoskeleton,[382] or the role of proteins of the reticulon family in ER membrane clearance.[398,399]

7.8 Concluding remarks

The main findings presented in this study are:

- A BCL-X_L inhibitor, either alone or in combination with a TKI, could be potentially used to treat CML.
- Combined inhibition of BCL-2 and MCL-1 are effective in promoting apoptosis in AML cell lines and primary patient samples.
- Inhibition of BCL-X_L and MCL-1 are highly efficacious in inducing cell death in HNSCC cell lines and patient samples.
- Inhibition of BCL-X_L and MCL-1 are highly efficacious in inducing cell death in PDAC cell lines.
- Inhibition of MCL-1 by BH3 mimetics induce DRP-1-dependent mitochondrial fragmentation.
- DRP-1 and CLIMP-63 are required for BH3 mimetic-mediated apoptosis, cytochrome *c* release and BAK/BAX activation.
- ER shaping proteins, such as RTN-4 and CLIMP-63, play an important role in BH3 mimetic-mediated apoptosis and cytochrome *c* release.
- DRP-1 and ER shaping proteins regulate ER-mitochondria contacts.

Taken together these findings have identified several novel aspects of BH3 mimetic mediated apoptosis and contributed important new knowledge to the fields of apoptosis and cell biology.

REFERENCES

1. Duque-Parra, J. E. Note on the origin and history of the term 'Apoptosis'. *Anat. Rec. Part B New Anat.* **283B**, 2–4 (2005).

2. Elmore, S. Apoptosis: a review of programmed cell death. *Toxicol. Pathol.* **35**, 495–516 (2007).

3. Kerr, J. F., Wyllie, A. H. & Currie, A. R. Apoptosis: a basic biological phenomenon with wide-ranging implications in tissue kinetics. *Br. J. Cancer* **26**, 239–57 (1972).

4. Savill, J. & Fadok, V. Corpse clearance defines the meaning of cell death. *Nature* **407**, 784–788 (2000).

5. Locksley, R. M., Killeen, N. & Lenardo, M. J. *The TNF and TNF Receptor Superfamilies: Integrating Mammalian Biology*. *Cell* **104**, (2001).

6. Tait, S. W. G. & Green, D. R. Mitochondria and cell death: outer membrane permeabilization and beyond. *Mol. cell Biol.* **11**, 621–32 (2010).

7. Westphal, D., Kluck, R. M. & Dewson, G. Building blocks of the apoptotic pore: How Bax and Bak are activated and oligomerize during apoptosis. *Cell Death Differ.* **21**, 196–205 (2014).

8. Bratton, S. B. *et al.* Recruitment, activation and retention of caspases-9 and-3 by Apaf-1 apoptosome and associated XIAP complexes. *EMBO J.* **20**, 998–1009 (2001).

9. Bratton, S. B. *et al.* Recruitment, activation and retention of caspases-9 and -3 by Apaf-1 apoptosome and associated XIAP complexes. *EMBO J.* **20**, 998–1009 (2001).

10. Renatus, M., Stennicke, H. R., Scott, F. L., Liddington, R. C. & Salvesen, G. S. Dimer formation drives the activation of the cell death protease caspase 9. *Proc. Natl. Acad. Sci.* **98**, 14250–14255 (2001).

11. Stennicke, H. R. *et al.* Caspase-9 can be activated without proteolytic processing. *J. Biol. Chem.* **274**, 8359–62 (1999).

12. Malladi, S., Challa-Malladi, M., Fearnhead, H. O. & Bratton, S. B. The Apaf-1•procaspase-9 apoptosome complex functions as a proteolytic-based molecular timer. *EMBO J.* **28**, 1916–1925 (2009).

13. Cohen, G. M. Caspases: Executioners of Apoptosis. *J. Biol. Chem.* **326**, 1–16 (1997).

14. Li, P. *et al.* Cytochrome c and dATP-Dependent Formation of Apaf-1/Caspase-9 Complex Initiates an Apoptotic Protease Cascade. *Cell* **91**, 479–489 (1997).

15. Srinivasula, S. M. *et al.* Generation of Constitutively Active Recombinant Caspases-3 and-6 by Rearrangement of Their Subunits. *J. Biol. Chem.* **273**, 10107–10111 (1998).

16. Kaufmann, S. H., Desnoyers, S., Ottaviano, Y., Davidson, N. E. & Poirier, G. G. Specific Proteolytic Cleavage of Poly (ADP-ribose) Polymerase : An Early Marker of Chemotherapy-induced Apoptosis. *Cancer Res.* **53**, 3976–3985 (1993).

17. Kale, J., Osterlund, E. J. & Andrews, D. W. BCL-2 family proteins: changing partners in the dance towards death. *Cell Death Differ.* **25**, 65–80 (2018).

18. Kischkel, F. C. *et al.* Cytotoxicity-dependent APO-1 (Fas/CD95)-associated proteins form a death-inducing signaling complex (DISC) with the receptor. *EMBO J.* **14**, 5579–88 (1995).

19. Fulda, S. & Vucic, D. Targeting IAP proteins for therapeutic intervention in cancer. *Nat. Rev. Drug Discov.* **11**, 109–123 (2012).

20. Du, C., Fang, M., Li, Y., Li, L. & Wang, X. Smac, a Mitochondrial Protein that

Promotes Cytochrome c–Dependent Caspase Activation by Eliminating IAP Inhibition. *Cell* **102**, 33–42 (2000).

21. Aouacheria, A., Combet, C., Tompa, P. & Hardwick, J. M. Redefining the BH3 death domain as a 'Short Linear Motif'. *Trends Biochem Sci* **40**, 736–748 (2015).

22. Schenk, R. L., Strasser, A. & Dewson, G. BCL-2: Long and winding path from discovery to therapeutic target. *Biochem. Biophys. Res. Commun.* **482**, 459–469 (2017).

23. Tsujimoto, Y., Finger, L., Yunis, J., Nowell, P. & Croce, C. Cloning of the chromosome breakpoint of neoplastic B cells with the t(14;18) chromosome translocation. *Science.* **226**, 1097–1099 (1984).

24. Lamers, F. *et al.* Targeted BCL2 inhibition effectively inhibits neuroblastoma tumour growth. *Eur. J. Cancer* **48**, 3093–3103 (2012).

25. Swellam, M., Abd-Elmaksoud, N., Halim, M. H., Khatab, H. & Khiry, H. Incidence of Bcl-2 expression in bladder cancer: Relation to schistosomiasis. *Clin. Biochem.* **37**, 798–802 (2004).

26. P Hellemans, PA van Dam, J Weyler, AT van Oosterom, P. B. and E. V. M. Prognostic value of bcl-2 expression in invasive breast cancer P. *Anticancer Res.* **18**, 4699–4704 (1998).

27. Dan-ping, Z., Xiao-wen, D., Jia-ping, P., Yi-xiong, Z., Su-zhan, Z. Prognostic significance of bcl-2 and p53 expression in colorectal carcinoma. *J. Zhejiang Univ. Sci. B* **6**, 1163–1169 (2005).

28. Jiang, S. -X, Sato, Y., Kuwao, S. & Kameya, T. Expression of bcl-2 oncogene protein is prevalent in small cell lung carcinomas. *J. Pathol.* **177**, 135–138 (1995).

29. Karnak, D. & Xu, L. Chemosensitization of prostate cancer by modulating Bcl-2 family proteins. *Curr. Drug Targets* **11**, 699–707 (2010).

30. Campos, L. *et al.* High expression of Bcl-2 protein in acute myeloid leukemia cells is associated with poor response to chemotherapy. *Blood* **81**, 3091–3096 (1993).

31. Vogler, M., Dinsdale, D., Dyer, M. J. S. & Cohen, G. M. ABT-199 selectively inhibits BCL2 but not BCL2L1 and efficiently induces apoptosis of chronic lymphocytic leukaemic cells but not platelets. *Br. J. Haematol.* **163**, 139–142 (2013).

32. Hermine, O. *et al.* Prognostic significance of bcl-2 protein expression in aggressive non-Hodgkin's lymphoma. *Blood* **87**, 265–272 (1996).

33. Warren, C. F. A., Wong-Brown, M. W. & Bowden, N. A. BCL-2 family isoforms in apoptosis and cancer. *Cell Death Dis.* **10**, 177 (2019).

34. Levine, B., Sinha, S. C. & Kroemer, G. Bcl-2 family members: Dual regulators of apoptosis and autophagy. *Autophagy* **4**, 600–606 (2008).

35. Lucas, C. M. *et al.* High CIP2A levels correlate with an antiapoptotic phenotype that can be overcome by targeting BCL-XL in chronic myeloid leukemia. *Leukemia* **42**, 1–9 (2016).

36. Harb, J. G. *et al.* Bcl-xL anti-apoptotic network is dispensable for development and maintenance of CML but is required for disease progression where it represents a new therapeutic target. *Leukemia* **27**, 1996–2005 (2013).

37. Zhang, K. *et al.* Bcl-xL overexpression and its association with the progress of tongue carcinoma. *Int. J. Clin. Exp. Pathol.* **7**, 7360–7377 (2014).

38. Scherr, A. L. *et al.* Bcl-xL is an oncogenic driver in colorectal cancer. *Cell Death Dis.* **7**, 1–10 (2016).

39. XiaoYing Li, Michela Marani, Roberta Mannucci, Berma Kinsey, Francesca Andriani, Ildo Nicoletti, Larry Denner, and M. M. Overexpression of BCL-XL Underlies the Molecular Basis for Resistance to Staurosporine-induced Apoptosis in PC-3 Cells. *Cancer Res.* **61**, 1699–1706 (2001).

40. Carolina Castilla, Bele´n Congregado, David Chincho´n, Francisco J. Torrubia, Miguel A. Japo´n, and C. S. Bcl-xL Is Overexpressed in Hormone-Resistant Prostate Cancer and Promotes Survival of LNCaP Cells via Interaction with Proapoptotic Bak Carolina. *Endocrinology* **147**, 4960–4967 (2006).

41. Minn, A. J., Boise, L. H. & Thompson, C. B. Bcl-XS Antagonizes the Protective Effects of Bcl-XL. *J. Biol. Chem.* **271**, 6306–6312 (1996).

42. Vaux, D. L., Cory, S., Adams, J. M. & David L. Vaux, S. C. & J. A. Bcl-2 gene promotes haemopoietic cell survival and cooperates with c-myc to immortalize pre-B cells. *Nature* **335**, 440–442 (1988).

43. Plö Tz, M., Gillissen, B., Hossini, A. M., Daniel, P. T. & Eberle, J. Disruption of the VDAC2–Bak interaction by Bcl-xS mediates efficient induction of apoptosis in melanoma cells. *Cell Death Differ.* **19**, 1928–1938 (2012).

44. Johnson, A. L., Bridgham, J. T. & Jensen, T. Bcl-XLONG Protein Expression and Phosphorylation in Granulosa Cells. *Endocrinology* **140**, 4521–4529 (1999).

45. Edlich, F. *et al.* Bcl-XL Retrotranslocates Bax from the Mitochondria into the Cytosol. *Cell* **145**, 104–116 (2011).

46. Kozopas, K. M., Yang, T., Buchan, H. L., Zhou, P. & Craig, R. W. MCL1, a gene expressed in programmed myeloid cell differentiation, has sequence similarity to BCL2. *Proc. Natl. Acad. Sci. U. S. A.* **90**, 3516–20 (1993).

47. Jorissen, R. N. *et al.* The landscape of somatic copy-number alteration across human cancers. *Cancer* **463**, 899–905 (2010).

48. Young, A. I. J. *et al.* MCL-1 inhibition provides a new way to suppress breast cancer metastasis and increase sensitivity to dasatinib. *Breast Cancer Res.* **18**, 125 (2016).

49. Campbell, K. J. *et al.* MCL-1 is a prognostic indicator and drug target in breast cancer article. *Cell Death Dis.* **9**, (2018).

50. Merino, D. *et al.* Synergistic action of the MCL-1 inhibitor S63845 with current therapies in preclinical models of triple-negative and HER2-amplified breast cancer. **2**, (2017).

51. Yin, J. *et al.* Copy-number variation of MCL1 predicts overall survival of non-small-cell lung cancer in a Southern Chinese population. *Cancer Med.* **5**, 2171–2179 (2016).

52. Zhang, H. *et al.* Mcl-1 is critical for survival in a subgroup of non-small-cell lung cancer cell lines. *Oncogene* **30**, 1963–1968 (2011).

53. Zervantonakis, I. K. *et al.* Systems analysis of apoptotic priming in ovarian cancer identifies vulnerabilities and predictors of drug response. *Nat. Commun.* **8**, (2017).

54. Palve, V., Mallick, N., Ghaisas, G., Kannan, S. & Teni, T. Overexpression of Mcl-1L splice variant is associated with poor and prognosis chemoresistance in oral cancers. *PLoS One* **9**, (2014).

55. Krajewski, S. *et al.* Immunohistochemical analysis of Mcl-1 protein in human tissues. Differential regulation of Mcl-1 and Bcl-2 protein production suggests a unique role for Mcl-1 in control of programmed cell death in vivo. *Am. J. Pathol.* **146**, 1309–19 (1995).

56. Wei, D. *et al.* Targeting Mcl-1 for radiosensitization of pancreatic cancers. *Transl. Oncol.* **8**, 47–54 (2015).

57. Reiner, T. *et al.* Mcl-1 protects prostate cancer cells from cell death mediated by chemotherapy-induced DNA damage. *Oncoscience* **2**, 703–715 (2015).

58. Wuillème-Toumi, S. *et al.* Mcl-1 is overexpressed in multiple myeloma and associated with relapse and shorter survival. *Leukemia* **19**, 1248–52 (2005).

59. Kaufmann, S. H. *et al.* Elevated expression of the apoptotic regulator Mcl-1 at the time of leukemic relapse. *Blood* **91**, 991–1000 (1998).

60. Yu, X. *et al.* Targeting MCL-1 sensitizes human esophageal squamous cell carcinoma cells to cisplatin-induced apoptosis. *BMC Cancer* **17**, 1–13 (2017).

61. Palve, V. C. & Teni, T. R. Association of anti-apoptotic Mcl-1L isoform expression with radioresistance of oral squamous carcinoma cells. *Radiat. Oncol.* **7**, 1–11 (2012).

62. Perciavalle, R. M. *et al.* Anti-apoptotic MCL-1 localizes to the mitochondrial matrix and couples mitochondrial fusion to respiration. *Nat. Cell Biol.* **14**, 575–83 (2012).

63. Kim, J. H. *et al.* MCL-1ES, a novel variant of MCL-1, associates with MCL-1L and induces mitochondrial cell death. *FEBS Lett.* **583**, 2758–2764 (2009).

64. Thomas, L. W., Lam, C. & Edwards, S. W. Mcl-1; the molecular regulation of protein function. *FEBS Lett.* **584**, 2981–9 (2010).

65. Warr, M. R. *et al.* BH3-ligand regulates access of MCL-1 to its E3 ligase. *FEBS Lett.* **579**, 5603–5608 (2005).

66. Zhong, Q., Gao, W., Du, F. & Wang, X. Mule/ARF-BP1, a BH3-only E3 ubiquitin ligase, catalyzes the polyubiquitination of Mcl-1 and regulates apoptosis. *Cell* **121**, 1085–1095 (2005).

67. Choudhary, G. S. *et al.* Cyclin E/Cdk2-dependent phosphorylation of Mcl-1 determines its stability and cellular sensitivity to BH3 mimetics. *Oncotarget* **6**, 16912–25 (2015).

68. Varadarajan, S. *et al.* Maritoclax and dinaciclib inhibit MCL-1 activity and induce apoptosis in both a MCL-1-dependent and -independent manner. *Oncotarget* **6**, 10–15 (2015).

69. Shen, L. *et al.* miR-497 induces apoptosis of breast cancer cells by targeting Bcl-w. *Exp. Ther. Med.* **3**, 475–480 (2012).

70. Placzek, W. J. *et al.* A survey of the anti-apoptotic Bcl-2 subfamily expression in cancer types provides a platform to predict the efficacy of Bcl-2 antagonists in cancer therapy. *Cell Death Dis.* **1**, e40 (2010).

71. Wilson, J. W. *et al.* Bcl-w expression in colorectal adenocarcinoma. **82**, 178–185 (2000).

72. Adams, C. M., Mitra, R., Gong, J. Z. & Eischen, C. M. Non-Hodgkin and Hodgkin lymphomas select for overexpression of BCLW. *Clin. Cancer Res.* **23**, 7119–7129 (2017).

73. Yoon, H. S. *et al.* Bfl-1 Gene Expression in Breast Cancer: Its Relationship with other Prognostic Factors. *J. Korean Med. Sci.* **18**, 225–230 (2003).

74. Park IC, Lee SH, Whang DY, Hong WS, Choi SS, Shin HS, Choe TB, H. S. Expression of a novel Bcl-2 related gene, Bfl-1, in various human cancers and cancer cell lines. *Anticancer Res.* **17**, 4619–4622 (1997).

75. Nagy, B. *et al.* Abnormal expression of apoptosis-related genes in haematological malignancies: Overexpression of MYC is poor prognostic sign in mantle cell lymphoma. *Br. J. Haematol.* **120**, 434–441 (2003).

76. Olsson, A. *et al.* Upregulation of bfl-1 is a potential mechanism of chemoresistance in B-cell chronic lymphocytic leukaemia. *Br. J. Cancer* **97**, 769–777 (2007).

77. Derek Yecies, Nicole E. Carlson, Jing Deng, and A. L. Acquired resistance to ABT-737 in lymphoma cells that up-regulate MCL-1 and BFL-1. *Lymphoid Neoplasia* **115**, 3304–3313 (2010).

78. Antignani, A. & Youle, R. J. How do Bax and Bak lead to permeabilization of the outer mitochondrial membrane? *Curr. Opin. Cell Biol.* **18**, 685–689 (2006).

79. Ionov, Y., Yamamoto, H., Krajewski, S., Reed, J. C. & Perucho, M. Mutational inactivation of the proapoptotic gene BAX confers selective advantage during tumor clonal evolution. *PNAS* **97**, 10872–10877 (2000).

80. Kondo, S. *et al.* Mutations of the bak gene in human gastric and colorectal cancers. *Cancer Res.* **60**, 4328–4330 (2000).

81. Hong Ouyang, Toni Furukawa, T. A. & Yo Kato, and A. H. The BAX Gene, the Promoter of Apoptosis, Is Mutated in Genetically Unstable Cancers of the Colorectum, Stomach, and Endometrium. **4**, 1071–1074 (1998).

82. Zoltan N. Oltvai, Curt L. Milkman, and S. J. K. Bcl-2 Heterodimerizes In Vivo with a Conserved Homolog, Bax, That Accelerates Programed Cell Death. *Cell* **74**, 609–619 (1993).

83. Gross, A., Jockel, J., Wei, M. C. & Korsmeyer, S. J. Enforced dimerization of BAX results in its translocation, mitochondrial dysfunction and apoptosis. *EMBO J.* **17**, 3878–3885 (1998).

84. Wolter, K. G. *et al.* Movement of Bax from the Cytosol to Mitochondria during Apoptosis. *J. Cell Biol.* **139**, 1281–1292 (1997).

85. Antonsson, B. *et al.* Inhibition of Bax Channel-Forming Activity by Bcl-2. *Science.* **277**, 370–372 (1997).

86. Westphal, D., Kluck, R. M. & Dewson, G. Building blocks of the apoptotic pore: how Bax and Bak are activated and oligomerize during apoptosis. *Cell Death Differ.* **21**, 196–205 (2014).

87. Farrow SN, White JH, Martinou I, Raven T, Pun KT, Grinham CJ, Martinou JC, B. R. Cloning of a bcl-2 homologue by interaction with adenovirus E1B 19K. *Lett. to Nat.* **374**, 731–733 (1995).

88. Chittenden, T. *et al.* Induction of apoptosis by the Bcl-2 homologue Bak. *Nature* **374**, 733–736 (1995).

89. Keifer, M. C. *et al.* Modulation of apoptosis by the widely distributed Bcl-2 homologue Bak. *Nature* **374**, 376–379 (1995).

90. Ku, B., Liang, C., Jung, J. U. & Oh, B.-H. Evidence that inhibition of BAX activation

by BCL-2 involves its tight and preferential interaction with the BH3 domain of BAX. *Cell Res.* **21**, 627–41 (2011).

91. Anasir, M. I., Caria, S., Skinner, M. A. & Kvansakul, M. Structural basis of apoptosis inhibition by the fowlpox virus protein FPV039. *J. Biol. Chem.* **292**, 9010–9021 (2017).

92. Gavathiotis, E. *et al.* BH3-Triggered Structural Reorganization Drives the Activation of Proapoptotic BAX. *Mol. Cell* **40**, 481–492 (2010).

93. Peyerl, F. W. *et al.* Elucidation of some Bax conformational changes through crystallization of an antibody-peptide complex. *Cell Death Differ.* **14**, 447–452 (2007).

94. Elizaveta S. Leshchinera, Craig R. Brauna, Gregory H. Birda, and L. D. W. Direct activation of full-length proapoptotic BAK. *HTM - Haerterei-Technische Mitteilungen* **55**, 10 pp (2000).

95. Todt, F. *et al.* Differential retrotranslocation of mitochondrial Bax and Bak. *EMBO J.* **34**, 67–80 (2014).

96. Ferrer, P. E., Frederick, P., Gulbis, J. M., Dewson, G. & Kluck, R. M. Translocation of a Bak C-Terminus Mutant from Cytosol to Mitochondria to Mediate Cytochrome c Release: Implications for Bak and Bax Apoptotic Function. *PLoS One* **7**, 1–13 (2012).

97. George, N. M., Evans, J. J. D. & Luo, X. A three-helix homo-oligomerization domain containing BH3 and BH1 is responsible for the apoptotic activity of Bax. *Genes Dev.* **21**, 1937–1948 (2007).

98. Brogden, K. A. Antimicrobial peptides: Pore formers or metabolic inhibitors in bacteria? *Nat. Rev. Microbiol.* **3**, 238–250 (2005).

99. Echeverry, N. *et al.* Intracellular localization of the BCL-2 family member BOK and functional implications. *Cell Death Differ.* **20**, 785–799 (2013).

100. Fernández-Marrero, Y. *et al.* The membrane activity of BOK involves formation of large, stable toroidal pores and is promoted by cBID. *FEBS J.* **284**, 711–724 (2017).

101. Einsele-Scholz, S. *et al.* Bok is a genuine multi-BH-domain protein that triggers apoptosis in the absence of Bax and Bak. *J. Cell Sci.* **129**, 2213–2223 (2016).

102. Llambi, F. *et al.* BOK Is a Non-canonical BCL-2 Family Effector of Apoptosis Regulated by ER-Associated Degradation. *Cell* **165**, 421–433 (2016).

103. Fernandez-Marrero, Y. *et al.* Is BOK required for apoptosis induced by endoplasmic reticulum stress? *Proc. Natl. Acad. Sci.* **113**, E492–E493 (2016).

104. Schulman, J. J. *et al.* Bok regulates mitochondrial fusion and morphology. *Cell Death Differ.* 1 (2019). doi:10.1038/s41418-019-0327-4

105. Korsmeyer, S. J., Shutter, J. R., Veis, D. J., Merry, D. E. & Oltvai, Z. N. Bcl-2/Bax: a rheostat that regulates an anti-oxidant pathway and cell death. *Semin. Cancer Biol.* **4**, 327–332 (1993).

106. Certo, M. *et al.* Mitochondria primed by death signals determine cellular addiction to antiapoptotic BCL-2 family members. *Cancer Cell* **9**, 351–65 (2006).

107. Kim, H. *et al.* Hierarchical regulation of mitochondrion-dependent apoptosis by BCL-2 subfamilies. *Nat. Cell Biol.* **8**, 1348–58 (2006).

108. Letai, A. *et al.* Distinct BH3 domains either sensitize or activate mitochondrial apoptosis, serving as prototype cancer therapeutics. *Cancer Cell* **2**, 183–192 (2002).

109. Kuwana, T. *et al.* BH3 domains of BH3-only proteins differentially regulate Bax-mediated mitochondrial membrane permeabilization both directly and indirectly. *Molecular Cell* **17**, 525–535 (2005).

110. Willis, S. N. *et al.* Apoptosis Initiated When BH3 Ligands Engage Multiple Bcl-2 Homologs, Not Bax or Bak. *Science.* **315**, 856–859 (2007).

111. Chen, L. *et al.* Differential targeting of prosurvival Bcl-2 proteins by their BH3-only ligands allows complementary apoptotic function. *Mol. Cell* **17**, 393–403 (2005).

112. Willis, S. N. *et al.* Proapoptotic Bak is sequestered by Mcl-1 and Bcl-xL, but not Bcl-2, until displaced by BH3-only proteins. *Genes and Development* **19**, 1294–1305 (2005).

113. Llambi, F. *et al.* A Unified Model of Mammalian BCL-2 Protein Family Interactions at the Mitochondria. *Mol. Cell* **44**, 517–531 (2011).

114. Isobe, K. *et al.* Clinical Significance of BIM Deletion Polymorphism in Non – Small-Cell Lung Cancer with Epidermal Growth. 483–487 (2014).

115. Faber, A. *et al.* BIM expression in treatment naïve cancers predicts responsiveness to kinase inhibitors. *Cancer Discov.* **1**, 352–365 (2012).

116. Ng, K. P. *et al.* A common BIM deletion polymorphism mediates intrinsic resistance and inferior responses to tyrosine kinase inhibitors in cancer. *Nat. Med.* **18**, 521–528 (2012).

117. Tagawa, H. *et al.* Genome-wide array-based CGH for mantle cell lymphoma: identification of homozygous deletions of the proapoptotic gene BIM. *Oncogene* **24**, 1348–1358 (2005).

118. Puthalakath, H., Huang, D. C. S., O'Reilly, L. A., King, S. M. & Strasser, A. The proapoptotic activity of the Bcl-2 family member Bim is regulated by interaction with the dynein motor complex. *Mol. Cell* **3**, 287–296 (1999).

119. O'connor, L. *et al. Bim: a novel member of the Bcl-2 family that promotes apoptosis*. *The EMBO Journal* **17**, (1998).

120. Eskes, R., Desagher, S., Antonsson, B. & Martinou, J.-C. Bid Induces the Oligomerization and Insertion of Bax into the Outer Mitochondrial Membrane. *Mol. Cell. Biol.* **20**, 929–935 (2000).

121. Wei, M. C. *et al.* tBID, a membrane-targeted death ligand, oligomerizes BAK to release cytochrome c. *Genes Dev.* **14**, 2060–2071 (2000).

122. Luo, X., Budihardjo, I., Zou, H., Slaughter, C. & Wang, X. Bid, a Bcl2 Interacting Protein, Mediates Cytochrome c Release from Mitochondria in Response to Activation of Cell Surface Death Receptors. *Cell* **94**, 481–490 (1998).

123. Gross, A. *et al.* Caspase cleaved BID targets mitochondria and is required for cytochrome c release, while BCL-X(L) prevents this release but not tumor necrosis factor-R1/Fas death. *J. Biol. Chem.* **274**, 1156–1163 (1999).

124. Li, H., Zhu, H., Xu, C. & Yuan, J. Cleavage of BID by Caspase 8 Mediates the Mitochondrial Damage in the Fas Pathway of Apoptosis. *Cell* **94**, 491–501 (1998).

125. Lee, J. H. *et al.* Inactivating mutation of the pro-apoptic gene BID in gastric cancer. *J. Pathol.* **202**, 439–445 (2004).

126. Goncharenko-Khaider, N., Lane, D., Matte, I., Rancourt, C. & Piché, A. The inhibition of Bid expression by Akt leads to resistance to TRAIL-induced apoptosis in ovarian cancer cells. *Oncogene* **29**, 5523–5536 (2010).

127. Yu, J. & Zhang, L. The transcriptional targets of p53 in apoptosis control. *Biochem. Biophys. Res. Commun.* **331**, 851–858 (2005).

128. Wu, D.-W. *et al.* FHIT loss confers cisplatin resistance in lung cancer via the AKT/NF-κB/Slug-mediated PUMA reduction. *Oncogene* **34**, 2505–2515 (2015).

129. Liu, B., Yuan, B., Zhang, L., Mu, W. & Wang, C. ROS/p38/p53/Puma signaling pathway is involved in emodin-induced apoptosis of human colorectal cancer cells. *Int. J. Clin. Exp. Med.* **8**, 15413–22 (2015).

130. Polzien, L. *et al.* Identification of Novel in Vivo Phosphorylation Sites of the Human Proapoptotic Protein BAD. *J. Biol. Chem.* **284**, 28004 (2009).

131. Datta, S. R. *et al.* 14-3-3 proteins and survival kinases cooperate to inactivate BAD by BH3 domain phosphorylation. *Mol. Cell* **6**, 41–51 (2000).

132. Troppmair, J. & Rapp, U. R. Raf and the road to cell survival: a tale of bad spells, ring bearers and detours. *Biochem. Pharmacol.* **66**, 1341–1345 (2003).

133. Marchion, D. C. *et al.* BAD Phosphorylation Determines Ovarian Cancer Chemosensitivity and Patient Survival. *Clin Cancer Res* **17**, 6356–66 (2011).

134. Smith, A. J., Karpova, Y., D'Agostino, R., Willingham, M. & Kulik, G. Expression of the Bcl-2 Protein BAD Promotes Prostate Cancer Growth. *PLoS One* **4**, e6224 (2009).

135. Oda, E. *et al.* Noxa, a BH3-Only Member of the Bcl-2 Family and Candidate Mediator of p53-Induced Apoptosis. *Science.* **288**, 1053–1058 (2000).

136. Inohara, N., Ding, L., Chen, S., Nunez, G. & Núñez, G. harakiri, a novel regulator of cell death, encodes a protein that activates apoptosis and interacts selectively with survival-promoting proteins Bcl-2 and Bcl-XL. *EMBO J.* **16**, 1686–1694 (1997).

137. Nakamura, M. *et al.* Frequent HRK inactivation associated with low apoptotic index in secondary glioblastomas. *Acta Neuropathol.* **110**, 402–410 (2005).

138. Li, H. *et al.* SUZ12 Promotes Human Epithelial Ovarian Cancer by Suppressing Apoptosis via Silencing HRK. *Mol. Cancer Res.* **10**, 1462–1472 (2012).

139. Higuchi, T. *et al.* HRK inactivation associated with promoter methylation and LOH in prostate cancer. *Prostate* **68**, 105–113 (2008).

140. Hur, J. *et al.* Regulation of Expression of BIK Proapoptotic Protein in Human Breast Cancer Cells: p53-Dependent Induction of BIK mRNA by Fulvestrant and Proteasomal Degradation of BIK Protein. *Cancer Res.* **66**, 10153–10161 (2006).

141. Fu, Y., Li, J. & Lee, A. S. GRP78/BiP Inhibits Endoplasmic Reticulum BIK and Protects Human Breast Cancer Cells against Estrogen Starvation–Induced Apoptosis. *Cancer Res.* **67**, 3734–3740 (2007).

142. Hur, J. *et al.* The Bik BH3-only protein is induced in estrogen-starved and antiestrogen-exposed breast cancer cells and provokes apoptosis. *Proc. Natl. Acad. Sci. U. S. A.* **101**, 2351–6 (2004).

143. Mathai, J. P., Germain, M. & Shore, G. C. BH3-only BIK Regulates BAX,BAK-dependent Release of Ca 2 from Endoplasmic Reticulum Stores and Mitochondrial Apoptosis during Stress-induced Cell Death*. *J. Biol. Chem.* **280**, 23829–23836

(2005).

144. Boyd, J. M. *et al.* Bik, a novel death-inducing protein shares a distinct sequence motif with Bcl-2 family proteins and interacts with viral and cellular survival-promoting proteins. *Oncogene* **11**, 1921–8 (1995).

145. Puthalakath, H. *et al.* Bmf: A proapoptotic BH3-only protein regulated by interaction with the myosin V actin motor complex, activated by anoikis. *Science.* **293**, 1829–1832 (2001).

146. Nguyen, M. *et al.* Small molecule obatoclax (GX15-070) antagonizes MCL-1 and overcomes MCL-1-mediated resistance to apoptosis. *Proc. Natl. Acad. Sci.* **104**, 19512–19517 (2007).

147. Wei, J. *et al.* An optically pure apogossypolone derivative as potent pan-active inhibitor of anti-apoptotic bcl-2 family proteins. *Front. Oncol.* **1**, 28 (2011).

148. Konopleva, M. *et al.* Mechanisms of antileukemic activity of the novel BH3 mimetic GX15-070 (obatoclax). **68**, 3413–3420 (2014).

149. Tse, C. *et al.* ABT-263: a potent and orally bioavailable Bcl-2 family inhibitor. *Cancer Res.* **68**, 3421–8 (2008).

150. Oltersdorf, T. *et al.* An inhibitor of Bcl-2 family proteins induces regression of solid tumours. *Nature* **435**, 677–81 (2005).

151. Sattler, M. *et al.* Structure of Bcl-x_L-Bak Peptide Complex: Recognition Between Regulators of Apoptosis. *Science.* **275**, 983–986 (1997).

152. Mason, K. D. *et al.* Programmed anuclear cell death delimits platelet life span. *Cell* **128**, 1173–1186 (2007).

153. Zhang, H. *et al.* Bcl-2 family proteins are essential for platelet survival. *Cell Death Differ.* **14**, 943 (2007).

154. Del Gaizo Moore, V. *et al.* Chronic lymphocytic leukemia requires BCL2 to sequester prodeath BIM, explaining sensitivity to BCL2 antagonist ABT-737. *J. Clin. Invest.* **117**, 112–21 (2007).

155. Souers, A. J. *et al.* ABT-199, a potent and selective BCL-2 inhibitor, achieves antitumor activity while sparing platelets. *Nat. Med.* **19**, 202–8 (2013).

156. Croce, C. M. & Reed, J. C. Finally, An Apoptosis-Targeting Therapeutic for Cancer. *Cancer Res.* **76**, 5914–5920 (2016).

157. Konopleva, M. *et al.* A Phase 2 Study of ABT-199 (GDC-0199) in Patients with Acute Myelogenous Leukemia (AML). *Blood* **124**, 118–118 (2014).

158. Sharp, C., Nooka, A. K., Kaufman, J. L., Lonial, S. & Boise, L. H. Efficacy Of ABT-199 In Multiple Myeloma. *Blood* **122**, 4453–4453 (2013).

159. Kumar, S. K. *et al.* Safety and Efficacy of Venetoclax (ABT-199/GDC-0199) Monotherapy for Relapsed/Refractory Multiple Myeloma: Phase 1 Preliminary Results. *Blood* **126**, 4219–4219 (2015).

160. Seymour, J. F. *et al.* The Single-Agent Bcl-2 Inhibitor ABT-199 (GDC-0199) In Patients With Relapsed/Refractory (R/R) Non-Hodgkin Lymphoma (NHL): Responses Observed In All Mantle Cell Lymphoma (MCL) Patients. *Blood* **122**, 1789 (2013).

161. Casara, P. *et al.* S55746 is a novel orally active BCL-2 selective and potent inhibitor

that impairs hematological tumor growth. *Oncotarget* **9**, 20075–20088 (2018).

162. Lessene, G. *et al.* Structure-guided design of a selective BCL-XL inhibitor. *Nat. Chem. Biol.* **9**, 390–397 (2013).

163. Tao, Z. F. *et al.* Discovery of a potent and selective BCL-XLinhibitor with in vivo activity. *ACS Med. Chem. Lett.* **5**, 1088–1093 (2014).

164. Leverson, J. D. *et al.* Exploiting selective BCL-2 family inhibitors to dissect cell survival dependencies and define improved strategies for cancer therapy. *Sci. Transl. Med.* **7**, 1–11 (2015).

165. Lee, E. F. *et al.* Conformational changes in Bcl-2 pro-survival proteins determine their capacity to bind ligands. *J. Biol. Chem.* **284**, 30508–30517 (2009).

166. Leverson, J. D. *et al.* Potent and selective small-molecule MCL-1 inhibitors demonstrate on-target cancer cell killing activity as single agents and in combination with ABT-263 (navitoclax). *Cell Death Dis.* **6**, 1–11 (2015).

167. Caenepeel, S. *et al.* AMG 176, a selective MCL1 inhibitor, is effective in hematologic cancer models alone and in combination with established therapies. *Cancer Discov.* **8**, 1582–1597 (2018).

168. Kotschy, A. *et al.* The MCL1 inhibitor S63845 is tolerable and effective in diverse cancer models. *Nature* **000**, 1–7 (2016).

169. Moujalled, D. M. *et al.* Combining BH3-mimetics to target both BCL-2 and MCL1 has potent activity in pre-clinical models of acute myeloid leukemia. *Leukemia* **33**, 905–917 (2019).

170. Lin, K. H. *et al.* Targeting MCL-1/BCL-XL Forestalls the Acquisition of Resistance to ABT-199 in Acute Myeloid Leukemia. *Sci. Rep.* **6**, 27696 (2016).

171. Tahir, S. K. *et al.* Potential mechanisms of resistance to venetoclax and strategies to circumvent it. *BMC Cancer* **17**, 399 (2017).

172. Bodo, J. *et al.* Acquired resistance to venetoclax (ABT-199) in t(14;18) positive lymphoma cells. *Oncotarget* **7**, (2016).

173. Fresquet, V. *et al.* Acquired mutations in BCL2 family proteins conferring resistance to the BH3 mimetic ABT-199 in lymphoma. *Blood* **123**, 4111–4119 (2014).

174. Jamil, S. *et al.* A proteolytic fragment of Mcl-1 exhibits nuclear localization and regulates cell growth by interaction with Cdk1. *Biochem. J.* **387**, 659–667 (2005).

175. Wang, X. *et al.* Deletion of MCL-1 causes lethal cardiac failure and mitochondrial dysfunction. *Genes Dev.* **27**, 1351–1364 (2013).

176. Thomas, R. L. *et al.* Loss of MCL-1 leads to impaired autophagy and rapid development of heart failure. *Genes Dev.* **27**, 1365–1377 (2013).

177. Merino, D. *et al.* BH3-Mimetic Drugs: Blazing the Trail for New Cancer Medicines. *Cancer Cell* **34**, 879–891 (2018).

178. Bankhead, P. *et al.* QuPath: Open source software for digital pathology image analysis. *Sci. Rep.* **7**, 1–7 (2017).

179. Di Veroli, G. Y. *et al.* Combenefit: an interactive platform for the analysis and visualization of drug combinations. *Bioinformatics* **32**, 2866–2868 (2016).

180. Tefferi, A. Classification, Diagnosis and Management of Myeloproliferative Disorders in the JAK2V617F Era. *Hematology* **2006**, 240–245 (2006).

181. Chereda, B. & Melo, J. V. Natural course and biology of CML. *Ann. Hematol.* **94**, 107–121 (2015).

182. An, X. *et al.* BCR-ABL tyrosine kinase inhibitors in the treatment of Philadelphia chromosome positive chronic myeloid leukemia: a review. *Leuk. Res.* **34**, 1255–1268 (2010).

183. Hochhaus, A., Ernst, T., Eigendorff, E. & Rosée, P. La. Causes of resistance and treatment choices of second- and third-line treatment in chronic myelogenous leukemia patients. *Ann. Hematol.* **94**, 133–140 (2015).

184. Manley, P. W. *et al.* Advances in the structural biology, design and clinical development of VEGF-R kinase inhibitors for the treatment of angiogenesis. *Biochim. Biophys. Acta - Proteins Proteomics* **1697**, 17–27 (2004).

185. O'Hare, T. *et al.* AP24534, a Pan-BCR-ABL Inhibitor for Chronic Myeloid Leukemia, Potently Inhibits the T315I Mutant and Overcomes Mutation-Based Resistance. *Cancer Cell* **16**, 401–412 (2009).

186. Yamamoto, J. F. & Goodman, M. T. Patterns of leukemia incidence in the United States by subtype and demographic characteristics, 1997–2002. *Cancer Causes Control* **19**, 379–390 (2008).

187. Kouchkovsky, I. De & Abdul-Hay, M. ' Acute myeloid leukemia : a comprehensive review and 2016 update '. *Blood Cancer J.* **6**, 1–10 (2016).

188. Tonks, a *et al.* Expression of AML1-ETO in human myelomonocytic cells selectively inhibits granulocytic differentiation and promotes their self-renewal. *Leukemia* **18**, 1238–45 (2004).

189. Meshinchi, S. *et al.* Clinical implications of FLT3 mutations in pediatric AML. *Blood* **108**, 3654–61 (2006).

190. Fathi, A. T. & Chen, Y.-B. Treatment of FLT3-ITD acute myeloid leukemia. *Am. J. Blood Res.* **1**, 175–89 (2011).

191. Weisberg, E. *et al.* Inhibition of mutant FLT3 receptors in leukemia cells by the small molecule tyrosine kinase inhibitor PKC412. *Cancer Cell* **1**, 433–443 (2002).

192. Wilhelm, S. *et al.* Discovery and development of sorafenib: a multikinase inhibitor for treating cancer. *Nat. Rev. Drug Discov.* **5**, 835–844 (2006).

193. Mak, D. H. *et al.* Activation of apoptosis signaling eliminates CD34+ progenitor cells in blast crisis CML independent of response to tyrosine kinase inhibitors. *Leukemia* **26**, 788–94 (2012).

194. de Groot, R. P., Raaijmakers, J. A. M., Lammers, J.-W. J. & Koenderman, L. STAT5-Dependent CyclinD1 and Bcl-xL Expression in Bcr-Abl-Transformed Cells. *Mol. Cell Biol. Res. Commun.* **3**, 299–305 (2000).

195. Horita, M. *et al.* Blockade of the Bcr-Abl Kinase Activity Induces Apoptosis of Chronic Myelogenous Leukemia Cells by Suppressing Signal Transducer and Activator of Transcription 5–Dependent Expression of Bcl-X L. *J. Exp. Med.* **191**, 977–984 (2000).

196. Salomoni, P., Condorelli, F., Sweeney, S. M. & Calabretta, B. Versatility of BCR/ABL-expressing leukemic cells in circumventing proapoptotic BAD effects. *Blood* **96**, 676–684 (2000).

197. Pan, R. *et al.* Selective BCL-2 inhibition by ABT-199 causes on-target cell death in acute myeloid Leukemia. *Cancer Discov.* **4**, 362–675 (2014).

198. Pasic, I. & Lipton, J. H. Current approach to the treatment of chronic myeloid leukaemia. *Leuk. Res.* **55**, 65–78 (2017).

199. Lozzio, C. B. & Lozzio, B. B. Human Chronic Myelogenous Leukemia Cell-Line With Positive Philadelphia Chromosome. *Blood* **45**, 321–334 (1975).

200. Kubonishi, I. & Miyoshi, I. Establishment of a Ph1 Chromosome-Positive Cell Line from Chronic Myelogenois Leukemia in Blast Crisis. *Int. J. Cell Cloning* **1**, 105–117 (1983).

201. Olivieri, A. & Manzione, L. symposium article Dasatinib : a new step in molecular target therapy. **18**, 42–46 (2007).

202. Dutta, S. *et al.* Potent and specific peptide inhibitors of human pro-survival protein Bcl-xL. *J. Mol. Biol.* **427**, 1241–1253 (2014).

203. Akçay, G. *et al.* Inhibition of Mcl-1 through covalent modification of a noncatalytic lysine side chain. *Nat. Chem. Biol.* **2174**, 1–8 (2016).

204. Teh, T.-C. *et al.* Eradication of Acute Myeloid Leukemia Is Enhanced By Combined Bcl-2 and Mcl-1 Targeting. *Blood* **124**, (2014).

205. Pan, R. *et al.* Inhibition of Mcl-1 with the pan-Bcl-2 family inhibitor (-)BI97D6 overcomes ABT-737 resistance in acute myeloid leukemia. *Blood* **126**, 363–372 (2015).

206. High, L. M. *et al.* The Bcl-2 Homology Domain 3 Mimetic ABT-737 Targets the Apoptotic Machinery in Acute Lymphoblastic Leukemia Resulting in Synergistic in Vitro and in Vivo Interactions with Established Drugs. *Mol. Pharmacol.* **77**, 483–494 (2010).

207. Foucquier, J. & Guedj, M. Analysis of drug combinations: current methodological landscape. *Pharmacol. Res. Perspect.* **3**, 1–11 (2015).

208. Geary, N. Understanding synergy. *AJP Endocrinol. Metab.* **304**, E237–E253 (2013).

209. Lucas, C. M. *et al.* A population study of imatinib in chronic myeloid leukaemia demonstrates lower efficacy than in clinical trials. *Leukemia* **22**, 1963–1966 (2008).

210. Gutiérrez-Castellanos, S. *et al.* Differences in BCL-X L expression and STAT5 phosphorylation in chronic myeloid leukaemia patients. *Eur. J. Haematol.* **72**, 231–238 (2004).

211. Bewry, N. N. *et al.* Stat3 contributes to resistance toward BCR-ABL inhibitors in a bone marrow microenvironment model of drug resistance. *Mol. Cancer Ther.* **7**, 3169–75 (2008).

212. Amarante-Mendes, G. P. *et al.* Bcl-2-independent Bcr-Abl-mediated resistance to apoptosis: protection is correlated with up regulation of Bcl-xL. *Oncogene* **16**, 1383–90 (1998).

213. Bai, H. *et al.* Bcl-xL enhances single-cell survival and expansion of human embryonic stem cells without affecting self-renewal. *Stem Cell Res.* **8**, 26–37 (2012).

214. Zeuner, A. *et al.* Elimination of quiescent/slow-proliferating cancer stem cells by Bcl-XL inhibition in non-small cell lung cancer. *Cell Death Differ.* **21**, 1877–88 (2014).

215. Vogler, M. *et al.* BCL2/BCL-X(L) inhibition induces apoptosis, disrupts cellular calcium homeostasis, and prevents platelet activation. *Blood* **117**, 7145–54 (2011).

216. Quentmeier, H., Reinhardt, J., Zaborski, M. & Drexler, H. G. FLT3 mutations in

acute myeloid leukemia cell lines. *Leuk. Off. J. Leuk. Soc. Am. Leuk. Res. Fund, U.K* **17**, 120–124 (2003).

217. Zhang, W. *et al.* Sorafenib induces apoptosis of AML cells via Bim-mediated activation of the intrinsic apoptotic pathway. *Leukemia* **22**, 808–818 (2008).

218. Chen, S., Dai, Y., Pei, X.-Y. & Grant, S. Bim Upregulation by Histone Deacetylase Inhibitors Mediates Interactions with the Bcl-2 Antagonist ABT-737: Evidence for Distinct Roles for Bcl-2, Bcl-xL, and Mcl-1. *Mol. Cell. Biol.* **29**, 6149–6169 (2009).

219. Konopleva, M. *et al.* MEK inhibition enhances ABT-737-induced leukemia cell apoptosis via prevention of ERK-activated MCL-1 induction and modulation of MCL-1/BIM complex. *Leukemia* **26**, 778–787 (2012).

220. Tron, A. E. *et al.* Abstract 302: Selective Mcl-1 inhibition by AZD5991 induces on-target cell death and achieves antitumor activity in multiple myeloma and acute myeloid leukemia. *Cancer Res.* **78**, 302–302 (2018).

221. Beauchamp, E. M. & Platanias, L. C. BH3 mimetics and multi-kinase inhibition in AML. *Blood* **119**, 5947–8 (2012).

222. Naqvi, K., Konopleva, M. & Ravandi, F. Targeted therapies in Acute Myeloid Leukemia: a focus on FLT-3 inhibitors and ABT199. *Expert Rev. Hematol.* **10**, 1–12 (2017).

223. Lee, J. S. *et al.* Statins enhance efficacy of venetoclax in blood cancers. *Sci. Transl. Med.* **10**, 1–22 (2018).

224. Grant, S. Rational combination strategies to enhance venetoclax activity and overcome resistance in hematologic malignancies. *Leuk. Lymphoma* **59**, 1292–1299 (2017).

225. Roberts, A. W. *et al.* Targeting BCL2 with Venetoclax in Relapsed Chronic Lymphocytic Leukemia. *N. Engl. J. Med.* **374**, 311–322 (2016).

226. Jou, A. & Hess, J. Epidemiology and Molecular Biology of Head and Neck Cancer. *Oncol. Res. Treat.* **40**, 328–332 (2017).

227. Leemans, C. R., Braakhuis, B. J. M. & Brakenhoff, R. H. The molecular biology of head and neck cancer. *Nat. Publ. Gr.* **11**, 9–22 (2011).

228. Herbst, R. S. *et al.* Phase II multicenter study of the epidermal growth factor receptor antibody cetuximab and cisplatin for recurrent and refractory squamous cell carcinoma of the head and neck. *J. Clin. Oncol.* **23**, 5578–87 (2005).

229. Gibson, M. K. & Forastiere, A. A. Review Reassessment of the role of induction chemotherapy for head and neck cancer. *Lancet* **7**, 565–574 (2006).

230. Chung, C. H. *et al.* Gene Expression Profiles Identify Epithelial-to-Mesenchymal Transition and Activation of Nuclear Factor-κB Signaling as Characteristics of a High-risk Head and Neck Squamous Cell Carcinoma. *Cancer Res.* **66**, 8210–8218 (2006).

231. Chung, C. H. *et al.* Molecular classification of head and neck squamous cell carcinomas using patterns of gene expression. *Cancer Cell* **5**, 489–500 (2004).

232. Trask, D. K. *et al.* Expression of Bcl-2 Family Proteins in Advanced Laryngeal Squamous Cell Carcinoma: Correlation With Response to Chemotherapy and Organ Preservation. *Laryngoscope* **112**, 638–644 (2002).

233. Li, R. *et al.* Targeting Antiapoptotic Bcl-2 Family Members with Cell-Permeable

BH3 Peptides Induces Apoptosis Signaling and Death in Head and Neck Squamous Cell Carcinoma Cells. *Neoplasia* **9**, 801–811 (2007).

234. Li, R. *et al.* ABT-737 Synergizes with Chemotherapy to Kill Head and Neck Squamous Cell Carcinoma Cells via a Noxa-Mediated Pathway. *Mol. Pharmacol.* **75**, 1231–39 (2009).

235. Westphal, S. & Kalthoff, H. Apoptosis: targets in pancreatic cancer. *Mol. Cancer* **2**, 1–14 (2003).

236. Siegel, R. L., Miller, K. D. & Jemal, A. Cancer statistics, 2016. *CA Cancer J Clin* **69**, 7–34 (2016).

237. Batty, G. D. *et al.* Risk factors for pancreatic cancer mortality: extended follow-up of the original Whitehall Study. *Cancer Epidemiol. Biomarkers Prev.* **18**, 673–5 (2009).

238. Hidalgo, M. Pancreatic Cancer. *N Engl J Med* **489**, 1605–1622 (2010).

239. Binenbaum, Y., Na'ara, S. & Gil, Z. Gemcitabine resistance in pancreatic ductal adenocarcinoma. *Drug Resist. Updat.* **23**, 55–68 (2015).

240. Lecca, P. Methods of biological network inference for reverse engineering cancer chemoresistance mechanisms. *Drug Discov. Today* **19**, 151–163 (2014).

241. Ceppi, P. *et al.* ERCC1 and RRM1 gene expressions but not EGFR are predictive of shorter survival in advanced non-small-cell lung cancer treated with cisplatin and gemcitabine. *Ann. Oncol.* **17**, 1818–1825 (2006).

242. Boucher, M. J. *et al.* MEK/ERK signaling pathway regulates the expression of Bcl-2, Bcl-X(L), and Mcl-1 and promotes survival of human pancreatic cancer cells. *J. Cell. Biochem.* **79**, 355–69 (2000).

243. Miyamoto, Y. *et al.* Immunohistochemical Analysis of Bcl-2, Bax, Bcl-X, and Mcl-1 Expression in Pancreatic Cancers. *Oncology* **56**, 73–82 (1999).

244. Muilenburg, D. J., Coates, J. M., Virudachalam, S. & Bold, R. J. Targeting Bcl-2-mediated cell death as a novel therapy in pancreatic cancer. *J. Surg. Res.* **163**, 276–281 (2010).

245. Zhou, Y., Liu, H., Xue, R., Tang, W. & Zhang, S. BH3 Mimetic ABT-199 Enhances the Sensitivity of Gemcitabine in Pancreatic Cancer in vitro and in vivo. *Dig. Dis. Sci.* **63**, 3367–3375 (2018).

246. Hari, Y., Harashima, N., Tajima, Y. & Harada, M. Bcl-xL inhibition by molecular-targeting drugs sensitizes human pancreatic cancer cells to TRAIL. *Oncotarget* **6**, 41902–41915 (2015).

247. Huang, S. & Sinicrope, F. A. BH3 Mimetic ABT-737 Potentiates TRAIL-Mediated Apoptotic Signaling by Unsequestering Bim and Bak in Human Pancreatic Cancer Cells. *Cancer Res* **68**, 2944–51 (2008).

248. Al-Zebeeby, A. *et al.* Targeting intermediary metabolism enhances the efficacy of BH3 mimetic therapy in hematologic malignancies. *Haematologica* **104**, 1016–1025 (2019).

249. Greaves, G. *et al.* BH3-only proteins are dispensable for apoptosis induced by pharmacological inhibition of both MCL-1 and BCL-XL. *Cell Death Differ.* **6**, 1037–1047 (2018).

250. Takahashi, H. *et al.* Simultaneous knock-down of Bcl-xL and MCL-1 induces apoptosis through Bax activation in pancreatic cancer cells. *Biochim. Biophys. Acta*

1833, 1199–1216 (2013).

251. Milani, M. *et al.* DRP-1 is required for BH3 mimetic-mediated mitochondrial fragmentation and apoptosis. *Cell Death Dis.* **8**, 1–9 (2017).

252. Cancer Research UK Website. (2019).

253. Le, X. & Hanna, E. Y. Optimal regimen of cisplatin in squamous cell carcinoma of head and neck yet to be determined. *Ann. Transl. Med.* **6**, 1–5 (2018).

254. Dorr, F. A. *et al.* Improvements in survival and clinical benefit with gemcitabine as first-line therapy for patients with advanced pancreas cancer: a randomized trial. *J. Clin. Oncol.* **15**, 2403–2413 (1997).

255. Wolter, K. G. *et al.* (-)-Gossypol Inhibits Growth and Promotes Apoptosis of Human Head and Neck Squamous Cell Carcinoma In Vivo. *Neoplasia* **8**, 163–172 (2006).

256. Banerjee, S. Preclinical Studies of Apogossypolone, a Novel Pan Inhibitor of Bcl-2 and Mcl-1, Synergistically Potentiates Cytotoxic Effect of Gemcitabine in Pancreatic Cancer Cells. *Pancreas* **39**, 323–331 (2010).

257. Quinn, B. A. *et al.* Pancreatic Cancer Combination Therapy Using a BH3 Mimetic and a Synthetic Tetracycline. *Cancer Res.* **75**, 2305–2315 (2015).

258. Varadarajan, S. *et al.* Evaluation and critical assessment of putative MCL-1 inhibitors. *Cell Death Differ.* **20**, 1475–84 (2013).

259. Gray, M. W. Mitochondrial evolution. *Cold Spring Harb. Perspect. Biol.* **4**, 1–16 (2012).

260. Westermann, B. Mitochondrial fusion and fission in cell life and death. *Nat. Rev. Mol. Cell Biol.* **11**, 872–884 (2010).

261. Ramachandran, R. Mitochondrial dynamics: The dynamin superfamily and execution by collusion. *Semin. Cell Dev. Biol.* **76**, 201–212 (2018).

262. Chappie, J. S., Acharya, S., Leonard, M., Schmid, S. L. & Dyda, F. G domain dimerization controls dynamin's assembly-stimulated GTPase activity. *Nature* **465**, 435–440 (2010).

263. Lima, A. R. *et al.* Dynamin-Related Protein 1 at the Crossroads of Cancer. *Genes (Basel).* **9**, 1–20 (2018).

264. Qi, X., Disatnik, M.-H., Shen, N., Sobel, R. A. & Mochly-Rosen, D. Aberrant mitochondrial fission in neurons induced by protein kinase C{delta} under oxidative stress conditions in vivo. *Mol. Biol. Cell* **22**, 256–65 (2011).

265. Han, X. J. *et al.* CaM kinase Iα-induced phosphorylation of Drp1 regulates mitochondrial morphology. *J. Cell Biol.* **182**, 573–585 (2008).

266. MacVicar, T. & Langer, T. OPA1 processing in cell death and disease – the long and short of it. *J. Cell Sci.* **129**, 2297–2306 (2016).

267. Quintana-cabrera, R. *et al.* The cristae modulator Optic atrophy 1 requires mitochondrial ATP synthase oligomers to safeguard mitochondrial function. *Nat. Commun.* **9**, 1–13 (2018).

268. Ishihara, N., Fujita, Y., Oka, T. & Mihara, K. Regulation of mitochondrial morphology through proteolytic cleavage of OPA1. *EMBO J.* **25**, 2966–2977 (2006).

269. Käser, M., Kambacheld, M., Kisters-Woike, B. & Langer, T. Oma1, a Novel Membrane-bound Metallopeptidase in Mitochondria with Activities Overlapping

with the m-AAA Protease. *J. Biol. Chem.* **278**, 46414–46423 (2003).

270. Faccenda, D. *et al.* Control of Mitochondrial Remodeling by the ATPase Inhibitory Factor 1 Unveils a Pro-survival Relay Report Control of Mitochondrial Remodeling by the ATPase Inhibitory Factor 1 Unveils a Pro-survival Relay via OPA1. *CellReports* **18**, 1869–1883 (2017).

271. Galluzzi, L. *et al.* Essential versus accessory aspects of cell death: recommendations of the NCCD 2015. *Cell Death Differ.* **22**, 58–73 (2015).

272. Bossy, B. *et al.* S-Nitrosylation of DRP1 Does Not Affect Enzymatic Activity and is Not Specific to Alzheimer's Disease. *J. Alzheimer's Dis.* **20**, S513–S526 (2010).

273. Dotto, V. Del *et al.* OPA1 Isoforms in the Hierarchical Organization of Mitochondrial Functions. *Cell Rep.* **19**, 2557–2571 (2017).

274. Olichon, A. *et al.* Loss of OPA1 perturbates the mitochondrial inner membrane structure and integrity, leading to cytochrome c release and apoptosis. *J. Biol. Chem.* **278**, 7743–7746 (2003).

275. Lee, J. E., Westrate, L. M., Wu, H., Page, C. & Voeltz, G. Multiple dynamin family members collaborate to drive mitochondrial division. *Mol. Biol. Cell.* **26**, 1–17 (2016).

276. Prudent, J. *et al.* MAPL SUMOylation of Drp1 Stabilizes an ER/Mitochondrial Platform Required for Cell Death. *Mol. Cell* **59**, 941–955 (2015).

277. Prudent, J. & McBride, H. M. Mitochondrial Dynamics: ER Actin Tightens the Drp1 Noose. *Curr. Biol.* **26**, 207–209 (2016).

278. Paupe, V. & Prudent, J. New insights into the role of mitochondrial calcium homeostasis in cell migration. *Biochem. Biophys. Res. Commun.* **xxx**, 1–12 (2017).

279. Vogler, M. *et al.* A novel paradigm for rapid ABT-737-induced apoptosis involving outer mitochondrial membrane rupture in primary leukemia and lymphoma cells. *Cell Death Differ.* **15**, 820–30 (2008).

280. Wei, J. *et al.* Sabutoclax (BI97C1) and BI112D1, putative inhibitors of MCL-1, induce mitochondrial fragmentation either upstream of or independent of apoptosis. *Neoplasia* **15**, 568–78 (2013).

281. Montero, J. & Letai, A. Why do BCL-2 inhibitors work and where should we use them in the clinic? *Cell Death Differ.* **183**, 1–9 (2017).

282. Kashatus, J. A., Nascimento, A., Counter, C. M. & Kashatus, D. F. Erk2 Phosphorylation of Drp1 Promotes Mitochondrial Fission and MAPK-Driven Tumor Growth. *Mol. Cell* **57**, 537–551 (2015).

283. Gan, X. *et al.* Inhibition of ERK-DLP1 signaling and mitochondrial division alleviates mitochondrial dysfunction in Alzheimer's disease cybrid cell. *Biochim. Biophys. Acta* **1842**, 220–231 (2014).

284. Trotta, A. P. & Chipuk, J. E. Mitochondrial dynamics as regulators of cancer biology. *Cell. Mol. Life Sci.* **74**, 1–19 (2017).

285. Tilokani, L., Nagashima, S., Paupe, V. & Prudent, J. Mitochondrial dynamics : overview of molecular mechanisms. **62**, 341–360 (2018).

286. Smirnova, E., Shurland, D. L., Ryazantsev, S. N. & van der Bliek, A. M. A human dynamin-related protein controls the distribution of mitochondria. *J. Cell Biol.* **143**, 351–8 (1998).

287. Chipuk, J. E. *et al.* Direct Activation of Bax by p55 Mediates Mitochondrial Membrane Permeabilization and Apoptosis. *Science.* **303**, 1010–1014 (2004).

288. Alsop, A. E. *et al.* Dissociation of Bak a1 helix from the core and latch domains is required for apoptosis. *Nat. Commun.* **6**, 1–13 (2015).

289. Del Dotto, V., Fogazza, M., Carelli, V., Rugolo, M. & Zanna, C. Eight human OPA1 isoforms, long and short: What are they for? *Biochim. Biophys. Acta - Bioenerg.* **1859**, 263–269 (2018).

290. Frank, S. *et al.* The Role of Dynamin-Related Protein 1, a Mediator of Mitochondrial Fission, in Apoptosis. *Dev. Cell* **1**, 515–525 (2001).

291. Perciavalle, R. M. & Opferman, J. T. Delving Deeper: MCL-1's Contributions to Normal and Cancer Biology. *Trends cell. biol.* **23**, 22–29 (2013).

292. Karbowski, M. *et al.* Spatial and temporal association of Bax with mitochondrial fission sites, Drp1, and Mfn2 during apoptosis. *J. Cell Biol.* **159**, 931–938 (2002).

293. Braschi, E., Zunino, R. & McBride, H. M. MAPL is a new mitochondrial SUMO E3 ligase that regulates mitochondrial fission. *EMBO Rep.* **10**, 748–54 (2009).

294. Smirnova, E., Griparic, L., Shurland, D. L. & van der Bliek, A. M. Dynamin-related protein Drp1 is required for mitochondrial division in mammalian cells. *Mol. Biol. Cell* **12**, 2245–56 (2001).

295. Wasiak, S., Zunino, R. & McBride, H. M. Bax/Bak promote sumoylation of DRP1 and its stable association with mitochondria during apoptotic cell death. *J. Cell Biol.* **177**, 439–450 (2007).

296. Kalkavan, H. & Green, D. R. MOMP, cell suicide as a BCL-2 family business. *Cell Death Differ.* **25**, 46–55 (2018).

297. Muñoz-Pinedo, C. *et al.* Different mitochondrial intermembrane space proteins are released during apoptosis in a manner that is coordinately initiated but can vary in duration. *PNAS* **103**, 11573–11578 (2006).

298. Parone, P. A. *et al.* Inhibiting the Mitochondrial Fission Machinery Does Not Prevent Bax/Bak-Dependent Apoptosis. *Mol. Cell. Biol.* **26**, 7397–7408 (2006).

299. Baumann, O. & Walz, B. Endoplasmic reticulum of animal cells and its organization into structural and functional domains. *Int. Rev. Cytol.* **205**, 149–214 (2001).

300. Shibata, Y., Hu, J., Kozlov, M. M. & Rapoport, T. A. Mechanisms Shaping the Membranes of Cellular Organelles. *Annu. Rev. Cell Dev. Biol.* **25**, 329–354 (2009).

301. Zhang, H. & Hu, J. Shaping the Endoplasmic Reticulum into a Social Network. *Trends Cell Biol.* **26**, 934–943 (2016).

302. Voeltz, G. K., Prinz, W. A., Shibata, Y., Rist, J. M. & Rapoport, T. A. A class of membrane proteins shaping the tubular endoplasmic reticulum. *Cell* **124**, 573–586 (2006).

303. Yamamoto, Y., Yoshida, A., Miyazaki, N., Iwasaki, K. & Sakisaka, T. Arl6IP1 has the ability to shape the mammalian ER membrane in a reticulon-like fashion. *Biochem. J* **458**, 69–79 (2014).

304. Klopfenstein, D. R. *et al.* Subdomain-specific Localization of CLIMP-63 (p63) in the Endoplasmic Reticulum Is Mediated by Its Luminal-Helical Segment. *J. Cell Biol.* **153**, 1287–1299 (2001).

305. Vance, J. E. Phospholipid Synthesis in a Membrane Fraction Associated with Mitochondria. *J. Biol. Chem.* **265**, 7248–7257 (1990).

306. Becker, G. L., Fiekums, G. & Lehningerg, A. L. Regulation of Free Ca2+ by Liver Mitochondria and Endoplasmic Reticulum. *J. Biol. Chem.* **255**, 9–9 (1980).

307. Herrera-Cruz, M. S. S. T. & Simmen, T. Of yeast, mice and men: MAMs come in two flavours. *Biol. Direct* **12**, 1–21 (2017).

308. Friedman, J. R. *et al.* ER Tubules Mark Sites of Mitochondrial Division. *Science.* **334**, 358–362 (2011).

309. Wu, W. *et al.* FUNDC1 regulates mitochondrial dynamics at the ER–mitochondrial contact site under hypoxic conditions. *EMBO J.* **35**, 1368–1384 (2016).

310. Rgy Csordá, G., Thomas, A. P., Rgy, G. & Czky, H. Quasi-synaptic calcium signal transmission between endoplasmic reticulum and mitochondria. *EMBO J.* **18**, 96–108 (1999).

311. Murley, A. *et al.* ER-associated mitochondrial division links the distribution of mitochondria and mitochondrial DNA in yeast. *Elife* **2**, 1–16 (2013).

312. Manor, U. *et al.* A mitochondria-anchored isoform of the actin-nucleating spire protein regulates mitochondrial division. *Elife* **4**, 1–27 (2015).

313. Pagliuso, A., Cossart, P. & Stavru, F. The ever-growing complexity of the mitochondrial fission machinery. *Cell. Mol. Life Sci.* **75**, 355–374 (2018).

314. Opydo-Chanek, M., Gonzalo, O. & Marzo, I. Multifaceted anticancer activity of BH3 mimetics: Current evidence and future prospects. *Biochem. Pharmacol.* **136**, 12–23 (2017).

315. Csordás, G., Weaver, D. & Hajnóczky, G. Endoplasmic Reticular–Mitochondrial Contactology: Structure and Signaling Functions. *Trends Cell Biol.* **28**, 523–540 (2018).

316. Prudent, J. & McBride, H. M. The mitochondria-endoplasmic reticulum contact sites: a signalling platform for cell death. *Curr. Opin. Cell Biol.* **47**, 52–63 (2017).

317. Korobova, F., Ramabhadran, V. & Higgs, H. N. An Actin-Dependent Step in Mitochondrial Fission Mediated by the ER-Associated Formin INF2. *Science.* **339**, 464–467 (2013).

318. Chang, C. R. & Blackstone, C. Dynamic regulation of mitochondrial fission through modification of the dynamin-related protein Drp1. *Ann. N. Y. Acad. Sci.* **1201**, 34–39 (2010).

319. Wang, S., Tukachinsky, H., Romano, F. B. & Rapoport, T. A. Cooperation of the ER-shaping proteins atlastin, lunapark, and reticulons to generate a tubular membrane network. *Elife* **5**, 1–29 (2016).

320. Goyal, U. & Blackstone, C. Untangling the web: Mechanisms underlying ER network formation. *BBA - Mol. Cell Res.* **1833**, 2492–2498 (2013).

321. Chen, S., Novick, P. & Ferro-Novick, S. ER network formation requires a balance of the dynamin-like GTPase Sey1p and the Lunapark family member Lnp1p. *Nat. Cell Biol.* **14**, 707–717 (2012).

322. Chen, S. *et al.* Lunapark stabilizes nascent three-way junctions in the endoplasmic reticulum. *PNAS* **112**, 418–423 (2015).

323. Rosselin, M., Santo-Domingo, J., Bermont, F., Giacomello, M. & Demaurex, N. L-OPA1 regulates mitoflash biogenesis independently from membrane fusion. *EMBO Rep.* **18**, 451–463 (2017).

324. Pellegrini, L. & Scorrano, L. A cut short to death: Parl and Opa1 in the regulation of mitochondrial morphology and apoptosis. *Cell Death Differ.* **14**, 1275–1284 (2007).

325. Reali, V. *et al.* Reticulon protein-1C is a key component of MAMs. *Biochim. Biophys. Acta - Mol. Cell Res.* **1853**, 733–745 (2015).

326. Shibata, Y. *et al.* Mechanisms determining the morphology of the peripheral ER. *Cell* **143**, 774–788 (2010).

327. Sandoz, P. A. & Gisou Van Der Goot, F. How many lives does CLIMP-63 have? *Biochem. Soc. Trans.* **43**, 222–228 (2015).

328. Gong, L. *et al.* RTN1-C mediates cerebral ischemia/reperfusion injury via ER stress and mitochondria-associated apoptosis pathways. *Cell Death.Dis.* **8**, 1–11 (2017).

329. Tagami, S., Eguchi, Y., Kinoshita, M., Takeda, M. & Tsujimoto, Y. A novel protein, RTN-XS, interacts with both Bcl-XL and Bcl-2 on endoplasmic reticulum and reduces their anti-apoptotic activity. *Oncogene* **19**, 5736–5746 (2000).

330. Cortes, J. *et al.* Phase 2 study of subcutaneous omacetaxine mepesuccinate after TKI failure in patients with chronic-phase CML with T315I mutation. *Blood* **120**, 2573–2580 (2012).

331. Naka, K., Hoshii, T. & Hirao, A. Novel therapeutic approach to eradicate tyrosine kinase inhibitor resistant chronic myeloid leukemia stem cells. *Cancer Sci.* **101**, 1577–1581 (2010).

332. Helgason, G. V., Karvela, M. & Holyoake, T. L. Kill one bird with two stones: potential efficacy of BCR-ABL and autophagy inhibition in CML. *Blood* **118**, 2035–2043 (2011).

333. Gonzalez, M. S. *et al.* BAX/BCL-XL gene expression ratio inversely correlates with disease progression in chronic myeloid leukemia. *Blood Cells, Mol. Dis.* **45**, 192–196 (2010).

334. Neviani, P. *et al.* The tumor suppressor PP2A is functionally inactivated in blast crisis CML through the inhibitory activity of the BCR/ABL-regulated SET protein. *Cancer Cell* **8**, 355–368 (2005).

335. Shafer, D. & Grant, S. Update on rational targeted therapy in AML. *Blood Rev.* **30**, 275–283 (2016).

336. Breitenbuecher, F. *et al.* A novel molecular mechanism of primary resistance to FLT3-kinase inhibitors in AML. *Blood* **113**, 4063–4073 (2009).

337. Kohl, T. M. *et al.* BH3 mimetic ABT-737 neutralizes resistance to FLT3 inhibitor treatment mediated by FLT3-independent expression of BCL2 in primary AML blasts. *Leukemia* **21**, 1763–1772 (2007).

338. Luedtke, D. A. *et al.* Inhibition of Mcl-1 enhances cell death induced by the Bcl-2-selective inhibitor ABT-199 in acute myeloid leukemia cells. *Signal Transduct. Target. Ther.* **2**, 1–9 (2017).

339. Li, Z., He, S. & Look, A. T. The MCL1-specific inhibitor S63845 acts synergistically with venetoclax/ABT-199 to induce apoptosis in T-cell acute lymphoblastic leukemia cells. *Leukemia* **33**, 262–266 (2019).

340. Stransky, N. *et al.* The Mutational Landscape of Head and Neck Squamous Cell Carcinoma. *Science.* **333**, 1157–1160 (2011).

341. Gadhikar, M. A. *et al.* Chk1/2 Inhibition Overcomes the Cisplatin Resistance of Head and Neck Cancer Cells Secondary to the Loss of Functional p53. *Mol. cancer th* **12**, 1860–1873 (2013).

342. Abuzeid, W. M. *et al.* Sensitization of head and neck cancer to cisplatin through the use of a novel curcumin analogue. *Arch. Otolaryngol. Head Neck Surg.* **137**, 499–507 (2011).

343. Jamil, S., Mojtabavi, S., Hojabrpour, P., Cheah, S. & Duronio, V. An Essential Role for MCL-1 in ATR-mediated CHK1 Phosphorylation. *Mol. Biol. Cell* **19**, 3212–3220 (2008).

344. Pena, J. C., Thompson, C. B., Recant, W., Vokes, E. E. & Rudin, C. M. Bcl-x L and Bcl-2 Expression in Squamous Cell Carcinoma of the Head and Neck. *Cancer* **85**, 164–170 (1999).

345. Yuen, A. P. W. *et al.* Clinicopathologic significance of bcl-2 expression in the surgical treatment of oral tongue carcinoma. *Eur. J. Surg. Oncol.* **28**, 667–72 (2002).

346. Wilson, G. D. *et al.* bcl-2 expression in head and neck cancer: an enigmatic prognostic marker. *Int. J. Radiat. Oncol. Biol. Phys.* **49**, 435–41 (2001).

347. Borner, M. M. *et al.* Spontaneous Apoptosis and the Expression of p53 and Bcl-2 Family Proteins in Locally Advanced Head and Neck Cancer. *Arch. Otolaryngol. Neck Surg.* **125**, 417–422 (1999).

348. Mallick, S. *et al.* Human oral cancers have altered expression of Bcl-2 family members and increased expression of the anti-apoptotic splice variant of *Mcl-1*. *J. Pathol.* **217**, 398–407 (2009).

349. Pallavi, N., Nalabolu, G. R. K. & Hiremath, S. K. S. Bcl-2 and c-Myc expression in oral dysplasia and oral squamous cell carcinoma: An immunohistochemical study to assess tumor progression. *J. Oral Maxillofac. Pathol.* **22**, 325–331 (2018).

350. Ow, T. J. *et al.* Optimal targeting of BCL-family proteins in head and neck squamous cell carcinoma requires inhibition of both BCL-xL and MCL-1. *Oncotarget* **10**, 494–510 (2019).

351. Grey, P. *et al.* Prognostic Significance of BCL-2 Expression in Localized Squamous Cell Carcinoma of the Head and Neck. *Ann. Otol. Rhinol. Laryngol.* **106**, 445–450 (1997).

352. Lo Muzio, L. *et al.* Bcl-2 as prognostic factor in head and neck squamous cell carcinoma. *Oncol. Res.* **15**, 249–55 (2005).

353. Redondo, M. *et al.* Expression of the Antiapoptotic Proteins Clusterin and Bcl-2 in Laryngeal Squamous Cell Carcinomas. *Tumor Biol.* **27**, 195–200 (2006).

354. Hezel, A. F., Kimmelman, A. C., Stanger, B. Z., Bardeesy, N. & Depinho, R. A. Genetics and biology of pancreatic ductal adenocarcinoma. *Genes Dev.* **20**, 1218–1249 (2006).

355. Liptay, S. *et al.* Mitogenic and antiapoptotic role of constitutive NF-κB/Rel activity in pancreatic cancer. *Int. J. Cancer* **105**, 735–746 (2003).

356. Bharti, A. C. & Aggarwal, B. B. Nuclear factor-kappa B and cancer: its role in prevention and therapy. *Biochem. Pharmacol.* **64**, 883–888 (2002).

357. Galmarini, C. M. *et al.* Expression of a non-functional p53 affects the sensitivity of cancer cells to gemcitabine. *Int. J. Cancer* **97**, 439–445 (2002).

358. Schwickart, M. *et al.* Deubiquitinase USP9X stabilizes MCL1 and promotes tumour cell survival. *Nature* **463**, 103–107 (2010).

359. Otera, H. *et al.* Mff is an essential factor for mitochondrial recruitment of Drp1 during mitochondrial fission in mammalian cells. *J. Cell Biol.* **191**, 1141–1158 (2010).

360. Mukherjee, N. *et al.* BH3 mimetics induce apoptosis independent of DRP-1 in melanoma. *Cell Death Dis.* **9**, 1–12 (2018).

361. Tanaka, A. & Youle, R. J. Molecular Cell Previews A Chemical Inhibitor of DRP1 Uncouples Mitochondrial Fission and Apoptosis. *Mol. Cell* **29**, 409–410 (2008).

362. Cassidy-Stone, A. *et al.* Chemical Inhibition of the Mitochondrial Division Dynamin Reveals Its Role in Bax/Bak-Dependent Mitochondrial Outer Membrane Permeabilization. *Dev. Cell* **14**, 193–204 (2008).

363. Pernas, L. & Scorrano, L. Mito-Morphosis: Mitochondrial Fusion, Fission, and Cristae Remodeling as Key Mediators of Cellular Function. *Annu. Rev. Physiol.* **78**, 505–531 (2015).

364. Bordt, E. A. *et al.* The Putative Drp1 Inhibitor mdivi-1 Is a Reversible Mitochondrial Complex I Inhibitor that Modulates Reactive Oxygen Species. *Dev. Cell* **40**, 583-594.e6 (2017).

365. Brooks, C. *et al.* Bak regulates mitochondrial morphology and pathology during apoptosis by interacting with mitofusins. *PNAS* **104**, 11649–11654 (2007).

366. Ferguson, S. M. & De Camilli, P. Dynamin, a membrane-remodelling GTPase. *Nat. Rev. Mol. Cell Biol.* **13**, 75–88 (2012).

367. Wu, H., Carvalho, P. & Voeltz, G. K. Here, there, and everywhere: The importance of ER membrane contact sites. *Science.* **361**, 1–9 (2018).

368. Lewis, S. C., Uchiyama, L. F. & Nunnari, J. ER-mitochondria contacts couple mtDNA synthesis with mitochondrial division in human cells. *Science.* **353**, 261–269 (2016).

369. Ban-ishihara, R., Ishihara, T., Sasaki, N., Mihara, K. & Ishihara, N. Dynamics of nucleoid structure regulated by mitochondrial fi ssion contributes to cristae reformation and release of cytochrome c. *PNAS* **110**, 11863–11868 (2013).

370. Riley, J. S. *et al.* Mitochondrial inner membrane permeabilisation enables mtDNA release during apoptosis. *EMBO J.* **37**, 1–16 (2018).

371. Pagliuso, A. *et al.* A role for septin 2 in Drp1-mediated mitochondrial fission. *EMBO Rep.* **17**, 858–873 (2016).

372. Korobova, F., Gauvin, T. J. & Higgs, H. N. A Role for Myosin II in Mammalian Mitochondrial Fission. *Curr. Biol.* **24**, 409–414 (2014).

373. Goldbeter, A. *et al.* An Actin-Dependent Step in Mitochondrial Fission Mediated by the ER-Associated Formin IFN2. **339**, 464–468 (2013).

374. Rowland, A. A. & Voeltz, G. K. Endoplasmic reticulum-mitochondria contacts: Function of the junction. *Nat. Rev. Mol. Cell Biol.* **13**, 607–615 (2012).

375. Xu, C., Bailly-Maitre, B. & Reed, J. Endoplasmic reticulum stress: cell life and death

decisions. *J. Clin. Invest.* **115**, 2656–2664 (2005).

376. Xia, M. *et al.* Communication between mitochondria and other organelles: a brand-new perspective on mitochondria in cancer. *Cell Biosci.* **9**, 1–19 (2019).

377. Sano, R. *et al.* Article GM1-Ganglioside Accumulation at the Mitochondria-Associated ER Membranes Links ER Stress to Ca 2+-Dependent Mitochondrial Apoptosis. *Mol. Cell* **36**, 500–511 (2009).

378. Jozsef, L. *et al.* Reticulon 4 is necessary for endoplasmic reticulum tubulation, STIM1-Orai1 coupling, and store-operated calcium entry. *J. Biol. Chem.* **289**, 9380–9395 (2014).

379. Dubois, C. *et al.* Remodeling of Channel-Forming ORAI Proteins Determines an Oncogenic Switch in Prostate Cancer. *Cancer Cell* **26**, 19–32 (2014).

380. McAndrew, D. *et al.* ORAI1-Mediated Calcium Influx in Lactation and in Breast Cancer. *Mol. Cancer Ther.* **10**, 448–460 (2011).

381. Chiurchiù, V., Maccarrone, M. & Orlacchio, A. The Role of Reticulons in Neurodegenerative Diseases. *NeuroMolecular Med.* **16**, 3–15 (2014).

382. Klopfenstein, D. R. C., Kappeler, F. & Hauri, H. P. A novel direct interaction of endoplasmic reticulum with microtubules. *EMBO J.* **17**, 6168–6177 (1998).

383. Dejgaard, K. *et al.* Organization of the Sec61 Translocon, Studied by High Resolution Native Electrophoresis. *J. Proteome Res.* **9**, 1763–1771 (2010).

384. Węsierska-Gądek, J. *et al.* A new, unexpected action of olomoucine, a CDK inhibitor, on normal human cells: Up-regulation of CLIMP-63, a cytoskeleton-linking membrane protein. *J. Cell. Biochem.* **102**, 1405–1419 (2007).

385. Karasawa, T., Wang, Q., David, L. L. & Steyger, P. S. CLIMP-63 is a gentamicin-binding protein that is involved in drug-induced cytotoxicity. *Cell Death Dis.* **1**, 102–111 (2010).

386. Polzien, L. *et al.* Identification of novel in vivo phosphorylation sites of the human proapoptotic protein BAD. Pore-forming activity of bad is regulated by phosphorylation. *J. Biol. Chem.* **284**, 28004–28020 (2009).

387. Williams, A. *et al.* The non-apoptotic action of Bcl-xL: regulating Ca2+ signaling and bioenergetics at the ER-mitochondrion interface. *J. Bioenerg. Biomembr.* **48**, 211–225 (2016).

388. Monaco, G. *et al.* The BH4 domain of anti-apoptotic Bcl-XL, but not that of the related Bcl-2, limits the voltage-dependent anion channel 1 (VDAC1)-mediated transfer of pro-apoptotic Ca^{2+} signals to mitochondria. *J. Biol. Chem.* **290**, 9150–9161 (2015).

389. Monaco, G. *et al.* Selective regulation of IP 3-receptor-mediated Ca 2+ signaling and apoptosis by the BH4 domain of Bcl-2 versus Bcl-Xl. *Cell Death Differ.* **19**, 295–309 (2012).

390. Chen, R. *et al.* Bcl-2 functionally interacts with inositol 1,4,5-trisphosphate receptors to regulate calcium release from the ER in response to inositol 1,4,5-trisphosphate. *J. Cell Biol.* **166**, 193–203 (2004).

391. Naon, D. *et al.* Critical reappraisal confirms that Mitofusin 2 is an endoplasmic reticulum–mitochondria tether. *PNAS* **113**, 11249–11254 (2016).

392. Vance, J. E. Phospholipid Synthesis and Transport in Mammalian Cells. *Traffic* **16**,

1–18 (2015).

393. Naon, D. & Scorrano, L. At the right distance: ER-mitochondria juxtaposition in cell life and death. *Biochim. Biophys. Acta - Mol. Cell Res.* **1843**, 2184–2194 (2014).

394. Stepanyants, N. *et al.* Cardiolipin's propensity for phase transition and its reorganization by dynamin-related protein 1 form a basis for mitochondrial membrane fission. *Mol. Biol. Cell* **26**, 3104–3116 (2015).

395. Kuwana, T. *et al.* Bid, Bax, and lipids cooperate to form supramolecular openings in the outer mitochondrial membrane. *Cell* **111**, 331–342 (2002).

396. Voss, C., Lahiri, S., Young, B. P., Loewen, C. J. & Prinz, W. A. ER-shaping proteins facilitate lipid exchange between the ER and mitochondria in S. cerevisiae. *J. Cell Sci.* **125**, 4791–4799 (2012).

397. Wang, Z., Jiang, H., Chen, S., Du, F. & Wang, X. The mitochondrial phosphatase PGAM5 functions at the convergence point of multiple necrotic death pathways. *Cell* **148**, 228–243 (2012).

398. Schuck, S., Gallagher, C. M. & Walter, P. ER-phagy mediates selective degradation of endoplasmic reticulum independently of the core autophagy machinery. *J. Cell Sci.* **127**, 4078–4088 (2014).

399. Forrester, A. *et al.* A selective ER-phagy exerts procollagen quality control via a Calnexin-FAM134B complex. *EMBO J.* **38**, 1–16 (2018).

APPENDIX

OPEN

Leukemia (2016), 1–9

www.nature.com/leu

ORIGINAL ARTICLE

High CIP2A levels correlate with an antiapoptotic phenotype that can be overcome by targeting BCL-X_L in chronic myeloid leukemia

CM Lucas[1], M Milani[1], M Butterworth[1], N Carmell[1], LJ Scott[1], RE Clark[1], GM Cohen[1,2] and S Varadarajan[1,2]

Cancerous inhibitor of protein phosphatase 2A (CIP2A) is a predictive biomarker of disease progression in many malignancies, including imatinib-treated chronic myeloid leukemia (CML). Although high CIP2A levels correlate with disease progression in CML, the underlying molecular mechanisms remain elusive. In a screen of diagnostic chronic phase samples from patients with high and low CIP2A protein levels, high CIP2A levels correlate with an antiapoptotic phenotype, characterized by downregulation of proapoptotic BCL-2 family members, including BIM, PUMA and HRK, and upregulation of the antiapoptotic protein BCL-X_L. These results suggest that the poor prognosis of patients with high CIP2A levels is due to an antiapoptotic phenotype. Disrupting this antiapoptotic phenotype by inhibition of BCL-X_L via RNA interference or A-1331852, a novel, potent and BCL-X_L-selective inhibitor, resulted in extensive apoptosis either alone or in combination with imatinib, dasatinib or nilotinib, both in cell lines and in primary $CD34^+$ cells from patients with high levels of CIP2A. These results demonstrate that BCL-X_L is the major antiapoptotic survival protein and may be a novel therapeutic target in CML.

Leukemia advance online publication, 18 March 2016; doi:10.1038/leu.2016.42

INTRODUCTION

Chronic myeloid leukemia (CML) is a malignant disease of a primitive hematopoietic cell, characterized by a reciprocal translocation between chromosomes 9 and 22 and creates the fusion gene *BCR-ABL1*, which is a deregulated tyrosine kinase that drives the leukemia.[1] CML treatment has been significantly improved by the tyrosine kinase inhibitor (TKI) imatinib, but some patients will eventually fail imatinib treatment and without a change in therapy, a significant proportion will progress towards blast crisis (BC), which is usually rapidly fatal.[2,3] The kinase activity of BCR-ABL is opposed by cellular phosphatases, such as protein phosphatase 2A (PP2A), which is impaired in several malignancies. PP2A plays an important role in regulating cell proliferation, differentiation and apoptosis. In CML, PP2A is inhibited by SET[4] and cancerous inhibitor of PP2A (CIP2A).[5] CIP2A inhibits PP2A activity and functions by preventing PP2A-driven dephosphorylation and stabilization of c-Myc.[6–8] CIP2A is a strong prospective predictor of subsequent development of BC in imatinib-treated CML patients,[5] although the underlying mechanisms remain unclear.

Apoptosis induction is tightly regulated by the BCL-2 family of proteins, which comprise several antiapoptotic members, such as BCL-2, BCL-X_L, MCL-1, BCL-w and BFL-1, together with proapoptotic molecules, such as the multidomain effectors BAX and BAK, as well as the BH3-only proteins, including the activators BIM, BID and PUMA, and sensitizers NOXA, HRK, BIK, BMF and BAD.[9,10] The BH3-only members can either be promiscuous or selective with respect to binding their antiapoptotic counterparts. The activators bind all antiapoptotic BCL-2 family members, whereas the sensitizers NOXA and HRK are more selective in binding MCL-1 and BCL-X_L, respectively.[11] BCR-ABL modulates the expression levels and/or the phosphorylation status of several BCL-2 family members, thus exerting important regulatory effects on apoptosis.[12–15] Furthermore, recent reports suggest important roles for several antiapoptotic BCL-2 family members in CML disease progression.[16–20] Elevated levels of these proteins in several cancers make them promising targets for drug therapy. Small-molecule inhibitors targeting specific members of the BCL-2 family, such as navitoclax/ABT-263 (BCL-2, BCL-X_L and BCL-w-specific) and venetoclax/ABT-199 (BCL-2-specific) are in clinical trials for several lymphoid malignancies.[21,22] Recently, selective inhibitors of BCL-X_L (A-1331852) and MCL-1 (A-1210477) have been synthesized.[23,24] These inhibitors target the antiapoptotic BCL-2 family members, displacing their sequestered proapoptotic counterparts, thereby resulting in apoptosis.

In this study, we demonstrate both a novel antiapoptotic role for CIP2A in CML pathogenesis and a key role for BCL-X_L in survival of CML cell lines and in primary $CD34^+$ cells from patients. These results raise the possibility that inhibition of BCL-X_L may be a novel therapeutic option in CML, especially in patients refractory to TKI therapy.

MATERIALS AND METHODS

Reagents and antibodies

Imatinib, nilotinib and dasatinib were from Selleck Chemicals (Houston, TX, USA). ABT-737, ABT-199, A-1331852 and A-1210477 were kindly provided by AbbVie (North Chicago, IL, USA). Antibodies against BIM, PUMA, BMF, BIK, BAD, BCL-X_L and BCL-w were from Cell Signaling Technology (Danvers, MA, USA), GAPDH and MCL-1 from Santa Cruz Biotechnology (Santa Cruz,

[1]Department of Molecular and Clinical Cancer Medicine, University of Liverpool, Liverpool, UK and [2]Department of Molecular and Clinical Pharmacology, University of Liverpool, Liverpool, UK. Correspondence: Dr S Varadarajan, Department of Molecular and Clinical Cancer Medicine, Institute of Translational Medicine, University of Liverpool, Sherrington Building, Ashton Street, Liverpool L69 3GE, UK.
E-mail: svar@liv.ac.uk
Received 28 August 2015; revised 10 February 2016; accepted 12 February 2016; accepted article preview online 29 February 2016

CA, USA), NOXA from Calbiochem (Darmstadt, Germany), BCL-2 from Dako (Ely, UK), BAX and BAK from Millipore (Watford, UK), HRK from Aviva Systems Biology (San Diego, CA, USA) and BID and BFL-1 were from Prof J Borst (The Netherlands Cancer Institute, Amsterdam, The Netherlands). All other reagents, unless mentioned otherwise, were from Sigma-Aldrich (St Louis, MO, USA).

Patient cohort

The study was approved by the Liverpool Central Research Ethics Committee; all 31 patients gave informed consent and were aged 18 or over. All have been seen since original diagnosis of chronic phase CML at our center and have been followed for at least 12 months (median follow-up: 39 months). Patients' characteristics are presented in Supplementary Table S1.

Sample collection, preparation and cell culture

At diagnosis, mononuclear cells from chronic phase CML patients were separated by density-dependent centrifugation (Lymphoprep Axis-Shield, Oslo, Norway), washed in RPMI 1640 (BioSera, Uckfield, UK) and resuspended in 10% dimethyl sulfoxide/10% fetal calf serum (BioSera)/ RPMI at 4 °C and cryopreserved in liquid nitrogen. Wherever possible, samples were enriched for $CD34^+$ cells using the CliniMACS kit (Miltenyi Biotec, Auburn, CA, USA). $CD34^+$ cells were cultured using StemSpan SFEMII media (Stemcell Technologies, Cambridge, UK). K562 and KCL22 cells were cultured in RPMI 1640 supplemented with 10% fetal calf serum and 5 mM L-glutamine.

BH3 profiling and flow cytometry

BH3 profiling was carried out using BH3 peptides from New England Peptide (Gardner, MA, USA) as previously described.[25] Loss of mitochondrial membrane potential and apoptosis were quantified by flow cytometry as described.[26] Patients with CIP2A levels $\geqslant 7.3$ mean fluorescence units by flow cytometry were defined as high CIP2A patients, as every patient that progressed to BC had CIP2A > 7.3 mean fluorescence units.[27] This cutoff value was derived using receiver operating characteristics (ROC) curve analysis for the prediction of BC based on the diagnostic CIP2A protein level; minimization of the Euclidian distance between the receiver operating characteristics curve and the corner (0, 1) was the criterion used. The optimal cutoff value produced an $AUC_{ROC} = 0.902$ (95% CI: 0.832, 0.973).

siRNA knockdowns, immunoprecipitation and western blotting

Cells were reverse-transfected with 10 nM of BAK (s1880 and s1881), BAX (s1888 and s1889), BIM (s195011), PUMA (pool of siRNAs), BMF (pool of siRNAs), BIK (s1989 and s1990), HRK (s194952), BCL-X_L (s1920), MCL-1 (s8583), BCL-w (s1924), BFL-1 (pool of siRNAs) from Life Technologies (Paisley, UK), BID (SI02654568), NOXA (SI00129430), BAD (SI00299348), BCL-2 (S100299411) from Qiagen (Manchester, UK) using Interferin

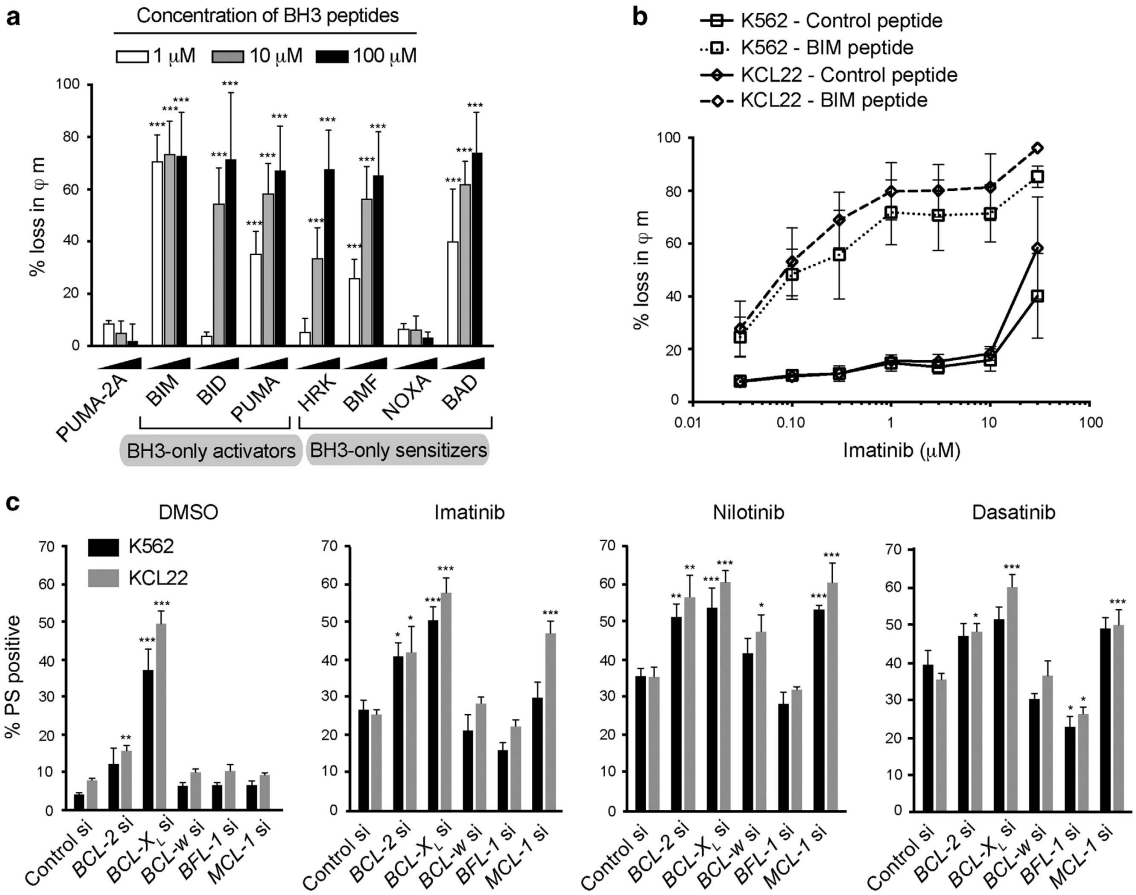

Figure 1. BH3 profiling and RNA interference implicate roles for BCL-2, BCL-X_L and MCL-1 in TKI-induced apoptosis. (**a**) BH3 profiling in K562 cells was carried out using the specified concentrations of different BH3 peptides for 2 h. PUMA-2A was used as the control peptide. (**b**) Dynamic BH3 profiling in K562 and KCL22 cells, exposed to increasing concentrations of imatinib for 16 h, was carried out using either control peptide (bold continuous lines) or BIM peptide (dotted lines) at 1 μM for 2 h. (**c**) K562 and KCL22 cells, reverse-transfected with the indicated siRNAs, were exposed for 48 h to dimethyl sulfoxide, imatinib (1 μM), nilotinib (50 nM) or dasatinib (3 nM) and apoptosis assessed by phosphatidylserine (PS) externalization. Statistical analysis was conducted using one-way analysis of variance applying the Welch correction and Dunnet's two-sided multiple comparison test to compare the different treatments to the appropriate control peptide/ siRNA (*$P \leqslant 0.05$, **$P \leqslant 0.01$, ***$P \leqslant 0.001$). Error bars represent standard error of mean (s.e.m.) from three independent experiments.

(Polyplus Transfection, NY, USA), according to the manufacturer's protocol and processed 48 h after transfection. Immunoprecipitation and western blotting were carried out according to the standard protocols.[26]

mRNA expression

Quantitative reverse transcription–PCR was performed using cDNA from total leukocytes. Pre-designed TaqMan real-time PCR assays were used for *BCL2L11* (Hs00708019_s1), *BCL2L1* (Hs00236329_m1), *BID* (Hs00609632_m1), *BBC3* (Hs00248075_m1), *HRK* (Hs02621354_s1) and *BAD* (Hs00188930_m1) and *GAPDH* (Hs99999905_m1) (Life Technologies). PCR was performed using a Stratagene MX3005P PCR machine (Agilent Technologies, Folsom, CA, USA). In evaluating the mRNA expression data, the comparative Ct method was used, with the $2^{-\Delta\Delta Ct}$ formula to achieve results for relative quantification. A pool of cDNA from four normal individuals was used as a calibrator and all samples were normalized to *GAPDH*.

Statistical analysis

Statistical analysis was conducted using one-way analysis of variance applying the Welch correction and Dunnet's two-sided multiple comparison test to compare the different treatments to the appropriate control peptide/siRNA (*$P \leqslant 0.05$, **$P \leqslant 0.01$, ***$P \leqslant 0.001$). For continuous variables, the Mann–Whitney *U*-test was used for comparisons between independent samples. For categorical variables, Fisher's exact test was used. Progression-free survival functions were estimated by the Kaplan–Meier estimator and the log-rank test was used for comparisons between groups. Statistical analysis was performed using GraphPad Prism (GraphPad Prism Software, Inc., La Jolla, CA, USA).

RESULTS

TKIs prime CML cell lines to undergo apoptosis

Since high levels of CIP2A contributed to imatinib resistance in CML, we wished to understand the role of BCL-2 family members in this resistance mechanism. Using BH3 profiling, a peptide-based technique to determine BCL-2 family dependencies,[25] we observed extensive loss of mitochondrial membrane potential (φ_m) in two CML cell lines, K562 and KCL22, following exposure to increasing concentrations of different BH3 peptides (Figure 1a and Supplementary Figure S1). Although all BH3-only activators exhibited extensive mitochondrial depolarization, BH3-only sensitizers demonstrated greater selectivity as demonstrated by a concentration-dependent loss in φ_m following BMF, BAD and HRK, but not NOXA (Figure 1a and Supplementary Figure S1). These results suggested that the survival of these cells depended more

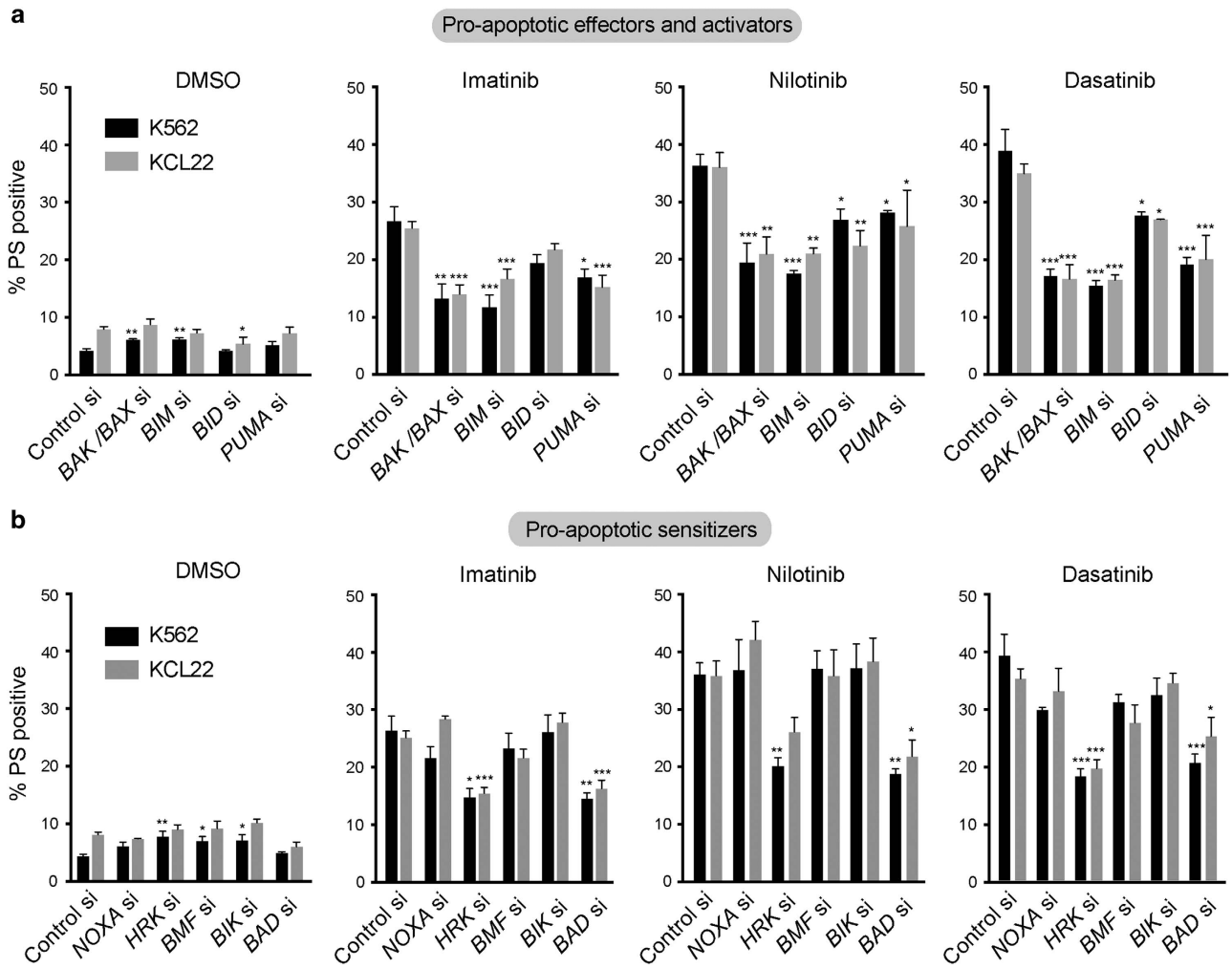

Figure 2. TKIs induce apoptosis in a BH3-dependent manner. (**a**, **b**) K562 and KCL22 cells, reverse-transfected with the indicated siRNAs, were exposed for 48 h to dimethyl sulfoxide, imatinib (1 μM), nilotinib (50 nM) and dasatinib (3 nM) and apoptosis assessed by phosphatidylserine (PS) externalization. Statistical analysis was conducted using one-way analysis of variance applying the Welch correction and Dunnet's two-sided multiple comparison test to compare the different siRNA transfections to their appropriate control siRNA in each treatment (*$P \leqslant 0.05$, **$P \leqslant 0.01$, ***$P \leqslant 0.001$). Error bars represent s.e.m. from three independent experiments.

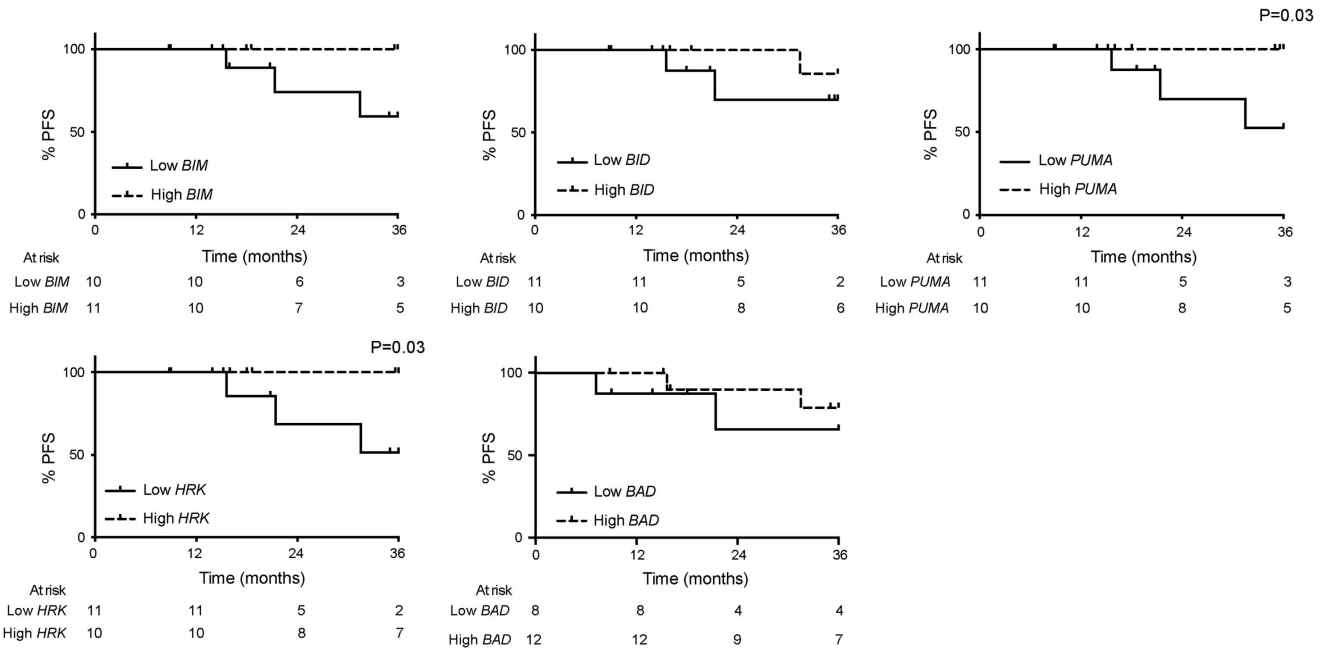

Figure 3. Expression levels of the proapoptotic BH3-only proteins correlate with progression-free survival in CML patients. Progression-free survival for patients treated with imatinib at initial diagnosis. PCR was performed using total leukocytes collected at initial diagnosis. Patients were stratified into high and low expression groups according to the median mRNA expression for *BIM, BID, PUMA, HRK* and *BAD* and the number of cases assessed presented below each graph. The log-rank test was used to determine the significance between high and low expressers.

on BCL-2, BCL-X_L and BCL-w, rather than on MCL-1 and BFL-1, as NOXA was the only sensitizer among the list to specifically target both MCL-1 and BFL-1 (Figure 1a and Supplementary Figure S1).[9–11] In dynamic BH3 profiling studies,[28] increasing concentrations of TKIs resulted in a significant loss of φ_m, only when the cells were subsequently exposed to the BIM peptide, suggesting that TKIs primed these cells to apoptosis and a combination therapy with another apoptotic stimuli could facilitate rapid apoptosis in these cells (Figure 1b and Supplementary Figure S2). Since our data implicated specific members of the BCL-2 family in antagonizing apoptosis, we performed RNA interference to silence the expression of different BCL-2 family members to study their effects on TKI-mediated apoptosis (Figure 1c). The concentrations of TKIs used in these studies were determined from their concentration–response curves (Supplementary Figure S3). Downregulation of BCL-X_L and to some extent BCL-2 resulted in apoptosis, suggesting that BCL-X_L is a critical survival factor in both CML cell lines (Figure 1c). Furthermore, downregulation of BCL-X_L, and to a lesser extent, BCL-2 and MCL-1, significantly potentiated TKI-mediated apoptosis in both K562 and KCL22 (Figure 1c), thus confirming an important role for antiapoptotic BCL-2 family members in TKI-mediated apoptosis.

TKIs induce apoptosis in a BH3-dependent manner

Exposure to TKIs caused a time-dependent decrease in the expression levels of most anti- and proapoptotic BCL-2 family members, with the notable exception of BAD, which was significantly upregulated (Supplementary Figure S4). To understand the relative contribution of different proapoptotic BCL-2 members in TKI-mediated apoptosis, we silenced the expression of BAX, BAK as well as BH3-only activators and sensitizers in K562 and KCL22 (Figure 2). Although all the proapoptotic effector and activator proteins were critical for TKI-mediated apoptosis, a selective dependence on HRK and BAD, but not NOXA, BMF or BIK was observed in TKI-mediated apoptosis (Figure 2 and

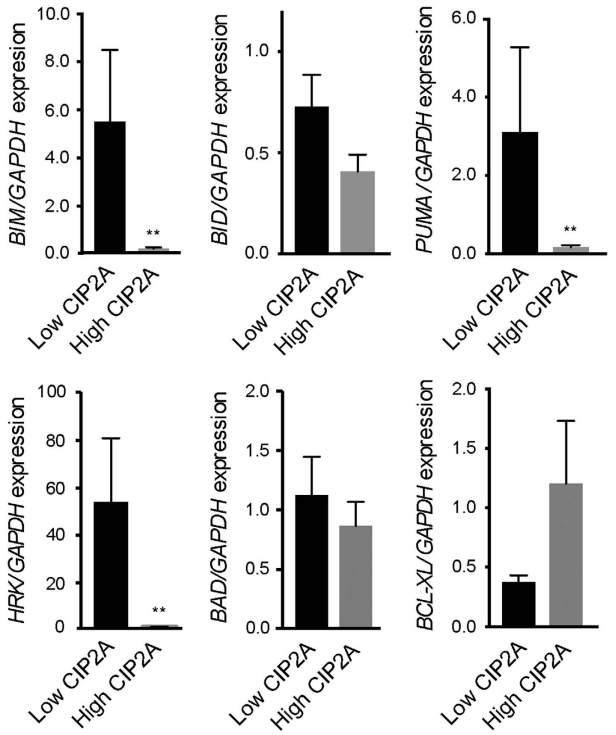

Figure 4. High CIP2A expression levels correlate with an antiapoptotic phenotype. mRNA expression for *BIM*, *BID, PUMA*, *HRK*, *BAD* and *BCL-X_L* in 31 newly diagnosed chronic phase CML patients stratified by their diagnostic CIP2A status. A pool of four normal healthy volunteers was used as a calibrator pool. Statistical analysis was conducted using a Mann–Whitney *U*-test comparing high and low CIP2A patients (**$P \leqslant 0.01$). Error bars represent s.e.m.

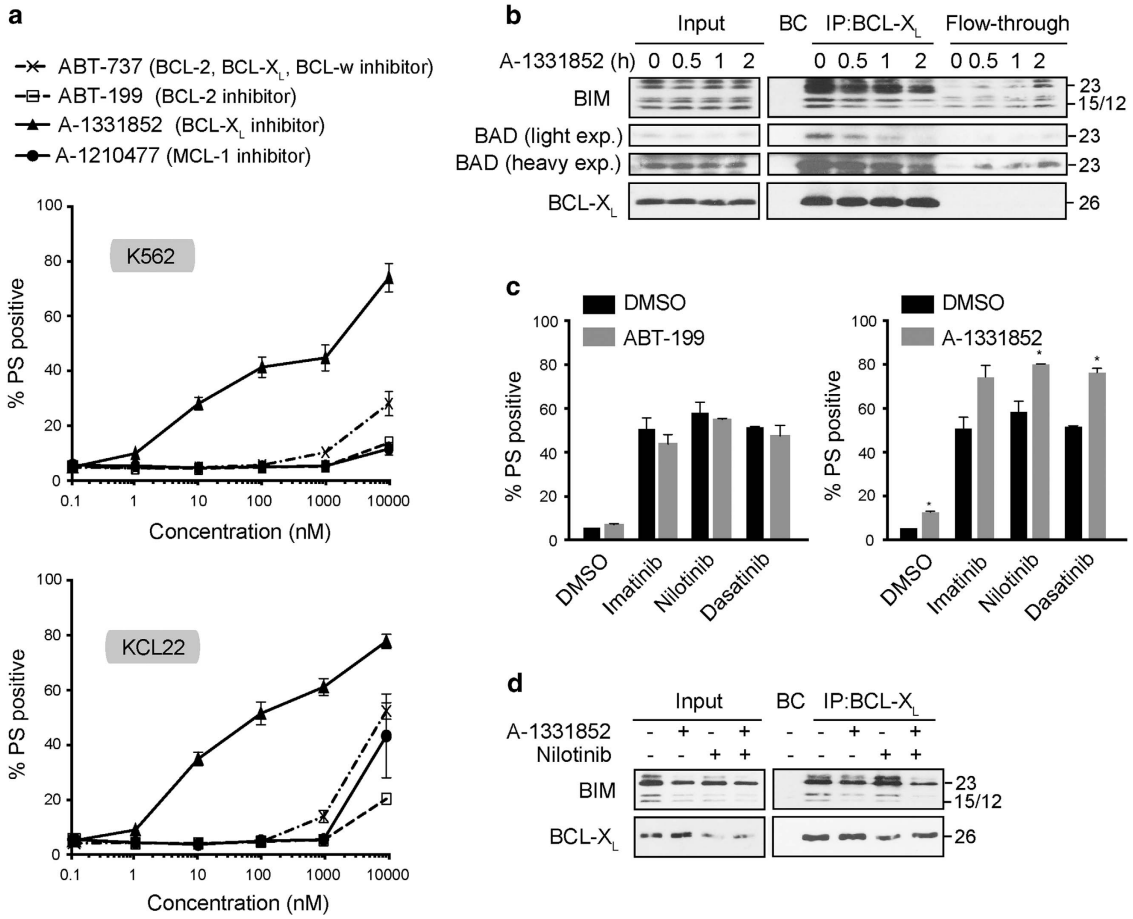

Figure 5. BCL-X_L is a critical survival factor and regulates TKI-induced apoptosis in CML cell lines. (**a**) K562 and KCL22 cells were exposed for 24 h to the specified inhibitors and apoptosis assessed by phosphatidylserine (PS) externalization. (**b**) Immunoprecipitation of BCL-X_L was carried out in K562 cells, exposed to A-1331852 (100 nM) for 0–2 h, and the eluted complexes were immunoblotted for the indicated proteins. The input cell lysates and the immunodepleted supernatant (labeled as Flow-through) were immunoblotted to check the efficiency of the immunoprecipitation. BC represents beads control. (**c**) K562 cells, exposed for 1 h to 1 nM of ABT-199 or A-1331852, were further exposed in the presence of the pretreated inhibitors to imatinib (1 μM), nilotinib (50 nM) or dasatinib (3 nM) for 24 h and apoptosis assessed. (**d**) Same as (**b**) but the immunoprecipitation was carried out with antibodies against BCL-X_L in K562 cells exposed to A-1331852 (1 nM) with or without nilotinib (50 nM) for 24 h. Statistical analysis was conducted using one-way analysis of variance applying the Welch correction and Dunnet's two-sided multiple comparison test to compare the TKI treatments with the combination treatments of A-1331852, represented by the black and gray histograms (*$P \leqslant 0.05$). Error bars represent s.e.m. from three independent experiments.

Supplementary Figure S4), thus implicating a regulatory role for several BH3-only members in TKI-induced apoptosis.

Downregulation of proapoptotic BCL-2 family proteins is associated with disease progression in imatinib-treated patients

To investigate a possible relationship between these BH3-only proteins and clinical outcome, we compared the mRNA expression levels of these proteins with progression-free survival of chronic phase CML patients, treated with imatinib at diagnosis (Figure 3). The median expression level for each gene was calculated and patients were stratified as high or low relative to the median. Low *BIM* expression was associated with an inferior progression-free survival, whereas *BID* or *BAD* expression did not correlate with clinical outcome (Figure 3). Low *PUMA* and *HRK* expression were significantly associated with disease progression to BC ($P = 0.03$; Figure 3). In this study, four patients progressed to BC and this disease progression was not associated with the presence of BCR-ABL kinase domain mutations. Low expression of *BIM, PUMA* and *HRK* was also associated with poor overall survival but this did not reach significance (data not shown). Moreover, 50% of patients with low *PUMA* or *HRK* expression at diagnosis had progressed by 36 months (Figure 3). In addition, low diagnostic levels of *BIM* and *HRK* were associated with a slower rate of deep molecular response (MR5) during the first three years of treatment (data not shown).

CIP2A levels correlate with the balance between pro- and antiapoptotic BCL-2 family proteins

Since CML disease progression correlates with high CIP2A levels,[5,29] as well as changes in expression levels of different BCL-2 family members (Figure 3), we speculated whether CIP2A levels could correlate with the expression levels of different BCL-2 family members. To investigate this possibility, we assessed mRNA expression for *BIM*, *BID, PUMA*, *HRK*, *BAD* and *BCL-X$_L$* in newly diagnosed chronic phase CML patients. Expression levels of *BIM*, *PUMA* and *HRK* were significantly lower in high compared with low CIP2A patients (Figure 4). A similar trend was observed for *BID* and *BAD* expression but this did not reach statistical significance (Figure 4). In contrast, patients with high CIP2A levels expressed high levels of *BCL-X$_L$*, although this did not reach statistical significance (Figure 4). Taken together these results suggest that CIP2A may exhibit its oncogenic activity by altering the balance of pro- and antiapoptotic proteins resulting in an antiapoptotic phenotype.

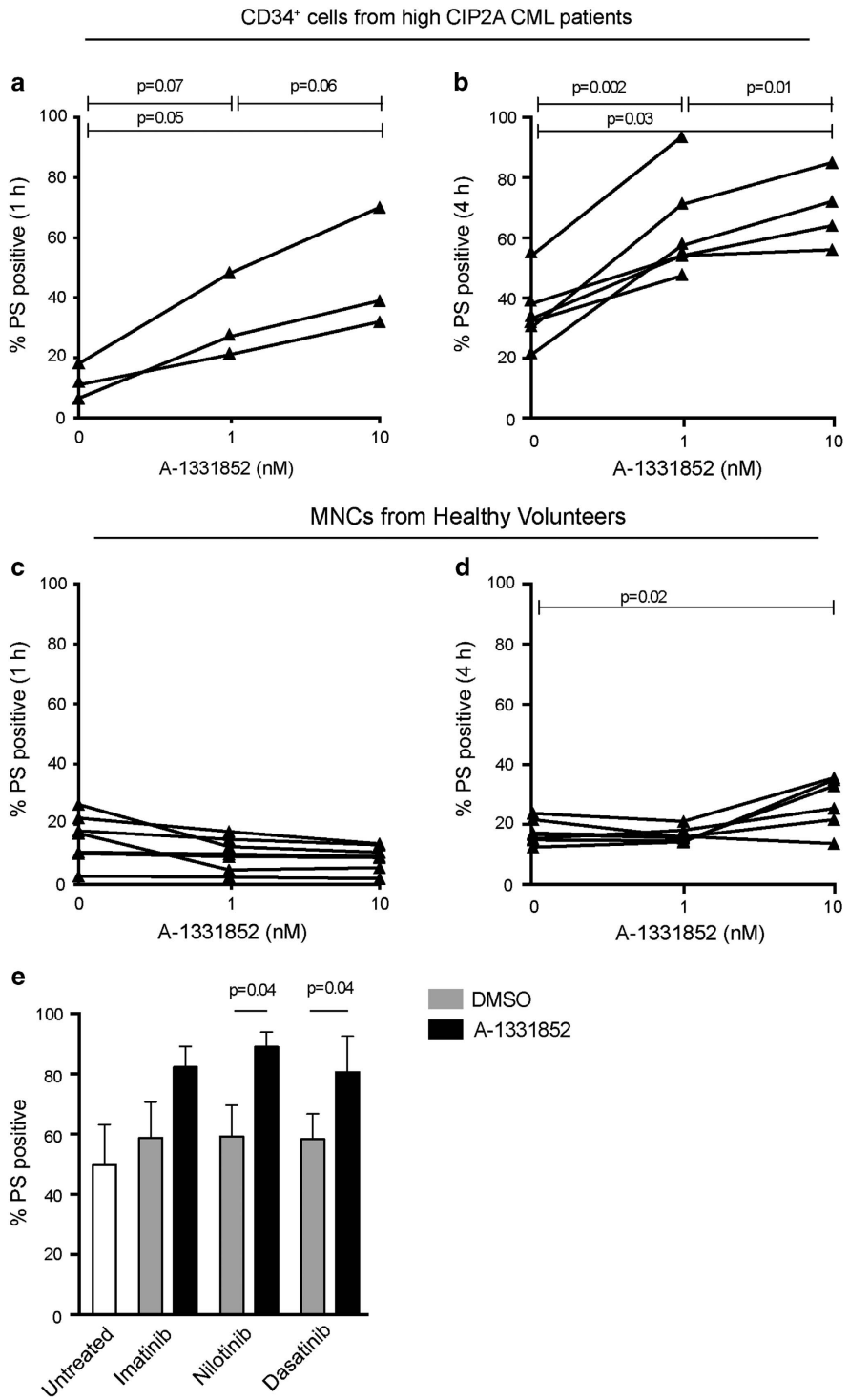

Figure 6. Inhibition of BCL-X_L promotes rapid apoptosis in primary CML cells. (**a**, **b**) Diagnostic chronic phase $CD34^+$ cells from high CIP2A patients were exposed to A-1331852 for 1 h ($n=3$) and 4 h ($n=5$) and apoptosis assessed. (**c**, **d**) Mononuclear cells (MNCs) from healthy volunteers were exposed to A-1331852 for 1 h ($n=8$) and 4 h ($n=6$) and apoptosis assessed. (**e**) Diagnostic chronic phase $CD34^+$ cells from high CIP2A patients were exposed to imatinib (5 μM), dasatinib (150 nM) and nilotinib (5 μM) for 24 h followed by the addition of A-1331852 (10 nM) to the cells for a further 1 h ($n=5$). Statistical analysis was conducted using a Mann–Whitney *U*-test and *P*-values specified, where significant. Error bars represent s.e.m.

BCL-X_L is a critical survival factor and antagonizes TKI-induced apoptosis in CML cell lines

Since our initial data identified BCL-X_L as a critical survival factor in CML cell lines, we used a toolkit of selective BCL-2 family inhibitors, comprising ABT-737 (BCL-2, BCL-X_L and BCL-w-specific inhibitor), ABT-199 (BCL-2-selective), A-1331852 (BCL-X_L-specific) and A-1210477 (MCL-1-selective) to further evaluate the role of BCL-X_L in CML cell survival. In both cell lines, A-1331852 was extremely potent, inducing apoptosis at low nanomolar concentrations, whereas the other inhibitors failed to induce apoptosis

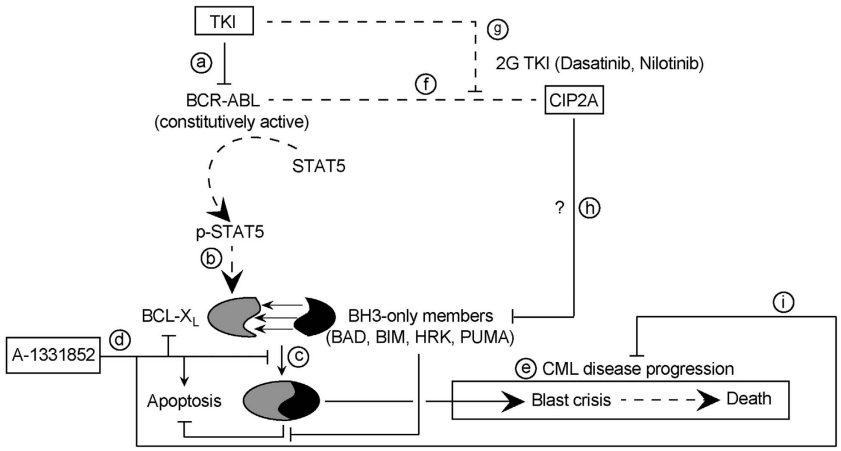

Figure 7. Selective inhibition of BCL-X_L overcomes CIP2A-mediated regulation of BCL-2 family members and disease progression in CML. The links that we have established/confirmed in this study are presented as bold lines whereas the dashed lines represent findings from literature. (a) The constitutively active kinase activity of BCR-ABL, antagonized by TKIs, results in phosphorylation of STAT5. (b) p-STAT5 induces the transcription of BCL-X_L. (c) BCL-X_L sequesters and inhibits BH3-only proteins. (d) This antiapoptotic activity is abolished by A-1331852. (e) Failure to achieve effective apoptosis results in disease progression. (f) High levels of CIP2A correlate with imatinib resistance in CML patients. (g) This can be overcome by second generation (2G) TKIs. (h) CIP2A expression levels correlate with an antiapoptotic phenotype characterized by changes in the balance between the pro- and antiapoptotic BCL-2 family members, thus conferring resistance to TKI therapy in CML. The precise mechanisms by which high CIP2A correlates with the antiapoptotic phenotype is unknown and hence marked with a '?' (i) Selective inhibition of BCL-X_L induces rapid apoptosis in CML cells, thus providing a novel and promising therapeutic option.

even at 100-fold higher concentrations (Figure 5a). A-1331852 was efficient in displacing both BIM and BAD from BCL-X_L and releasing them into the cytosol (Figure 5b). Furthermore, A-1331852, but not ABT-199, was efficacious in potentiating TKI-mediated apoptosis for 2G TKIs (Figure 5c). A combination of nilotinib and A-1331852 was more potent than either A-1331852 or nilotinib alone in displacing BIM from BCL-X_L (Figure 5d), further suggesting that A-1331852 can be effective in inducing apoptosis in CML cell lines, either as a single agent or in combination with TKIs.

A-1331852 exhibits remarkable potency both as a single agent and in combination with TKIs in killing primary CD34$^+$ CML cells

We next investigated the ability of A-1331852 to induce apoptosis in primary CD34$^+$ progenitor cells from high CIP2A patients. In agreement with our data in CML cell lines, A-1331852 displayed remarkable potency in inducing apoptosis in these cells at low nanomolar concentrations as early as 1 h post-treatment (Figure 6a). Prolonged exposure (4 h) resulted in improved potency as A-1331852 induced extensive apoptosis ($P = 0.002$) at concentrations as low as 1 nM in these cells (Figure 6b). Similar results were observed in CD34$^+$ progenitor cells from low CIP2A patients (Supplementary Figure S5). In contrast, mononuclear cells isolated from healthy volunteers generally remained insensitive to the treatment (Figures 6c and d). This is particularly significant as clinically achievable concentrations of imatinib (5 μM), nilotinib (5 μM) or dasatinib (150 nM) did not induce significant apoptosis in primary CD34$^+$ cells after 4 h exposure (data not shown). Even after 24 h exposure, none of these TKIs induced much if any apoptosis above the high spontaneous apoptosis observed in the progenitor cells (Figure 6e). However a subsequent and short exposure to A-1331852 (1 h) following the initial 24 h exposure to TKIs was sufficient to induce enhanced apoptosis in these CD34$^+$ cells ($P \leqslant 0.01$, Figure 6e). These data support the possibility of targeting BCL-X_L, as a novel and effective therapeutic strategy in CML (Figure 7).

DISCUSSION

High expression of CIP2A contributes to imatinib resistance in CML and is a strong prospective predictor of subsequent development of BC in imatinib-treated patients.[5] However the mechanism(s) by which CIP2A increases the risk of disease progression is poorly understood. In this study, we have identified several proapoptotic BCL-2 family members to be critical in TKI-mediated apoptosis (Figures 1 and 2). These findings also extended to CML patients, as decreased expression of specific proapoptotic BH3-only members *PUMA*, *HRK* and possibly *BIM* correlated with disease progression in CML patients (Figure 3). To our knowledge, this is the first study to link several proapoptotic BCL-2 family members to progression-free survival in imatinib-treated CML patients. We show that high CIP2A expression levels correspond to low expression of specific BH3-only proteins, *BIM*, *PUMA* and *HRK*, and an increase in the expression of *BCL-X$_L$* (Figure 4), highly characteristic of an antiapoptotic phenotype.

Recently, we have shown that administration of 2G TKIs, such as nilotinib and dasatinib, can overcome high CIP2A and prevent disease progression.[5,27] However, this is not without worrying side effects, as dasatinib has a 25% risk of pleural effusion within ~3 years and nilotinib therapy is associated with hyperglycemia in some patients and a dose-related (8–10%) risk of myocardial infarction, cerebrovascular event or peripheral arterial occlusive event by 6 years.[30,31] This necessitates research into possible alternate therapeutic strategies. In this study, using a BCL-X_L-specific inhibitor, A-1331852,[23] we demonstrate for the first time, an effective therapeutic option for CML patients with high CIP2A expression levels. A-1331852 displayed remarkable potency, both as a single agent and in combination with TKIs, to induce apoptosis in cell lines and in progenitor CD34$^+$ primary cells (Figures 5 and 6) demonstrating the critical importance of BCL-X_L in the survival of CML cells. Although BCL-X_L has been associated with disease progression,[12,19,32–34] this is the first study that demonstrates a novel antiapoptotic role for CIP2A in CML pathogenesis and how this can be overcome by selectively targeting BCL-X_L. This therapeutic option appears particularly promising because the CD34$^+$ progenitor cells were highly sensitive to nanomolar concentrations of A-1331852 but

insensitive to even prolonged exposure of the TKIs (Figure 6). This observation is in agreement with previous studies demonstrating a BCL-X_L dependence of stem cell survival for human embryonic stem cells as well as non-small-cell lung cancer cells.[35,36] Thus, targeting BCL-X_L potentially offers great therapeutic benefits in CML, especially due to the insensitivity of quiescent $CD34^+$ progenitor CML cells to imatinib, which is a major factor in the recurrence of the disease on discontinuation of therapy,[17,37] although it will be necessary to overcome potential toxicities, such as thrombocytopenia, associated with BCL-X_L inhibition.[22,38]

In summary, we clearly demonstrate that high CIP2A corresponds to an antiapoptotic phenotype, which may contribute to the poor prognosis of CML patients. We have also shown that this antiapoptotic phenotype can be overcome in CML by targeting BCL-X_L, thus identifying an effective therapeutic option for CML patients with high expression levels of CIP2A (Figure 7). As high CIP2A levels are also implicated in disease progression in acute myeloid leukemia, breast, bladder, cervical, colon, hepatocellular and lung cancer,[39–46] it will be of interest to ascertain if these tumors also exhibit an antiapoptotic phenotype. Targeting this antiapoptotic phenotype with selective BCL-2 family antagonists may offer novel therapeutic approaches to these malignancies.

CONFLICT OF INTEREST

REC has received research funding from Novartis, Bristol Myers Squibb and Pfizer and is a member of the speakers' bureau for Novartis. All authors report no conflict of interest.

ACKNOWLEDGEMENTS

We thank AbbVie for inhibitors, Prof. A Letai for expert guidance on BH3 profiling, Prof. J Borst for antibodies and Dr RJ Harris for support and advice. This work was supported by the NorthWest Cancer Research Grants CR994 (GMC) and CR1040 (SV and GMC).

REFERENCES

1 Ben-Neriah Y, Daley GQ, Mes-Masson AM, Witte ON, Baltimore D. The chronic myelogenous leukemia-specific P210 protein is the product of the bcr/abl hybrid gene. *Science* 1986; **233**: 212–214.
2 Lucas CM, Wang L, Austin GM, Knight K, Watmough SJ, Shwe KH *et al.* A population study of imatinib in chronic myeloid leukaemia demonstrates lower efficacy than in clinical trials. *Leukemia* 2008; **22**: 1963–1966.
3 de Lavallade H, Apperley JF, Khorashad JS, Milojkovic D, Reid AG, Bua M *et al.* Imatinib for newly diagnosed patients with chronic myeloid leukemia: incidence of sustained responses in an intention-to-treat analysis. *J Clin Oncol* 2008; **26**: 3358–3363.
4 Neviani P, Santhanam R, Trotta R, Notari M, Blaser BW, Liu S *et al.* The tumor suppressor PP2A is functionally inactivated in blast crisis CML through the inhibitory activity of the BCR/ABL-regulated SET protein. *Cancer Cell* 2005; **8**: 355–368.
5 Lucas CM, Harris RJ, Giannoudis A, Copland M, Slupsky JR, Clark RE. Cancerous inhibitor of PP2A (CIP2A) at diagnosis of chronic myeloid leukemia is a critical determinant of disease progression. *Blood* 2011; **117**: 6660–6668.
6 Junttila MR, Puustinen P, Niemelä M, Ahola R, Arnold H, Böttzauw T *et al.* CIP2A inhibits PP2A in human malignancies. *Cell* 2007; **130**: 51–62.
7 Khanna A, Böckelman C, Hemmes A, Junttila MR, Wiksten J-P, Lundin M *et al.* MYC-dependent regulation and prognostic role of CIP2A in gastric cancer. *J Natl Cancer Inst* 2009; **101**: 793–805.
8 Lucas CM, Harris RJ, Giannoudis A, Clark RE. c-Myc inhibition decreases CIP2A and reduces BCR-ABL1 tyrosine kinase activity in chronic myeloid leukemia. *Haematologica* 2015; **100**: e179–e182.
9 Kim H, Rafiuddin-Shah M, Tu H-C, Jeffers JR, Zambetti GP, Hsieh JJ-D *et al.* Hierarchical regulation of mitochondrion-dependent apoptosis by BCL-2 subfamilies. *Nat Cell Biol* 2006; **8**: 1348–1358.
10 Certo M, Del Gaizo Moore V, Nishino M, Wei G, Korsmeyer S, Armstrong SA *et al.* Mitochondria primed by death signals determine cellular addiction to antiapoptotic BCL-2 family members. *Cancer Cell* 2006; **9**: 351–365.
11 Ku B, Liang C, Jung JU, Oh B-H. Evidence that inhibition of BAX activation by BCL-2 involves its tight and preferential interaction with the BH3 domain of BAX. *Cell Res* 2011; **21**: 627–641.
12 de Groot RP, Raaijmakers JA, Lammers JW, Koenderman L. STAT5-dependent CyclinD1 and Bcl-xL expression in Bcr-Abl-transformed cells. *Mol Cell Biol Res Commun* 2000; **3**: 299–305.
13 Horita M, Andreu EJ, Benito A, Arbona C, Sanz C, Benet I *et al.* Blockade of the Bcr-Abl kinase activity induces apoptosis of chronic myelogenous leukemia cells by suppressing signal transducer and activator of transcription 5-dependent expression of Bcl-xL. *J Exp Med* 2000; **191**: 977–984.
14 Neshat MS, Raitano AB, Wang HG, Reed JC, Sawyers CL. The survival function of the Bcr-Abl oncogene is mediated by Bad-dependent and -independent pathways: roles for phosphatidylinositol 3-kinase and Raf. *Mol Cell Biol* 2000; **20**: 1179–1186.
15 Salomoni P, Condorelli F, Sweeney SM, Calabretta B. Versatility of BCR/ABL-expressing leukemic cells in circumventing proapoptotic BAD effects. *Blood* 2000; **96**: 676–684.
16 Korfi K, Mandal A, Furney SJ, Wiseman D, Somervaille TCP, Marais R. A personalised medicine approach for ponatinib-resistant chronic myeloid leukaemia. *Ann Oncol* 2015; **26**: 1180–1187.
17 Mak DH, Wang R-Y, Schober WD, Konopleva M, Cortes J, Kantarjian H *et al.* Activation of apoptosis signaling eliminates CD34+ progenitor cells in blast crisis CML independent of response to tyrosine kinase inhibitors. *Leukemia* 2012; **26**: 788–794.
18 Ko TK, Chuah CTH, Huang JWJ, Ng K-P, Ong ST. The BCL2 inhibitor ABT-199 significantly enhances imatinib-induced cell death in chronic myeloid leukemia progenitors. *Oncotarget* 2014; **5**: 9033–9038.
19 Harb JG, Neviani P, Chyla BJ, Ellis JJ, Ferenchak GJ, Oaks JJ *et al.* Bcl-xL anti-apoptotic network is dispensable for development and maintenance of CML but is required for disease progression where it represents a new therapeutic target. *Leukemia* 2013; **27**: 1996–2005.
20 Song T, Chai G, Liu Y, Xie M, Chen Q, Yu X *et al.* Mechanism of synergy of BH3 mimetics and paclitaxel in chronic myeloid leukemia cells: Mcl-1 inhibition. *Eur J Pharm Sci* 2015; **70**: 64–71.
21 Tse C, Shoemaker AR, Adickes J, Anderson MG, Chen J, Jin S *et al.* ABT-263: a potent and orally bioavailable Bcl-2 family inhibitor. *Cancer Res* 2008; **68**: 3421–3428.
22 Souers AJ, Leverson JD, Boghaert ER, Ackler SL, Catron ND, Chen J *et al.* ABT-199, a potent and selective BCL-2 inhibitor, achieves antitumor activity while sparing platelets. *Nat Med* 2013; **19**: 202–208.
23 Leverson JD, Phillips DC, Mitten MJ, Boghaert ER, Diaz D, Tahir SK *et al.* Exploiting selective BCL-2 family inhibitors to dissect cell survival dependencies and define improved strategies for cancer therapy. *Sci Transl Med* 2015; **7**: 279ra40.
24 Leverson JD, Zhang H, Chen J, Tahir SK, Phillips DC, Xue J *et al.* Potent and selective small-molecule MCL-1 inhibitors demonstrate on-target cancer cell killing activity as single agents and in combination with ABT-263 (navitoclax). *Cell Death Dis* 2015; **6**: e1590.
25 Ryan J, Letai A. BH3 profiling in whole cells by fluorimeter or FACS. *Methods* 2013; **61**: 156–164.
26 Vogler M, Butterworth M, Majid A, Walewska RJ, Sun X-M, Dyer MJS *et al.* Concurrent up-regulation of BCL-XL and BCL2A1 induces approximately 1000-fold resistance to ABT-737 in chronic lymphocytic leukemia. *Blood* 2009; **113**: 4403–4413.
27 Lucas CM, Harris RJ, Holcroft AK, Scott LJ, Carmell N, McDonald E *et al.* Second generation tyrosine kinase inhibitors prevent disease progression in high-risk (high CIP2A) chronic myeloid leukaemia patients. *Leukemia* 2015; **29**: 1514–1523.
28 Montero J, Sarosiek KA, DeAngelo JD, Maertens O, Ryan J, Ercan D *et al.* Drug-induced death signaling strategy rapidly predicts cancer response to chemotherapy. *Cell* 2015; **160**: 977–989.
29 Neelakantan P, Gerrard G, Lucas C, Milojkovic D, May P, Wang L *et al.* Combining BCR-ABL1 transcript levels at 3 and 6 months in chronic myeloid leukemia: implications for early intervention strategies. *Blood* 2013; **121**: 2739–2742.
30 O'Brien S, Hedgley C, Foroni L, Apperley J, Osborne W, Zwingers T *et al.* SPIRIT 2: an NCRI randomised study comparing dasatinib with imatinib in patients with newly diagnosed chronic myeloid leukaemia – 2 year follow up. *Accepted for the European Haematology Association Annual Meeting*: Vienna, June 2015 (oral presentation).
31 Hughes TP, Larson RA, Kim D-W, Issaragrisil S, le Coutre PD, Lobo C *et al.* Efficacy and safety of nilotinib (NIL) vs. imatinib (IM) in patients with newly diagnosed chronic myeloid leukaemia in chronic phase (CML-CP): 6-year follow-up of ENESTnd. *Accepted for the European Haematology Association Annual Meeting*: Vienna, Austria, June 2015 (poster presentation).
32 Gutiérrez-Castellanos S, Cruz M, Rabelo L, Godínez R, Reyes-Maldonado E, Riebeling-Navarro C. Differences in BCL-X(L) expression and STAT5

phosphorylation in chronic myeloid leukaemia patients. *Eur J Haematol* 2004; **72**: 231–238.
33 Bewry NN, Nair RR, Emmons MF, Boulware D, Pinilla-Ibarz J, Hazlehurst LA. Stat3 contributes to resistance toward BCR-ABL inhibitors in a bone marrow microenvironment model of drug resistance. *Mol Cancer Ther* 2008; **7**: 3169–3175.
34 Amarante-Mendes GP, McGahon AJ, Nishioka WK, Afar DE, Witte ON, Green DR. Bcl-2-independent Bcr-Abl-mediated resistance to apoptosis: protection is correlated with up regulation of Bcl-xL. *Oncogene* 1998; **16**: 1383–1390.
35 Bai H, Chen K, Gao Y-X, Arzigian M, Xie Y-L, Malcosky C *et al.* Bcl-xL enhances single-cell survival and expansion of human embryonic stem cells without affecting self-renewal. *Stem Cell Res* 2012; **8**: 26–37.
36 Zeuner A, Francescangeli F, Contavalli P, Zapparelli G, Apuzzo T, Eramo A *et al.* Elimination of quiescent/slow-proliferating cancer stem cells by Bcl-XL inhibition in non-small cell lung cancer. *Cell Death Differ* 2014; **21**: 1877–1888.
37 Corbin AS, Agarwal A, Loriaux M, Cortes J, Deininger MW, Druker BJ. Human chronic myeloid leukemia stem cells are insensitive to imatinib despite inhibition of BCR-ABL activity. *J Clin Invest* 2011; **121**: 396–409.
38 Vogler M, Hamali HA, Sun X-M, Bampton ETW, Dinsdale D, Snowden RT *et al.* BCL2/BCL-X(L) inhibition induces apoptosis, disrupts cellular calcium homeostasis, and prevents platelet activation. *Blood* 2011; **117**: 7145–7154.
39 Cristóbal I, Garcia-Orti L, Cirauqui C, Alonso MM, Calasanz MJ, Odero MD. PP2A impaired activity is a common event in acute myeloid leukemia and its activation by forskolin has a potent anti-leukemic effect. *Leukemia* 2011; **25**: 606–614.
40 Come C, Laine A, Chanrion M, Edgren H, Mattila E, Liu X *et al.* CIP2A is associated with human breast cancer aggressivity. *Clin Cancer Res* 2009; **15**: 5092–5100.
41 Huang LP, Adelson ME, Mordechai E, Trama JP. CIP2A expression is elevated in cervical cancer. *Cancer Biomark* 2010; **8**: 309–317.
42 Huang LP, Savoly D, Sidi AA, Adelson ME, Mordechai E, Trama JP. CIP2A protein expression in high-grade, high-stage bladder cancer. *Cancer Med* 2012; **1**: 76–81.
43 Teng H-W, Yang S-H, Lin J-K, Chen W-S, Lin T-C, Jiang J-K *et al.* CIP2A is a predictor of poor prognosis in colon cancer. *J Gastrointest Surg* 2012; **16**: 1037–1047.
44 He H, Wu G, Li W, Cao Y, Liu Y. CIP2A is highly expressed in hepatocellular carcinoma and predicts poor prognosis. *Diagn Mol Pathol* 2012; **21**: 143–149.
45 Dong Q-Z, Wang Y, Dong X-J, Li Z-X, Tang Z-P, Cui Q-Z *et al.* CIP2A is overexpressed in non-small cell lung cancer and correlates with poor prognosis. *Ann Surg Oncol* 2011; **18**: 857–865.
46 De P, Carlson J, Leyland-Jones B, Dey N. Oncogenic nexus of cancerous inhibitor of protein phosphatase 2A (CIP2A): an oncoprotein with many hands. *Oncotarget* 2014; **5**: 4581–4602.

Supplementary Information accompanies this paper on the Leukemia website (http://www.nature.com/leu)

OPEN

Citation: Cell Death and Disease (2017) 8, e2552; doi:10.1038/cddis.2016.485
Official journal of the Cell Death Differentiation Association

www.nature.com/cddis

DRP-1 is required for BH3 mimetic-mediated mitochondrial fragmentation and apoptosis

Mateus Milani[1,4], Dominic P Byrne[2,4], Georgia Greaves[1], Michael Butterworth[1], Gerald M Cohen[1,3], Patrick A Eyers*[,2] and Shankar Varadarajan*[,1,3]

The concept of using BH3 mimetics as anticancer agents has been substantiated by the efficacy of selective drugs, such as Navitoclax and Venetoclax, in treating BCL-2-dependent haematological malignancies. However, most solid tumours depend on MCL-1 for survival, which is highly amplified in multiple cancers and a major factor determining chemoresistance. Most MCL-1 inhibitors that have been generated so far, while demonstrating early promise *in vitro*, fail to exhibit specificity and potency in a cellular context. To address the lack of standardised assays for benchmarking the *in vitro* binding of putative inhibitors before analysis of their cellular effects, we developed a rapid differential scanning fluorimetry (DSF)-based assay, and used it to screen a panel of BH3 mimetics. We next contrasted their binding signatures with their ability to induce apoptosis in a MCL-1 dependent cell line. Of all the MCL-1 inhibitors tested, only A-1210477 induced rapid, concentration-dependent apoptosis, which strongly correlated with a thermal protective effect on MCL-1 in the DSF assay. In cells that depend on both MCL-1 and BCL-X_L, A-1210477 exhibited marked synergy with A-1331852, a BCL-X_L specific inhibitor, to induce cell death. Despite this selectivity and potency, A-1210477 induced profound structural changes in the mitochondrial network in several cell lines that were not phenocopied following MCL-1 RNA interference or transcriptional repression, suggesting that A-1210477 induces mitochondrial fragmentation in an MCL-1-independent manner. However, A-1210477-induced mitochondrial fragmentation was dependent upon DRP-1, and silencing expression levels of DRP-1 diminished not just mitochondrial fragmentation but also BH3 mimetic-mediated apoptosis. These findings provide new insights into MCL-1 ligands, and the interplay between DRP-1 and the anti-apoptotic BCL-2 family members in the regulation of apoptosis.

Cell Death and Disease (2017) **8,** e2552; doi:10.1038/cddis.2016.485; published online 12 January 2017

Targeting the diverse anti-apoptotic BCL-2 family of proteins offers substantial promise for cancer treatment and has the potential to be valuable in overcoming tumour recurrence and chemoresistance. In particular, the BCL-2 selective inhibitor, ABT-199 (Venetoclax) and ABT-263 (Navitoclax), which also targets BCL-2, BCL-X_L and BCL-w, have been employed successfully for treating haematological malignancies.[1–3] However, these inhibitors are ineffective in treating solid tumours, whose survival often depends on the overexpression of the anti-apoptotic protein MCL-1. MCL-1 is one of the most widely expressed pathologic factors in human cancers,[4] and many putative MCL-1 inhibitors have been synthesised, several of which have demonstrated selectivity in different types of *in vitro* assays.[5–13]

Inhibitors of the BCL-2 family of proteins, widely referred to as BH3 mimetics, elicit their pro-apoptotic roles by activating BAX and or BAK, which perturbs mitochondrial integrity resulting in the release of cytochrome *c* and caspase activation.[14] The putative inhibitors of MCL-1 evaluated in the current study have all been designed to function as BH3 mimetics, and a variety of analytical data from different *in vitro* studies has demonstrated their ability to target MCL-1.[5–13] However, the lack of a single benchmarked binding assay to evaluate compound binding and reproducibility has hindered compound comparisons, with most assays relying upon fluorescence polarisation, which is subject to signal-to-noise artefacts and potential interference from the compounds. Indeed, many described MCL-1 inhibitors have failed to enter clinical trials, potentially due to a lack of specificity and potency.

In this study, we purified recombinant human MCL-1 from bacteria and developed a rapid, simple differential scanning fluorimetry (DSF) assay, which we exploit to screen a broad panel of BH3 mimetics. Using a thermostability protocol, we validate A-1210477 as a potent and selective MCL-1 ligand *in vitro*. We corroborate our DSF assay in a series of cellular experiments, showing that A-1210477 induces rapid apoptosis in an MCL-1-dependent cell line. Furthermore, we observe rapid and extensive mitochondrial fission following A-1210477 that occurs in a DRP-1-dependent manner. Finally, we

[1]Department of Molecular and Clinical Cancer Medicine, Institute of Translational Medicine, University of Liverpool, Ashton Street, Liverpool L69 3GE, UK; [2]Department of Biochemistry, Institute of Integrative Biology, University of Liverpool, Crown Street, Liverpool L69 7ZB, UK and [3]Department of Molecular and Clinical Pharmacology, Institute of Translational Medicine, University of Liverpool, Liverpool, Ashton Street, Liverpool L69 3GE, UK
*Corresponding author: PA Eyers, Department of Biochemistry, Institute of Integrative Biology, University of Liverpool, Crown Street, Liverpool L69 3ZB, UK.
Tel:/Fax: 44-151-7954465; E-mail: patrick.eyers@liverpool.ac.uk
or S Varadarajan, Department of Molecular and Clinical Cancer Medicine, Institute of Translational Medicine, University of Liverpool, Ashton Street, Liverpool L69 3GE, UK.
Tel: 44-151-7949576; Fax: 44-151-7065826; E-mail: svar@liv.ac.uk
[4]These authors contributed equally to this work.
Received 06.12.16; accepted 16.12.16; Edited by G Raschella'

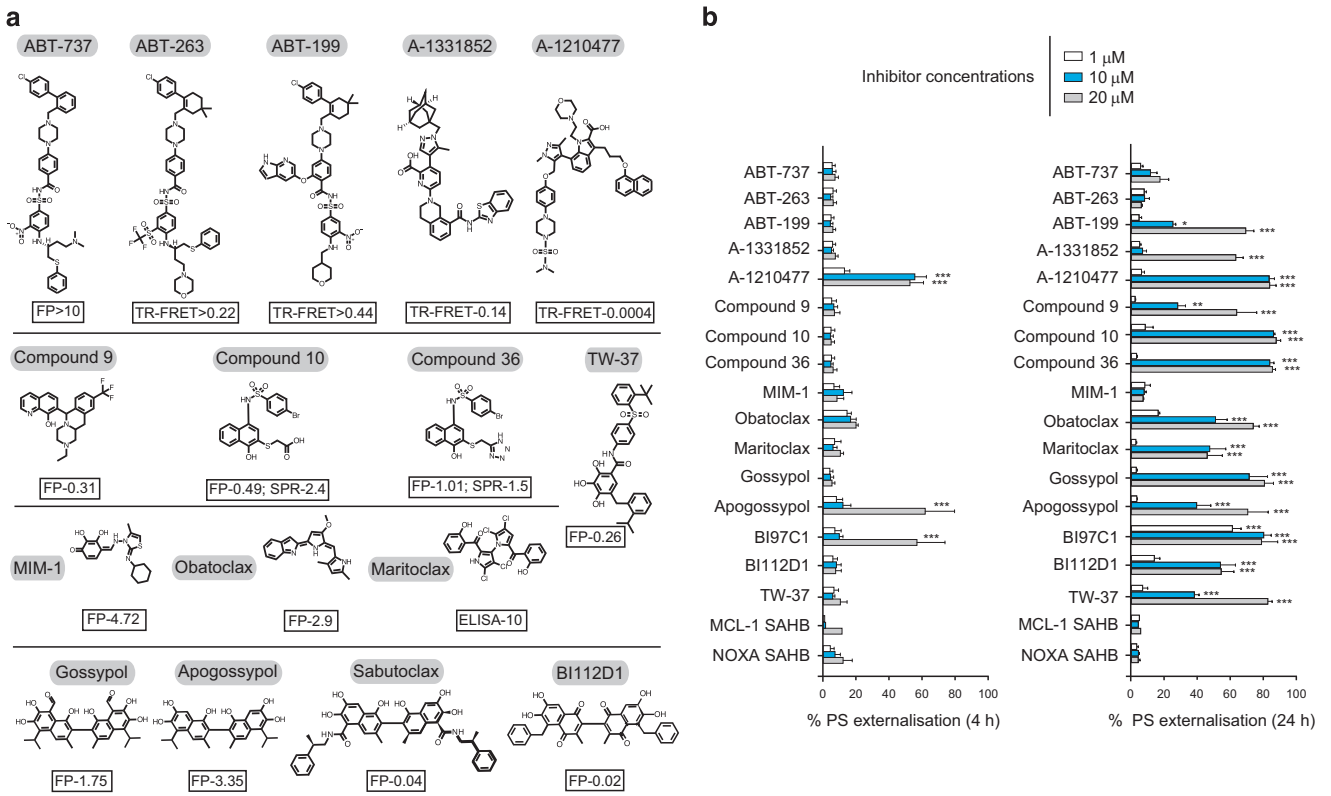

Figure 1 Reported *in vitro* binding constants of MCL-1 inhibitors correlate poorly with the ability to induce apoptosis in a cellular context. (**a**) Chemical structures of reported BH3 mimetics used in this study along with literature binding affinities (μM), assessed by fluorescence polarisation (FP), surface plasmon resonance (SPR) or time-resolved fluorescence resonance energy transfer (TR-FRET). (**b**) Analysis of concentration-dependent effects of MCL-1 inhibitors on cellular apoptosis, assessed by the extent of phosphatidylserine (PS) externalisation following 4 and 24 h of exposure in MCL-1 addicted H929 cells. Statistical analysis was conducted using one-way ANOVA and *P*-values depicted as ***$P \leqslant 0.001$. Results are shown as the mean $\pm$ S.E.M. (standard error of the mean) from at least three independent experiments

characterise roles for DRP-1 in A-1210477-mediated mitochondrial fragmentation as well as in BH3 mimetic-mediated apoptosis. Thus, our report identifies A-1210477 as a bona fide MCL-1 inhibitor that not only facilitates apoptosis but also grossly perturbs mitochondrial membrane dynamics.

Results

Most described MCL-1 inhibitors fail to potently induce apoptosis in a MCL-1 dependent cell line. The literature contains numerous examples of small molecule MCL-1 inhibitors that exhibit a wide range of reported binding affinities for MCL-1 (Figure 1). These have been calculated using a variety of *in vitro* approaches, including fluorescence polarisation (FP), surface plasmon resonance (SPR), ELISA and time-resolved fluorescence resonance energy transfer (TR-FRET; Figure 1). The first selective inhibitors of the BCL-2 family of proteins, ABT-737 and its orally available analogue, ABT-263 (Navitoclax) target BCL-2, BCL-X_L and BCL-w, but not MCL-1, at low nanomolar concentrations.[1] These compounds have been followed by ABT-199 (Venetoclax), A-1331852 and A-1210477, which, respectively, target BCL-2, BCL-X_L and MCL-1.[2,5,15] The MCL-1 ligand 'Compound 9' was generated as a result of a HTS strategy coupled to direct hit optimisation,[6] while MIM-1 was identified by a stapled peptide-based competitive screen.[7] A series of 3-substituted-N-(4-Hydroxynaphthalen-1-yl) arylsulphonamides, including compounds 10 and 36, have been reported to bind and inhibit MCL-1.[8] Obatoclax mesylate is a pan-BCL-2 inhibitor with reported specificity for MCL-1.[9] Maritoclax (marinopyrrole A1) is a natural product that directly binds MCL-1 and targets it for proteasomal degradation.[10] Removal of the toxic aldehyde groups in the naturally occurring polyphenol, gossypol, resulted in apogossypol, which upon further substitution yielded BI97C1 (Sabutoclax) and BI112D1, both of which are claimed to target all members of the BCL-2 family.[11,12] TW-37 is a benzenesulphonyl derivative of gossypol reported to bind to MCL-1 with a higher affinity than BCL-2 or BCL-X_L (Figure 1a).[13]

To investigate whether these compounds induce cellular apoptosis by inhibiting MCL-1, we exposed MCL-1-addicted H929 cells to this broad panel of putative inhibitors (Figure 1a) and assessed the extent of apoptosis induction. Also included in our panel as negative controls were ABT-737, ABT-263, ABT-199 and A-1331852, which were assessed alongside the stabilised alpha-helix of BCL-2 domains (SAHBs), which were designed to mimic the BH3 binding helix of MCL-1 and NOXA, respectively.[16] Remarkably, only A-1210477 induced extensive concentration-dependent apoptosis in H929 cells following a brief (4 h) exposure (Figure 1b). Both apogossypol and

BI97C1 (Sabutoclax) induced apoptosis at high micromolar concentrations, whereas all other inhibitors failed to exhibit any enhanced apoptosis (Figure 1b). In contrast, a prolonged exposure (24 h) to several compounds, including ABT-199, A-1331852, Obatoclax, Maritoclax, gossypol derivatives and compounds 9, 10 and 36, resulted in a marked increase in cell death (Figure 1b), suggesting that they function through an indirect or off-target effect.

Design and validation of a new assay to evaluate MCL-1 compound binding. Since *in vitro* binding assays for these drugs were carried out using different assays under distinct experimental conditions, it is impossible to correlate discrepancies between reported *in vitro* binding affinities (Figure 1a) and quantified cellular effects (Figure 1b) without introducing some form of standardisation. To overcome this technical challenge, we developed and validated a new *in vitro* assay that enabled us to compare, under identical experimental conditions, the relative effects of putative MCL-1 inhibitors. DSF is a biophysical method that can be used in a thermostability assay (TSA) workflow to monitor shifts in unfolding parameters as a measure of ligand binding affinity.[17–22] We initially isolated a recombinant truncated version of human MCL-1 (amino acids 172-329, corresponding to the BH1-3 domains) as well as a R263A mutant to serve as negative control, as the conserved arginine at position 263 of MCL-1 is critical for ligand and substrate binding in all BCL-2 family members (Figures 2a and b).[23] Both wild-type (WT) and R263A MCL-1 exhibited similar folded secondary structure profiles (assessed by circular dichroism) and thermal unfolding profiles (assessed by DSF; Figures 2c and d), although R263A MCL-1 (Tm ~66 °C) was slightly less stable than WT MCL-1 (Tm ~67.5 °C). To validate whether recombinant MCL-1 proteins were functionally relevant for screening putative MCL-1 inhibitors, we assessed the ability of different synthetic BH3 peptides to bind WT and R263A MCL-1. As expected, the MCL-1 specific synthetic peptide, MS-1, and a peptide corresponding to the BH3 domain of BIM, were both very efficient MCL-1 binding partners, with temperature shifts of ~10 °C recorded at equimolar peptide and MCL-1 protein concentration. In contrast, PUMA and NOXA peptides showed more modest MCL-1 binding signals, even at high concentrations (Figure 2e). Under identical conditions, no detectable MCL-1 binding was observed for BAD (which binds specifically to BCL-2, BCL-X_L and BCL-w but not MCL-1), HRK (BCL-X_L-specific) and PUMA-2A (a negative control) synthetic peptides (Figure 2e). These results were entirely consistent with the extent of mitochondrial depolarisation induced by these peptides in a cellular BH3 profiling assay using H929 cells (compare Figures 2e and f). Furthermore, none of the BH3 peptides bound/stabilised the R263A mutated MCL-1 protein (Figure 2g), validating the importance of this highly conserved basic residue for peptide binding, and creating a powerful dual recombinant protein screening system for further mechanistic analysis of MCL-1 ligands.

DSF identifies A-1210477 as a MCL-1 specific inhibitor. Next, we next used DSF to screen 18 compounds that have been reported to be MCL-1 inhibitors, concluding that A-1210477 elicited the most marked thermal shift (ΔT_m value of 6–8 °C), in contrast to the weak thermal shifts observed with other inhibitors of <2 °C, which is within the cut-off for a weak or nonspecific binding event, as defined for ligand binding to protein kinases and bromodomains.[22] MCL-1 SAHB was the next-best inducer of MCL-1 stabilisation, exhibiting a thermal shift of ~4 °C at a concentration of 10 μM (Figure 3a). Interestingly, the BCL-X_L ligand A-1331852 consistently destabilised MCL-1 protein at concentrations of 10 μM and above (Figure 3a). This effect was specific to MCL-1 protein, and did not occur with any other proteins tested. However, destabilisation also occurred with MCL-1 R263A, suggesting a nonspecific interaction elsewhere on the MCL-1 protein (data not shown). In contrast, MCL-1 thermal shifts with A-1210477 and MCL-1 SAHB were both concentration-dependent and completely abolished in MCL-1 R263A (Figure 3b and c). Finally, we directly measured the affinity of the interaction between MCL-1 and A-1210477 using Microscale Thermophoresis (MST), which confirmed a sub-micromolar K_d value of ~740 nM (Figure 3d). Taken together, these data strongly suggest that A-1210477 is a bona fide MCL-1 inhibitor in a cellular context (Figure 1b) and represents the most potent MCL-1 ligand evaluated using our thermal shift assay, with concentration-dependent ΔT_m values suggestive of high-affinity (nM) binding, corroborated by MST analysis.[24–26]

A-1210477 synergises with a BCL-X_L inhibitor to induce the intrinsic apoptotic pathway. Next, we wished to confirm whether A-1210477 could synergise with distinct BH3 mimetics to induce apoptosis in cells that depend on another BCL-2 family member, in addition to MCL-1. Individual exposure of H1299 cells, which depend on both MCL-1 and BCL-X_L for survival,[27,28] to either A-1210477 or A-1331852 (a specific BCL-X_L inhibitor) had little effect on apoptosis, whereas a combination of the two compounds resulted in a marked induction of apoptosis (Figure 4a). This was accompanied by a concomitant loss of the mitochondrial membrane potential, activation and oligomerisation of BAK and release of mitochondrial cytochrome *c* (Figures 4b–f).

A-1210477 induces DRP-1-mediated mitochondrial fission. The exposure of H1299 cells to A-1210477 resulted in a highly fragmented mitochondrial network, whereas the cells exposed to A-1331852 retained normal mitochondrial structure (Figure 4f). A-1210477-mediated mitochondrial fragmentation was observed in multiple cancer cell lines (Figure 5a) but these mitochondrial changes did not result in apoptosis (data not shown). Interestingly, neither genetic MCL-1 silencing (RNA interference) nor transcriptional MCL-1 repression (using the CDK inhibitor dinaciclib) phenocopied A-1210477-mediated mitochondrial fragmentation (Figure 5b), strongly suggesting that these effects occurred in a MCL-1-independent manner. As the length and continuity of the filamentous mitochondrial network is regulated by specific fission and fusion proteins, we speculated that A-1210477 may alter expression levels of mitochondrial fission and/or fusion GTPases. However, A-1210477-mediated mitochondrial fragmentation was not accompanied by a loss of fusion proteins, such as MFN1 or MFN2 and/or enhanced OPA1 proteolysis (Figure 5c), almost

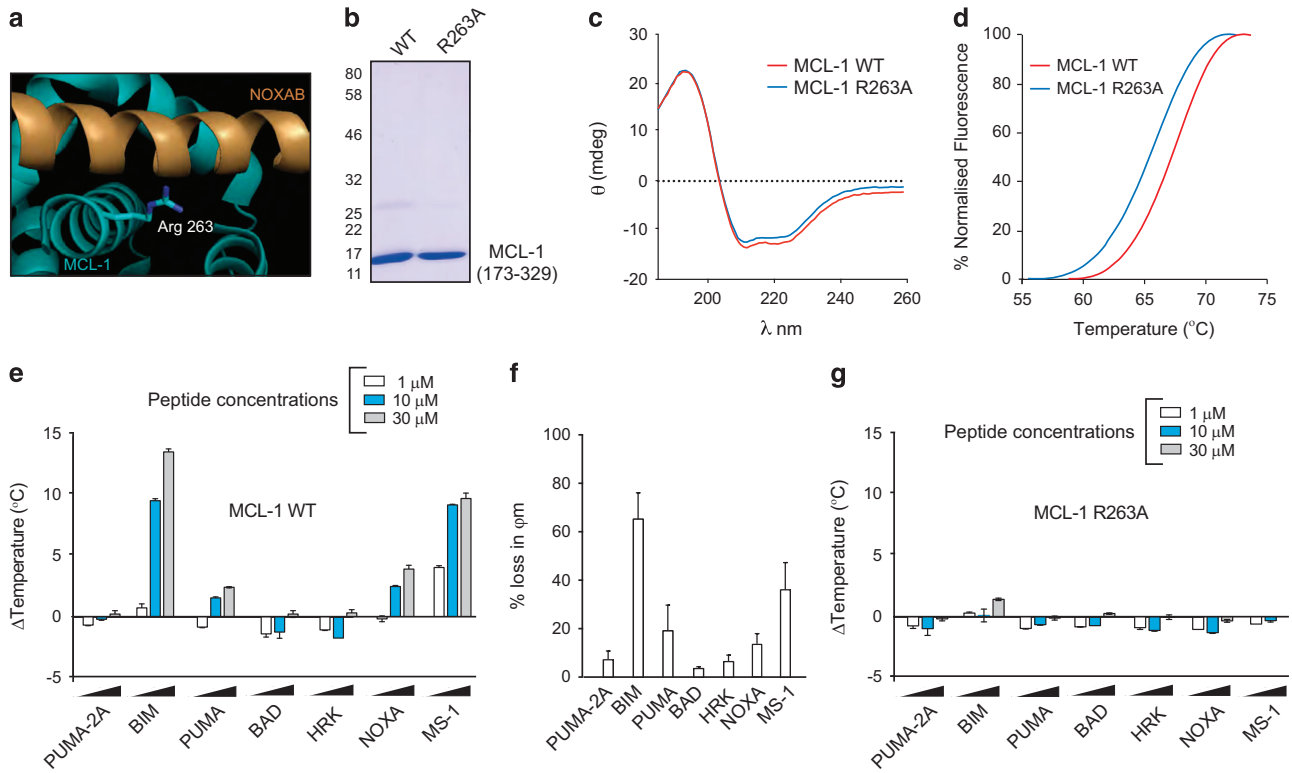

Figure 2 Analysis of purified recombinant WT and R263A MCL-1 (E173-R329) proteins. (**a**) Modelled binding mode of NOXAB peptide engaged with MCL-1 BH3 domain (PDB: 2JM6) with the critical Arg 263 side-chain highlighted. (**b**) SDS-PAGE and Coomassie blue staining of gel filtered, purified recombinant WT and R263A MCL-1 (2 μg) proteins. (**c**) Circular dichroism spectra showing similar secondary structures of WT (red) and R263A (blue) MCL-1 (E173-R329) proteins. (**d**) TSA comparing thermal denaturation (unfolding) profiles for WT (red) and R263A (blue) MCL-1 (E173-R329) proteins. (**e**) Validation of a MCL-1 TSA using synthetic BH3 peptides, demonstrating concentration-dependent binding, characterised by a positive shift of change in the unfolding temperature (ΔTemperature). (**f**) BH3 profiling in H929 cells reveals an enhanced loss in mitochondrial membrane potential (φm) following exposure to BIM, PUMA, NOXA and MS-1 peptides, consistent with their ability to bind to MCL-1. (**g**) ΔTemperature (ΔT_m) values for R263A MCL-1 confirms little, or no, detectable binding of MCL-1 to the indicated synthetic peptides. Mean ΔT_m values ± S.D. ($n=2$) were calculated by subtracting the control T_m value (buffer, no peptide) from the measured T_m value. The TSA graphs are plotted as duplicate data points (0.3 °C separation per point) and are representative of a single experiment performed in duplicate, which was repeated at least three times

certainly excluding a fusion defect. In contrast, inactivation of the fission protein, DRP-1 using either a siRNA or a dominant-negative DRP-1 mutant (K38A) efficiently reduced mitochondrial fragmentation following A-1210477 exposure (Figure 5d), confirming the absolute requirement of DRP-1 in A-1210477-mediated mitochondrial fission.

DRP-1-is required for BH3 mimetic-mediated apoptosis. Although A-1210477-mediated mitochondrial fragmentation did not directly result in apoptosis, it remained possible that such major structural alterations could sensitise cells to apoptosis. Interestingly, downregulation of DRP-1 not only prevented mitochondrial fragmentation but also markedly reduced the extent of apoptosis, following exposure to the combination of A-1210477 and A-1331852 (Figures 6a–c). Silencing the dual expression of BCL-X_L and MCL-1 resulted in extensive apoptosis (Figure 6d), independent of any mitochondrial fragmentation (data not shown). DRP-1 deficiency also diminished apoptosis in these cells (Figure 6d) suggesting that the protective effect of DRP-1 siRNA was independent of mitochondrial fragmentation, and occurred most likely due to its known effects on mitochondrial outer membrane permeabilisation (MOMP; Figure 6e).[29] Taken together, these results strongly suggested that DRP-1 was required both for BH3 mimetic-induced mitochondrial fragmentation as well as apoptosis.

Discussion

Several promising small molecule inhibitors reported to target MCL-1 *in vitro* have been largely ineffective in a cellular context.[27] The failure to convert a 'high-affinity' (often reported as nM) *in vitro* MCL-1 binding affinity into an enhanced apoptosis phenotype in a physiological context might be partly due to the lack of accessibility of the drugs at sites of action, thus rendering it more difficult to treat solid tumours than circulating B cells in lymphoid malignancies. Alternatively, high expression levels of additional BCL-2 family members in solid tumours could result in functional target redundancy, raising the prospects of a requirement for pan-BCL-2 family inhibition as a therapeutic strategy. With the exception of A-1210477, most of the other putative MCL-1 inhibitors tested here induced cell death in a MCL-1-dependent cell line only after prolonged cellular exposure (Figure 1b). This is in stark contrast to the rapid and extensive apoptosis observed with

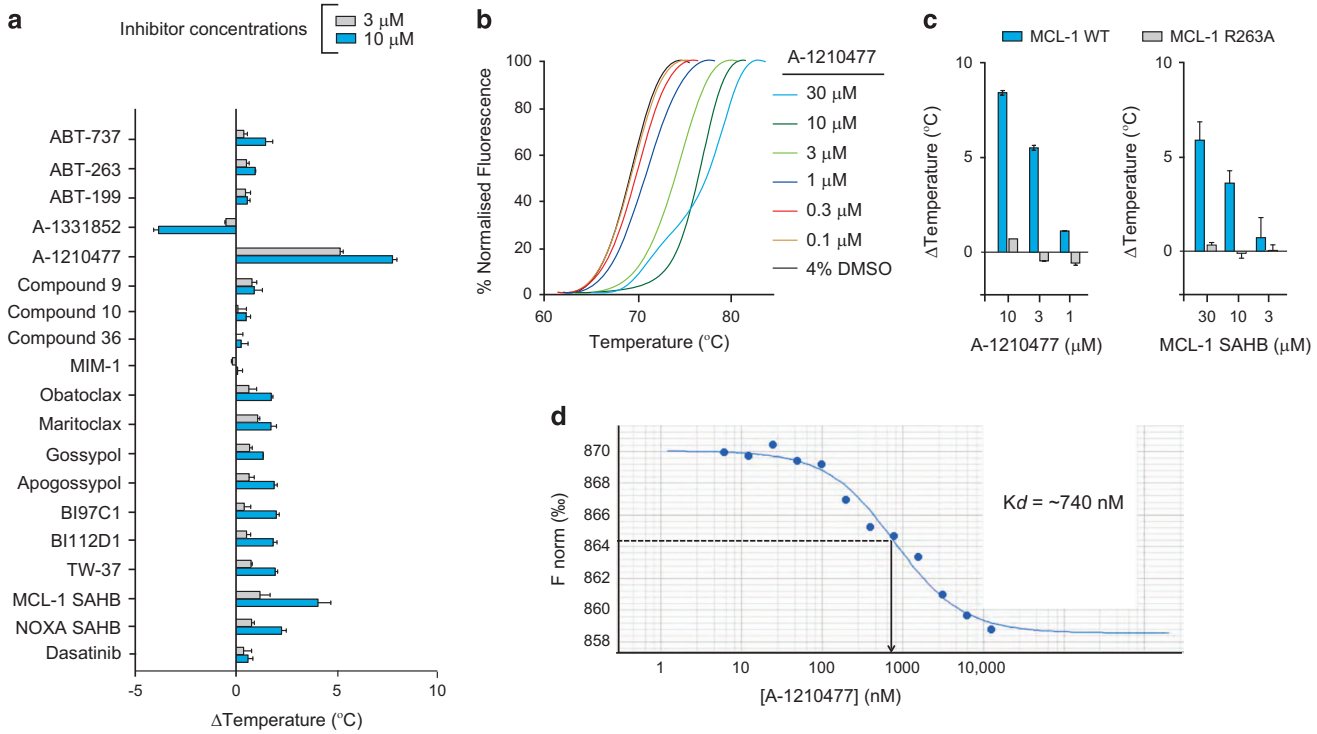

Figure 3 Inhibitor screening using differential scanning fluorimetry (DSF) reveals that A-1210477, but not other BH3 mimetics, exhibit marked MCL-1 binding and thermal stabilisation. (**a**) MCL-1 TSA screen of BH3 mimetics evaluated in the study reveals marked stabilisation of MCL-1 by A-1210477 and MCL-1 SAHB. In contrast, A-1331852 exhibits a negative perturbation (destabilisation) in thermal stability, possibly suggesting either nonspecific binding or an unusual binding mode to MCL-1. (**b**) A-1210477 exhibits a concentration-dependent increase in MCL-1 stabilisation. (**c**) A-1210477 and MCL-1 SAHB exhibit concentration-dependent binding to WT but not R263A MCL-1. (**d**) MCL-1 protein (173–329) was covalently labelled with the fluorescent red dye NT-647 and binding to A-1210477 analysed using microscale thermophoresis. The TSA graphs are plotted as duplicate data points (0.3 °C separation per point) and are representative of a single experiment performed in duplicate, which was repeated at least three times

other potent clinical BH3 mimetics, such as ABT-263 and ABT-199.[2,27,30] Indeed, the induction of cell death at these later times might be attributed to either other indirect measures of downregulating MCL-1 (such as transcriptional or translational repression and NOXA upregulation) or other off-target effects associated with these inhibitors.[27,31]

In this study, we developed a novel DSF approach to evaluate the effects of a panel of putative MCL-1 inhibitory ligands, characterising A-1210477 as the only compound in our panel that bound MCL-1 in a R263-dependent manner and induced concentration-dependent apoptosis (Figures 1–3). Although MCL-1 SAHB also bound MCL-1 rather specifically (Figure 3), it was inefficient in inducing apoptosis in a cellular context, either due to weak target engagement or weak cell permeability. In contrast to most other putative inhibitors tested, A-1210477 also readily perturbed the thermal-induced unfolding of MCL-1 at concentrations consistent with high-affinity binding to MCL-1 (Figure 3), providing strong support for the exploitation of this assay for the identification and benchmarking of other MCL-1 ligands. We believe that this simple and rapid method could readily be exploited to compare and contrast both potency and mechanistic aspects of compound binding for MCL-1, circumventing issues associated with data comparison and poor reliability demonstrated for more complex fluorescence assays (most of which involve FRET or FP).

Indeed, there is now an urgent need for specific and potent small molecule inhibitors of MCL-1 that efficiently target cancer cells while sparing physiological cellular functions of MCL-1. While this manuscript was in preparation, a new single-digit nanomolar MCL-1 inhibitor, S63845, which induces rapid apoptosis in MCL-1-dependent cells, was reported.[32] It will be interesting to assess whether S63845 exhibits mitochondrial structural changes similar to those observed with A-1210477. Nonetheless, of all the compounds tested in the current study, only A-1210477 was prominent in terms of MCL-1 binding in DSF assay and rapid induction of apoptosis in cellular assays. However, A-1210477 still requires micromolar concentrations in a cellular context to exert apoptotic effects, and is predicted to lack the potency for *in vivo* efficacy, where nanomolar compounds are likely to be a prerequisite. The discovery of high-affinity compounds such as S63845 that reportedly possess this higher cellular efficacy in tumour models might help alleviate this issue in the clinic.

Materials and Methods

Cell culture. The H929 cells from ECACC (Salisbury, UK), H23 and H1299 cells from ATCC (Middlesex, UK) were cultured in RPMI 1640 medium supplemented with 10% fetal calf serum (FCS) from Life Technologies, Inc., (Paisley, UK). HeLa and MCF7 from ATCC were cultured in DMEM medium supplemented with 10% FCS (all from Life Technologies, Inc.).

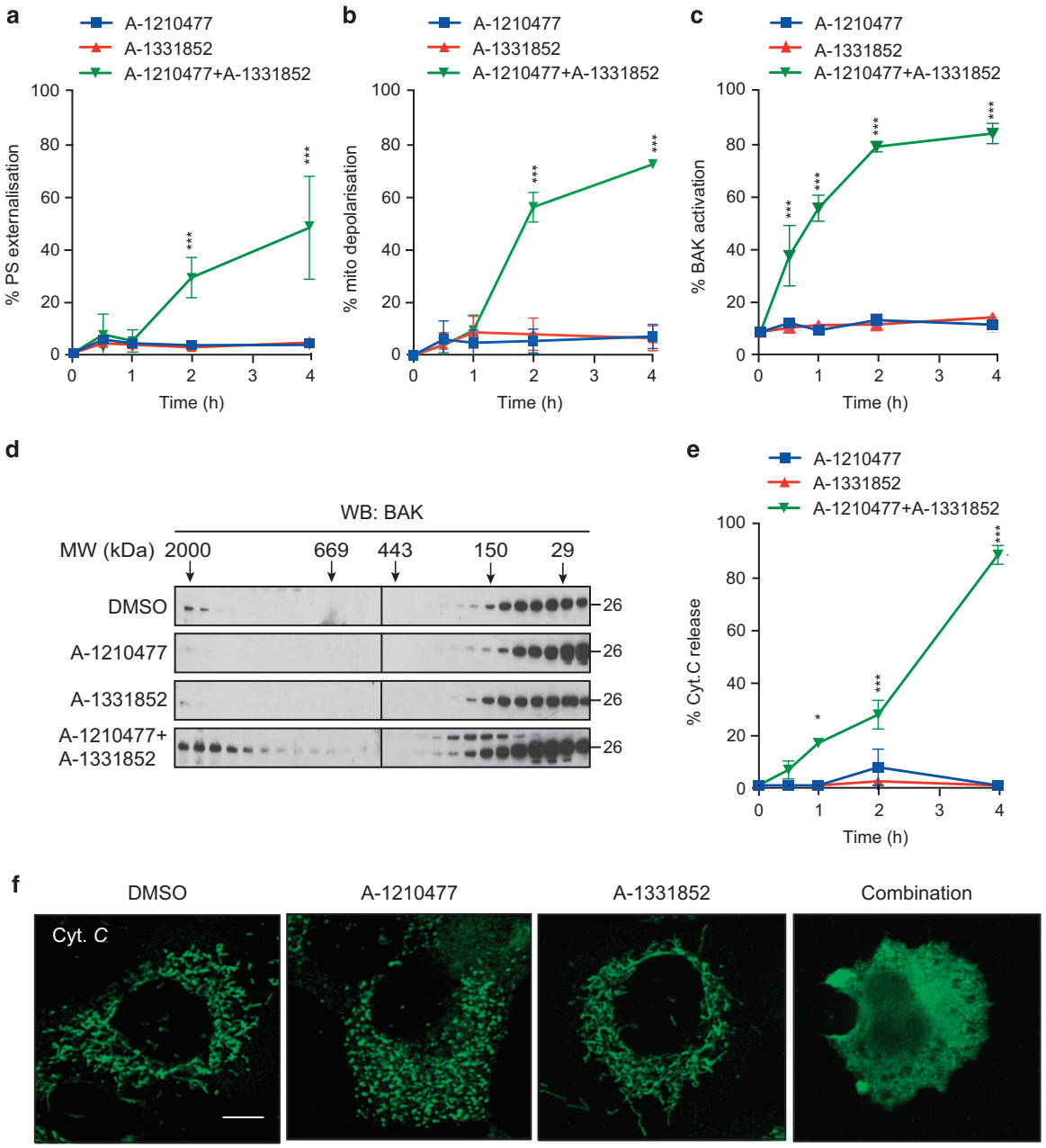

Figure 4 Inhibition of both BCL-X_L and MCL-1 is required to release mitochondrial cytochrome *c* in H1299 cells. (**a**) H1299 cells were exposed to A-1210477 (10 μM), A-1331852 (100 nM) or both compounds. Only the combined treatment lead to a time-dependent increase in apoptosis, as assessed by (**a**) PS externalisation, (**b**) mitochondrial depolarisation, (**c**) BAK activation, (**d**) BAK oligomerisation and (**e** and **f**) mitochondrial cytochrome *c* release. For cytochrome *c* release, the cells were immunostained with cytochrome *c* antibody (scale bar, 10 μm) and ~100 cells for each treatment in three independent experiments were quantified for the loss of mitochondrial cytochrome *c*. Statistical analysis was conducted using one-way ANOVA and *P*-values depicted as $^*P \leqslant 0.05$ and $^{***}P \leqslant 0.001$

BCL-2 family inhibitors. ABT-737, ABT-263, ABT-199, A-1331852 and A-1210477 were kindly provided by AbbVie Inc. (North Chicago, IL, USA). Compounds 10, 20, 21, 22, 36, 37 and 41 were provided by Dr. Z Nikolovska-Coleska (University of Michigan, Ann Arbor, MI, USA).[8] Compound 9 was custom-synthesised and purchased from Molport (Riga, Latvia).[6] MIM-1 and the stapled peptides against MCL-1 and NOXA were kindly provided by Dr. L Walensky (Dana-Farber Cancer Institute, Boston, MA, USA).[7,16] Maritoclax was provided by Professor H-G Wang (Pennsylvania State University College of Medicine, Hershey, PA, USA).[10] Apogossypol, Sabutoclax and BI112D1 were provided by Professor M. Pellecchia (Sanford-Burnham Institute, La Jolla, CA, USA).[11,12] Gossypol, Obatoclax and TW-37 were obtained from Selleck Chemicals Co. (Houston, TX, USA).

Reagents and plasmids. Peptides for BIM (MRPEIWIAQELRRIGDEFNA), BID (EDIIRNIARHLAQVGDSMDRY), NOXA (AELPPEFAAQ LRKIGDKVYC), PUMA (EQWAREIGAQLRRMADDLNA), HRK (WSSAAQLTAARLKALGDE LHQ), MS-1 (RPEIWMTQGLRRLGDEINAYYAR), BAD (LWAAQRYGRELRRMSDEFEGSFKGL) and PUMA-2 A (EQWAREIGAQARRMAADLNA) were from New England Peptide (Gardner, MA, USA) or GenScript (Piscataway, NJ, USA). Antibodies against MCL-1, BAK and GAPDH from Santa Cruz Biotechnology (Santa Cruz, CA, USA); OPA1, DRP-1, HSP60 and Cytochrome *C* from BD Biosciences (Oxford, UK); Tubulin, MFN1, MFN2, Caspase-3, MCL-1 (RC-13) from Abcam (Cambridge, UK); BAK (Ab-1) from Merck Chemicals Ltd (Nottingham, UK) were used. For bacterial expression of recombinant proteins, a human MCL-1 dsDNA corresponding to

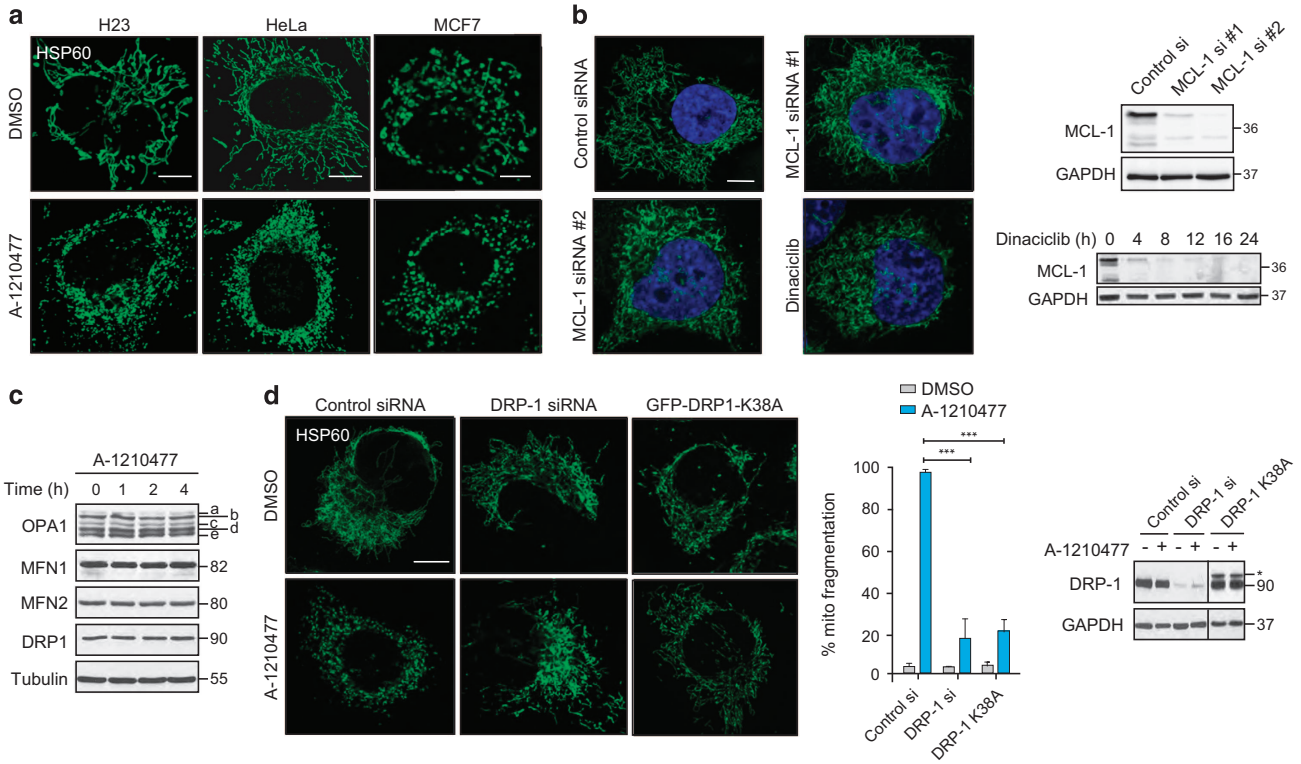

Figure 5 A-1210477 induces extensive mitochondrial fragmentation in a DRP-1-dependent manner. (**a**) H23, HeLa and MCF7 cells exposed to A-1210477 (10 μM) for 2 h resulted in extensive mitochondrial fragmentation, as assessed by immunostaining with HSP60 antibody (scale bar, 10 μm). (**b**) H1299 cells were either transfected with control siRNA, two different MCL-1 siRNAs for 72 h or exposed to Dinacilib (30 nM) for 4 h and assessed for mitochondrial integrity by immunostaining with HSP60 antibody (scale bar, 10 μm). The blots show knockdown efficiency of MCL-1 siRNAs and downregulation of MCL-1 by Dinaciclib. (**c**) Western blot of H1299 cells exposed to A-1210477 (10 μM) for the indicated times revealed no major changes in total expression levels of mitochondrial fission or fusion proteins. Tubulin was used as a loading control. (**d**) H1299 cells were either transfected with control siRNA, DRP-1 siRNA or GFP-DRP-1 K38A plasmid, then exposed to A-1210477 (10 μM) for 2 h and the decrease in the extent of mitochondrial fragmentation was quantified by assessing ~ 100 cells from each treatment in three independent experiments (scale bar, 10 μm). Statistical analysis was conducted using one-way ANOVA (***$P \leqslant 0.001$). The blots show the knockdown efficiency of DRP-1 siRNA and the overexpression of GFP-DRP-1 K38A (denoted by*)

amino acids E173- R329 was amplified using the primer sets, 5′-AAGTTCTG TTTCAGGGCCCGGAGTTGTACCGGCAGTCG-3′ and 5′-ATGGTCTAGAAAGCTTT ACCTGATGCCACCTTCTAGGTC-3′ and cloned into pOPIN F (OPPF-UK, Oxford, UK) to generate N-terminally His6-tag fusion protein. This was used as a template to generate the R263A mutant using site-directed mutagenesis with the primer sets, 5′-CGTAACAAACTGGGGCGCGATTGTGACTCTC-3′ and 5′-GAGAGTCACAATCG CGCCCCAGTTTGTTACG-3′. GFP-DRP-1 K38A plasmid was described previously.[33] All other reagents, unless mentioned otherwise, were from Sigma-Aldrich Co. (St. Louis, MO, USA).

Protein purification. WT MCL-1 fusion protein (N-terminal His6-tag fused to amino acids Glu173-Arg329, containing the BH3, BH1 and BH2 domains) and an R263A substitution in the WGRIV motif found in the MCL-1 BH1 domain were produced in BL21 (DE3) pLysS *E. coli* cells (Novagen, Nottingham, UK), induced with 0.4 mM IPTG for 18 h at 18 °C and purified by immobilised metal affinity chromatography (IMAC) using Ni-NTA agarose (Qiagen, Manchester, UK) and size exclusion chromatography using a HiLoad 16/600 Superdex 200 column (GE Healthcare, Chicago, IL, USA), equilibrated in 50 mM Tris HCl, pH 7.4, 100 mM NaCl, 10 % (v/v) glycerol and 1 mM DTT. Secondary structure compositions of WT and R263A MCL-1 proteins (0.9 mg/ml) were analysed by circular dichroism in the far UV range (180–260 nm) using a Jasco 1100 CD spectrometer with a path length of 0.1 cm, following buffer exchange into 10 mM sodium phosphate (pH 7.4) and 25 mM NaF.

DSF assays. Thermal shift assays (TSA) were performed using a StepOnePlus Real-Time PCR machine (Life Technologies, Paisley, UK) using Sypro-Orange dye (Invitrogen, Paisley, UK). Thermal ramping (0.3 °C per min between 25 and 94 °C) was used to generate thermal denaturation curves for purified MCL-1 proteins (10 μM) in the presence or absence of the indicated concentrations of ligand (final DMSO concentration 4% v/v). Data were processed using the Boltzmann equation to generate sigmoidal denaturation curves, and average $T_m/\Delta T_m$ values calculated as previously described,[26] using GraphPad Prism software.

Microscale thermophoresis. MCL-1 protein (173–329) was covalently labelled with the fluorescent red dye NT-647, which reacts with primary amines present on MCL-1 Lys residues to form a stable dye–protein conjugate before analysis. The concentration of MCL-1 was kept constant in the assay and the concentration of the unlabelled A-1210477 ligand diluted in buffer was varied between 6 nM and 200 μM. The assay was performed after loading into capilliaries 25 mM HEPES, pH 7.4 containing 0.05% Tween-20. MST analysis was performed using the Monolith NT.115 instrument and data were plotted using Monolith software.

BH3 profiling and flow cytometry. BH3 profiling was carried out as previously described.[34] In brief, the cells were permeabilised with digitonin (0.002 %) in DTEB buffer (10 mM HEPES, 135 mM Trehalose, 20 μM EDTA, 20 μM EGTA, 5 mM succinic acid, 0.1 % BSA, 50 mM potassium chloride, pH 7.5) containing oligomycin (10 μg/ml) and incubated for 2 h with varying concentrations of BH3 peptides. The loss of mitochondrial membrane potential (φm) was measured by observing the loss of TMRE (200 nM) using an Attune NxT flow cytometer (ThermoFisher Scientific, Paisley, UK). The extent of apoptosis in cells following different treatments was quantified by FACS following staining of the cells with Annexin V-FITC and propidium iodide to measure phosphatidylserine externalisation, as previously described.[33] For monitoring BAK activation, the cells pre-treated

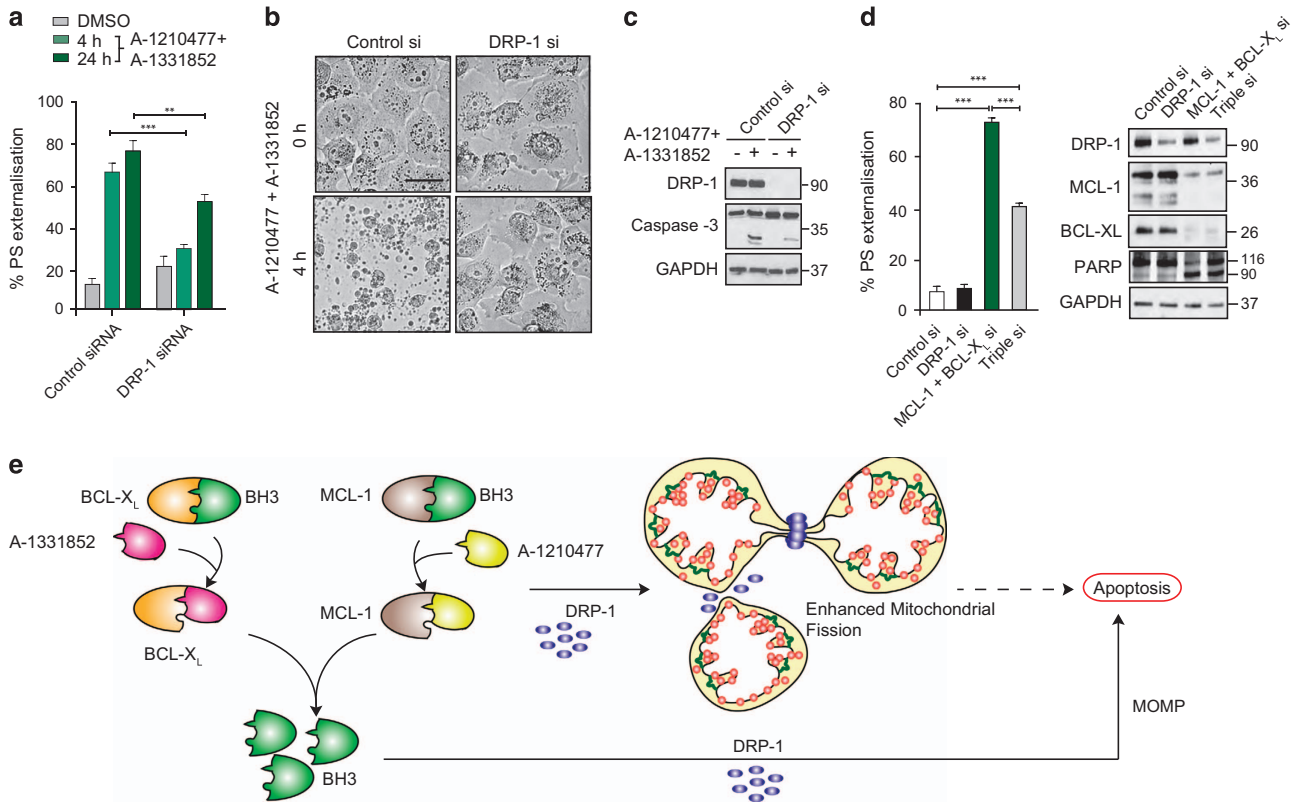

Figure 6 BH3 mimetics induce apoptosis in a DRP-1-dependent manner. (**a**) H1299 cells, transfected with DRP-1 siRNA and exposed to a combination of A-1210477 (10 μM) and A-1331852 (100 nM) demonstrate a marked decrease in apoptosis at 4 and 24 h. Statistical analysis was conducted using one-way ANOVA (**$P<0.005$, ***$P\leqslant 0.001$). (**b**) Bright-field microscopy of H1299 cells transfected with control or DRP-1 siRNA and treated with A-1210477 (10 μM) and A-1331852 (100 nM) for 4 h reveals the extent of DRP-1-dependent cell death (scale bar, 30 μm). (**c**) Immunoblots showing the knockdown efficiency of DRP-1 siRNA as well as its anti-apoptotic effects, as evident from the decrease in the processing of pro-caspase-3 following DRP-1 downregulation. (**d**) H1299 cells were transfected with siRNAs against both BCL-X_L and MCL-1 in the absence or presence (Triple si) of DRP-1 siRNA for 36 h and the extent of apoptosis assessed by PS externalisation. Blots showing the knockdown efficiency of the siRNAs and the anti-apoptotic effects associated with DRP-1 deficiency, as evident from the decrease in the processing of the caspase substrate, PARP. Statistical analysis was conducted using one-way ANOVA (***$P\leqslant 0.001$). (**e**) Scheme representing the distinct functions of A-1210477 in apoptosis induction (by releasing BH3-only members from the hydrophobic groove and causing mitochondrial outer membrane permeabilisation; MOMP) as well as increased mitochondrial fission in a DRP-1 dependent manner

with Z-VAD(OMe).fmk (Selleck Chemicals) for 30 min were exposed to the indicated drugs, fixed in 1 % (w/v) paraformaldehyde and stained with conformation-specific AP-1 BAK antibody (1 μg/ml), corresponding fluorophore- conjugated secondary antibody and quantified by FACS.

siRNA knockdowns. For transient transfections, the cells were transfected using TransIT-LT-1 transfection reagent (Mirus Bio LLC, Madison, WI, USA) and left for 48 h, according to the manufacturer's instructions. For siRNA knockdowns, the cells were transfected for 72 h with DRP-1 siRNA (S104274235; Qiagen), MCL-1 siRNA (s8585; Ambion and SI02781205; Qiagen) or BCL-XL siRNA (s1920; Ambion) using Interferin Reagent (Polyplus transfection Inc, NY, USA), according to the manufacturer's protocol.

Gel filtration and western blotting. For gel filtration experiments, the cells were lysed in CHAPS lysis buffer containing 1 % CHAPS, 20 mM Tris HCl (pH 8), 150 mM NaCl, 20 μM MG132 and protease inhibitor cocktail, incubated on ice for 30 mins, and centrifuged at 14 000 × *g* for 3 min at 4 °C. The pellet was discarded and supernatant (500 μl; 25 mg of protein per ml) was injected onto both Superose 6 and Superdex S200 size exclusion columns (GE Healthcare) and eluted using a running buffer containing 50 mM Tris HCl (pH 8), 150 mM KCl, 1 mM EDTA, 5 % glycerol, 1 mM DTT and 1 mM PMSF. 500 μl fractions eluted from the columns were collected for immunoblotting. Western blotting was carried out according to standard protocols. Briefly, 50 μg of total protein lysate was subjected to SDS-PAGE electrophoresis. Subsequently proteins were transferred to nitrocellulose membrane and protein bands visualised with ECL reagents (GE Healthcare).

Microscopy. Bright-field microscopy of cells was performed using EVOS FLOID cell imaging station (ThermoFisher Scientific). For immunofluorescent staining, the cells grown on coverslips were fixed with 4 % (w/v) paraformaldehyde, permeabilised with 0.5 % (v/v) Triton X-100 in PBS and followed by incubations with primary antibodies, the appropriate fluorophore-conjugated secondary antibodies, mounted on glass slides and imaged using a 3i Marianas spinning disk confocal microscope, fitted with a Plan-Apochromat ×63/1.4 NA Oil Objective, M27 and a Hamamatsu ORCA-Flash4.0 v2 sCMOS Camera (all from Intelligent Imaging Innovations, GmbH, Gottingen, Germany).

Statistical analysis. For time-course studies, a two-way ANOVA was performed and other studies were analysed for statistical significance with one-way ANOVA and the asterisks depicted correspond to the following *P*-values: *$P\leqslant 0.05$, **$P\leqslant 0.005$ and ***$P\leqslant 0.001$.

Conflict of Interest

The authors declare no conflict of interest.

Acknowledgements. We thank AbbVie, Drs Z Nikolovska-Coleska, L Walensky, H-G Wang and M Pellecchia for providing different BH3 mimetics used in this study. This work was supported by the North West Cancer Research Grants CR994 (to GMC), CR1040 (to SV and GMC), CR1037 (to PAE), a BBSRC TRDF grant (to PAE) and a Science Without Borders, CNPq 233624/2014-7, Ministry of Education, Brazil (to MM).

1. Tse C, Shoemaker AR, Adickes J, Anderson MG, Chen J, Jin S *et al.* ABT-263: a potent and orally bioavailable Bcl-2 family inhibitor. *Cancer Res* 2008; **68**: 3421–3428.
2. Souers AJ, Leverson JD, Boghaert ER, Ackler SL, Catron ND, Chen J *et al.* ABT-199, a potent and selective BCL-2 inhibitor, achieves antitumor activity while sparing platelets. *Nat Med* 2013; **19**: 202–208.
3. Roberts AW, Davids MS, Pagel JM, Kahl BS, Puvvada SD, Gerecitano JF *et al.* Targeting BCL2 with venetoclax in relapsed chronic lymphocytic leukemia. *N Engl J Med* 2015; **374**: 311–322.
4. Beroukhim R, Mermel CH, Porter D, Wei G, Raychaudhuri S, Donovan J *et al.* The landscape of somatic copy-number alteration across human cancers. *Nature* 2010; **463**: 899–905.
5. Leverson JD, Zhang H, Chen J, Tahir SK, Phillips DC, Xue J *et al.* Potent and selective small-molecule MCL-1 inhibitors demonstrate on-target cancer cell killing activity as single agents and in combination with ABT-263 (navitoclax). *Cell Death Dis* 2015; **6**: e1590.
6. Richard DJ, Lena R, Bannister T, Blake N, Pierceall WE, Carlson NE *et al.* Hydroxyquinoline-derived compounds and analoguing of selective Mcl-1 inhibitors using a functional biomarker. *Bioorg Med Chem* 2013; **21**: 6642–6649.
7. Cohen NA, Stewart ML, Gavathiotis E, Tepper JL, Bruekner SR, Koss B *et al.* A competitive stapled peptide screen identifies a selective small molecule that overcomes MCL-1-dependent leukemia cell survival. *Chem Biol* 2012; **19**: 1175–1186.
8. Abulwerdi FA, Liao C, Mady AS, Gavin J, Shen C, Cierpicki T *et al.* 3-Substituted-N-(4-hydroxynaphthalen-1-yl)arylsulfonamides as a novel class of selective Mcl-1 inhibitors: structure-based design, synthesis, SAR, and biological evaluation. *J Med Chem* 2014; **57**: 4111–4133.
9. Nguyen M, Marcellus RC, Roulston A, Watson M, Serfass L, Murthy Madiraju SR *et al.* Small molecule obatoclax (GX15-070) antagonizes MCL-1 and overcomes MCL-1-mediated resistance to apoptosis. *Proc Natl Acad Sci USA* 2007; **104**: 19512–19517.
10. Doi K, Li R, Sung SS, Wu H, Liu Y, Manieri W *et al.* Discovery of marinopyrrole A (Maritoclax) as a selective Mcl-1 antagonist that overcomes ABT-737 resistance by binding to and targeting Mcl-1 for proteasomal degradation. *J Biol Chem* 2012; **287**: 10224–10235.
11. Wei J, Kitada S, Rega MF, Stebbins JL, Zhai D, Cellitti J *et al.* Apogossypol derivatives as pan-active inhibitors of antiapoptotic B-cell lymphoma/leukemia-2 (Bcl-2) family proteins. *J Med Chem* 2009; **52**: 4511–4523.
12. Wei J, Stebbins JL, Kitada S, Dash R, Zhai D, Placzek WJ *et al.* An optically pure apogossypolone derivative as potent pan-active inhibitor of anti-apoptotic bcl-2 family proteins. *Front Oncol* 2011; **1**: 28.
13. Wang Z, Song W, Aboukameel A, Mohammad M, Wang G, Banerjee S *et al.* TW-37, a small-molecule inhibitor of Bcl-2, inhibits cell growth and invasion in pancreatic cancer. *Int J Cancer* 2008; **123**: 958–966.
14. Youle RJ, Strasser A. The BCL-2 protein family: opposing activities that mediate cell death. *Nat Rev Mol Cell Biol* 2008; **9**: 47–59.
15. Leverson JD, Phillips DC, Mitten MJ, Boghaert ER, Diaz D, Tahir SK *et al.* Exploiting selective BCL-2 family inhibitors to dissect cell survival dependencies and define improved strategies for cancer therapy. *Sci Transl Med* 2015; **7**: 279ra40.
16. Stewart ML, Fire E, Keating AE, Walensky LD. The MCL-1 BH3 helix is an exclusive MCL-1 inhibitor and apoptosis sensitizer. *Nat Chem Biol* 2010; **6**: 595–601.
17. Pantoliano MW, Petrella EC, Kwasnoski JD, Lobanov VS, Myslik J, Graf E *et al.* High-density miniaturized thermal shift assays as a general strategy for drug discovery. *J Biomol Screen* 2001; **6**: 429–440.
18. Lo M-C, Aulabaugh A, Jin G, Cowling R, Bard J, Malamas M *et al.* Evaluation of fluorescence-based thermal shift assays for hit identification in drug discovery. *Anal Biochem* 2004; **332**: 153–159.
19. Brandts JF, Lin LN. Study of strong to ultratight protein interactions using differential scanning calorimetry. *Biochemistry* 1990; **29**: 6927–6940.
20. Layton CJ, Hellinga HW. Thermodynamic analysis of ligand-induced changes in protein thermal unfolding applied to high-throughput determination of ligand affinities with extrinsic fluorescent dyes. *Biochemistry* 2010; **49**: 10831–10841.
21. Jung M, Philpott M, Müller S, Schulze J, Badock V, Eberspächer U *et al.* Affinity map of bromodomain protein 4 (BRD4) interactions with the histone H4 tail and the small molecule inhibitor JQ1. *J Biol Chem* 2014; **289**: 9304–9319.
22. Filippakopoulos P, Qi J, Picaud S, Shen Y, Smith WB, Fedorov O *et al.* Selective inhibition of BET bromodomains. *Nature* 2010; **468**: 1067–1073.
23. Friberg A, Vigil D, Zhao B, Daniels RN, Burke JP, Garcia-Barrantes PM *et al.* Discovery of potent myeloid cell leukemia 1 (Mcl-1) inhibitors using fragment-based methods and structure-based design. *J Med Chem* 2013; **56**: 15–30.
24. Bailey FP, Byrne DP, McSkimming D, Kannan N, Eyers PA. Going for broke: targeting the human cancer pseudokinome. *Biochem J* 2015; **465**: 195–211.
25. Mohanty S, Oruganty K, Kwon A, Byrne DP, Ferries S, Ruan Z *et al.* Hydrophobic core variations provide a structural framework for tyrosine kinase evolution and functional specialization. *PLoS Genet* 2016; **12**: e1005885.
26. Murphy JM, Zhang Q, Young SN, Reese ML, Bailey FP, Eyers PA *et al.* A robust methodology to subclassify pseudokinases based on their nucleotide-binding properties. *Biochem J* 2014; **457**: 323–334.
27. Varadarajan S, Vogler M, Butterworth M, Dinsdale D, Walensky LD, Cohen GM. Evaluation and critical assessment of putative MCL-1 inhibitors. *Cell Death Differ* 2013; **20**: 1475–1484.
28. Butterworth M, Pettitt A, Varadarajan S, Cohen GM. BH3 profiling and a toolkit of BH3-mimetic drugs predict anti-apoptotic dependence of cancer cells. *Br J Cancer* 2016; **114**: 638–641.
29. Otera H, Miyata N, Kuge O, Mihara K. Drp1-dependent mitochondrial fission via MiD49/51 is essential for apoptotic cristae remodeling. *J Cell Biol* 2016; **212**: 531–544.
30. S Soderquist R, Eastman A. BCL2 inhibitors as anticancer drugs: a plethora of misleading BH3 mimetics. *Mol Cancer Ther* 2016; **15**: 2011–2017.
31. Varadarajan S, Poornima P, Milani M, Gowda K, Amin S, Wang H-G *et al.* Maritoclax and dinaciclib inhibit MCL-1 activity and induce apoptosis in both a MCL-1-dependent and -independent manner. *Oncotarget* 2015; **6**: 12668–12681.
32. Kotschy A, Szlavik Z, Murray J, Davidson J, Maragno AL, Le Toumelin-Braizat G *et al.* The MCL1 inhibitor S63845 is tolerable and effective in diverse cancer models. *Nature* 2016; **538**: 477–482.
33. Varadarajan S, Butterworth M, Wei J, Pellecchia M, Dinsdale D, Cohen GM. Sabutoclax (BI97C1) and BI112D1, putative inhibitors of MCL-1, induce mitochondrial fragmentation either upstream of or independent of apoptosis. *Neoplasia* 2013; **15**: 568–578.
34. Lucas CM, Milani M, Butterworth M, Carmell N, Scott LJ, Clark RE *et al.* High CIP2A levels correlate with an antiapoptotic phenotype that can be overcome by targeting BCL-XL in chronic myeloid leukemia. *Leukemia* 2016; **30**: 1273–1281.

Milani et al. *Cell Death Discovery* (2019)5:117
https://doi.org/10.1038/s41420-019-0199-x

Cell Death Discovery

ARTICLE Open Access

DRP-1 functions independently of mitochondrial structural perturbations to facilitate BH3 mimetic-mediated apoptosis

Mateus Milani[1], Alison J. Beckett[2], Aoula Al-Zebeeby[1], Xu Luo[3], Ian A. Prior[2], Gerald M. Cohen[1,4] and Shankar Varadarajan[1,4]

Abstract

Maintenance of mitochondrial integrity is critical for normal cellular homoeostasis. Most cells respond to stress stimuli and undergo apoptosis by perturbing mitochondrial structure and function to release proteins, such as cytochrome *c*, which are essential for the execution of the intrinsic apoptotic cascade. Cancer cells evade these events by overexpressing the anti-apoptotic BCL-2 family of proteins on mitochondrial membranes. Inhibitors of the anti-apoptotic BCL-2 family proteins, also known as BH3 mimetics, antagonise the pro-survival functions of these proteins and result in rapid apoptosis. Although the precise mechanism by which BH3 mimetics induce apoptosis has been well characterised, not much is known in terms of the structural changes that occur in mitochondria during apoptosis. Using a panel of highly selective BH3 mimetics and a wide range of cell lines, we demonstrate that BH3 mimetics induce extensive mitochondrial fission, accompanied by swelling of the mitochondrial matrix and rupture of the outer mitochondrial membrane. These changes occur in a BAX/ BAK-dependent manner. Although a major mitochondrial fission GTPase, DRP-1, has been implicated in mitochondrial apoptosis, our data demonstrate that DRP-1 might function independently/downstream of BH3 mimetic-mediated mitochondrial fission to facilitate the release of cytochrome *c* and apoptosis. Moreover, downregulation of DRP-1 prevented cytochrome *c* release and apoptosis even when OPA1, a protein mediating mitochondrial fusion, was silenced. Although BH3 mimetic-mediated displacement of BAK and other BH3-only proteins from BCL-X_L and MCL-1 was unaffected by DRP-1 downregulation, it prevented BAK activation significantly, thus placing DRP-1 as one of the most critical players, along with BAX and BAK, that governs BH3 mimetic-mediated cytochrome *c* release and apoptosis.

Introduction

Most chemotherapeutic agents kill cancer cells by executing the intrinsic apoptotic pathway, which is characterised by mitochondrial outer membrane permeabilization (MOMP), release of cytochrome *c* from the inner mitochondrial membrane (IMM) and formation of the apoptosome that activates the initiator and effector caspases. MOMP is regulated by the BCL-2 family, whereby BAX and BAK, undergo specific conformational changes to form oligomeric pores that insert into the outer mitochondrial membrane (OMM) to release cytochrome *c*[1,2]. Activation of BAX and BAK is achieved by several pro-apoptotic BH3-only members, which are generally rendered ineffective by sequestration with specific anti-apoptotic BCL-2 family of proteins, such as BCL-2, BCL-X_L and MCL-1[3,4]. These anti-apoptotic proteins are highly expressed in many cancers and inhibitors known as BH3 mimetics have been designed to target them in order

Correspondence: Shankar Varadarajan (svar@liv.ac.uk)
[1]Department of Molecular and Clinical Cancer Medicine, Institute of Translational Medicine, University of Liverpool, Liverpool, Ashton Street, Liverpool L69 3GE, UK
[2]Department of Cellular and Molecular Physiology, Institute of Translational Medicine, University of Liverpool, Liverpool, Ashton Street, Liverpool L69 3GE, UK
Full list of author information is available at the end of the article.
Edited by I. Amelio

SPRINGER NATURE CDDpress

to displace the BH3-only proteins, activate BAX and BAK, thereby inducing MOMP and apoptosis of cancer cells[5].

ABT-737, and its orally available analogue, ABT-263 (Navitoclax) were the first bona fide BH3 mimetics developed to target BCL-2, BCL-X_L and BCL-w[6,7]. Subsequently, BH3 mimetics that specifically target BCL-2 (ABT-199 (Venetoclax), S55746), BCL-X_L (A-1331852) and MCL-1 (A-1210477, S63845, AMG 176 and AZD5991) have been synthesised[8–14]. These inhibitors, as single agents, have demonstrated much promise in treating a wide variety of haematological malignancies, and have had limited success in combination with conventional chemotherapy against several solid tumours[8,12–17]. BH3 mimetics induce apoptosis primarily by targeting protein–protein interactions between the anti- and pro-apoptotic BCL-2 family members[18]. Subsequently, BH3 mimetics have been shown to induce significant structural changes in the mitochondria, ranging from mitochondrial matrix swelling to discontinuities in the OMM, upstream of caspase activation[19,20]. Furthermore, BAX and BAK localise to the breakpoints in OMM and may facilitate cytochrome *c* release at such breakpoints[19]. Although BCL-2 family members have been implicated in regulating mitochondrial membrane dynamics and functions[21–24], putative inhibitors of MCL-1 have often resulted in extensive mitochondrial fission in various cell lines[25–27]. The regulation of this fission and its relationship to BH3 mimetic-mediated apoptosis remains to be determined.

Mitochondrial structure is maintained through an intricate balance between the activities of several fusion and fission proteins, which belong to a conserved family of GTPases that reside in the OMM or IMM. Mitofusins 1 and 2 (MFN1/ 2) and optic atrophy 1 (OPA1) are essential for mitochondrial fusion, whereas dynamin related protein 1 (DRP-1) is essential for mitochondrial fission[28]. Defects in mitochondrial fusion and fission have been implicated in a range of pathophysiological conditions including poor brain development, optic atrophy, cardiomyopathy and neurodegenerative diseases[29,30]. Mounting evidence now suggests the involvement of several members of BCL-2 family members, particularly MCL-1, in the regulation of mitochondrial structure and function[22–25,29]. However, the mechanism by which MCL-1 regulates mitochondrial membrane dynamics and the potential cross-talk with its conventional role in antagonising apoptosis remain to be characterised.

In this study, we use a panel of highly selective BH3 mimetics together with cell lines that depend on specific BCL-2 family members for survival to demonstrate that BH3 mimetics induce significant ultrastructural mitochondrial changes upstream of caspase activation. DRP-1 plays a role downstream of these changes but upstream of MOMP to facilitate cytochrome *c* release and apoptosis, following exposure to BH3 mimetics.

Results

BH3 mimetics induce marked mitochondrial structural changes

Previously, we have reported that BH3 mimetics induce a novel paradigm of apoptosis characterised by marked ultrastructural changes in the mitochondria, involving the loss of mitochondrial cristae and the appearance of breaks in the OMM, resulting from mitochondrial matrix swelling[19,20,31]. In cell lines that depend for survival almost exclusively on BCL-2 (MAVER-1), BCL-X_L-(K562) and MCL-1 (H929)[32], exposure to the relevant BH3 mimetics, such as ABT-199, A-1331852 and A-1210477, respectively, resulted in similar mitochondrial matrix swelling and rupture of the OMM (Fig. 1a–c). Such mitochondrial changes were also evident in H1299 cells following exposure to a combination of A-1331852 and A-1210477, as these cells depend on both BCL-X_L and MCL-1 for survival (Fig. 1d). These mitochondrial ultrastructural changes were independent of effector caspases, as they were observed in cells pre-treated with Z-VAD.fmk, a broad-spectrum caspase inhibitor (Fig. 1). Exposure of the different cells to their appropriate BH3 mimetic resulted in mitochondrial membrane depolarisation, loss of cytochrome *c* and induction of apoptosis, as assessed by phosphatidylserine externalisation (Supplementary Fig. S1). Exposure of the cells to Z-VAD.fmk almost completely inhibited BH3 mimetic-mediated apoptosis, assessed by PS externalisation, whereas little if any inhibition of cytochrome *c* release was observed (Supplementary Fig. S1). Taken together these results suggested that the mitochondrial structural changes occurred upstream of effector caspase activation and accompanied cytochrome *c* release, as well as a loss of mitochondrial membrane potential.

BH3 mimetic-mediated mitochondrial perturbations occur in a BAX/BAK-dependent manner

To assess whether BAX and BAK play crucial roles in BH3 mimetic-mediated ultrastructural changes in mitochondria, we exposed HCT-116 WT and BAX/BAK double knock-out (DKO) cells to a combination of A-1331852 and A-1210477, as HCT-116 cells also depend on both BCL-X_L and MCL-1 for survival[33]. Exposure of the HCT-116 WT cells to the BH3 mimetics resulted in significant mitochondrial matrix swelling accompanied by a loss of mitochondrial cristae, although rupture of the OMM was not readily apparent (Fig. 2). However, all these mitochondrial changes were clearly prevented in the HCT-116 BAX/BAK DKO cells, demonstrating a requirement for BAX and/or BAK for the perturbation of the mitochondria. Since BH3-only members are generally required to activate BAX and BAK, we wished to assess whether BH3 mimetics could induce mitochondrial structural perturbations in the absence of all known pro-

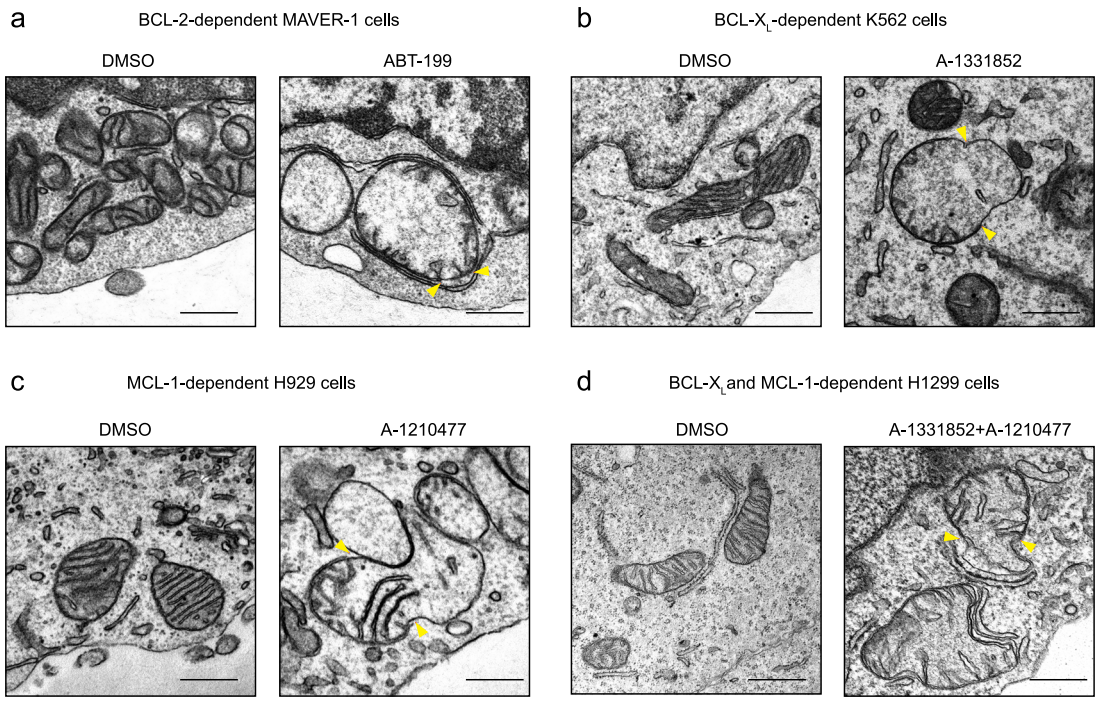

Fig. 1 BH3 mimetics induce marked ultrastructural changes in mitochondria of different cells. a MAVER-1, **b** K562, **c** H929 and **d** H1299 cells were exposed to Z-VAD.fmk (30 μM) for 0.5 h, followed by ABT-199 (100 nM), A-1331852 (100 nM), A-1210477 (10 μM), or a combination of A-1331852 (100 nM) and A-1210477 (10 μM), respectively, for 4 h and assessed for mitochondrial structural changes by electron microscopy. Yellow arrowheads indicate regions of breaks at the outer mitochondrial membrane. Scale bars: 500 nm

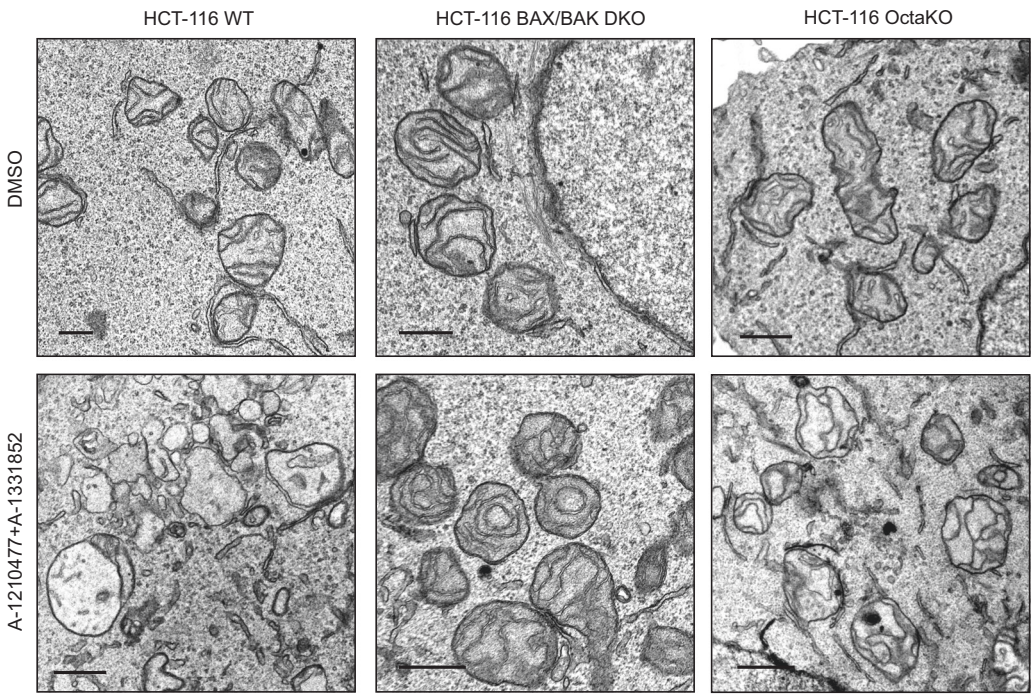

Fig. 2 BH3 mimetics disrupt mitochondria in a BAX- and BAK-dependent but BH3-independent manner. HCT-116 WT, DKO (BAX/BAK deficient) and OctaKO cells were exposed to Z-VAD.fmk (30 μM) for 0.5 h, followed by a combination of A-1331852 (100 nM) and A-1210477 (10 μM) for 4 h and assessed for mitochondrial structural changes by electron microscopy. Scale bars: 500 nm

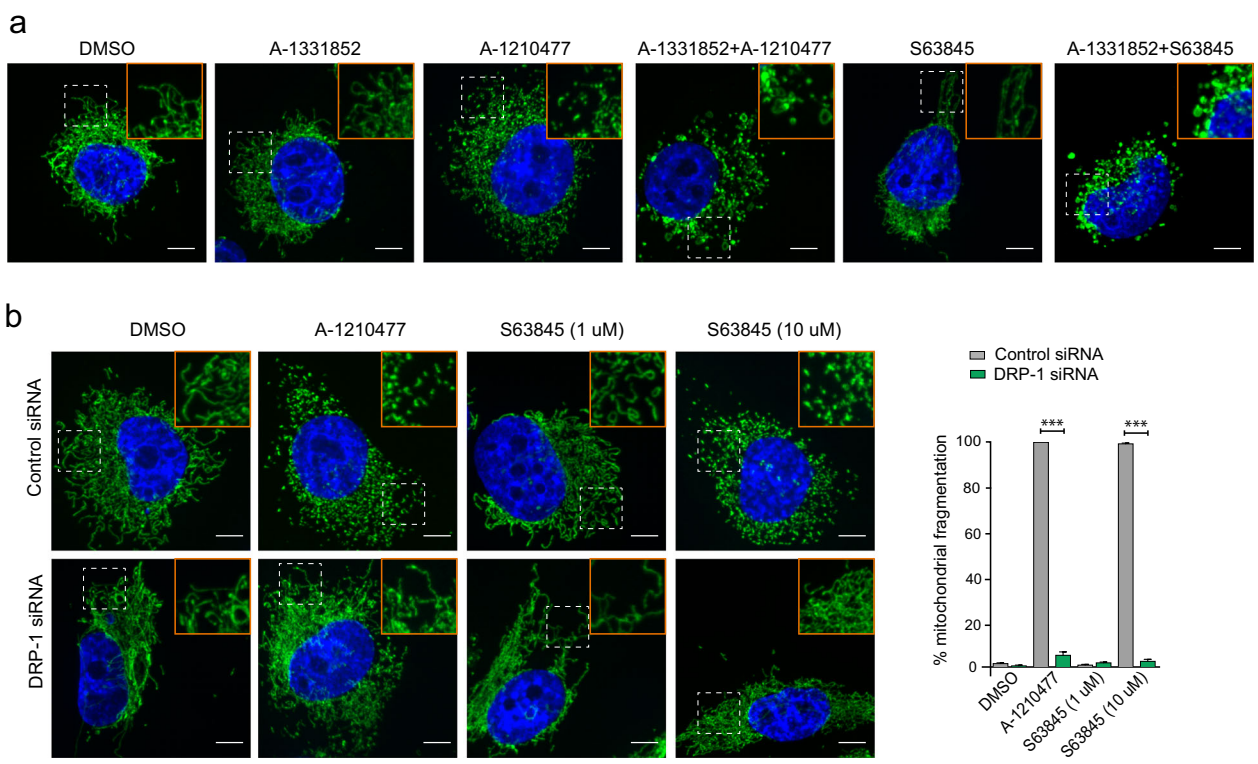

Fig. 3 Mitochondrial fission mediated by A-1210477 and S63845 occurs in a DRP-1-dependent manner. a H1299 cells were exposed to Z-VAD.fmk (30 μM) for 0.5 h, followed by either A-1331852 (100 nM), A-1210477 (10 μM), S63845 (100 nM), or a combination of the different inhibitors for 4 h and assessed for mitochondrial integrity by immunostaining with HSP70 antibody. **b** H1299 cells were transfected with control or DRP-1 siRNA for 72 h and exposed to A-1210477 (10 μM) or S63845 (1 and 10 μM) for 4 h and assessed for mitochondrial integrity. The extent of mitochondrial fragmentation was quantified by analysing ~100 cells for each condition in three independent experiments. Scale bar: 10 μm. Error bars = mean ± SEM. Statistical analysis was conducted by one-way ANOVA (***$P \leq 0.001$)

apoptotic BH3-only members. For this, we used HCT-116 OctaKO cells, which lack the BH3-only members namely, BIM, BID, PUMA, BAD, BIK, HRK, BMF and NOXA[33]. Exposure of these cells to a combination of A-1331852 and A-1210477 resulted in mitochondrial structural changes, characteristic of significant cristae remodelling (Fig. 2). However, the swelling of mitochondrial matrix and the accompanying loss of cristae observed in the HCT-116 WT cells following BH3 mimetics were not apparent in HCT-116 OctaKO cells (Fig. 2). This is consistent with earlier findings demonstrating that the pro-apoptotic BH3-only members are dispensable for BH3 mimetic-mediated apoptosis[34]. Taken together, our data demonstrated that the activation of BAX and/or BAK, either in a BH3-dependent or independent manner, is essential for the ultrastructural changes observed in the mitochondria, following exposure to BH3 mimetics.

DRP-1 is not required for the mitochondrial structural changes that occur during the onset of apoptosis

We previously reported that putative inhibitors of MCL-1 induced extensive mitochondrial fission and suggested that this could be a prerequisite for the ensuing apoptosis in MCL-1-dependent cell lines[25–27]. In support of this suggestion, exposure of A-1210477 but not A-1331852 resulted in extensive mitochondrial fission that resembled mitochondrial fragmentation in H1299 cells (Fig. 3a, Supplementary Fig. S2). The ability of A-1210477 to induce mitochondrial fission was also clearly evident when used in combination with A-1331852 to induce apoptosis in these cells (Fig. 3a, Supplementary Fig. S2). However, mitochondria in this instance appeared swollen, potentially indicating swollen matrix and loss of cristae that were previously observed at the level of electron microscopy (compare Figs. 1d and 3a). In marked contrast, S63845 at a concentration (100 nM) sufficient to induce apoptosis in a MCL-1-dependent manner[34] failed to demonstrate mitochondrial fission (Fig. 3a, Supplementary Fig. S2). However, S63845 (100 nM) when used in conjunction with A-1331852 resulted in mitochondrial structural changes that resembled the swollen mitochondria observed following a combination of A-1210477 and A-1331852 (Fig. 3a, Supplementary Fig. S2). Taken together, our results suggested that mitochondrial fission

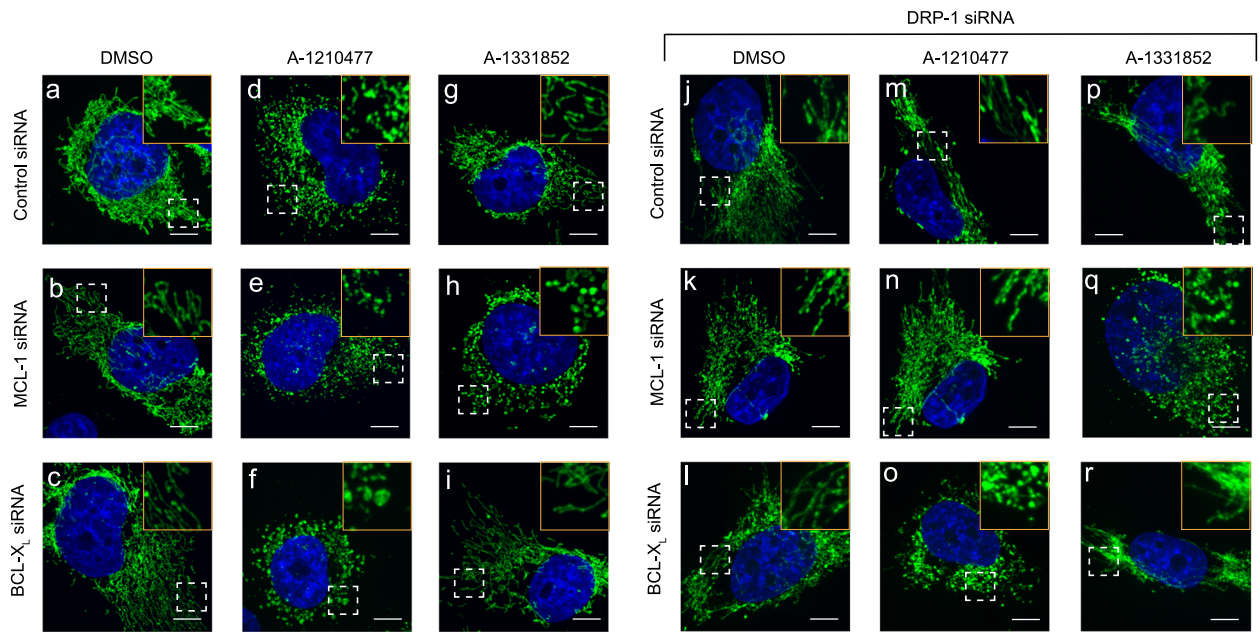

Fig. 4 DRP-1 is not required for mitochondrial fission during BH3 mimetic-mediated apoptosis. H1299 cells were transfected with control, MCL-1, or BCL-X_L siRNAs, either alone or in combination with DRP-1 siRNA for 72 h, then exposed to Z-VAD.fmk (30 μM) for 0.5 h, followed by A-1210477 (10 μM) and/or A-1331852 (100 nM) for 4 h and assessed for mitochondrial integrity by immunostaining with HSP70 antibody. The boxed regions in the images are enlarged to show mitochondrial structural changes in the indicated cells. Scale bar: 10 μm

mediated by A-1210477 versus a combination of MCL-1 and BCL-X_L inhibitors was distinct. Moreover, while S63845 failed to exhibit mitochondrial fission at low concentrations (100–1000 nM), higher concentrations (10 μM) of S63845 resulted in significant mitochondrial fission, which mimicked A-1210477-mediated mitochondrial fragmentation (Fig. 3b).

We previously reported that A-1210477-mediated mitochondrial fission occurred in a DRP-1-dependent manner[27]. A similar dependence on DRP-1 was also observed in cells exhibiting extensive mitochondrial fission, following exposure to high concentrations of S63845 (Fig. 3b). Thus both the MCL-1 inhibitors, A-1210477 and S63845, induced mitochondrial fission, which was clearly dependent on DRP-1 (Fig. 3b). We wished to assess if such mitochondrial fission was a prerequisite for apoptosis induction. Since H1299 cells depend on both BCL-X_L and MCL-1 for survival, we exposed cells to either A-1210477 or A-1331852 and simultaneously silenced the expression levels of either BCL-X_L or MCL-1 to facilitate apoptosis. Although downregulation of BCL-XL or MCL-1 did not result in mitochondrial fission and maintained the filamentous structure, exposure of the cells to A-1210477 resulted in significant mitochondrial fission, which resembled fragmented mitochondria (Fig. 4a–d, Supplementary Fig. S3). In the MCL-1-downregulated cells, A-1210477 still retained its ability to cause mitochondrial fragmentation (Fig. 4e), but when BCL-X_L was downregulated, A-1210477 resulted in mitochondrial structural changes that resembled matrix swelling (Fig. 4f, Supplementary Fig. S3), as previously described (Fig. 1d). In contrast, exposure to A-1331852 only resulted in similar mitochondrial swelling when MCL-1 was also downregulated (Fig. 4g–I, Supplementary Fig. S3). These results suggested that mitochondrial fission, mediated by MCL-1 inhibitors, appeared to exhibit a distinct morphology from that observed following the induction of apoptosis. This was more apparent following DRP-1 downregulation, which prevented A-1210477-mediated mitochondrial fission (Fig. 4m, n), but did not appear to alter mitochondrial swelling observed during apoptosis induction (Fig. 4o, q, Supplementary Fig. S3). Taken together, these results exclude an involvement of DRP-1 in the early mitochondrial structural changes including mitochondrial swelling associated with the onset of apoptosis (Fig. 4).

Consistent with the above hypothesis, electron micrographs revealed marked structural alterations of the mitochondria in cells exposed to both A-121077 and A-1331852, characterised by breaks in the OMM (denoted by the yellow arrowheads), mitochondrial matrix swelling and a concomitant loss of cristae (Fig. 5a). Downregulation of DRP-1 alone resulted in elongated mitochondria, consistent with its known role in mitochondrial fission (Fig. 5a). However, the mitochondria in the DRP-1-downregulated cells following exposure to BH3 mimetics

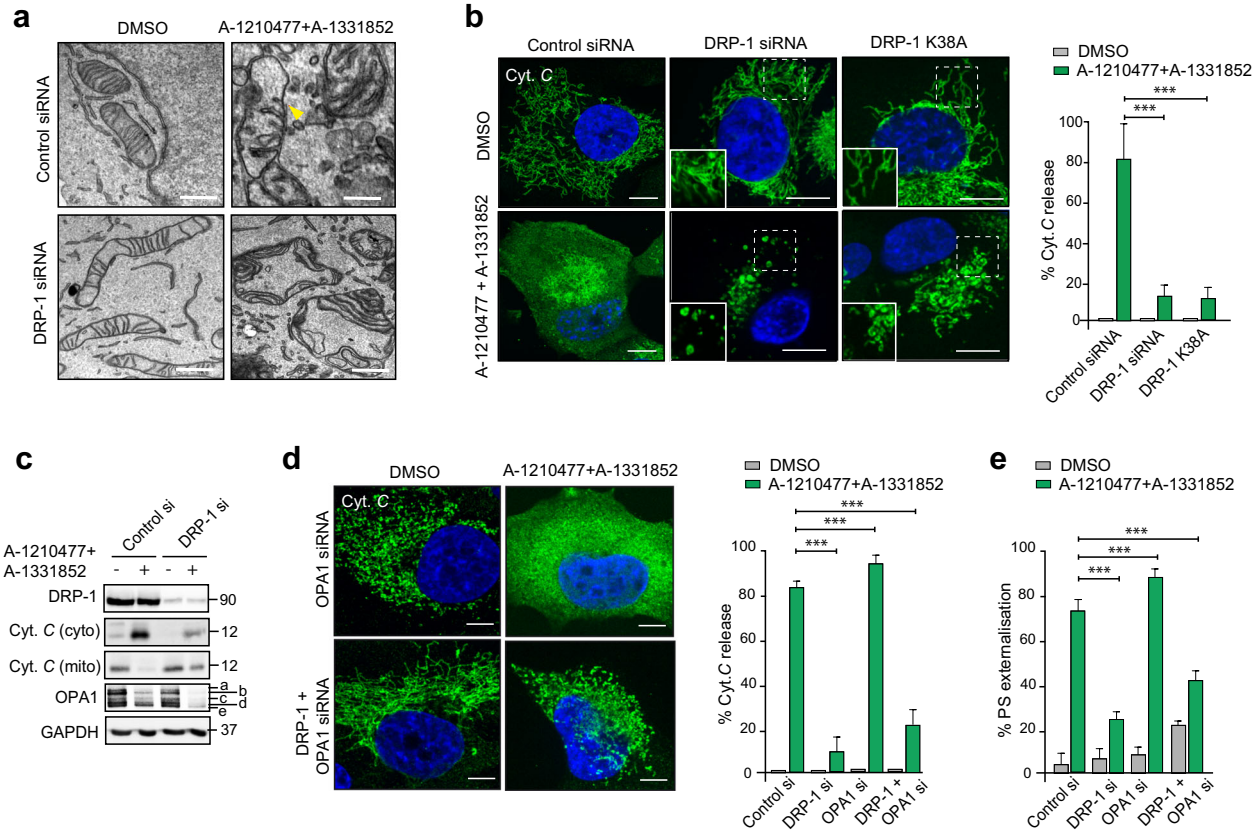

Fig. 5 DRP-1 regulates BH3 mimetic-induced cytochrome *c* release and apoptosis downstream of mitochondrial cristae remodelling. a Electron microscopy of H1299 cells, transfected with DRP-1 siRNA for 72 h in the presence or absence of the indicated BH3 mimetics for 2 h. Breaks in the outer mitochondrial membrane are indicated by the yellow arrowhead. Scale bars = 10 nm. **b** H1299 cells were transfected with DRP-1 siRNA or GFP-DRP-1 K38A plasmid for 72 h, exposed to Z-VAD.fmk (30 μM) for 0.5 h, followed by a combination of A-1331852 (100 nM) and A-1210477 (10 μM) for 4 h and the extent of cytochrome *c* released from mitochondria assessed by confocal microscopy. The boxed regions in the images are enlarged to show mitochondrial structural changes in the indicated cells. The extent of cytochrome *c* release was quantified by counting at least 100 cells from three independent experiments. **c** Same as **b**, but the extent of cytochrome *c* release as well as OPA1 processing and the silencing efficiency of DRP-1 siRNA were analysed by western blotting. **d** H1299 cells were transfected with the indicated siRNAs for 72 h, treated as described in **b** and the extent of cytochrome *c* release assessed and quantified. The extent of cytochrome *c* release was quantified by counting at least 100 cells from three independent experiments. **e** Same as **d** but the cells were exposed to BH3 mimetics in the absence of Z-VAD.fmk and the extent of apoptosis assessed by PS externalisation from at least three independent experiments. All scale bars, unless indicated: 10 μm. Error bars = mean ± SEM. Statistical analysis was conducted by one-way ANOVA (***$P \leq 0.001$)

appeared visibly swollen with intact cristae and few if any breaks in the OMM (Fig. 5a). Taken together, our data suggested that mitochondrial fission observed following exposure to MCL-1 inhibitors was distinct from the structural perturbations (characterised by OMM breaks and IMM swelling) observed as a result of apoptosis induction.

DRP-1 is critical for the release of cytochrome *c* from mitochondria during apoptosis

Permeabilisation of the OMM, otherwise known as MOMP, occurs as a consequence of BAX and/or BAK oligomerization and is generally accompanied by the release of mitochondrial cytochrome *c* into the cytosol. Exposure of cells to a combination of A-1210477 and A-1331852 resulted in an almost complete release of mitochondrial cytochrome *c* into the cytosol (Fig. 5b, c). This was markedly inhibited in cells, following inactivation of DRP-1 using siRNA or overexpression of the DRP-1 K38A plasmid (Fig. 5b, c), thus placing DRP-1 upstream of cytochrome *c* release. While cytochrome *c* was still retained in mitochondria following DRP-1 down-regulation, mitochondria in these cells appeared swollen (Fig. 5b), consistent with those observed in the electron micrographs (Fig. 5a). As cytochrome *c* release occurs as a consequence of mitochondrial cristae remodelling[35], exposure to BH3 mimetics not only resulted in the release of mitochondrial cytochrome *c* but also caused a loss of

the high molecular weight isoforms of OPA1, characteristic of mitochondrial cristae remodelling (Fig. 5c). While downregulation of DRP-1 markedly diminished BH3 mimetic-mediated release of cytochrome *c*, it did not prevent BH3 mimetic-mediated loss of OPA1 (Fig. 5c), thus placing DRP-1 upstream of cytochrome *c* release but downstream of mitochondrial cristae remodelling. This was further confirmed following exposure of DRP-1 and/or OPA1-downregulated cells to BH3 mimetics. While downregulation of OPA1 resulted in significant mitochondrial fission, as well as a near-complete release of cytochrome *c* following BH3 mimetics, a simultaneous downregulation of DRP-1 diminished these effects (Fig. 5d). Similarly downregulation of DRP-1 prevented BH3 mimetic-induced apoptosis, even in the absence of OPA1 (Fig. 5e), thus placing DRP-1 downstream of OPA1 proteolysis but upstream of cytochrome *c* release in BH3 mimetic-mediated apoptosis.

DRP-1 is critical for BAK activation during BH3 mimetic-mediated apoptosis

Our results indicated that BH3 mimetics could induce structural perturbations in the mitochondria, characterised by OPA1 proteolysis, cristae remodelling and the accompanying redistribution of cytochrome *c* from cristae to mitochondrial inner membrane space, all irrespective of the presence or absence of DRP-1. Since the role of DRP-1 was placed upstream of cytochrome *c* release, we wished to assess whether DRP-1 impacted on any upstream events during BH3 mimetic-mediated apoptosis. The primary function of BH3 mimetics is to disrupt the protein–protein interactions between the anti-apoptotic (BCL-X_L and MCL-1, in this instance) and pro-apoptotic members of the BCL-2 family. The released pro-apoptotic proteins could then activate the effector proteins (BAK, in H1299 as these cells lack BAX) to oligomerise on mitochondrial membranes to subsequently release cytochrome *c* (Fig. 6a).

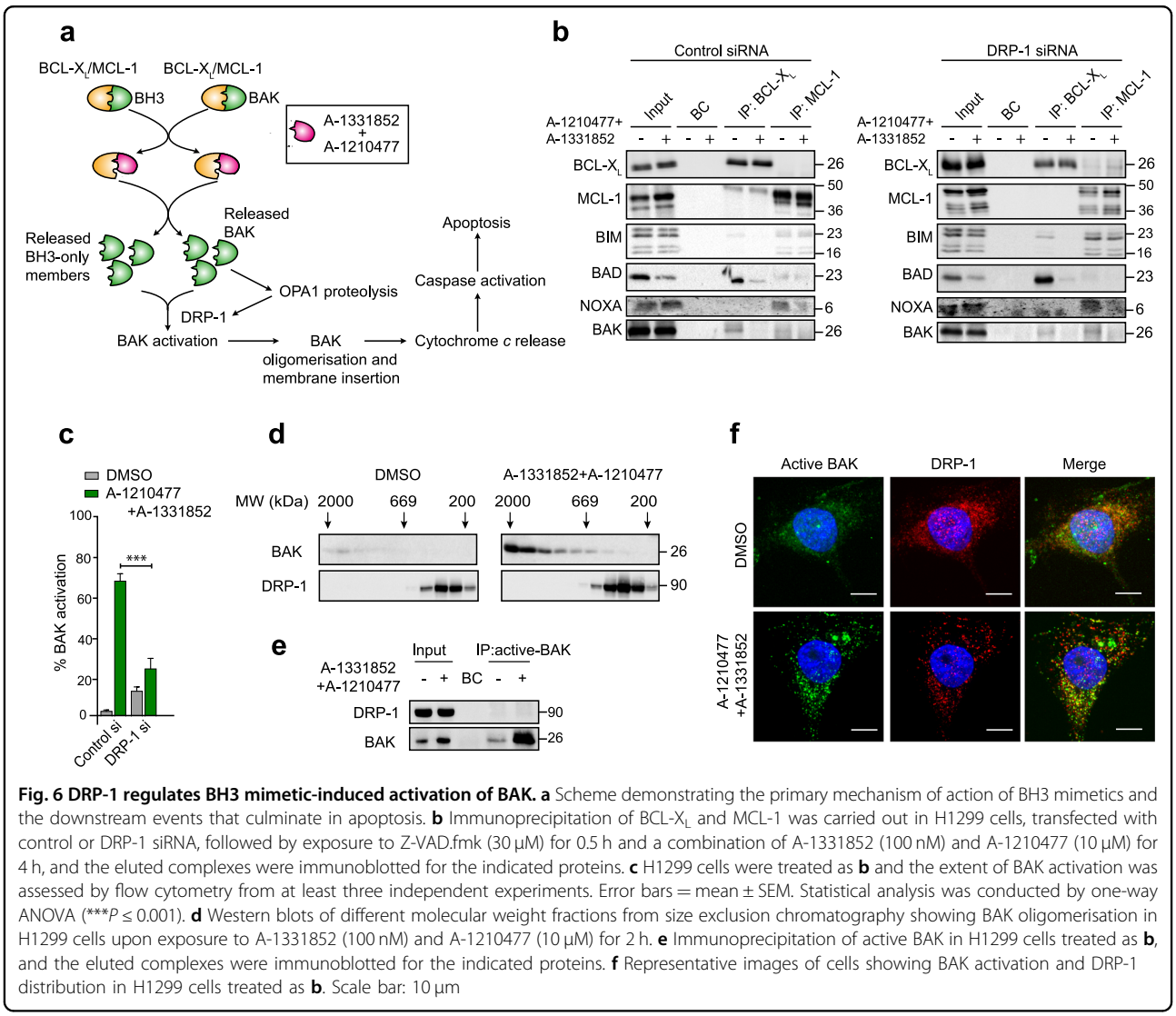

Fig. 6 DRP-1 regulates BH3 mimetic-induced activation of BAK. a Scheme demonstrating the primary mechanism of action of BH3 mimetics and the downstream events that culminate in apoptosis. **b** Immunoprecipitation of BCL-X_L and MCL-1 was carried out in H1299 cells, transfected with control or DRP-1 siRNA, followed by exposure to Z-VAD.fmk (30 μM) for 0.5 h and a combination of A-1331852 (100 nM) and A-1210477 (10 μM) for 4 h, and the eluted complexes were immunoblotted for the indicated proteins. **c** H1299 cells were treated as **b** and the extent of BAK activation was assessed by flow cytometry from at least three independent experiments. Error bars = mean ± SEM. Statistical analysis was conducted by one-way ANOVA (***$P \leq 0.001$). **d** Western blots of different molecular weight fractions from size exclusion chromatography showing BAK oligomerisation in H1299 cells upon exposure to A-1331852 (100 nM) and A-1210477 (10 μM) for 2 h. **e** Immunoprecipitation of active BAK in H1299 cells treated as **b**, and the eluted complexes were immunoblotted for the indicated proteins. **f** Representative images of cells showing BAK activation and DRP-1 distribution in H1299 cells treated as **b**. Scale bar: 10 μm

Immunoprecipitation of BCL-X_L and MCL-1 to identify their associated pro-apoptotic proteins revealed that in H1299 cells, BIM and BAK were bound to both BCL-X_L and MCL-1, whereas NOXA and BAD exclusively bound to MCL-1 and BCL-X_L, respectively (Fig. 6b). Exposure of these cells to a combination of A-1331852 and A-1210477 resulted in displacement of most of these pro-apoptotic proteins from their corresponding ant-apoptotic partners (Fig. 6b). Importantly, none of these interactions/displacements were altered in cells following DRP-1 downregulation, thus suggesting that DRP-1 played no role in the early events of BH3 mimetic-mediated apoptosis. Since BAK and other BH3-only proteins were released following BH3 mimetics, we next wished to assess if BAK activation was altered in the absence of DRP-1. Downregulation of DRP-1 resulted in a significant decrease in BH3 mimetic-mediated activation of BAK (Fig. 6c), suggesting that DRP-1 was critical in the activation of BAK during BH3 mimetic-mediated apoptosis. Although the requirement of DRP-1 for BAK activation could be demonstrated, no binding of DRP-1 to the oligomerised/active BAK was observed in these cells (Fig. 6d–f), thus suggesting the involvement of other protein(s) in BAK activation immediately preceding cytochrome *c* release. Taken together, our data confirm that DRP-1 plays a critical role at the level of BAK activation, facilitating OMM breaks, cytochrome *c* release and apoptosis.

Discussion

BH3 mimetics, in particular ABT-737 and ABT-199, induce a novel paradigm of cell death, characterised by excessive swelling of mitochondrial matrix and discontinuities in the OMM in BCL-2-dependent chronic lymphocytic leukaemia cells[19,31]. BH3 mimetics targeting BCL-X_L and MCL-1 also induce similar mitochondrial ultrastructural changes in cells that exclusively depend on BCL-X_L and MCL-1, respectively (Fig. 1)[20]. However, cells exposed to the MCL-1 inhibitor, A-1210477, exhibit marked mitochondrial changes, in particular mitochondrial fission, irrespective of their dependencies on a specific BCL-2 family member for survival (Fig. 3). This is in agreement with our previous findings[27]. Mitochondrial fission mediated by A-1210477 alone did not result in apoptosis in these cell lines, even after prolonged exposure[27]. This was most probably because most cell lines derived from solid tumours depend on both BCL-X_L and MCL-1 for survival, and inhibition of MCL-1 alone was not sufficient to result in apoptosis. This was further supported by our observation that inhibition of MCL-1 using A-1210477 while resulting in extensive mitochondrial fission did not induce OMM breaks and cell death, unless the activity of BCL-X_L was also neutralised.

Although A-1210477-mediated mitochondrial fission did not necessarily result in apoptosis, it was difficult to ascertain whether such fission was a prerequisite for apoptosis. This difficulty was partly because DRP-1 appeared to play important but distinct roles both in A-1210477-mediated mitochondrial fission and BH3 mimetic-mediated apoptosis[27]. Moreover, DRP-1 also interacted with MCL-1 and BCL-X_L, thus coupling mitochondrial fission and apoptosis[23,27,36]. However, with the development of more potent inhibitors, such as S63845, we have demonstrated that mitochondrial fission does not occur at concentrations sufficient to inhibit MCL-1 (Fig. 3). Furthermore, while mitochondrial fission induced by A-1210477 and high concentrations of S63845 was mediated by DRP-1, mitochondrial swelling that occurred at the onset of apoptosis induction was largely independent of DRP-1 (Figs. 3 and 4), thus differentiating the distinct types of mitochondrial fission.

Our data in the HCT-116 WT and BAX/BAK DKO cells convincingly demonstrate that BH3 mimetic-mediated OMM breaks and swelling of matrix compartment are essential for BAX/BAK to facilitate cytochrome *c* release (Fig. 2). The inability of HCT-116 OctaKO cells to prevent BH3 mimetic-mediated mitochondrial changes further supports our findings that BAX and BAK but not the known BH3-only members are critical for BH3 mimetic-mediated apoptosis[33,34]. How BAX and BAK localise to the sites of OMM breaks to facilitate cytochrome *c* release is not entirely known. The involvement of DRP-1, Dynamin-2, and even membranes of the endoplasmic reticulum in these events have been previously proposed[37–42]. Downregulation of DRP-1 or its receptors, MID49 and MID51, have been shown to antagonise cytochrome *c* release and apoptosis in response to a wide variety of apoptotic stimuli[43]. DRP-1 functions downstream of OPA1-mediated cristae remodelling (Fig. 5), to activate BAK (Fig. 6), which in turn precedes BAK oligomerisation and membrane insertion for the execution of MOMP and apoptosis. However, mitochondrial cristae remodelling requires the presence of BAX and BAK (Fig. 2)[44]. Thus DRP-1 could function either downstream or independent of OPA1 proteolysis to activate BAK and ensuing apoptosis. Taken together, our data suggest that BH3 mimetics most likely activate BAX/BAK independently of the eight known BH3-only members, which further results in OPA1-mediated cristae remodelling to redistribute cytochrome *c* within the mitochondria, thus priming the mitochondria to undergo MOMP, upon sensing the stress signal. DRP-1 plays a critical role at this stage to activate BAK and/or BAX to insert these effector proteins on mitochondrial membranes. This along with the constriction of the primed mitochondria by DRP-1 constitute the so-called stress signals that cause OMM breaks, efficiently releasing the redistributed cytochrome *c* into the cytosol and initiating apoptosis.

Materials and methods

Cell culture

H1299 (purchased from ATCC), K562 (provided by Prof. R. Clark, University of Liverpool) and MAVER-1 cells (provided by Dr. J. Slupsky, University of Liverpool) were cultured in RPMI 1640 medium (Life Technologies). H929 cells (purchased from DMSZ, Braunshweig, Germany) were cultured in RPMI 1640 medium supplemented with 0.05 mM β-mercaptoethanol (BME). Colon cancer cell lines HCT-116 (wild-type and DKO) (from R. J. Youle, National Institute of Health, USA) and HCT-116-OctaKO[33] were cultured in McCoy's 5A Modified media. All culture media were supplemented with 10% FBS (Life Technologies) and maintained at 37 °C in a humidified atmosphere of 5% CO_2. All cell lines used in this study were subjected to short tandem repeat (STR) profiling to ensure quality and integrity.

Reagents

ABT-199, A-1210477 and Z-VAD.FMK from Selleck (Houston, TX, USA), S63845 from Active Biochem (Kowloon, Hong Kong) and A-1331852 from AbbVie Inc. (North Chicago, IL, USA) were used. Antibodies against HSP70 (cat#ab2799) from Abcam (Cambridge, UK), OPA1 (cat#612607), cytochrome *c* (cat#556432) and DRP-1 (cat#611113) from BD Biosciences (San Jose, CA, USA); BCL-X_L (cat#2762), BIM (cat#2933) and BAD (cat#9292) from Cell Signalling Technology (MA, USA); BAK (AB-1) (cat#AM-03) and NOXA (cat#OP180) from Millipore (Watford, UK) and MCL-1 (cat#sc-819), BAK (cat#sc-832) and GAPDH (cat#sc-25778) from Santa Cruz Biotechnologies (Santa Cruz, CA, USA) were used. All other reagents were obtained from Sigma Aldrich (St. Louis, MO, USA).

Overexpression and genetic silencing

For transient overexpression studies, cells were transfected with GFP-DRP1 K38A plasmid (provided by Dr. E. Bampton, University of Leicester, UK), using TransIT-LT-1 transfection reagent (Mirus Bio LLC, Madison, WI, USA), according to the manufacturer's protocol. For RNA interference, cells were transfected with 10 nM of siRNAs against DRP-1 (s104274235), MCL-1 (s8585 or SI02781205) or BCL-X_L siRNA (s1920) purchased from Qiagen Ltd (Manchester, UK) or ThermoFisher Scientific (Waltham, MA, USA). Cells were transfected using 0.33% (v/v) Interferin reagent (Polyplus Transfection Inc., NY) to culture media, according to the manufacturer's protocol and processed 72 h after transfection.

Microscopy

For electron microscopy, cells were fixed in 2.5% (w/v) glutaraldehyde and 2 mM calcium chloride in 0.1 M cacodylate buffer (pH 7.4). This was followed by heavy metal staining, which consisted of two consecutive osmium tetroxide steps (2% (w/v) OsO4 in ddh_2O), followed by 1% (w/v) aqueous uranyl acetate. To prevent precipitation artefacts, the cells were washed copiously with ddH_2O between each staining step. All fixation and staining steps were performed in a Pelco Biowave®Pro (Ted Pella Inc., Redding, California, USA) at 100w 20Hg, for 3 min and 1 min, respectively. Dehydration was in a graded ethanol series before filtration and embedding in medium premix resin (TAAB, Reading, UK). Seventy to 74 nm serial sections were cut using a UC6 ultra microtome (Leica Microsystems, Wetzlar, Germany) and collected on Formvar (0.25% (w/v) in chloroform (TAAB, Reading, UK) coated Gilder 200 mesh copper grids (GG017/C; TAAB, Reading, UK). Images were acquired on a 120 kV Tecnai G2 Spirit BioTWIN (FEI, Hillsboro, Oregon, USA) using a MegaView III camera and analySIS software (Olympus, Germany). For immunocytochemistry, cells grown on coverslips were fixed with 4% (w/v) paraformaldehyde, permeabilised with 0.5% (v/v) Triton X-100 in PBS, followed by incubations with primary antibodies (diluted 1:250 in 3% BSA in PBS), the appropriate fluorophore-conjugated secondary antibodies (diluted 1:1000 in 3% BSA in PBS), mounted on glass slides and imaged using a 3i Marianas spinning disk confocal microscope, fitted with a Plan-Apochromat ×63/1.4 NA oil objective, M27 and a Hamamatsu ORCA-Flash4.0 v2 sCMOS Camera (all from Intelligent Imaging Innovations, GmbH, Germany).

Cytochrome *c* release assay

Approximately 10^6 cells were washed in cold PBS and resuspended in mitochondrial isolation buffer (250 mM sucrose, 20 mM HEPES, pH 7.4, 5 mM $MgCl_2$ and 10 mM KCl) containing 0.01% digitonin. Cells were left on ice for 5 min followed by centrifugation at 13000 *g* for 3 min at 4 °C. Subsequently, the supernatant (cytosolic fraction) and pellet (mitochondrial fraction) were processed for western blotting.

Size exclusion chromatography, immunoprecipitation and western blotting

Size exclusion chromatography and immunoprecipitation experiments were carried out as previously described[16,27]. Western blotting was carried out according to standard protocols. Briefly, 50 µg of total protein lysate was subjected to SDS-PAGE electrophoresis. Subsequently proteins were transferred to nitrocellulose membrane, probed with appropriate primary antibodies (diluted 1:1000 in Tris-buffered saline with 0.1% Tween-20), species-specific secondary antibodies (diluted 1:2000 in Tris-buffered saline with 0.1% Tween-20) and protein bands visualised with ECL reagents (GE Healthcare).

Flow cytometry

The extent of apoptosis in cells following different treatments was quantified by using an Attune NxT flow cytometer (ThermoFisher Scientific, Paisley, UK) following staining of the cells with AnnexinV-FITC and propidium iodide to measure phosphatidylserine externalisation, as previously described[45]. Loss in mitochondrial membrane potential (ψ_m) was assessed as described previously[19] by staining cells with TMRE, a lipophilic fluorescent dye that accumulates in the mitochondria in relation to the membrane potential, and quantified by flow cytometry. For BAK activation, cells were fixed with 2% paraformaldehyde at room temperature for 10 min, washed with PBS and resuspended in a buffer containing 0.1% saponin and 0.5% BSA in PBS for 10 min. The cell suspension was then incubated with 0.1 mg/ml of anti-BAK AB-1 (Calbiochem Research Biochemicals—now Merck, cat#AM-03) antibody for 1 h at 4 °C, followed by further incubation with goat-anti-mouse IgG-AlexaFluor-488 conjugated secondary antibody for 1 h at 4 °C, before being subjected to flow cytometry.

Statistical analysis

Statistical analysis was conducted by using one-way ANOVA with Bonferroni's multiple comparison test was performed to evaluate differences between numerical variables. Asterisks depicted correspond to the following p values: $^{*}p \le 0.05$, $^{**}p \le 0.005$ and $^{***}p \le 0.001$.

Acknowledgements
We thank AbbVie for the BH3 mimetics and Drs. Youle, Clark, Slupsky and Bampton for the different cells and plasmids used in the study. This work was supported by a Science Without Borders Scholarship, CNPq 233624/2014-7, Ministry of Education, Brazil (to MM), studentship by Ministry of Higher Education and Scientific Research and University of Al-Qadisiyah, Iraq (to AA), NIH Grants R03CA205496 and R01GM118437 (to XL) and a North West Cancer Research Grant CR1040 (to SV and GMC).

Author details
[1]Department of Molecular and Clinical Cancer Medicine, Institute of Translational Medicine, University of Liverpool, Liverpool, Ashton Street, Liverpool L69 3GE, UK. [2]Department of Cellular and Molecular Physiology, Institute of Translational Medicine, University of Liverpool, Liverpool, Ashton Street, Liverpool L69 3GE, UK. [3]Eppley Institute for Research in Cancer and Allied Diseases, Fred and Pamela Buffett Cancer Center, University of Nebraska Medical Center, Omaha, NE 68198, USA. [4]Department of Molecular and Clinical Pharmacology, Institute of Translational Medicine, University of Liverpool, Liverpool, Ashton Street, Liverpool L69 3GE, UK

Conflict of interest
The authors declare that they have no conflict of interest.

The online version of this article (https://doi.org/10.1038/s41420-019-0199-x) contains supplementary material, which is available to authorised users.

Received: 5 June 2019 Revised: 17 June 2019 Accepted: 23 June 2019
Published online: 17 July 2019

References

1. Adams, J. M. & Cory, S. The Bcl-2 apoptotic switch in cancer development and therapy. *Oncogene* **26**, 1324–1337 (2007).
2. Danial, N. N. & Korsmeyer, S. J. Cell death: critical control points. *Cell* **116**, 205–219 (2004).
3. Youle, R. J. & Strasser, A. The BCL-2 protein family: opposing activities that mediate cell death. *Nat. Rev. Mol. Cell Biol.* **9**, 47–59 (2008).
4. Chen, L. et al. Differential targeting of prosurvival Bcl-2 proteins by their BH3-only ligands allows complementary apoptotic function. *Mol. Cell* **17**, 393–403 (2005).
5. Lessene, G., Czabotar, P. E. & Colman, P. M. BCL-2 family antagonists for cancer therapy. *Nat. Rev. Drug Discov.* **7**, 989–1000 (2008).
6. van Delft, M. F. et al. The BH3 mimetic ABT-737 targets selective Bcl-2 proteins and efficiently induces apoptosis via Bak/Bax if Mcl-1 is neutralized. *Cancer Cell* **10**, 389–399 (2006).
7. Tse, C. et al. ABT-263: a potent and orally bioavailable Bcl-2 family inhibitor. *Cancer Res.* **68**, 3421–3428 (2008).
8. Souers, A. J. et al. ABT-199, a potent and selective BCL-2 inhibitor, achieves antitumor activity while sparing platelets. *Nat. Med.* **19**, 202–208 (2013).
9. Leverson, J. D. et al. Exploiting selective BCL-2 family inhibitors to dissect cell survival dependencies and define improved strategies for cancer therapy. *Sci. Transl. Med.* **7**, 279ra40 (2015).
10. Leverson, J. D. et al. Potent and selective small-molecule MCL-1 inhibitors demonstrate on-target cancer cell killing activity as single agents and in combination with ABT-263 (navitoclax). *Cell Death Dis.* **6**, e1590 (2015).
11. Kotschy, A. et al. The MCL1 inhibitor S63845 is tolerable and effective in diverse cancer models. *Nature* **538**, 477–482 (2016).
12. Caenepeel, S. et al. AMG 176, a selective MCL1 inhibitor, is effective in hematologic cancer models alone and in combination with established therapies. *Cancer Discov.* **8**, 1582–1597 (2018).
13. Tron, A. E. et al. Discovery of Mcl-1-specific inhibitor AZD5991 and preclinical activity in multiple myeloma and acute myeloid leukemia. *Nat. Commun.* **9**, 5341 (2018).
14. Casara, P. et al. S55746 is a novel orally active BCL-2 selective and potent inhibitor that impairs hematological tumor growth. *Oncotarget* **9**, 20075–20088 (2018).
15. Roberts, A. W. et al. Targeting BCL2 with Venetoclax in relapsed chronic lymphocytic leukemia. *N. Engl. J. Med.* **374**, 311–322 (2015).
16. Lucas, C. M. et al. High CIP2A levels correlate with an antiapoptotic phenotype that can be overcome by targeting BCL-XL in chronic myeloid leukemia. *Leukemia* **30**, 1273–1281 (2016).
17. Vaillant, F. et al. Targeting BCL-2 with the BH3 mimetic ABT-199 in estrogen receptor-positive breast cancer. *Cancer Cell* **24**, 120–129 (2013).
18. Oltersdorf, T. et al. An inhibitor of Bcl-2 family proteins induces regression of solid tumours. *Nature* **435**, 677–681 (2005).
19. Vogler, M. et al. A novel paradigm for rapid ABT-737-induced apoptosis involving outer mitochondrial membrane rupture in primary leukemia and lymphoma cells. *Cell Death Differ.* **15**, 820–830 (2008).
20. Henz, K. et al. Selective BH3-mimetics targeting BCL-2, BCL-XL or MCL-1 induce severe mitochondrial perturbations. *Biol. Chem.* **400**, 181–185 (2019).
21. Hardwick, J. M., Chen, Y.-B. & Jonas, E. A. Multipolar functions of BCL-2 proteins link energetics to apoptosis. *Trends Cell Biol.* **22**, 318–328 (2012).
22. Chen, Y.-B. et al. Bcl-xL regulates mitochondrial energetics by stabilizing the inner membrane potential. *J. Cell Biol.* **195**, 263–276 (2011).
23. Li, H. et al. A Bcl-xL-Drp1 complex regulates synaptic vesicle membrane dynamics during endocytosis. *Nat. Cell Biol.* **15**, 773–785 (2013).
24. Perciavalle, R. M. et al. Anti-apoptotic MCL-1 localizes to the mitochondrial matrix and couples mitochondrial fusion to respiration. *Nat. Cell Biol.* **14**, 575–583 (2012).
25. Varadarajan, S. et al. Sabutoclax (BI97C1) and BI112D1, putative inhibitors of MCL-1, induce mitochondrial fragmentation either upstream of or independent of apoptosis. *Neoplasia* **15**, 568–578 (2013).
26. Varadarajan, S. et al. Maritoclax and dinaciclib inhibit MCL-1 activity and induce apoptosis in both a MCL-1-dependent and -independent manner. *Oncotarget* **6**, 12668–12681 (2015).
27. Milani, M. et al. DRP-1 is required for BH3 mimetic-mediated mitochondrial fragmentation and apoptosis. *Cell Death Dis.* **8**, e2552 (2017).

28. Hoppins, S., Lackner, L. & Nunnari, J. The machines that divide and fuse mitochondria. *Annu. Rev. Biochem.* **76**, 751–780 (2007).
29. Marín-García, J. & Akhmedov, A. T. Mitochondrial dynamics and cell death in heart failure. *Heart Fail. Rev.* **21**, 123–136 (2016).
30. Bertholet, A. M. et al. Mitochondrial fusion/fission dynamics in neurodegeneration and neuronal plasticity. *Neurobiol. Dis.* **90**, 3–19 (2016).
31. Vogler, M., Dinsdale, D., Dyer, M. J. S. & Cohen, G. M. ABT-199 selectively inhibits BCL2 but not BCL2L1 and efficiently induces apoptosis of chronic lymphocytic leukaemic cells but not platelets. *Br. J. Haematol.* **163**, 139–142 (2013).
32. Al-Zebeeby A. et al. Targeting intermediary metabolism enhances the efficacy of BH3 mimetic therapy in haematological malignancies. *Haematologica*. **104**, 1016–1025 (2019).
33. O'Neill, K. L., Huang, K., Zhang, J., Chen, Y. & Luo, X. Inactivation of prosurvival Bcl-2 proteins activates Bax/Bak through the outer mitochondrial membrane. *Genes Dev.* **30**, 973–988 (2016).
34. Greaves, G. et al. BH3-only proteins are dispensable for apoptosis induced by pharmacological inhibition of both MCL-1 and BCL-XL. *Cell Death Differ.* **26**, 1037–1047 (2019).
35. Scorrano, L. et al. A distinct pathway remodels mitochondrial cristae and mobilizes cytochrome c during apoptosis. *Dev. Cell* **2**, 55–67 (2002).
36. Morciano, G. et al. Mcl-1 involvement in mitochondrial dynamics is associated with apoptotic cell death. *Mol. Biol. Cell* **27**, 20–34 (2016).
37. Prudent, J. et al. MAPL SUMOylation of Drp1 Stabilizes an ER/ Mitochondrial Platform Required for Cell Death. *Mol. Cell* **59**, 941–955 (2015).
38. Wang, P. et al. Dynamin-related protein Drp1 is required for Bax translocation to mitochondria in response to irradiation-induced apoptosis. *Oncotarget* **6**, 22598–22612 (2015).
39. Xu, W. et al. Bax-PGAM5L-Drp1 complex is required for intrinsic apoptosis execution. *Oncotarget* **6**, 30017–30034 (2015).
40. Lee, J. E., Westrate, L. M., Wu, H., Page, C. & Voeltz, G. K. Multiple dynamin family members collaborate to drive mitochondrial division. *Nature* **540**, 139–143 (2016).
41. Friedman, J. R. et al. ER tubules mark sites of mitochondrial division. *Science* **334**, 358–362 (2011).
42. Cho, B. et al. Constriction of the mitochondrial inner compartment is a priming event for mitochondrial division. *Nat. Commun.* **8**, 15754 (2017).
43. Otera, H., Miyata, N., Kuge, O. & Mihara, K. Drp1-dependent mitochondrial fission via MiD49/51 is essential for apoptotic cristae remodeling. *J. Cell Biol.* **212**, 531–544 (2016).
44. Yamaguchi, R. et al. Opa1-mediated cristae opening is Bax/Bak and BH3 dependent, required for apoptosis, and independent of Bak oligomerization. *Mol. Cell* **31**, 557–569 (2008).
45. Vogler, M. et al. Concurrent up-regulation of BCL-XL and BCL2A1 induces approximately 1000-fold resistance to ABT-737 in chronic lymphocytic leukemia. *Blood* **113**, 4403–4413 (2009).